Biochemical Characterisation of pre-Replicative Complex Architecture

Amina Mehanna

University College London

and

Cancer Research UK London Research Institute

PhD Supervisor: John Diffley

A thesis submitted for the degree of

Doctor of Philosophy

University College London

September 2013

Declaration

I Amina Mehanna confirm that the work presented in this thesis is my own. Where information has been derived from other sources, I confirm that this has been indicated in the thesis.

Abstract

Pre-replicative complexes (pre-RCs), containing the helicase Mcm2-7, are assembled on origins of replication during G1 phase of the cell cycle. This 'licenses' origins for subsequent activation during S-phase. The loading of the Mcm2-7 complex requires ATP hydrolysis and the licensing factors ORC, Cdc6 and Cdt1, and results in the assembly of a head-to-head double hexamer of Mcm2-7 bound around duplex DNA.

To understand how the Mcm2-7 complex is loaded into a double hexamer, we need a better understanding of the stoichiometry and positioning of licensing factors relative to each other during pre-RC assembly. To address this, I used a tagging and immunoaffinity purification strategy. For this purpose, I generated purified protein preparations where subunits of the licensing proteins were fused to either a 9x Myc or a 3x FLAG tag. These proteins were tested for their ability to support loading of the Mcm2-7 complex *in vitro*.

I used the tagged proteins in an established *in vitro* pre-RC assembly assay coupled with an immunoaffinity purification approach. I found that in the absence of ATP hydrolysis, one molecule each of ORC, Cdc6 and Cdt1 recruit a single Mcm2-7 hexamer to origin DNA. Using an ATPase mutant, I showed that ATP hydrolysis by Cdc6 is not required for Mcm2-7 double hexamer formation. I found that a conserved C-terminal region of Mcm3 is critical for Mcm2-7 recruitment to ORC-Cdc6-DNA. Mutations in this C-terminal domain were lethal *in vivo* and inhibited Mcm2-7 loading onto origin DNA *in vitro*. I used the tagged proteins coupled with crosslinking and denaturing immunoaffinity purifications and found that Mcm3 interacts with Orc2 and Cdc6 during Mcm2-7/Cdt1 recruitment to ORC-Cdc6-DNA.

The results of this thesis suggest that Mcm2-7 is recruited to origin DNA via Mcm3 interaction with Orc2 and Cdc6 and that the Mcm2-7 hexamers are loaded in a sequential manner.

Acknowledgements

First and foremost I would like to thank my supervisor John Diffley for his support, excellent guidance and patience over the past four years. I would also like to thank members of the lab, past and present; Dirk Remus, Boris Pfander, Jordi Frigola, Mona Yekezare, Agnieszka Janska, Corella Casas Delucchi, Anne Early, Tom Deegan, Stephanie Carter, Gideon Coster, Belen Gomez Gonzalez, Dominik Boos, Max Douglas, Lucy Drury, Khalid Siddiqui, Kenneth On, Joe Yeeles and Christoph Kurat. Lab members have been abundantly helpful and supportive throughout this project and have created a wonderful atmosphere to work in.

I would also like to express my gratitude to LRI Fermentation Services; Alireza Alidoust and Namita Patel. Finally I would like to thank my friends and family for their continuing belief, patience and support.

Table of Contents

List of figures

List of tables

Abbreviations

ARS: Autonomously Replicating Sequence

Cdc6: Cell Division Cycle 6

CDK: Cyclin Dependent Kinase

Cdt1: CDC10 Dependent Transcript

DNA: Deoxyribonucleic acid

dsDNA: Double Stranded DNA

MCM: MiniChromosome Maintenance

ORC: Origin Recognition Complex

Pre-RC: pre-Replicative Complex

ssDNA: Single Stranded DNA

Chapter 1. Introduction

Deoxyribonucleic acid (DNA) is a polymer of nucleotides that provides genetic instructions to cells. Most DNA is composed of two polymer strands of nucleotides that are complementary to each other. These two strands are entwined in a DNA double helix, the structure of which was first elucidated in 1953 by Watson and Crick (Watson and Crick, 1953).

The replication or copying of DNA is a biological process that occurs in all cell types, from the simplest bacterium to the most complex multicellular organism. This process takes place prior to cell division and acts as the basis for biological inheritance. During DNA replication, a multiprotein replication machine, the replisome, separates the two strands of double helical DNA and uses each as a template to assemble nucleotides into a new complementary strand. The outcome is a pair of DNA double helices, each identical to the original. This is referred to as semiconservative DNA replication.

Accurate and efficient DNA replication is fundamental to ensure that daughter cells inherit an intact copy of the genetic material and to ensure a species' genetic continuity from generation to generation. More than four decades ago, Jacob et al., proposed the "replicon model" of DNA replication to describe the regulation of *Escherichia coli* chromosomal duplication (Jacob et al., 1963). The model postulated that a trans-acting factor called an "initiator" would activate DNA replication through a cis-acting DNA sequence called a "replicator". Indeed, replicators were subsequently identified in prokaryotes, DNA viruses and lower eukaryotes by their ability to confer DNA replication in extrachromosomal replication of plasmids. Initiator proteins were also identified by their ability to bind replicators. This largely validated the "replicon model" and revealed the basic mechanisms by which cells regulate their DNA replication (Bell and Dutta, 2002).

However, it turns out that the replication of DNA is not as simple as an initiator and replicator; instead it is a highly orchestrated process that requires the concerted actions of several proteins. Initiator proteins not only recognize the "replicator" but also act together to load DNA helicase enzymes (replicative helicases) that unwind

the DNA duplex. Subsequently, strand synthesis machineries are recruited to complete replisome formation. These include; primases, DNA polymerases that copy single stranded DNA templates and polymerase clamp-loader complexes. In a further layer of complexity, specific “replicator” sequences have not been identified in higher eukaryotes.

There are also several key steps involved in the accurate and efficient replication of DNA. The “replicator” or origin of replication must first be determined and then recognized. Next, in order for the duplex DNA to function as a template during DNA replication, the two entwined strands must first be exposed. DNA helicases, the enzymes that unwind the DNA, are incapable of initiating unwinding from a completely double-stranded DNA molecule. There is therefore an activity, other than the helicase, that induces the initial opening or melting of the DNA duplex. The DNA helicase also has to, somehow, be loaded onto the DNA in order to initiate DNA unwinding. Furthermore, a series of other steps are then required for the DNA polymerase to begin copying of the template strands and synthesis of new complementary DNA.

There are therefore several issues that need to be overcome in order for efficient replication to take place. Organisms have developed elegant mechanisms to deal with each of the steps involved in replicating their DNA. This introduction will discuss these mechanisms with a focus on DNA helicases, their role in replication and how a DNA helicase is loaded onto origin DNA.

Cells encode many different helicases that contribute to different aspects of nucleic acid metabolism. DNA helicases are motors that couple nucleoside triphosphate binding and hydrolysis to double strand DNA separation and translocation along single-stranded DNA (Lohman and Bjornson, 1996). Generally DNA helicases are oligomeric (mostly functioning as dimers or hexamers), which allows them to contact the DNA at multiple sites (Lohman and Bjornson, 1996). Unwinding of the DNA at replication origins results in the formation of two replication forks, which move in opposite directions. The replicative helicase tracks along with the replication forks unwinding the DNA.

In both prokaryotes and eukaryotes, loading of the replicative helicase at origins represents a key step in replisome assembly. This loading is mediated by initiator proteins and occurs before the recruitment of DNA polymerases that copy the template strands. In *E.coli,* DNA replication is initiated from a single sequence-specific "replicator" or origin known as *OriC* by binding of the initiator protein DnaA. This binding triggers local DNA melting and loading of the replicative helicase DnaB with the aid of another protein, DnaC. In eukaryotes, the initiator origin recognition complex (ORC) binds at origins and together with two other proteins, Cdc6 and Cdt1, loads the replicative helicase Mcm2-7. It is still unclear at which stage and how initial DNA melting occurs in eukaryotes. Loading of the replicative helicase is tightly regulated in both bacteria and eukaryotes. The reason for this is to ensure that daughter cells inherit an intact and error-free copy of the genome. These mechanisms and their significance will be further reviewed later.

The following discussion will focus on the mechanisms of helicase loading and regulation in prokaryotes and eukaryotes with particular focus on the bacterium *Escherichia coli* and the yeast *Saccharomyces cerevisiae* in which these events are best understood.

1.1 DNA Replication in *Escherichia coli*

1.1.1 *E.coli* Origin of Replication

An origin of DNA replication is a site on the DNA at which DNA replication initiates. In bacteria, DNA replication initiates from a single well-defined "replicator" or origin on a circular chromosome. The time taken to replicate the chromosome is therefore proportional to its size. The *E.coli* origin of DNA replication, *OriC* was identified as a 232-245 base pair (bp) region carrying the necessary information for autonomous replication (Oka et al., 1980). *OriC* was further characterised as containing five 9 bp elements (DnaA boxes) that bind the initiator protein DnaA (Fuller et al., 1984, Matsui et al., 1985) as well as three AT-rich 13 bp repeats that are unwound by DnaA binding (Bramhill and Kornberg, 1988). The three 13-mer repeats were then identified as a DNA unwinding element (DUE) that unwinds locally in the absence of replication proteins due to the effects of supercoiling (Kowalski and Eddy, 1989).

Details of DNA sequence motifs in *OriC* are reviewed in (Leonard and Mechali, 2013). A schematic of *OriC* is shown in Figure 1.1. The main functions of *OriC* are to act as a site of replication fork assembly and DNA replication control, for a recent review see (Skarstad and Katayama, 2013).

1.1.2 DnaA binding at *OriC*

The *E.coli* replication initiator, DnaA is a member of the AAA^+ (ATPase associated with various cellular activities) family and is highly conserved amongst bacteria (Katayama, 2008). DNA replication initiator proteins in most cell types share this membership in the AAA^+ protein family. The AAA^+ proteins are involved in a diverse range of cellular activities and usually couple ATP hydrolysis to their activity (Koonin, 1993). AAA^+ proteins often assemble into oligomeric assembles where ATPase active sites are formed at dimer interfaces (Koonin, 1993). The AAA^+ protein, DnaA exists in two states, an ATP-bound active form (DnaA-ATP) and an ADP-bound inactive form (DnaA-ADP).

DnaA performs a central role in binding at *OriC* and initiating DNA replication. DnaA binds with highest affinity to the consensus sequence 5′-TTATCCAC-3′ within the DnaA boxes (Schaper and Messer, 1995). It binds to 3 of these 9 bp elements throughout the cell cycle and forms a nucleoprotein complex (Nievera et al., 2006). Upon initiation, DnaA-ATP rapidly forms a larger nucleoprotein complex of 20-30 monomers (Figure 1.1, step 1) by binding of extra DnaA at two lower affinity 9 bp elements in *OriC* (Nievera et al., 2006). This has been visualised by electron microscopy with negative staining (Fuller et al., 1984). The lower affinity 9 bp elements in *OriC* preferentially bind DnaA-ATP (McGarry et al., 2004) and together with the high affinity 9 bp elements are essential for formation of the DnaA-*OriC* nucleoprotein complex (Miller et al., 2009).

Assembly of the DnaA-*OriC* nucleoprotein complex, together with negatively supercoiled DNA, directly induces DNA unwinding at the DUE (Figure 1.1, step 1), therefore generating single-stranded DNA (open complex formation) suitable for helicase loading and subsequent replisome assembly (Bramhill and Kornberg,

1988). Following replication initiation, DnaA-ATP is prohibited from accessing OriC by several mechanisms including decreasing the levels of available ATP and blocking binding sites in *OriC* (reviewed in (Leonard and Grimwade, 2010)). This ensures that initiations from *OriC* are limited to once per cell cycle, and a complete copy of the genome is available for each daughter cell upon cell division.

1.1.3 Loading of the replicative helicase in *E.coli*

DnaB is the replicative helicase in *E.coli* (LeBowitz and McMacken, 1986). Purification and biochemical characterisation of this helicase found that it is a hexamer composed of six identical subunits (Reha-Krantz and Hurwitz, 1978a, Arai et al., 1981). DnaB was also found to preferentially bind to single stranded DNA and require Mg^{2+} to stabilize its structure (Reha-Krantz and Hurwitz, 1978b). In the absence of Mg^{2+}, DnaB dissociates into monomers and trimers (Bujalowski et al., 1994). Crystal structures of DnaB from other prokarya revealed that the DnaB monomer is a highly flexible molecule consisting of two domains when outside of the confines of the hexamer (Bailey et al., 2007a). Furthermore, electron microscopy data showed that DnaB can exist in a 3-fold symmetry conformation (trimer of dimers) or a 6-fold symmetry (all subunits equivalent) (Yang et al., 2002). DnaB is loaded onto single-stranded DNA and several studies have shown that the enzyme unwinds DNA by translocating in a 5'-3' direction (LeBowitz and McMacken, 1986). A crystal structure of DnaB in complex with single-stranded DNA revealed that DnaB forms a closed spiral staircase structure around the DNA with each C-terminal domain contacting two nucleotides (Itsathitphaisarn et al., 2012).

In order for DnaB to be loaded onto single stranded DNA at *OriC*, it requires a binding partner called DnaC. Like DnaA, DnaC is a member of the AAA^+ family of ATPases (Bell and Kaguni, 2013). It was first thought that DnaC had to bind ATP to interact with DnaB (Wickner and Hurwitz, 1975), however more recent studies, using mutants defective in ATP binding, have demonstrated that DnaC does not need to bind ATP to interact with DnaB (Davey et al., 2002). Three-dimensional reconstruction of cryo-electron microscopy revealed that DnaC binds to the C-

terminal face of the helicase as three dumb-bell-shaped dimers that lock DnaB in the 3-fold symmetry conformation (Barcena et al., 2001).

After single stranded DNA is exposed on *OriC* by formation of the DnaA-*OriC* nucleoprotein complex, DnaA loads two DnaB-DnaC complexes onto this unwound DNA at opposing sides of the resulting bubble (Figure 1.1, step 2), expanding it further (Fang et al., 1999, Carr and Kaguni, 2001). This presents an interesting problem of how to coordinate loading of two DnaB-DnaC complexes on opposing sides of the bubble, in the correct conformation and orientation. It is still unclear how this is achieved. One suggestion, based on structural studies of DnaC from *Aquifex aelicus*, is that DnaC functions as a molecular adapter that uses DnaA-ATP as a docking site to regulate correct spatial deposition of the helicase (Mott et al., 2008). Another intriguing event that occurs during helicase loading is that the DnaB helicase must somehow open up at one of its interfaces to encircle the single-stranded DNA. A recent study using electron microscopy and small angle X-ray scatter (SAXS) determined the ATP-bound structure of the DnaB-DnaC complex (Arias-Palomo et al., 2013). They found that DnaC adopts a spiral conformation that remodels both the N-terminal and C-terminal portions of DnaB, giving rise to a break in the hexameric ring (Arias-Palomo et al., 2013). This could possibly be a mechanism for DnaB loading onto single stranded DNA. Once the DnaB helicase is loaded, it is straight away active for DNA unwinding ahead of the replication fork.

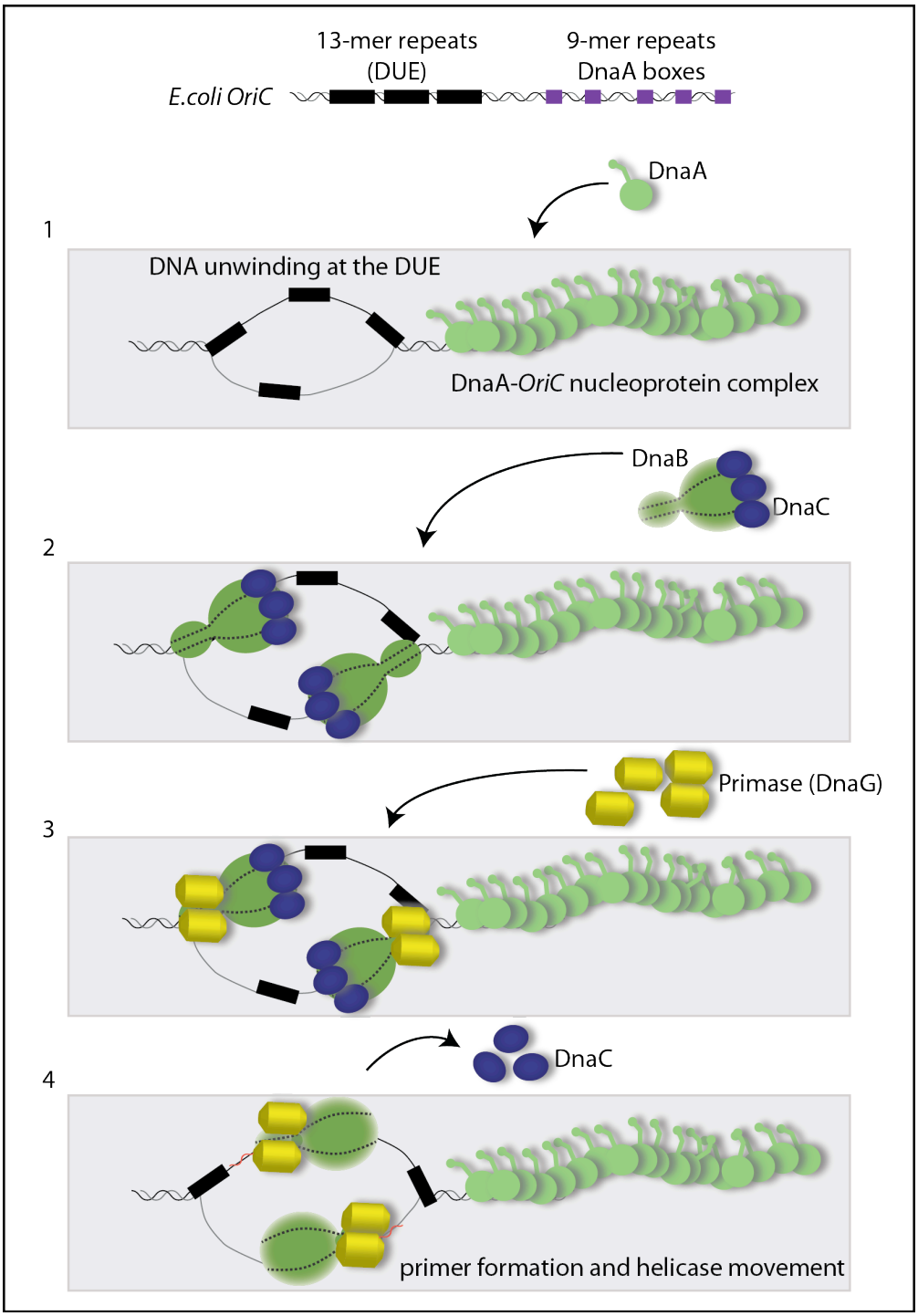

Figure 1.1 Helicase loading at the *E.coli* replication origin, *OriC*

The *E.coli* origin of replication, *OriC*, is shown at the top of the figure. Some sequence elements have been highlighted. In step 1, DnaA-ATP binds the 9-mer repeats (DnaA boxes) to form the DnaA nucleoprotein filament. This, along with the effects of negative supercoiling, induces DNA unwinding at the DUE. In step 2, DnaA loads the helicase DnaB in a complex with DnaC on to opposing sides of the replication bubble. In step 3, the primase DnaG binds to DnaB at its N-terminus. This binding and RNA primer formation (in red) is thought to induce release of DnaC (step 4).

After loading of the DnaB helicase, DnaC dissociates. DnaC bound to ATP (DnaC-ATP), or the poorly hydrolysed analogue ATPγS, is capable of loading DnaB in a DnaA dependent manner (Davey et al., 2002). This indicates that ATP hydrolysis by DnaC is not required for DnaB loading. However, DnaC-ATP is inhibitory to the helicase function of DnaB and it must be hydrolysed after depositing the helicase (Davey et al., 2002). The combined presence of DnaB and single-stranded DNA seem to trigger this ATP hydrolysis, alleviating the inhibitory effect (Davey et al., 2002). The hydrolysis does not however appear to induce release of DnaC, instead its dissociation seems to be induced by a primase (DnaG) that interacts with DnaB at its N-terminus (Figure 1.1, steps 3 and 4) (Makowska-Grzyska and Kaguni, 2010). It is thought that DnaG synthesising a RNA primer whilst interacting with DnaB somehow alters the conformation of DnaB therefore inducing release of DnaC (Figure 1.1, step 4) (Makowska-Grzyska and Kaguni, 2010).

1.1.4 Regulation of helicase loading

Initiation of replication in prokaryotes must be regulated in two ways, firstly to ensure that the whole genome is replicated once per generation and secondly to prevent extra initiation events. One way to achieve this control is by regulating helicase loading. *E.coli* generally regulate helicase loading by controlling the production and activity of the initiator protein DnaA and by inhibiting its access to the origin (reviewed in (Skarstad and Katayama, 2013)).

One way to prevent re-initiation during a single cell cycle, is to prevent DnaA binding to *OriC*. In *E.coli* this is achieved by binding of a protein called SeqA to newly replicated origins, which acts to sequester the origin, preventing excess initiations (Lu et al., 1994, von Freiesleben et al., 1994). SeqA is able to discriminate between unreplicated and newly replicated *OriC* by the methylation status of GATC sequences, which are enriched at the origin (Slater et al., 1995). Adenines in these sequences are methylated by Dam methylase and remain hemi-methylated for a short while (about a third of a generation in the case of *OriC*) after the replication fork has passed (Campbell and Kleckner, 1990, Lu et al., 1994). SeqA recognises these hemi-methylated sequences at the origin and binds them, preventing re-initiation of replication and also Dam methylation (Lu et al., 1994,

Slater et al., 1995, Guarne et al., 2002). SeqA binds to *OriC* in a multimeric form altering the superhelical structure of the DNA and hindering DnaA access to the origin (Torheim and Skarstad, 1999). These mechanisms help to prevent re-initiation of DNA replication within a single cell cycle.

The transcription of DnaA varies with the cell cycle (Bogan and Helmstetter, 1997). An additional important mechanism of SeqA is to bind at the *dnaA* gene promoter, during which time the promoter becomes unavailable to the transcription machinery (Skarstad and Katayama, 2013). This occurs soon after origin firing, thus reducing the ability of DnaA to load the helicase and preventing re-initiation. DnaA also binds at sites other than OriC and acts as a gene regulatory protein. As regions are replicated, this doubles the number of DnaA binding sites and titrates the protein away from the origin, making it unavailable for helicase loading. Another mechanism is regulation of the nucleotide binding state of DnaA (Reviewed in, Skarstad and Katayama, 2013)). DnaA-ATP can bind *OriC* and load the replicative helicase, as discussed previously. The *E.coli* chromosome contains sequences called DARS1 and DARS2 that facilitate the release of ADP from DnaA, therefore activating it (Kaguni, 2006). DARS1 and DARS2 are regulated to ensure timely initiation of DNA replication, however the mechanism of this regulation remains to be elucidated (Kaguni, 2006).

1.1.5 Events downstream of helicase loading

Following primer formation by DnaG (Figure 1.1, step 4, red lines), the primers are extended by the bacterial replicase, DNA polymerase III (Pol III) holoenzyme (reviewed in (Johansson and Dixon, 2013)). Pol III requires a primer to initiate synthesis, and translocates in a 5' to 3' direction (Kornberg and Gefter, 1972). Pol III is composed of around 17 subunits, containing a polymerase core (αεθ), a sliding clamp (β_2), and a clamp loader complex (DnaX) (Johansson and Dixon, 2013). It is thought that a dimer of pol III functions at each replication fork (Maki et al., 1988, Kim et al., 1996). Pol III synthesizes leading and lagging strands simultaneously. The leading strand is synthesised in a continuous fashion. On the lagging strand, however, pol III is only able to synthesize Okazaki fragments up to the 5' end of a preceding RNA primer, at which point it is recycled to the next

primer at the replication fork, resulting in a gap (Kornberg and Baker, 1992). Another polymerase, pol I, then excises the RNA primers and extends the DNA primer filling in this gap (Kornberg and Baker, 1992). The activity of pol I leaves a nick with a 3'-OH and 5'-phosphate that is a substrate for DNA ligase which seals the nick, making a continuous lagging strand (Kornberg and Baker, 1992).

1.2 DNA Replication in Eukaryotes

The eukaryotic cell cycle is composed of four distinct phases; S phase, in which DNA replication occurs, M phase, in which segregation of sister chromatids and cell division takes place, and two gap phases G1 and G2 (Figure 1.2). The order of the cell cycle is as follows: G1, S, G2 and M and is shown in Figure 1.2.

Replication origins are tightly regulated to ensure that they fire once and only once during a cell cycle and produce a single error-free copy of the genome. Loss of this control may cause genome instability, which can contribute to human disease (Arias and Walter, 2007). Re-replication during a single cell cycle has been shown to lead to gene copy number changes, which in turn may promote oncogenesis (Green et al., 2010).

It is therefore crucial that eukaryotic cells have evolved mechanisms to regulate once per cell cycle replication. This is achieved by initiating DNA replication in two discrete steps. In the first step, the Mcm2-7 replicative helicase, which unwinds DNA, is loaded into pre-replicative complexes (pre-RCs) in an inactive form. This is in contrast to *E.coli* where the DnaB helicase is loaded in an active form. The loading of inactive Mcm2-7 into pre-RCs is known as origin licensing, and occurs in late M to G1 phase of the cell cycle (Figure 1.2). Importantly this can only occur when the level of CDK is low and that of the anaphase promoting complex (APC/C) is high (Diffley, 1996). In the second step, origins are activated by recruitment of initiation factors to pre-RCs, which induces replisome formation and unwinding of the DNA by the replicative helicase. This in turn allows polymerases to access and copy the template strands. Origin activation occurs in S phase of the cell cycle and

is triggered by an increase in the level of S-phase CDK and inactivation of the APC/C at the G1/S transition (Diffley, 1996).

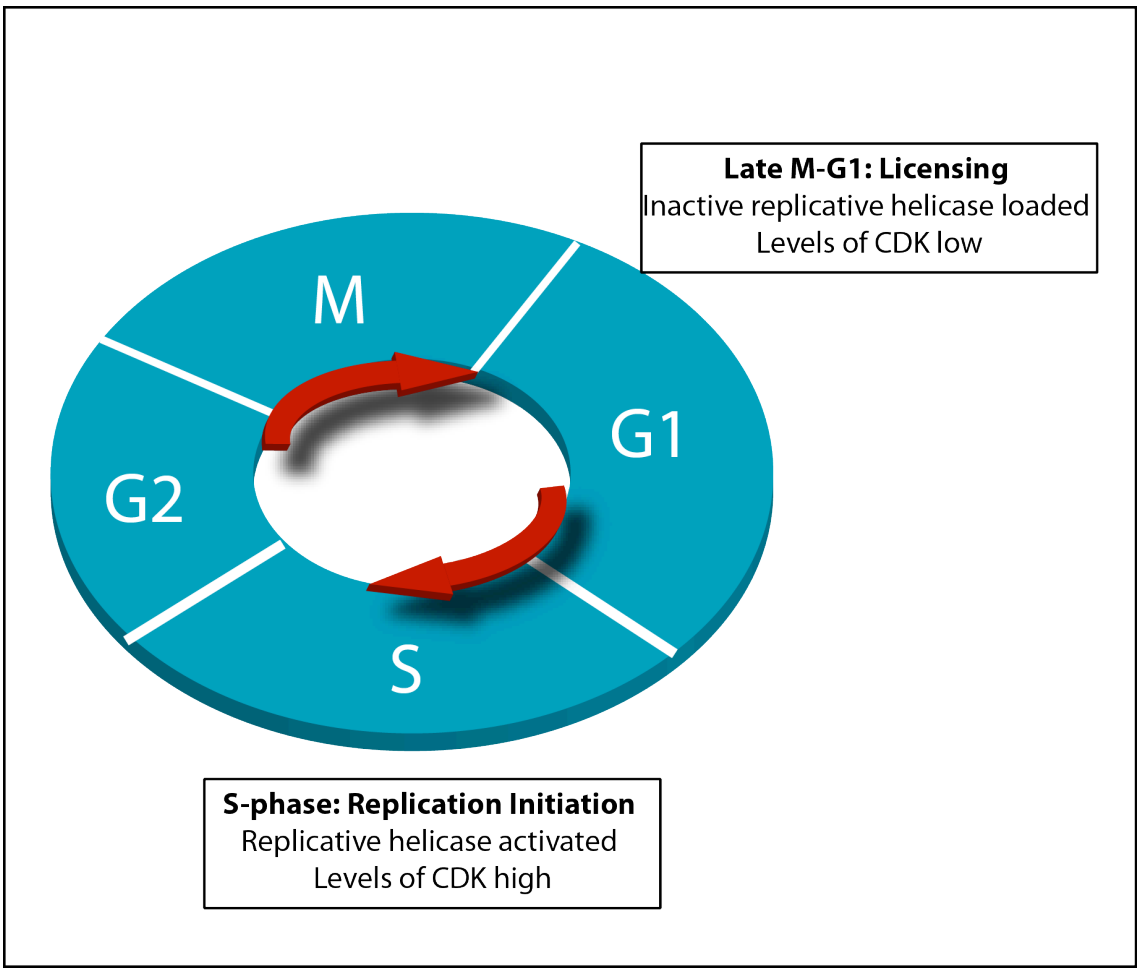

Figure 1.2 Cell cycle regulation of DNA replication

The eukaryotic cell cycle is composed of four phases, M, G1, S and G2. Licensing of origins of DNA replication can only take place in late M to G1 phase, when the levels of CDK are low. This licensing involves assembly of the replicative helicase into pre-replicative complexes. At this stage the helicase is inactive. Upon transition into S phase, the levels of CDK rise and this triggers activation of the helicase and replisome progression. This temporal separation of assembly and then activation, ensures that DNA replication is restricted to once per cell cycle.

1.2.1 Eukaryotic origins of DNA replication

In contrast to bacterial genomes, in eukaryotic cells, DNA replication is initiated from hundreds to thousands of origins along chromosomes. The number of origins

used is generally related to the size of an organism's genome and length of its cell cycle (Leonard and Mechali, 2013). This means that if all origins fire at the same time, the time taken to replicate the genome is directly proportional to inter-origin distance, as opposed to the size of the genome. The presence of multiple origins ensures that every region of the genome is replicated in a rapid and efficient manner. Origins of DNA replication act as sites where pre-replicative complexes, containing the replicative helicase, are assembled. The replicative helicases are then activated in a timely fashion in S phase, when DNA unwinding is required (Reviewed in Remus and Diffley, 2009).

1.2.1.1 DNA replication origins in the yeast Saccharomyces cerevisiae

The first "replicators" or origins in *S. cerevisiae* were identified due to their ability to confer autonomous replication to plasmid DNA (Stinchcomb et al., 1979, Struhl et al., 1979, Hsiao and Carbon, 1979). The first origin was termed Autonomously Replicating Sequence 1 (ARS1). Since then, many other ARSs have been identified and the *S.cerevisiae* genome is estimated to contain some 400 origins (Leonard and Mechali, 2013). Mutational analysis revealed that each ARS contains an 11 bp consensus sequence [5'-(A/T)TTTA(T/C)(A/G)TTT(A/T)-3'], called the ARS consensus sequence (ACS) (Broach et al., 1983, Van Houten and Newlon, 1990). Three elements close to the ACS, termed B1, B2 and B3, have also been identified, and these appear to contribute to origin function (Marahrens and Stillman, 1992, Huang and Kowalski, 1996). The B1 element, most proximal to the ACS, is important for binding of the origin recognition complex (ORC) (Rowley et al., 1995), the B2 element may be a binding site for the replicative helicase (Mcm2-7) (Wilmes and Bell, 2002) and the B3 element binds a DNA-binding factor Abf1 that functions in transcription (Diffley et al., 1994).

Interestingly, *S.cerevisiae* is the only species for which a "replicator" or specific consensus sequence for origins has been identified. Even in other yeast species, a clear consensus sequence is not found. In addition to the ACS and B elements, *S.cerevisiae* origins exhibit a nucleosome-free region and the ACS is necessary to confer this nucleosome exclusion (Eaton et al., 2010).

1.2.1.2 DNA replication origins in metazoans

Due to the larger size of their genomes, metazoans require activation of thousands of origins of replication in a single cell cycle. For example, in the early cleavage stages of the *Xenopus leavis* embryo, DNA replication initiates from some 300,000 origins that are ~ 5-15 kb apart (Blow et al., 2001). Replication origins occur at specific sites in the genome, but their genetic characteristics are still somewhat unclear. A long-standing question has been whether metazoans initiate DNA replication from sequence specific "replicators" as per the replicon model and as in *S.cerevisiae*. This question still remains unresolved. However, genome-wide analysis of active sites of DNA replication initiation in mouse and *drosophila* cells highlighted a preference of an initiator protein, ORC, for CpG islands (Cayrou et al., 2011). In addition, there appear to be G-rich motifs in 80-90% of replication origins close to sites of initiation (Cayrou et al., 2011). These motifs are termed origin G-rich repeated elements (OGREs) and are capable of forming G quadruplexes (Reviewed in, Cayrou et al., 2012).

Another feature of metazoan origins is that there are many more origins than needed during a cell cycle. Approximately, one out of every five potential origins fires during a single cell cycle (Cayrou et al., 2011). This is a feature shared by budding yeast origins (Friedman et al., 1997) and selection of which origins fire seems to occur stochastically. These excess origins may function as back up, which could be important for example if a replication fork encounters difficult to replicate regions that affect its stability (Blow and Ge, 2009). If a fork stalls and is unable to continue replication, spare or "dormant" origins could fire and replicate the DNA up to the stalled fork (Yekezare et al., 2013). There is an increasing body of evidence indicating that such dormant origins are important for genomic stability and cell viability, particularly under conditions of replication stress. For example, when dormant origin activation was inhibited in human cells, reduced viability was observed upon induction of replicative stress (Ge et al., 2007).

1.2.2 Loading of the Replicative Helicase – pre-replicative complex formation

Several early studies revealed that, in eukaryotes, events during replication initiation are separated into distinct stages of the cell cycle. Cell fusion experiments using the mammalian cell line HeLa, showed that fusion of a G1 cell with an S phase cell resulted in rapid induction of DNA replication (Rao and Johnson, 1970). However, when an S phase cell was fused with a G2 phase cell, there was no effect on the normal course of S phase DNA replication (Rao and Johnson, 1970). This indicated that there were positive factors in S phase cells that caused G1 cells to initiate DNA replication. Other studies in *Xenopus* egg extracts showed that G2 nuclei were unable to undergo re-replication when added to a G1 extract, unless the nuclear envelope was permeabilised, suggesting the existence of a 'licensing' factor that could only gain access to DNA during mitosis, after nuclear envelope breakdown (Blow and Laskey, 1988).

Later, *in vivo* footprinting experiments in *S.cerevisiae* revealed that during G1 there is a more extensive protection pattern on origins when compared to S, G2 and M phases of the cell cycle (Diffley et al., 1994). These data indicated that origins are in a 'pre-replicative' state in G1 and then a 'post-replicative' state in later stages of the cell cycle. The pre-replicative state visualised by footprinting represents a pre-replicative complex (pre-RC) at the origin that is lost upon entry into S phase (Diffley et al., 1995). This pre-RC footprint is due to binding of the replicative helicase and its loading factors at origin DNA (Santocanale and Diffley, 1996, Aparicio et al., 1997, Labib et al., 2001). Therefore, the term 'pre-RC formation' has become synonymous with helicase loading and origin licensing.

We now know that origins are licensed in G1 phase by pre-replicative formation, which essentially results in loading of an inactive replicative helicase and then in S phase the poised helicase is activated for replication.

1.2.2.1 Helicase Loading Proteins

The eukaryotic replicative helicase Mcm2-7 (MCM) is loaded onto origin DNA by the combined actions of three proteins, the Origin Recognition Complex (ORC), Cdc6 and Cdt1.

ORC

The very first step in loading the eukaryotic replicative helicase is binding of the origin recognition complex (ORC) to origin DNA. ORC was identified by footprinting studies on *S.cerevisiae* ARS1, followed by fractionation and purification (Bell and Stillman, 1992). ORC was found to be a complex consisting of six subunits. Subsequently, genetic evidence showed that ORC plays a pivotal role early on in DNA replication (Micklem et al., 1993, Foss et al., 1993, Bell et al., 1993). In yeast, ORC is bound at replication origins throughout the cell cycle and requires both the ACS and the B1 element for this binding (Diffley and Cocker, 1992, Diffley et al., 1995, Rowley et al., 1995).

Following studies in yeast, the ORC subunits were found to be conserved in other eukaryotes and play a crucial role in their DNA replication (Gavin et al., 1995, Gossen et al., 1995, Carpenter et al., 1996, Muzi-Falconi and Kelly, 1995). Whereas ORC binds a specific sequence in yeast, the determinants for ORC binding in metazoans are less clear. Interestingly, human ORC binds to a WD40 repeat-containing protein called ORCA that interacts with methylated nucleosomes (Shen et al., 2010, Chakraborty et al., 2011). This could be one method of directing ORC to compacted chromatin.

ORC is a heterohexamer consisting of Orc1-Orc6. Five of these subunits, Orc1-5 are part of the AAA^+ family of proteins, but only Orc1 and Orc5 have been shown to bind ATP (Klemm et al., 1997). Binding of ATP by ORC is essential for its binding to the ACS (Bell and Stillman, 1992) and for pre-RC formation (Klemm and Bell, 2001). Orc1 but not Orc5 has been shown to hydrolyse ATP *in vitro* (Klemm et al., 1997) and an arginine finger in Orc4 is critical for ATP hydrolysis by Orc1 (Bowers et al., 2004). In addition, a mutation in this arginine finger of Orc4 that blocks ATP hydrolysis by Orc1 was shown to block re-iterative Mcm2-7 loading (multiple

Mcm2-7 molecules are loaded at origins of replication) (Bowers et al., 2004). Studies from *Drosophila melanogaster* have shown that dmORC binds DNA and chromatin *in vitro* in an ATP-dependent manner, similar to *S.cerevisiae* (Remus et al., 2004). Interestingly, in human cells ATP binding by Orc4 and Orc5 seems to be required for assembly of hsORC (Siddiqui and Stillman, 2007). It is probable that the ATP binding and hydrolysis functions of ORC differ across domains of life.

ORC1, -2, -4 and -5 contain potential winged helices at their C-termini, which could play a role in ORC-protein and ORC-DNA interactions. Electron microscopy studies coupled with epitope tagging, using *S.cerevisiae* purified ORC, have identified the subunit arrangement within the ORC hexamer (Chen et al., 2008).

Cdc6

Cell Division Cycle 6 (Cdc6) was first identified in *S.cerevisiae,* in a screen for cell cycle mutants (Hartwell et al., 1973). Cdc6 was thought to play a role in replication since temperature sensitive mutants of *CDC6* resulted in mini-chromosome loss, and it was presumed that this protein functioned at the beginning of S phase in replication initiation (Hogan and Koshland, 1992). However, later studies showed that Cdc6 was in fact required for pre-RC formation (late M to G1 phase), but not for ORC binding at origins (Santocanale and Diffley, 1996, Cocker et al., 1996). Concurrently studies in *Xenopus* identified a Cdc6 homologue that is essential for replication initiation (Coleman et al., 1996). Data showed that xCdc6 can only bind chromatin in the presence of Xorc2 and moreover it was required for loading of xMcm3 (part of the Mcm2-7 replicative helicase), suggesting that ORC, Cdc6 and MCM proteins associate with chromatin sequentially (Coleman et al., 1996).

Furthermore, Cdc6 was also found to be required for loading the replicative helicase Mcm2-7 onto chromatin in *S.cerevisiae* (Donovan et al., 1997). Cdc6 can only bind origins in the presence of ORC, and interacts directly with this complex (Liang et al., 1995, Seki and Diffley, 2000).

The Cdc6 protein, like Orc1-5, DnaA and DnaC, is also a member of the AAA^+ family of proteins and it binds and hydrolyses ATP. Mutations in the Walker A and B motifs, responsible for ATP binding and hydrolysis respectively, indicated

genetically separable roles for these functions in pre-RC assembly (Perkins and Diffley, 1998). Genetic data suggested that ATP binding by Cdc6 is required for its interaction with replication origins in G1, whereas ATP hydrolysis is required for loading Mcm2-7 onto chromatin (Perkins and Diffley, 1998, Weinreich et al., 1999). *In vitro* data using yeast G1 extracts also suggested that ATP hydrolysis by Cdc6 is required for Mcm2-7 loading, and that this occurs prior to ATP hydrolysis by ORC (Randell et al., 2006).

Orthologues of Cdc6 have been identified in higher eukaryotes by sequence homology to the *S.cerevisiae* protein, and these also play a role in pre-RC formation (Coleman et al., 1996, Williams et al., 1997).

Cdt1

Cdt1 (Cdc10 Dependent Transcript 1) was first discovered in *S.pombe* as a cell cycle regulated gene required for DNA replication (Hofmann and Beach, 1994). Subsequently homologues of Cdt1 were identified in *Xenopus laevis*, human cells, *Drosophila* and *S.cerevisiae* and this protein was found to play a role in pre-RC formation (Maiorano et al., 2000, Tanaka and Diffley, 2002, Nishitani et al., 2000, Nishitani et al., 2001, Devault et al., 2002, Whittaker et al., 2000). Cdt1 is quite poorly conserved in terms of primary sequence, but all Cdt1 proteins identified contain a pair of winged helices towards their C-termini (Bell and Kaguni, 2013).

In the absence of Cdt1, Cdc6 can still bind origins when ORC is already bound, both *in vivo* and *in vitro* (Maiorano et al., 2000, Nishitani et al., 2000, Remus et al., 2009). In contrast, Cdt1 is unable to bind origins *in vitro* in the absence of Cdc6 (Randell et al., 2006, Remus et al., 2009). Having said this, in *Xenopus* extracts depleted of Cdc6, Cdt1 is still able to bind the origin but Mcm2-7 loading is not supported in this scenario (Gillespie et al., 2001). Cdt1 binds to Mcm2-7 via its C-terminal winged helices (Zhang et al., 2010, Ferenbach et al., 2005). It primarily binds to the C-terminus of Mcm6 (Yanagi et al., 2002). In the yeast *S.cerevisiae,* Cdt1 is constitutively bound to Mcm2-7 and together this complex is shuttled into the nucleus for pre-RC formation in late M/G1 phase of the cell cycle (Tanaka and Diffley, 2002). These studies show that there are probably subtle differences in Cdt1 function and interaction with Mcm2-7 in different species.

Mcm8 and Mcm9

In all eukaryotes, Mcm2-7 loading is dependent on ORC, Cdc6 and Cdt1. Metazoans may employ additional proteins for loading of the Mcm2-7 complex. For example, Mcm8 and Mcm9 are proteins related to the Mcm2-7 subunits that may act to assist in the loading of Mcm2-7 onto chromatin (Lutzmann and Mechali, 2008, Volkening and Hoffmann, 2005, Maiorano et al., 2005). Mcm8 and Mcm9 have also been implicated in homologous recombination (Lutzmann et al., 2012) and may function as a complex that recruits Rad51 to sites of DNA damage (Park et al., 2013).

1.2.2.2 The Mcm2-7 helicase

The MCM proteins were identified in a screen for mutants defective in minichromosome maintenance in yeast (Maine et al., 1984). It was later shown that two of these proteins, Mcm2 and Mcm3, are required for initiation of DNA replication and their subnuclear localization is temporally regulated with respect to the cell cycle (Yan et al., 1993, Hennessy et al., 1990). These proteins localise to the nucleus at the end of mitosis and then exit at the beginning of S-phase, and once in the nucleus both Mcm2 and Mcm3 bind tightly to chromatin. Evidence that the role of the MCM proteins is conserved, came from studies in *Xenopus* eggs whereby a homologue of Mcm3 was identified and found to be important for licensing (Kubota et al., 1995). Furthermore, several studies showed that the MCM proteins form a complex, composed of Mcm2-7, that associates with chromatin in G1 in an ORC and Cdc6-dependent manner (Donovan et al., 1997, Romanowski et al., 1996, Thommes et al., 1997). In addition, the Mcm2-7 proteins were found to be loaded onto chromatin in a salt-stable complex (Donovan et al., 1997), indicating that this complex is topologically linked with the DNA. ORC and Cdc6 are required to load the Mcm2-7 complex onto chromatin in late M to G1 phase, but neither is required for maintenance of the complex on DNA (Donovan et al., 1997).

It was first thought that the Mcm2-7 complex was a poor candidate for the eukaryotic replicative helicase, since a subcomplex containing Mcm4/6/7 has limited helicase activity (acts 3'-5') *in vitro* and is non-processive (Ishimi, 1997). The

full Mcm2-7 complex displayed no helicase activity *in vitro* (Lee and Hurwitz, 2000). Also, yeast genetic analysis showed that these proteins are not essential for replication elongation (Nasmyth and Nurse, 1981, Yan et al., 1993) and mammalian studies failed to show co-localisation between Mcm3 and replication fork foci (Kimura et al., 1994).

However, a later study, using an *in vitro* replication system derived from *Xenopus* egg extracts, showed that DNA unwinding at an early stage of replication is dependent on Mcm2-7 (Walter and Newport, 2000). An Archaeal protein related to the eukaryotic MCM proteins was found to act as an ATP dependent DNA helicase with a 3'-5' polarity similar to the Mcm4/6/7 subcomplex (Shechter et al., 2000). Importantly, Mcm2-7 was shown to be required for progression of DNA replication forks (Labib et al., 2000). Finally, biochemical experiments in *Drosophila* provided evidence that Mcm2-7 stably associates with a protein called Cdc45 and a complex GINS, forming a CMG complex, and that this large assembly has an ATP-dependent helicase activity (Moyer et al., 2006). The Mcm2-7 complex was therefore found to be a helicase that is activated only upon the G1-S phase transition by association with these accessory factors, Cdc45 and GINS (Ilves et al., 2010). This provided an answer as to why the Mcm2-7 complex did not exhibit helicase activity on its own *in vitro*.

The eukaryotic replicative helicase therefore consists of the Mcm2-7 complex associated with Cdc45 and GINS, forming the CMG. Mcm2-7 is composed of 6 essential and related subunits, Mcm2, Mcm3, Mcm4, Mcm5, Mcm6 and Mcm7 (reviewed in (Bochman and Schwacha, 2009). Whilst DnaA and ORC belong to the same clade of AAA^+ proteins, the Mcm2-7 complex is not an orthologue of DnaB. This suggests that whilst some aspects of replication may be conserved, helicase function and loading are likely to be different. The six eukaryotic MCM proteins share significant sequence similarity with each other, particularly in a central region that encodes a AAA^+ domain (ATPase active site) (Koonin, 1993). In addition, the Mcm2-7 proteins have characteristic N and C terminal extensions that are conserved amongst eukaryotes (Figure 1.3A). This suggests that the Mcm2-7 subunits have distinct functions. The MCM proteins contain unique insertions in their AAA^+ domains that are predicted to form β-hairpins that may interact with

single-stranded DNA during unwinding (Bochman and Schwacha, 2009). As is common with members of the AAA^+ family and replicative helicases, the Mcm2-7 proteins oligomerize into a toroidal complex (Figure 1.3B). Electron microscopy and subunit interaction studies have shown that the Mcm2-7 subunits interact in a defined order (Figure 1.3B) forming a ring with a positively charged central channel (Remus et al., 2009, Bochman et al., 2008, Costa et al., 2011, Davey et al., 2003) (Figure 1.3). Interestingly, a direct interaction between Mcm2 and Mcm5 has never been observed, instead the subunit arrangement depicted in Figure 1.3B has been inferred from interactions between the other subunits and the ring structure observed by EM (Davey et al., 2003, Bochman et al., 2008). Consistent with this, the Mcm2-7 complex has been visualised both as a closed ring (Remus et al., 2009) and a gapped ring (Costa et al., 2011). This discontinuity in the ring may be important for helicase loading and DNA unwinding.

AAA^+ proteins form ATPase active sites at dimer interfaces whereby one subunit contributes a Walker A motif (involved in ATP binding) and a Walker B motif (orients a nucleophilic water molecule) and the other subunit contributes a catalytically essential arginine finger (contacts the γ-phosphate of ATP) (Bochman and Schwacha, 2009). This is true of the Mcm2-7 complex, where ATPase active sites are formed at the interfaces between subunits and these sites appear to play distinct functional roles (Bochman et al., 2008), which remain to be fully characterised.

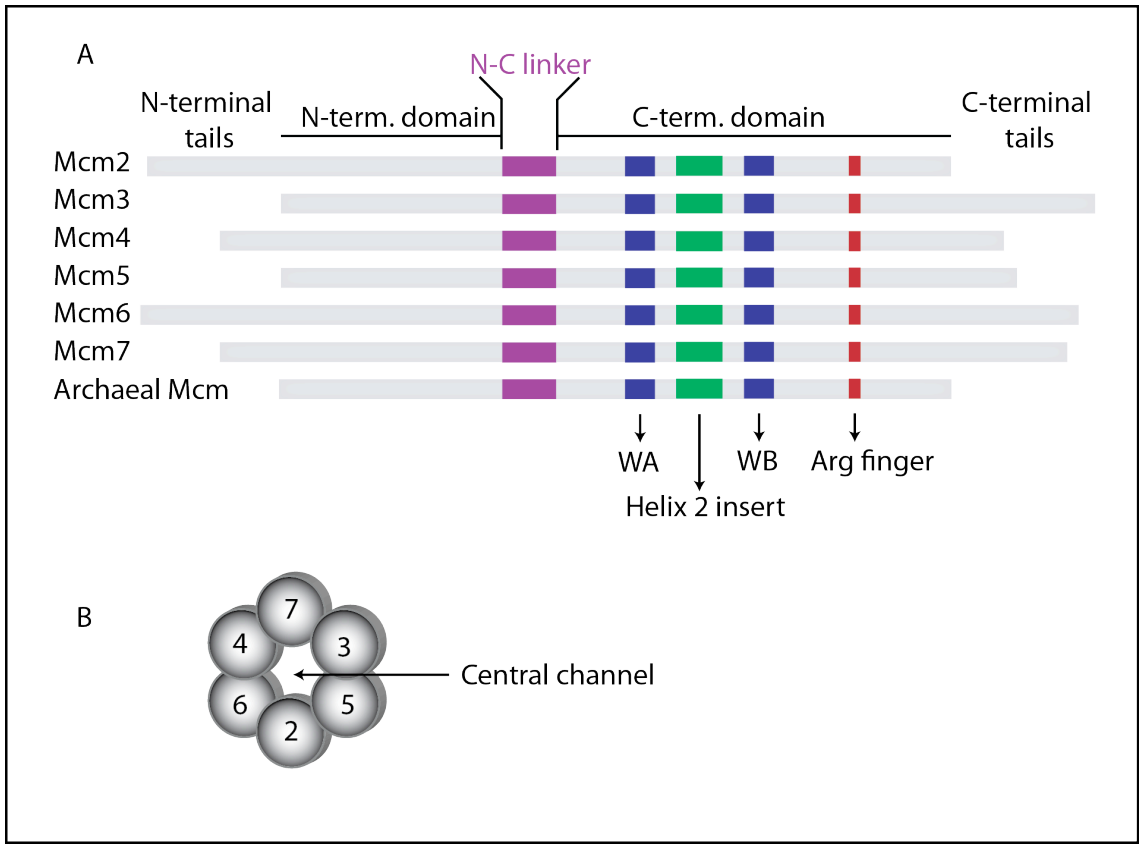

Figure 1.3 Structure of the Mcm2-7 helicase

(A) The Mcm2-7 proteins share a conserved AAA^+ domain consisting of a walker A motif (WA), a walker B motif (WB) and an arginine finger (Arg finger) They also have unique C-terminal and N-terminal extensions, which are absent form Archaeal MCMs. (B) The Mcm2-7 proteins assemble into a toroid. In a ring there is a single copy of each subunit and these are assembled in the order indicated, around a positively charged central channel.

1.2.2.3 Mechanism of Mcm2-7 loading

Here I will discuss what was known about the mechanism of Mcm2-7 loading at the beginning of my PhD. More recent published studies from the end of my PhD will be presented in the results and discussion chapters, as they are relevant to our current work.

Origin licensing takes place in late M to G1 phase of the cell cycle and involves the assembly of pre-replicative complexes that contain the Mcm2-7 helicase. The first step in helicase loading is binding of ORC to origin DNA. ORC then cooperates

with Cdc6 and Cdt1 to load the Mcm2-7 complex onto DNA in a reaction requiring ATP binding and hydrolysis. Although ORC, Cdc6 and Cdt1 are required to load the Mcm2-7 complex onto DNA, they are not required to maintain it (Donovan et al., 1997, Edwards et al., 2002, Rowles et al., 1999). Upon ATP hydrolysis, and therefore helicase loading, Cdc6 and Cdt1 are released from the origin, which explains why *in vivo* chromatin immunoprecipitation assays only detect ORC and Mcm2-7 at origins (Aparicio et al., 1997, Tanaka et al., 1997). The replicative helicase is inactive at this stage and DNA unwinding is not yet detected (Geraghty et al., 2000, Walter and Newport, 2000). The absence of detectable single-stranded DNA, suggested that the Mcm2-7 complex may be loaded onto double-stranded DNA.

Recent work has greatly enhanced our understanding of helicase loading. Reconstitution of pre-RC formation *in vitro* has played a large part in this work. This began with the assembly of pre-RCs in *Saccharomyces cerevisiae* G1 extracts by the addition of exogenous ARS1 DNA (Seki and Diffley, 2000). Using this system, the authors tested the requirements for nucleotides in pre-RC assembly and found that ATP is required for the binding of ORC to origin DNA (as shown *in vivo* by Bell and Stillman, 1992) and for the association of Cdc6 and Mcm2-7 with ORC (Seki and Diffley, 2000). Subsequent studies using similar extract-based systems proposed that there are distinct functions for the ATPase activities of ORC and Cdc6 (Bowers et al., 2004, Randell et al., 2006). As mentioned previously, a point mutation in the Walker B motif of Cdc6, that inhibits ATP hydrolysis but not ATP binding, appeared to block Mcm2-7 loading. In addition, blocking ATP hydrolysis by ORC, by mutating a catalytically essential arginine finger in Orc4, seemed to reduce the number of Mcm2-7 complexes bound at origins (multiple Mcm2-7 complexes are normally loaded at origins) (Bowers et al., 2004). Importantly, mutations that eliminate ORC ATP hydrolysis in *S.cerevisiae* do not support viability (Bowers et al., 2004). This led to a model that sequential ATP hydrolysis by Cdc6 then ORC is required for proper Mcm2-7 loading at origins. In addition, Orc6 was found to interact with Cdt1, thus providing a mechanism for Mcm2-7/Cdt1 interaction with ORC-Cdc6 (Chen et al., 2007). In light of these data, it was proposed that ORC-Cdc6, is not just a landing pad for factors, but rather acts as a molecular machine to load the Mcm2-7 complex onto DNA.

Since relatively little was known about the biochemical mechanisms of pre-RC assembly, it was necessary to reconstitute the pre-RC with purified proteins. This was achieved by using purified *S.cerevisiae* ORC, Cdc6 and Mcm2-7 in complex with Cdt1 and assembling a loading reaction on origin DNA coupled to beads (Evrin et al., 2009, Remus et al., 2009, Tsakraklides and Bell, 2010, Kawasaki et al., 2006). Results from these studies showed that ORC, Cdc6 and Cdt1 are sufficient to perform Mcm2-7 loading *in vitro*, consistent with previous work (Kawasaki et al., 2006). Incubation of ORC, Cdc6 and Mcm2-7/Cdt1 in the presence of ATP with origin DNA coupled to beads, allowed Mcm2-7 loading onto DNA-beads in a salt-resistant manner. In this reaction Cdc6 and Cdt1 are released. In contrast, when ATP hydrolysis was blocked by performing the loading reactions in the presence of the non-hydrolysable ATP analogue ATPγS: ORC, Cdc6, and Mcm2-7/Cdt1 were all detectable on the DNA in low salt but were quantitatively removed by high salt extraction (for a schematic of these reactions, refer to Figure 1.5). This has led to the model that before helicase loading, ORC, Cdc6 and Mcm2-7/Cdt1 are "recruited" to origins in a short-lived complex and upon ATP hydrolysis, Cdc6 and Cdt1 are released and the Mcm2-7 helicase is stably "loaded" onto DNA.

Using electron microscopy, these studies demonstrated that single heptamers of Mcm2-7/Cdt1 are stably loaded onto origin DNA as head-to-head double hexamers connected by their N-terminal rings (Evrin et al., 2009, Remus et al., 2009). Similarly, double hexamers of Mcm2-7 have been observed at licensed origins in *Xenopus* egg extracts (Gambus et al., 2011). The loaded double hexamer of Mcm2-7 is reminiscent of structures observed for Archaeal MCM homohexamers (Chong et al., 2000, Fletcher et al., 2003). However, unlike the Archaeal MCMs, the eukaryotic Mcm2-7 double hexamer is only detected after loading onto DNA (Remus et al., 2009). The double hexamer of Mcm2-7 appears to be stable, as it is capable of surviving gel filtration and treatment with DNase (Gambus et al., 2011, Evrin et al., 2009). It also appears to be able to slide along the DNA (Remus et al., 2009). Importantly, EM data indicate that the Mcm2-7 double hexamer encircles double stranded DNA that runs through its central channel (Figure 1.4) (Remus et al., 2009, Evrin et al., 2009). There are several lines of evidence that show that the Mcm2-7 double hexamer encircles double stranded DNA. Firstly, EM with rotary

shadowing was performed on the double hexamer using a technique that does not allow visualisation of single-stranded DNA (mica adsorption) and strong contrasts of DNA molecules going through the central channel were observed (Evrin et al., 2009). Secondly, when Mcm2-7 double hexamers were bound to circular DNA, the DNA appeared to be relaxed, consistent with the absence of single-stranded DNA (Remus et al., 2009). Finally, studies showed that the double hexamer encircles and slides non-directionally on DNA, indicating that this DNA is double-stranded (Remus et al., 2009, Evrin et al., 2009).

Since single hexamers of Mcm2-7 were never observed on DNA by EM (Remus et al., 2009) and multiple Cdt1 molecules were detected in ATPγS (Takara and Bell, 2011), it was thought that both Mcm2-7 hexamers are loaded at the same time, in a concerted manner. In addition, Cdt1 was found to interact with Orc6 and this ORC subunit appeared to have two Cdt1 interaction sites (Takara and Bell, 2011, Chen et al., 2007). This gave a possible mechanism for loading of two Mcm2-7 hexamers at the same time via Cdt1 interaction with Orc6. Information about the stoichiometry and interactions of loading factors would provide additional insight into this mechanism. In addition, it is still unclear when during the loading process, the Mcm2-7 ring opens and whether the DNA enters the central channel through the Mcm2-5 weakest interface.

Towards the beginning of my PhD project, the discussed published data seemed to suggest the following model for Mcm2-7 loading: ORC recruitment to the origin is first directed by sequence (in budding yeast), local chromatin structure and interaction with other proteins (e.g. ORCA in human cells). Upon entry into G1, ORC recruits Cdc6 and this interaction is dependent on ATP binding. This perhaps reveals two Cdt1 binding sites on Orc6 allowing for the recruitment of two Mcm2-7/Cdt1 hetero-heptamers. It is unclear whether the Mcm2-7 ring is open at this point. If the ring were open, this would indicate that the two hexamers would be aligned to form a single open gate for loading onto the DNA. ATP hydrolysis by Cdc6 then triggers release of Cdc6 itself and Cdt1 and closure of the Mcm2-7 double hexamer around double stranded DNA. Finally, ATP hydrolysis by ORC would probably cause its release from loaded Mcm2-7 and ORC would then be free to direct a new loading event. This model shall be discussed further throughout this

thesis with new data, both published and unpublished shedding light on various steps. A basic model of Mcm2-7 helicase loading is shown is Figure 1.4, whereby ATP binding and hydrolysis lead to assembly of a head-to-head double hexamer bound around double-stranded DNA.

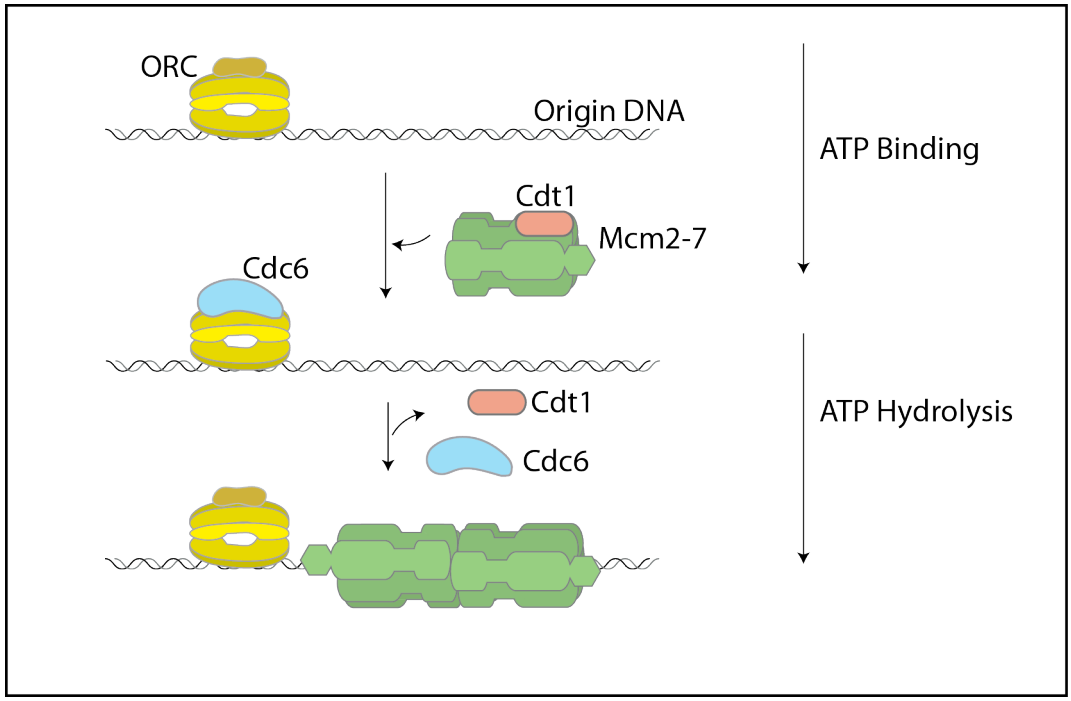

Figure 1.4 Schematic of Mcm2-7 helicase loading

The Origin Recognition Complex, ORC, binds to replication origins. In late M to G1 phase, ORC along with Cdc6 and Cdt1, recruits then loads a double hexamer of the Mcm2-7 helicase around double stranded DNA in a reaction that requires ATP binding and hydrolysis.

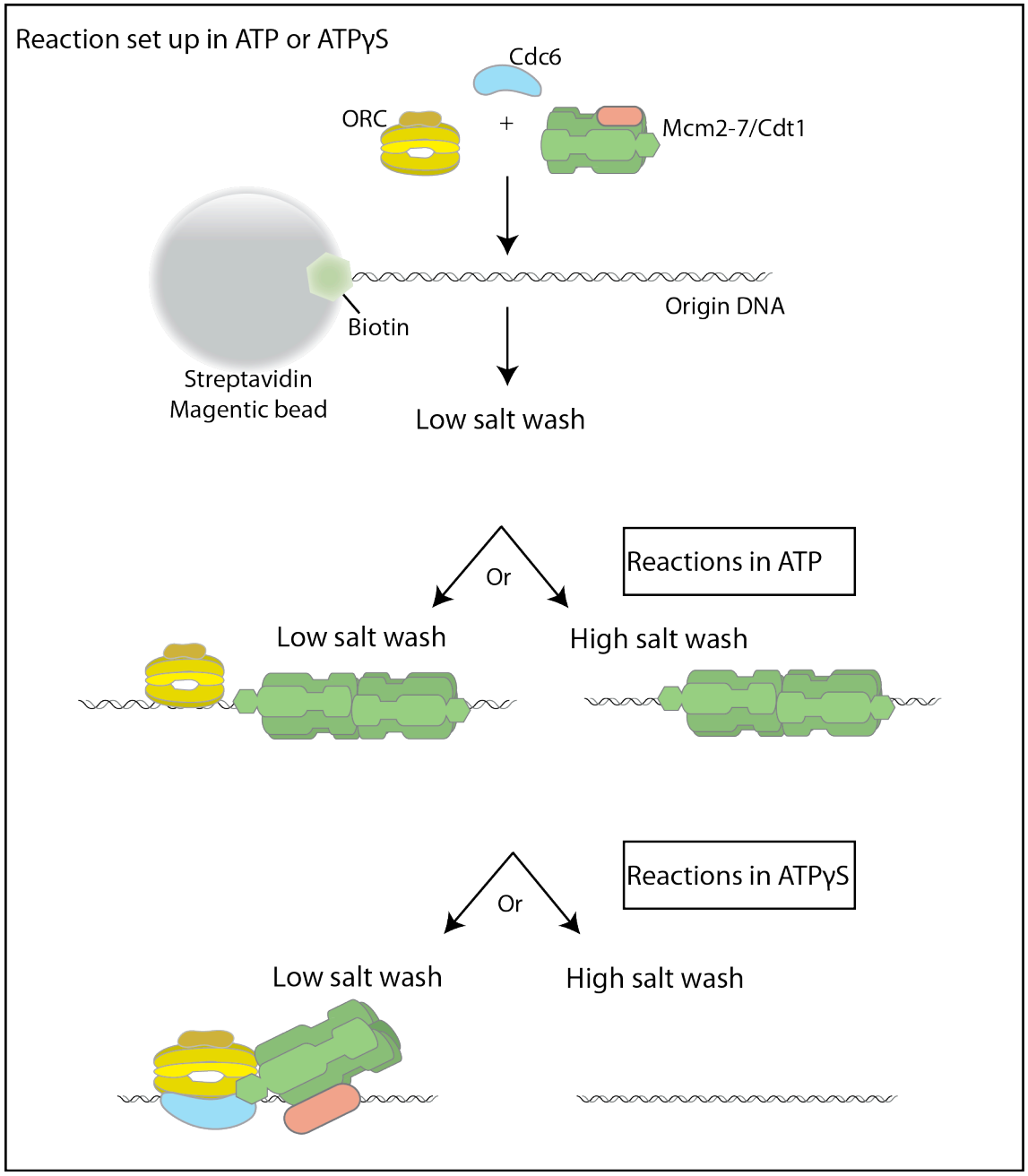

Figure 1.5 Schematic of *in vitro* reconstitution of pre-RC formation

Purified ORC, Cdc6 and Mcm2-7/Cdt1 are incubated with biotinylated origin-containing DNA coupled to streptavidin coated magnetic beads. This is performed in the presence of ATP or ATPγS. All reactions are washed in low salt. Reactions can then be washed in low salt or high salt wash buffers. For reactions set up in ATP, a low salt wash gives rise to ORC and Mcm2-7 on the DNA, as Cdc6 and Cdt1 are released upon ATP hydrolysis. Under high salt wash conditions, ATP reactions give rise to a loaded double hexamer of Mcm2-7 whilst other proteins are washed away. For reactions set up in ATPγS, a low salt wash shows that all proteins are bound (recruited) at the origin. In contrast, under high salt wash conditions, all proteins are washed away. (Evrin et al., 2009, Remus et al., 2009).

1.2.3 Comparison of helicase loading in E.coli and eukaryotes

There are several similarities between helicase loading in *E.coli* and eukaryotes. Firstly, helicase loading in both relies on recognition of the origin by an initiator protein, DnaA in *E.coli* and ORC in eukaryotes. The replicative helicases in E.coli (DnaB) and eukaryotes (Mcm2-7) assemble into six-subunit rings. Interestingly, helicase loading in both is dependent on at least one additional factor. In *E.coli*, DnaC binds DnaB and is required for its loading. In eukaryotes, Cdc6 and Cdt1 are required for Mcm2-7 loading and share some properties with DnaC. Cdc6, like DnaC belongs to the AAA^+ family of proteins and has weak ATPase activity on its own. Cdt1 on the other hand shares with DnaC the ability to associate with its helicase. Finally, the replicative helicase must be activated, either by release of DnaC in *E.coli* or by recruitment of GINS and Cdc45 in eukaryotes.

However, there are a number of important differences both in the mechanism of helicase loading and helicase function. In terms of structure, DnaB is a monohexamer that contains a RecA-like ATPase domain (Bailey et al., 2007b), whereas Mcm2-7 is a heterohexamer composed of AAA^+ ATPase domains (Bochman and Schwacha, 2009). Whilst in prokaryotes origin DNA is unwound and the helicase loads around single-stranded DNA, in eukaryotes no DNA unwinding is observed before S phase and the helicase is loaded around double-stranded DNA. In addition, unlike DnaB, Mcm2-7 appears to track along the DNA in a 3'-5' direction. I.e. DnaB moves along the lagging-strand whilst Mcm2-7 moves along the leading-strand template. DnaB is loaded as two single hexamers on either side of the replication bubble whereas Mcm2-7 is loaded as a head-to-head double hexamer around double stranded DNA.

These differences are likely due to activation timing of the helicase. In *E.coli,* DnaB is rapidly activated after loading, whereas Mcm2-7 is not activated until S phase. This means that the eukaryotic helicase needs to be restrained in an inactive form for longer. Probably, the Mcm2-7 complex assembles into a double hexamer since this structure is more difficult to activate and therefore restrains origin firing. In addition, the double hexamer perhaps encircles double stranded DNA to reduce the time that single-stranded DNA is exposed and maintain genome stability.

In fact, the Mcm2-7 helicase is more reminiscent of the simian virus 40 large T-antigen and the papilloma virus E1 helicase which form hexameric or double hexameric rings around DNA and move in a 3'-5' direction (Enemark and Joshua-Tor, 2008).

1.2.4 Regulation of Mcm2-7 helicase loading

The loading of the Mcm2-7 helicase is tightly restricted to late M/G1 phase of the cell cycle, therefore ensuring that DNA replication occurs once per cell cycle (Arias and Walter, 2007, Symeonidou et al., 2012, Siddiqui et al., 2013). This restriction to late M/G1 is mainly mediated by inhibiting helicase loading at other stages of the cell cycle. The mechanisms of this control vary amongst organisms.

In the yeast *S.cerevisiae,* inhibition of helicase loading outside of late M/G1 is primarily achieved by CDK-mediated phosphorylation. CDK phosphorylates Orc2 and Orc6 (Nguyen et al., 2001), which is thought to disrupt an interaction between Orc6 and Cdt1 therefore impeding Mcm2-7 loading (Chen and Bell, 2011, Chen et al., 2007). In addition, CDK-phosphorylated ORC was recently shown to recruit Mcm2-7 to origin DNA *in vitro*, but ATP hydrolysis then promotes Mcm2-7 release (Frigola et al., 2013). This indicates the presence of an ATP-dependent quality control mechanism that inhibits licensing outside of G1 phase. CDK also phosphorylates Cdc6, which promotes its degradation by the SCF-Cdc4 complex (Drury et al., 2000). Finally, Mcm2-7 in complex with Cdt1 is regulated by CDK phosphorylation of Mcm3, which results in soluble Mcm2-7/Cdt1 being exported from the nucleus (Labib et al., 1999, Liku et al., 2005). Together these mechanisms act to inhibit re-replication by blocking helicase loading outside of G1 phase.

In metazoans, Cdt1 is the primary target for regulation of helicase loading. Outside of G1 phase, Cdt1 is bound by a protein called geminin that inhibits its association with Mcm2-7 (Wohlschlegel et al., 2000). In addition, Cdt1 is degraded during S phase in a PCNA or CDK-dependent manner (Fujita, 2006). Cdt1 is believed to be the main target for regulating once per cell cycle replication since deregulation of

metazoan Cdt1 is sufficient to cause significant re-replication (Fujita, 2006). Cdc6 is also targeted in metazoans by CDK phosphorylation which mediates its nuclear export (Petersen et al., 1999). Finally CDK phosphorylation of ORC inhibits its interaction with origin DNA during G2 and M phases of the cell cycle (Siddiqui et al., 2013). These pathways act to prevent re-replication during the cell cycle in order to preserve genome integrity.

1.2.5 Activation of the replicative helicase

In S-phase the loaded replicative helicase is activated, promoting unwinding of the DNA duplex and allowing DNA polymerases to access and copy the template strands. This step is triggered by an increase in S-phase CDK activity and inactivation of the APC/C at the G1/S transition (Diffley, 1996). Activation of the helicase occurs through the action of two protein kinases, CDK and DDK. In yeast, CDK phosphorylates two proteins, Sld2 and Sld3. This generates binding sites for a set of tandem BRCT repeats on another protein, Dpb11 (Zegerman and Diffley, 2007, Tanaka et al., 2007). Sld3, with its binding partner Sld7 (Tanaka et al., 2011), and Cdc45 associate with origins in a mutually dependent manner (Kamimura et al., 2001). It is thought that Sld3-7 together recruit Cdc45 onto pre-RCs. Sld2, as part of a multi-protein complex, is thought to guide GINS to origins (Muramatsu et al., 2010).

In vertebrates, TopBP1 is the orthologue of Dpb11, whilst Treslin/TICRR was recently identified as the orthologue of Sld3 (Boos et al., 2011, Sanchez-Pulido et al., 2010). Treslin/TICRR has additional domains over Sld3 and was found to interact with a protein called MTBP which is required for GINS, Cdc45 and PCNA recruitment to chromatin in S phase (Boos et al., 2013). It was therefore suggested that MTBP in higher eukaryotes could play a similar role to Sld7.

DDK, comprising a heterodimer of Cdc7 and Dbf4, phosphorylates several of the MCM subunits specifically once they are loaded on chromatin (Francis et al., 2009). Phosphorylation of Mcm4 relieves an auto-inhibitory activity and promotes S phase progression (Sheu and Stillman, 2006, Sheu and Stillman, 2010). DDK also

phosphorylates Mcm2 and Mcm6 (Randell et al., 2010), although the exact function of this is currently unknown.

These events and the action of other factors such as Mcm10, lead to formation and activation of the CMG complex. This complex has been described in *Drosophila melanogaster* embryo extracts (Moyer et al., 2006) and *Saccharomyces cerevisiae* lysates (Gambus et al., 2006). The recruitment of Cdc45 and GINS activates the Mcm2-7 complex (Ilves et al., 2010). The Mcm2-7 helicase in complex with Cdc45 and GINS, translocates along single-stranded DNA in a 3'-5' direction on the leading strand, displacing the lagging strand as it moves (Fu et al., 2011). In addition, the CMG has been found to contain just one copy of Mcm2-7 (Moyer et al., 2006).

Therefore transition from a Mcm2-7 double hexamer to an active CMG complex is a highly complex process (reviewed in (Boos et al., 2012)). For one, the loaded Mcm2-7 double hexamer must split into two individual hexamers upon or after its activation. Additionally, the Mcm2-7 ring must have to open to extrude a strand from its central channel and retain the correct strand within. It is still unclear how these events occur and in what succession. It is likely that the Mcm2-7 complex itself induces origin melting. Recent development of an assay for *in vitro* DNA replication (Heller et al., 2011) will be useful in addressing these questions.

1.2.6 Replisome progression

This thesis focuses on the mechanism of helicase loading in eukaryotes, here I will only briefly describe events downstream of origin unwinding. Replisome mechanics are described in detail elsewhere (Pomerantz and O'Donnell, 2007, Johnson and O'Donnell, 2005, Zheng and Shen, 2011).

Due to the anti-parallel nature of DNA and the direction in which nucleic acid synthesis occurs (5'-3'), leading and lagging strands are synthesised continuously and discontinuously, respectively. Once origin unwinding occurs, a specialised RNA polymerase called primase is recruited and synthesizes short RNA primers

(~12 nucleotides in length) which are extended by DNA Pol α/primase (Frick and Richardson, 2001). These primers are required since cellular DNA polymerases are unable to initiate synthesis in their absence (Kornberg and Baker, 1992). Synthesis of the leading strand is thought to require only one or very few of these priming events and is hence said to occur in a continuous manner. In contrast, synthesis of the lagging strand requires multiple priming events and occurs as a series of discontinuous Okazaki fragments (Kornberg and Baker, 1992).

A clamp loader, replication factor C (RFC), recognizes the RNA-DNA primer synthesised by Pol α/primase. It is then able to displace the primase and recruit the sliding clamp PCNA that acts as a processivity factor for DNA polymerases. RFC loads PCNA in an ATP dependent manner and contact with primed DNA stimulates ATP hydrolysis by RFC, leaving PCNA encircling the DNA (Bowman et al., 2004). This is reminiscent of ORC-Cdc6 loading the Mcm2-7 complex in an ATP binding and hydrolysis-dependent manner. The leading strand polymerase, Pol ε (Pursell et al., 2007), uses only one or very few sliding clamps since synthesis occurs in a continuous and processive manner. The lagging strand polymerase, Pol δ (Nick McElhinny et al., 2008) which physically interacts with Pol α (Johansson et al., 2004), is in contrast recycled amongst several PCNA sliding clamps to synthesise multiple Okazaki fragments.

Once synthesis of Okazaki fragments is completed, Pol δ initiates removal of the RNA primers (Zheng and Shen, 2011). It does this by regulating displacement of the 5' end of a downstream Okazaki fragment creating a 5' flap substrate on the RNA primer for nucleases called Dna2 and Fen1 (Garg et al., 2004). The Okazaki fragments are then joined together to form an intact lagging DNA strand.

1.3 Summary

Much progress has been made in the field of DNA replication over the last 25 years. Many of the events involved in replisome formation in *E.coli* are now relatively well understood and mechanistic details are being unravelled. Studies in *E.coli* have served as a platform for understanding the mechanisms of DNA replication in eukaryotic cells.

The advance in biochemical assays to study replication in eukaryotes has greatly enhanced our understanding of pre-RC assembly and we now know that ORC, Cdc6 and Cdt1 function together to load a double hexamer of Mcm2-7 around double stranded DNA. We also know that in S phase, the Mcm2-7 replicative helicase is activated by incorporation into the CMG complex that tracks along single stranded DNA in a 3'-5' direction to unwind the DNA. With such advanced knowledge, many more fundamental questions about the mechanistic details arise.

It is still unclear how exactly ORC, Cdc6 and Cdt1 are able to coordinate loading of a double hexamer of Mcm2-7. Is one ORC molecule required for this loading? Or is the loading achieved by binding of two ORC molecules on either side of the origin? A similar question may be asked of Cdc6. How are the ATPase activities of the loading proteins coordinated for double hexamer formation? Which proteins are required to interact during helicase loading? Answering any of these questions would enhance our understanding of how a pre-RC is assembled.

Equally there are many questions surrounding eukaryotic replisome assembly and helicase activation. It is intriguing how the helicase must transition from a double hexamer around double stranded DNA to a single hexamer around single stranded DNA.

This thesis will focus on characterising the biochemical architecture of pre-replicative complex formation using the yeast *S.cerevisiae* as a model system. In particular the stoichiometry of loading factors and some of their interactions are revealed. The results of this thesis give some insight into how the Mcm2-7 double hexamer is loaded onto DNA.

Chapter 2. Materials & Methods

2.1 Solutions

TBS

20 mM Tris-HCl pH 7.5, 150 mM NaCl

TBST

20 mM Tris-HCl pH 7.5, 150 mM NaCl, 1 mM Tween 20

TE

10 mM Tris-HCl pH 8.0, 1 mM EDTA

Western transfer buffer

48 mM Trizma base, 39 mM glycine, 0.0375% SDS, 20% methanol

Milk TBST

5% Marvel Milk in TBST

TAE

40 mM Tris acetate, 1 mM EDTA

2.2 *E.coli* manipulation

2.2.1 Cell growth

Cells were grown in suspension in LB (0.5% bacto-tryptone, 0.25% bacto-yeast extract, 170 mM NaCl, pH 7.0) at 37°C. For growth on solid media, LB was supplemented with 2% agar. For selective growth, media was supplemented with ampicillin (75 µg/ml) and/or chloramphenicol (34 µg/ml).

All media was obtained from Cancer Research UK, Clare Hall laboratories, media services.

2.2.2 Transformation

DH5α cells (NEB) were used for routine transformation and cells were transformed according to manufacturer's guidelines (NEB).

BL21 CodonPlus RIL cells (Stratagene) or BL21 DE3 Codon+ RIL cells (Stratagene) were used for protein expression and cells were transformed according to manufacturer's guidelines (Stratagene).

2.2.3 Plasmid DNA preparation

2 or 5 ml of cell cultures were grown overnight in selective LB to amplify plasmid DNA. Plasmid DNA was purified using a Mini-Prep kit (QIAGEN) according to manufacturer's guidelines.

2.3 Yeast manipulation

2.3.1 Cell growth

Cells were grown in suspension in YP (1% yeast extract, 2% bacto-peptone) with 2% glucose, galactose or raffinose at 30°C. For growth on solid media YP was supplemented with 2% agar and 2% glucose (YPD agar).

For selective growth, drop-in media (2% agar, 1x yeast nitrogen base, 2% glucose in ddH_2O) was supplemented with the required amino acids (adenine 5 mg/ml, uracil 2 mg/ml, leucine 10 mg/ml, tryptophan 2 mg/ml, histidine 10 mg/ml).

For selection of the NatNT2 marker, cells were grown on YPD agar supplemented with 100 µg/ml Nourseothricin (LEXSY NTC, Jena Bioscience)

For G1 phase arrest, alpha factor was added for 2 hours to log phase cultures at 5 µg/ml (all strains were Δ*bar1*.

2.3.2 Transformation

Cells were transformed according to Gietz et al. (Gietz et al., 1992).

2.3.3 Mating, sporulation and tetrad dissection

Mating was achieved by mixing together a MATa and a MATalpha strain in a 1 cm patch on a YPD agar plate. The plate was incubated overnight at 25°C. Heterozygotes were selected by streaking the mated strains on plates that selected for the diploid strain. Single colonies were then patched onto rich sporulation media. The plate was incubated at 25°C for 2-3 days and sporulation was checked microscopically for the presence of tetrads.

Asci were digested in a solution of zymolyase (0.25 mg/ml in 1 M sorbitol) at 37°C for 5 mins. Digested asci were spread in a line on a YPD agar plate and tetrads were dissected using a tetrad dissection microscope (Singer).

2.3.4 Genomic DNA extraction

To extract yeast genomic DNA, cells were grown overnight in 5 ml of YP (see 2.3.1) supplemented with 2% glucose. Cells were collected by centrifugation at 3000 rpm for 2 minutes. Cells were washed with 1 ml ddH_2O and resuspended in 400 µl extract solution (2% Triton X-100, 1% SDS, 100 mM NaCl, 10 mM Tris-HCl pH 8.0, 1 mM EDTA). 2- mercaptoethanol (0.14 M) and lyticase (100 U/ml) were added to this suspension and the mixture was incubated for 5 minutes at 37°C. An equal volume of phenol/chloroform was added and the cells were broken open by vortexing for 10 seconds. The mixture was centrifuged for 2 minutes at 13,000 rpm in a benchtop centrifuge and the aqueous phase was recovered. The DNA was precipitated by adding an equal volume of iso-propanol and centrifuging as before. The DNA pellet was washed twice with 70% ethanol by centrifugation as before. The DNA pellet was then resuspended in 50 µl TE supplemented with 50 µg/ml RNaseA. RNA was degraded by incubation at 37°C for 1 hour and DNA was stored at -20°C.

2.3.5 Protein extraction

Whole cell protein extractions were carried out by subjecting yeast cells to mild alkali treatment and boiling in SDS sample buffer (Kushnirov, 2000).

2.4 Protein analysis

2.4.1 SDS-Polyacrylamide Gel Electrophoresis (SDS-PAGE)

SDS PAGE was carried out using either pre-cast or home-made gels. For home-made gels, 10% or 7.5% polyacrylamide gels were prepared according to (Sambrook and Russell, 2001) using a Mini-Protean II gel system (BioRad).

For pre-cast SDS-PAGE the following were used:

Criterion XT 3-8% Tris-acetate with XT Tricine running buffer (Bio-Rad)
NuPage 4-12% Bis-Tris with MOPS running buffer (Invitrogen)
NuPage 10% Bis-Tris with MOPS running buffer (Invitrogen).

2x SDS PAGE loading buffer was prepared according to (Sambrook and Russell, 2001).

2.4.2 Immunoblotting

Following SDS-PAGE, gels were equilibrated in western transfer buffer and transferred to Hybond ECL nitrocellulose membranes (GE Healthcare) by wet transfer at 400 mA for 2 hours at 4°C. Membranes were blocked in milk TBST for 30 mins and then incubated with primary antibodies for 2 hours in milk TBST. Membranes were washed 2 x 10 mins in TBST and incubated with secondary antibody (HRP-conjugated) for 1 hour in milk TBST if required. Membranes were then washed 3 x 10 mins in TBST and blots were visualised by Enhanced Chemiluminesence (ECL) reagents (Amersham) or ECL Dura (Pierce).

2.4.3 Protein Staining

Coomassie staining: Instant Blue (Expedeon), according to manufacturer's guidelines

Silver staining: Silver Quest (Invitrogen), according to manufacturer's guidelines

2.4.4 ^{32}P visualisation

Radiolabel incorporation into dried gels was visualised using a phosphorimager. Dried gels were exposed to a phosphorscreen (Molecular Dynamics) for 1 hour – overnight before analysis using a Typhoon phosphorimager (GE Healthcare).

2.5 Cloning

All restriction digested plasmids and PCR products were purified from agarose gels using Roche PCR purification kit (according to manufacturer's guidelines). All generated plasmids were sequenced using Big Dye Terminator Kit version 3.1 (Invitrogen, and LRI sequencing facility).

2.5.1 Cloning Cdc6 and E224G Cdc6 in pGEX-6p-1

S.cerevisaie CDC6 was amplified from pET15b-*CDC6* using the primers AM1 and AM2. The PCR product was cloned between BamHI and XhoI restriction sites in pGEX-6p-1 (GE Healthcare), generating pAM3.

E224G *CDC6* was amplified from pET15b-*E224G-CDC6* using the primers AM1 and AM2 and cloned in pGEX-6p-1 as above, generating pAM4.

2.5.2 Cloning the 3x FLAG and 9x Myc epitope tags in pAM3

The 9x Myc epitope tag was amplified from pYM21 by PCR using AM71 and AM72. The PCR product was cloned into the BamHI site of pAM3. This resulted in Cdc6 tagged at its 5' end with 9x Myc (pAM36).

The 3 x FLAG epitope tag was generated by annealing the AM81 and AM86 oligos. The product was cloned into the BamHI site of pAM3. This gave rise to Cdc6 tagged at its 5' end with 3x FLAG (pAM37).

2.5.3 Cloning the 3x FLAG epitope tag in ORC overexpression vectors

The 3 x FLAG epitope tag was generated by annealing the AM140 and AM141 oligos. The product was cloned into the SgrA1 site of pJF17 and pJF18. This gave rise to pAM15 and pAM17, where Orc4 and Orc6 were tagged at their 5' ends with 3x FLAG respectively.

A 3 x FLAG epitope tag was also generated by annealing the AM142 and AM143 oligos. The product was cloned into the AscI site of pJF19, pJF17, and pJF18. This gave rise to pAM18, pAM14 and pAM16, where Orc1, Orc3 and Orc5 were tagged at their 5' ends respectively.

2.5.4 Cloning the 9x Myc epitope tags in ORC overexpression vectors

The 9x Myc epitope tag was amplified from pYM21 by PCR using AM117 and AM119. The PCR product was cloned into the SgrA1 site of pJF17 and pJF18. This gave rise to pAM9 and pAM11, where Orc4 and Orc6 were tagged at their 5' ends with 9 x Myc respectively.

The 9x Myc epitope tag was also amplified from pYM21 by PCR using AM120 and AM122. The PCR product was cloned into the AscI site of pJF17 and pJF18. This gave rise to pAM8 and pAM10, where Orc3 and Orc5 were tagged at their 5' ends respectively.

2.5.5 Cloning CBP-TEV at the 5' end of Mcm3 in a MCM overexpression vector

CBP-TEV was amplified from pJF19 by PCR using the primers GC090 and AM75. The PCR product was cloned into the SgrA1 site of pJF5. This resulted in CBP-TEV at the 5' end of Mcm3 (pAM38).

2.5.6 Cloning 9x Myc at the 5' end of Mcm3 in pAM38

9x Myc was amplified from pYM21 using the primers AM117 and AM119. The PCR product was cloned into the SgrA1 site of pAM38. This resulted in tagged Mcm3 as follows: CBP-TEV-9x Myc-Mcm3 (5'-3'), pAM27.

2.5.7 Cloning 3x FLAG and 9x Myc at the 5' end of Cdt1

The 3 x FLAG epitope tag was generated by annealing the AM140 and AM141 oligos. The product was cloned into the SgrA1 site of pJF2. This gave rise to Cdt1 tagged at its 5' end with 3x FLAG (pAM28)

The 9x Myc epitope tag was amplified from pYM21 using the primers AM117 and AM119. The PCR product was cloned into the SgrA1 site of pJF2. This gave rise to Cdt1 tagged at its 5' end with 9x Myc (pAM22)

2.5.8 Cloning Mcm3 and deletion fragments into an MBP expression vector

Mcm3 and deletion fragments were cloned into the MBP expression plasmid pMAL-C2P. pMAL-C2P was a gift from Satoru Mochida and was derived from pMAL-C2 (NEB) by introducing a PreScission protease site before the EcoRI site in the polylinker region. MCM3 was amplified from S.cerevisiae genomic DNA using AM51 and AM52 and cloned into pMAL-C2P using XbaI and SalI sites (pAM5).

A C-terminal fragment of *MCM3* consisting of 588 bp was amplified from *S.cerevisiae* genomic DNA using AM54 and AM52. This PCR product was cloned

in pMAL-C2P using XbaI and SalI sites (pAM6).

An N-terminal fragment of *MCM3* consisting of 2331 bp was amplified from *S.cerevisiae* genomic DNA using AM51 and AM53. This PCR product was cloned in pMAL-C2P using XbaI and SalI sites (pAM7).

2.6 Construction of yeast strains

2.6.1 Background strains for ORC 3x FLAG and 9x Myc fusions

Background strains for tagging the ORC subunits were generated by linearizing ORC overexpression vectors and transforming these one by one into yJF1. yAM4 was generated by transforming pJF17 and pJF18 in yJF1. yAM5 was generated by transforming pJF17 and pJF19 in yJF1. yAM6 was generated by transforming pJF18 and pJF19 in yJF1.

2.6.2 ORC Strains containing 3x FLAG or 9x Myc fusions

ORC strains containing 5' fusions to 3x FLAG or 9x Myc were generated by transforming linearized tagged ORC overexpression vectors into the background strains described above (Refer to Table 5 for more information). This generated the strains yAM8 (*3x FLAG-ORC1*), yAM12 (*3x FLAG-ORC3*), yAM14 (*3x FLAG-ORC4*), yAM16 (*3x FLAG-ORC5*), yAM18 (*3x FLAG-ORC6*), yAM11 (*9x MYC-ORC3*), yAM13 (*9x MYC-ORC4*), yAM15 (*9x MYC-ORC5*), yAM17 (*9x MYC-ORC6*).

ORC strains containing 3' fusions of 3x FLAG or 9x Myc to Orc2 were generated by amplification of the 3x FLAG or 9x Myc tags from pBP83 or pYM21 respectively.

3x FLAG was amplified from pBP83 using the primers AM88 and AM89, the PCR product was then transformed into ySD-ORC. This gave rise to the strain yAM44 (*ORC2-3x FLAG*).

9x Myc was amplified from pYM21 using the primers AM88 and AM89, the PCR product was then transformed into ySD-ORC. This gave rise to the strain yAM43 (*ORC2-9x Myc*).

2.6.3 Background strains for Mcm2-7/Cdt1 3x FLAG and 9x Myc fusions

Background strains were generated by mating yJF21 and yAM37, heterozygote selection, sporulation and tetrad dissection. Background strains were identified by selecting for markers. This generated yAM22.

2.6.4 Mcm2-7/Cdt1 strains containing 3x FLAG or 9x Myc fusions

Mcm2-7/Cdt1 strains containing 5' fusions to CBP or 3x FLAG or 9x Myc were generated by transforming linearized tagged Mcm2-7/Cdt1 overexpression vectors into the background strain described above and into yJF21 (Refer to Table 5 for more information). This generated the strains yAM33 (*CBP-TEV-MCM3*), yAM34 (*9x MYC-CDT1*), yAM35 (*3x FLAG-CDT1*), yAM25 (*CBP-TEV-9x MYC-MCM3*).

2.7 Protein Purification

2.7.1 Purification of ORC from yDR11

In this strain *ORC1* has a C-terminal TAP-TCP tag consisting of: TEV protease site, calmodulin binding protein (CBP) and protein A (from N-term to C-term). Each of the ORC subunits is overexpressed in yDR11 from the *Gal1-10* promoter. ORC was purified from this strain as described in Remus et al., 2009 with minor alterations, in salt type and concentration. The purification is described below.

Starter cultures of yDR11 in YP + 2% raffinose were incubated overnight with shaking at 30°C. These were then inoculated in a 50 L fermentor culture in YP + 2% raffinose at 30°C and grown to a cell density of 2 x 10^7 cells/ml. The cells were then arrested for 3 hours with 100 ng/ml of the yeast mating pheromone alpha factor. ORC expression was induced overnight by addition of 2 % galactose. Cells

were harvested by centrifugation, washed twice in wash buffer (25 mM Hepes-KOH pH 7.6, 1 M Sorbitol) and once in lysis buffer (25 mM Hepes-KOH pH 7.6, 0.05% NP-40, 10% Glycerol) + 0.1 M KCl by 10 min centrifugations at 4500 rpm. The pellet was then resuspended in 0.5 volumes of lysis buffer + 0.1 M KCl + 2 mM β-mercaptoethanol + Complete EDTA-free protease inhibitors (Roche: 1 tablet/25 ml buffer). The cell suspension was frozen drop-wise into liquid nitrogen creating balls of cells known as popcorn. The popcorn was crushed under liquid nitrogen in a freezer mill using 6 cycles of 2 minutes (crushing at rate setting 15) creating frozen powder. Whole cell extracts were prepared on ice by adding an equal volume of lysis buffer + 0.1 M KCl + 2 mM β-mercaptoethanol + Complete EDTA-free protease inhibitors (Roche: 1 tablet/25 ml buffer) and mixing vigorously with a glass rod. The salt concentration was increased to 0.5 M KCl and the suspension centrifuged at 42000 rpm for 1 hour using a Ti45 ultracentrifuge rotor (Beckman). The soluble clear phase, which contains ORC, was then collected and at this stage could be frozen in liquid nitrogen and stored at -80°C.

2 mM $CaCl_2$ was added to thawed extracts and the suspension subjected to ultracentrifugation as above for 30 mins. The supernatants were transferred to 50 ml falcon tubes and 200 µl packed bed resin Calmodulin affinity resin (Stratagene; pre-equilibrated in lysis buffer + 0.3 M KCl) added per 50 ml of extract. These tubes were rotated for 3 hours at 4°C. Using a disposable gravity flow column, Calmodulin beads and bound proteins were recovered and washed with 10 bed resin volumes of lysis buffer + 0.3 M KCl + 2 mM $CaCl_2$ + 2 mM β-mercaptoethanol. ORC was then eluted with 10 bed resin volumes of lysis buffer + 0.3 M KCl + 1 mM EDTA + 1 mM EGTA + 2 mM β-mercaptoethanol. ORC eluted in the 2^{nd}, 3^{rd} and 4^{th} fractions.

ORC containing fractions were pooled and concentrated to 2 ml using a Centricon Plus-20 Centrifugal Filter (Millipore) and incubated with an approximately equal amount of TEV protease (w/w), overnight at 4°C. The mixture was then passed over a superdex 200 (Hiload 16/60, GE Healthcare) resin using lysis buffer + 0.3 M KCl + 1 mM EDTA + 1 mM EGTA + 2 mM β-mercaptoethanol. ORC-containing peak fractions were pooled and passed over 400 µl washed IgG sepharose beads (Amersham) to remove uncleaved protein. The resulting untagged ORC was

dialysed for 2 hours against lysis buffer + 0.15 M KCl + 1 mM EDTA + 1 mM EGTA + 2 mM β-mercaptoethanol and fractionated over a 1 ml MonoQ column using a gradient of 0.15-0.5 M KCl over 20 column volumes. The MonoQ column removed a truncation of Orc1. Peak-containing fractions (containing full length Orc1) were pooled and dialysed for 2 hours against lysis buffer + 0.1 M KOAc + 1 mM EDTA + 1 mM EGTA + 2 mM β-mercaptoethanol.

2.7.2 ORC purification from ySDORC

The ySDORC strain is codon optimised to increase protein expression of the ORC subunits. This allows purification of high protein yields from smaller volumes of cells compared to yDR11 (see above). In this strain *ORC1* has an N-terminal tag consisting of a calmodulin binding protein (CBP) and a TEV protease site. Also in this strain the codon optimised ORC subunits are expressed from the *Gal1-10* promoter. The ySDORC strain was used to construct all the tagged ORC complexes described in Chapter 4.

Starter cultures of ySDORC in YP + 2% raffinose were incubated overnight with shaking at 30°C. These were then inoculated in a 2 L culture in YP + 2% raffinose at 30°C and grown to a cell density of 2 x 10^7 cells/ml. The cells were then arrested for 3 hours with 100 ng/ml of the yeast mating pheromone alpha factor. ORC expression was induced for 3 hours by addition of 2 % galactose. Cells were harvested by centrifugation, washed twice in wash buffer (25 mM Hepes-KOH pH 7.6, 1 M Sorbitol) and once in lysis buffer (25 mM Hepes-KOH pH 7.6, 0.05% NP-40, 10% Glycerol) + 0.1 M KCl by 10 min centrifugations at 4500 rpm. The pellet was then resuspended in 0.5 volumes of lysis buffer + 0.1 M KCl + 2 mM β-mercaptoethanol + Complete EDTA-free protease inhibitors (Roche: 1 tablet/25 ml buffer). Preparation of “popcorn”, freezer milling and whole cell extracts was performed as for purification of ORC from yDR11, except a Ti70.1 rotor was used for ultracentrifugation.

2 mM $CaCl_2$ was added to thawed extracts and the suspension subjected to ultracentrifugation at 50,000 rpm for 30 mins using a Ti70.1 ultracentrifuge rotor

(Beckman). The supernatant was transferred to 600 µl packed bed volume of Calmodulin affinity resin (Stratagene; pre-equilibrated in lysis buffer + 0.3 M KCl) in a disposable gravity flow column. The column was rotated for 3 hours at 4°C. Calmodulin beads and bound proteins were washed with 10 bed resin volumes of lysis buffer + 0.3 M KCl + 2 mM $CaCl_2$ + 2 mM β-mercaptoethanol. ORC was then eluted with 10 bed resin volumes of lysis buffer + 0.3 M KCl + 1 mM EDTA + 1 mM EGTA + 2 mM β-mercaptoethanol. ORC eluted in the 2nd, 3rd and 4th fractions as for purification from yDR11.
ORC containing fractions were pooled and concentrated to 0.4 ml using a Centricon Plus-20 Centrifugal Filter (Millipore) and incubated with an approximately equal amount of TEV protease (w/w), overnight at 4°C. Note that ORC is still functional when the CBP tag is not cleaved off, this step was therefore sometimes left out from the purification protocol. The mixture was then passed over a superdex 200 (10/300, GE Healthcare) resin using lysis buffer + 0.3 M KCl + 1 mM EDTA + 1 mM EGTA + 2 mM β-mercaptoethanol. ORC was dialysed for 2 hours against lysis buffer + 0.1 M KOAc + 1 mM EDTA + 1 mM EGTA + 2 mM β-mercaptoethanol.

All 3x FLAG and 9x Myc-tagged ORC complexes were purified in this manner.

2.7.3 Mcm2-7/Cdt1 Purification from yDR17

In this strain Mcm4 is tagged at its C-terminus with 3 x FLAG and Cdt1 co-purifies with the MCM complex. Mcm2-7/Cdt1 was purified from yDR17 as in Remus et al., 2009 with minor differences.

Starter cultures of yDR17 in YP + 2% glucose were incubated overnight with shaking at 30°C. These were then inoculated in a 100 L fermentor culture in YP + 2% glucose at 30°C and grown to a cell density of 8 x 10^7 cells/ml. The fermentor culture was supplemented with an extra 1% glucose and arrested for 3 hours with 100 ng/ml alpha factor. Cells were harvested by centrifugation, washed twice in wash buffer (25 mM Hepes-KOH pH 7.6, 1 M Sorbital) and once in lysis buffer (45 mM Hepes-KOH pH 7.6, 0.02% NP-40, 10% Glycerol) + 0.1 M KOAc + 5 mM

$Mg(OAc)_2$ by 10 min centrifugations at 4500 rpm. The pellet was then resuspended in 0.5 volumes of lysis buffer + 0.1 M KOAc + 2mM β-mercaptoethanol + Complete EDTA-free protease inhibitors (Roche: 1 tablet/25 ml buffer). Popcorn preparation and freezer milling was carried out as for ORC purifications.

To make whole cell extracts, the yeast powder was thawed in a room temperature water bath. Then, on ice, an equal volume of lysis buffer + 0.1 M KOAc + 2 mM β-mercaptoethanol + Complete EDTA-free protease inhibitors (Roche: 1 tablet/25 ml buffer) was added and mixed vigorously with a glass rod. The salt concentration was increased to 0.5 M KOAc and the suspension centrifuged at 42000 rpm for 1 hour using a Ti45 ultracentrifuge rotor (Beckman). The soluble clear phase which contains Mcm2-7/Cdt1 was then collected and at this stage could be frozen in liquid nitrogen and stored at -80°C.

The soluble clear phase was dialysed against lysis buffer + 0.1 M KOAc + 2 mM β-mercaptoethanol + Complete EDTA-free protease inhibitors (Roche: 1 tablet/25 ml buffer) for 2 x 1.5 hours and centrifuged at 42000 rpm for 30 min using a Ti45 ultracentrifuge rotor. The supernatants were transferred to 50 ml falcon tubes and supplemented with 3 mM ATP. 200 µl packed bed resin Anti-FLAG M2 Agarose (Sigma; pre-equilibrated in lysis buffer + 0.1 M KOAc) was then added to each 50 ml of extract. These tubes were rotated for 3 hours at 4°C. Using a disposable gravity flow column, Anti-FLAG beads and bound proteins were recovered and washed with 10 bed resin volumes of lysis buffer + 0.1 M KOAc + 1 mM ATP + 2 mM β-mercaptoethanol. Washed beads were resuspended in 1 bed-resin volume of lysis buffer + 0.1 M KOAc + 1 mM ATP + 2 mM β-mercaptoethanol supplemented with 1 mg/ml 3 x FLAG peptide (Sigma) and rotated at 4°C for 30 mins. The flow-through fraction was concentrated using Microcon YM-10, 10000 MWCO (Millipore) and fractionated over a 24 ml Superdex 200 10/300 column (GE Healthcare) equilibrated in lysis buffer + 0.1 M KOAc + 1 mM ATP + 2 mM β-mercaptoethanol. Mcm2-7/Cdt1 eluted in the 670 kDa fraction (Thyroglobulin fraction). Peak fractions were pooled and concentrated as above, then frozen in aliquots of 10 µl.

2.7.4 Mcm2-7/Cdt1 purification from yJF38

In this strain Mcm3 is tagged at its N-terminus with 3 x FLAG and Cdt1 co-purifies with the MCM complex. In contrast to the yDR17 strain, in yJF38 Mcm2-7 and Cdt1 are overexpressed from the *Gal1-10* promoter. Mcm2-7/Cdt1 was purified from yJF38 as in Frigola et al., 2013, the only exception being that KOAc was used instead of K-glutamate in all buffers.

2.7.5 Mcm2-7/Cdt1 purification from yAM33

In this strain, Mcm3 is fused to a CBP (Calmodulin Binding Peptide) at its N-terminus and Cdt1 co-purifies with the MCM complex. Starter cultures of yAM33 in YP + 2% rafinose were incubated overnight with shaking at 30°C. These were then inoculated in a 2 L culture in YP + 2% raffinose at 30°C and grown to a cell density of 2 x 10^7 cells/ml. The cells were then arrested for 3 hours with 100 ng/ml of the yeast mating pheromone alpha factor. Mcm2-7/Cdt1 expression was induced for 3 hours by addition of 2 % galactose. Cells were harvested by centrifugation, washed twice in wash buffer (25 mM Hepes-KOH pH 7.6, 1 M Sorbitol) and once in lysis buffer (45 mM Hepes-KOH pH 7.6, 0.05% NP-40, 10% Glycerol) + 100 mM KOAc by 10 min centrifugations at 4500 rpm. The pellet was then resuspended in 0.5 volumes of lysis buffer + 0.1 M KOAc + 2 mM β-mercaptoethanol + Complete EDTA-free protease inhibitors (Roche: 1 tablet/25 ml buffer). Preparation of “popcorn”, freezer milling and whole cell extracts was performed as for purification of Mcm2-7/Cdt1 from yDR17, except a Ti70.1 rotor was used for ultracentrifugation.

The soluble clear phase was dialysed against lysis buffer + 0.1 M KOAc + 2 mM β-mercaptoethanol + Complete EDTA-free protease inhibitors (Roche: 1 tablet/25 ml buffer) for 2 x 1.5 hours. 2 mM $CaCl_2$ was added to extracts and the suspension subjected to ultracentrifugation at 50,000 rpm for 30 mins using a Ti70.1 ultracentrifuge rotor (Beckman). The supernatant was transferred to 600 µl packed bed volume of Calmodulin affinity resin (Stratagene; pre-equilibrated in lysis buffer + 0.1 M KOAc) in a disposable gravity flow column. The column was rotated for 3 hours at 4°C. Calmodulin beads and bound proteins were washed with 10 bed resin volumes of lysis buffer + 0.1 M KOAc + 2 mM $CaCl_2$ + 2 mM β-

mercaptoethanol. ORC was then eluted with 10 bed resin volumes of lysis buffer + 0.1 M KOAc + 1 mM EDTA + 1 mM EGTA + 2 mM β-mercaptoethanol. Mcm2-7/Cdt1 eluted in the 2nd, 3rd and 4th fractions. The elution fractions were concentrated using Microcon YM-10, 10000 MWCO (Millipore) and fractionated over a 24 ml Superdex 200 10/300 column (GE Healthcare) equilibrated in lysis buffer + 0.1 M KOAc + 2 mM β-mercaptoethanol. Mcm2-7/Cdt1 eluted in the 670 kDa fraction (Thyroglobulin fraction). Peak fractions were pooled and concentrated as above, then frozen in aliquots of 10 µl.

Mcm2-7/Cdt1 complexes containing 9x Myc-Mcm3, 3x FLAG-Cdt1 or 9x Myc-Cdt1 were all purified in this manner.

2.7.6 Cdc6 purification from Baculovirus

Cdc6 purification from a baculovirus expression vector was performed exactly as described in Remus et al., 2009.

2.7.7 Cdc6 purification from *E.coli*

Cdc6 purification from *E.coli* was modified from Speck et al. 2005. The plasmid pGEX-6p-1/Cdc6 (pAM3) was transformed into BL21 CodonPlus RIL cells (Stratagene) following manufacturer's guidelines. A 10 ml starter culture of LB/ampicillin (100 µg/ml)/ chloramphenicol (34 µg/ml) was grown overnight at 37°C with shaking then diluted 1:100 in 1 L of LB/amplicillin (100 µg/ml)/ chloramphenicol (34 µg/ml). The 1 L culture at OD_{600} 0.6 was placed on ice for 10 minutes and induced with 0.5 mM IPTG for 5 hours at 18°C with shaking. Cells were then harvested at 6000 rpm for 10 mins. To lyse cells, the pellet was resuspended in 50 ml buffer A (50 mM $KXPO_4$ pH7.6, 150 mM KOAc, 5 mM $MgCl_2$, 2 mM ATP, 1% Triton X-100, 1 mM DTT, Complete EDTA-free protease inhibitors (Roche; 1/25 ml)) and 100 µg/ml lysozyme was added. The mixture was incubated on ice for 30 minutes and then sonicated for 2 mins (5 sec off 5 sec on) at maximum intensity. The suspension was then centrifuged at 15000 rpm for 15 mins in a SS34 rotor (Sorvall) and the supernatant transferred to 2 ml bed-resin pre-washed glutathione sepharose (GE Healthcare) in a disposable gravity flow column. This was rotated at

4°C for 3 hours. Glutathione beads and bound proteins were recovered in the column and washed with 20 column volumes of buffer A. A 50% slurry was then prepared with buffer A and 50 µl preScission protease (GE Healthcare) added. The mixture was incubated for 2 hrs at 4°C with rotation. The flow-through was then recovered and the concentration of KOAc diluted to 75 mM. This was incubated with 2 ml hydroxyapatite pre-equilibrated in buffer B (50 mM $KXPO_4$ pH7.5, 75 mM KOAc, 5 mM $MgCl_2$, 2 mM ATP, 0.1% Triton x-100, 1 mM DTT) for 15 mins at 4°C with rotation. The protein-hydroxyapatite was washed with 5 column volumes of buffer B and then washed with 5 column volumes of buffer C (50 mM $KXPO_4$ pH7.5, 150 mM KOAc, 5 mM $MgCl_2$, 15% glycerol, 0.1% Triton x-100, 1 mM DTT). Cdc6 was finally eluted with 10 column volumes buffer D (50 mM $KXPO_4$ pH7.5, 400 mM KOAc, 5 mM $MgCl_2$, 15% glycerol, 0.1% Triton x-100, 1 mM DTT). Peak fractions were pooled and concentrated using a Centricon Plus-20 Centrifugal Filter (Millipore), then aliquoted in 10 µl volumes and snap-frozen in liquid nitrogen.

3x FLAG-Cdc6 and 9x Myc-Cdc6 were also purified in this manner.

2.7.8 Purification of MBP-Mcm3

Plasmids expressing MBP-Mcm3 (pAM5, pAM6 or pAM7) were transformed into BL21 DE3 Codon+ RIL cells (Stratagene). 0.5 L of cells were grown at 37°C to a density of OD_{600}=0.5-0.8. Cells were chilled on ice, and then 1 mM IPTG was added. Induction of protein expression was carried out overnight at 18ºC with shaking.

Cells were harvested, washed once with ice-cold 25 mM Hepes-KOH pH7.6/1M sorbitol, once with buffer B (50 mM Tris-HCl pH 7.5, 0.05% NP-40, 10% glycerol)/1 M NaCl and then the pellet was resuspended in 20 ml of buffer B/1 M NaCl/2 mM ß-mercapethanol/protease inhibitors (Roche). 50 µl of lysozyme (50 mg/ml) was added and the suspension incubated for 20 minutes at 4ºC. Cells were kept on ice and sonicated 3 x 30 sec at 15 microns using a sonicator (Soniprep 150 (Sanyo)). The lysate was centrifuged for 1 hour at 45000 rpm using a Ti45 rotor. The soluble phase was collected and incubated with 2 ml packed amylose bead volume (NEB)

at 4ºC for 1 hour. Beads were washed with ten bed resin volumes of buffer B/0.3 M NaCl/2 mM ß-mercaptoethanol. Elution was performed with buffer B/0.3 M NaCl/2 mM ß-mercaptoethanol/10 mM Maltose. Peak fractions were pooled and concentrated using a Centricon Plus-20 Centrifugal Filter (Millipore), then aliquoted in 10 µl volumes and snap-frozen in liquid nitrogen.

2.8 Preparation of DNA-Beads

The *in vitro* reconstitution assay involves assembly of purified pre-RC proteins on linear yeast origin DNA conjugated to magnetic beads. I used two types of DNA-beads, one where the DNA was conjugated to beads via a biotin-streptavidin linkage, and one where the DNA was conjugated to beads via a photocleavable biotin-streptavidin linkage.

2.8.1 Amplification of origin DNA

A 1048 bp fragment containing the yeast origin ARS305 was generated by PCR with the primers ARS305-F-Eco-Bio (biotinylated primer) or ARS305-F-PC-Bio (primer containing a photocleavable biotin) and ARS305-R (Remus et al., 2009) and using p305bp as a template (Huang and Kowalski, 1996). The resulting linear PCR product was biotinylated either with or without a photocleavable site at one end. Eight 50 µl PCR reactions were setup and subsequently purified using the High Pure PCR Product Purification Kit (Roche).

2.8.2 Conjugation of Origin DNA to Magnetic Beads

200 µl streptavidin-coated M-280 Dynabeads (Invitrogen) were washed twice using a magnetic rack in 500 µl buffer 1 (10 mM Tris-HCL pH 7.5, 1 mM EDTA, 2 M NaCl) and resuspended in 200 µl buffer 1 (N.B should be carried out in non-stick eppendorf tubes). The purified PCR reactions from 2.9.1 were pooled, added to the washed bead suspension and rotated overnight at 4°C. The beads were then washed twice in 500 µl buffer 2 (10 mM Hepes-KOH pH 7.6, 1 mM EDTA, 1 M KOAc) and twice in 500 µl buffer 3 (10 mM Hepes-KOH pH 7.6, 1 mM EDTA). The DNA-beads were then resuspended in 200 µl buffer 3 and stored at 4°C.

2.9 In Vitro Reconstitution of Mcm2-7 Loading

2.9.1 Setting up the reactions

This method is described based on the setup of four standard reactions as follows; reaction 1 (ATP, low salt wash), reaction 2 (ATP, high salt wash), reaction 3 (ATPγS, low salt wash) and reaction 4 (ATPγS, high salt wash). To set up the reactions, 5 µl DNA-beads (2.2) per reaction were placed in non-stick eppendorf tubes and 2.5 µl supernatant buffer removed on a magnetic rack. On ice, the reactions were setup as in Table 1, making sure to add the purified proteins to the reactions last and in the order ORC, Cdc6 then Mcm2-7/Cdt1.

Table 1 Reaction composition for *in vitro* pre-RC assembly

Component	Per reaction
5 x Binding buffer (Table 2)	8 µl
ATP/ ATPγS (100 mM)	2 µl
DTT (0.1 M)	0.4 µl
ORC	50 nM final concentration
Cdc6	50 nM final concentration
Mcm2-7/Cdt1	100 nM final concentration
Distilled Water	Up to 40 µl
DNA-Beads	2.5 µl

The reactions were mixed on ice by pipetting and then placed at 30°C for 30 mins, shaking at 1000 rpm.

2.9.2 Washing the Reactions

Following incubation, unbound proteins were removed by placing the tubes on a magnetic rack and aspirating the supernatants. All reactions were washed once with low salt wash buffer (Table 2) by resuspending the beads in the buffer and

pipetting up and down an equal amount in each tube. A further wash was then carried out as above either in low salt wash buffer or high salt wash buffer as required (Table 2). The DNA-beads and bound proteins were then resuspended in 40 µl Laemmli buffer and boiled for 5 min (if DNA-beads with a streptavidin-biotin linkage were used).

If DNA-beads with a photocleavable biotin were used, then DNA-beads and bound proteins were re-suspended in 20 µl of low salt wash buffer. DNA was then removed from the beads by irradiating with UVA for 10 min at 330 nM.

Table 2 Buffer compositions for pre-RC assembly *in vitro*

5 x binding buffer	
Hepes-KOH pH 7.6	125 mM
MgOAc	50 mM
NP-40	0.10%
KOAc	Final concentration of 100 mM in the reactions; including salt contributed by purified proteins
Glycerol	25%
Low salt wash buffer	
Hepes-KOH pH 7.6	45 mM
MgOAc	5 mM
NP-40	0.02%
EDTA	1 mM
EGTA	1 mM
KOAc	0.3 M
Glycerol	10%
High salt wash buffer	
Hepes-KOH pH 7.6	45 mM
MgOAc	5 mM
NP-40	0.02%
EDTA	1 mM
EGTA	1 mM
NaCl	0.5 M
Glycerol	10%

2.9.3 Analysis of Loading Reactions

The reactions were analysed by SDS PAGE and immunoblotting with specific antibodies or silver staining (Invitrogen, Silver Quest). Loading of ¼ of a sample on an SDS PAGE gel was sufficient for western blotting and similarly ½ a sample for silver staining. Silver staining provides the advantage of being able to visualize all the proteins at once to which there may not be antibodies available. Quantification may also be performed on silver-stained gels in a more linear manner compared to film.

2.10 Electromobility shift assays

Origin DNA probes were generated by PCR amplification. The 1 kb orign probe was amplified from p305bp using ARS305F and ARS305R. The 247 bp probe was amplified from pUC19-ARS305 using M13F and M13R. The PCR products were labelled using ^{32}P γ ATP and polynucleotide kinase (PNK). The following reaction was set up: 10 µl ^{32}P γ ATP (6000 Ci/mmol), 2 µl 10x PNK buffer, 1.32 µl PNK (10 U/µl), 581.16 fmol PCR product, distilled water to make up 20 µl. The reaction was placed on ice for 1 hour. Then 80 µl of Hepes-EDTA (10 mM Hepes-KOH pH 7.6, 1 mM EDTA) was added. The reaction was purified through a Sephadex G-25 column and DNA concentration was checked. A final concentration of 12 fmol/µl in Hepes-EDTA was then prepared.

EMSA reactions were set up as follows: 4 µl 5x binding buffer (See table 2), 1 µl ATP (100 mM), 2 µl DTT (10 mM), 160 fmol ORC, 80 fmol Cdc6, 320 fmol Mcm2-7/Cdt1 (or as otherwise indicated), 1 µl probe DNA (12 fmol/µl) and distilled water up to 20 µl. Reactions were incubated for 30 mins at 30°C with shaking at 800 rpm. To crosslink reactions, glutaraldehyde was added to a final concentration of 0.1%. Reactions were incubated for a further 5 mins at 24°C with shaking at 800 rpm. Crosslinking was arrested with 50 mM TRIS-HCl Ph 7.5, 15 mins at 24°C with shaking at 800 rpm. Native loading dye was added to samples (6x recipe: 30% v/v glycerol, 0.1% Xylene cyanol, 0.1% Bromophenol blue, in distilled water). Whole reactions were then loaded either onto a 0.8% agarose gel (pre-run at 4°C for 1 hour). Electrophoresis was either performed for 16 hours at 25 V or for 4.5 hours at

100 V. Gels were dried onto DE81 paper (Whatman) in a vacuum gel dryer. Dried gels were exposed for 16 hours in phosphorimager cassettes. Results were visualised using a Typhoon scanner.

2.11 Stoichiometry assays

To examine protein stoichiometry reactions were set up as for “Reconstitution of Mcm2-7 loading” reactions (section 2.9), using equimolar amounts of tagged proteins (refer to Tables 1 and 2). Reactions were incubated, washed, and DNA and bound proteins cleaved from the magnetic beads by UVA irradiation as described in section 2.9.

Reactions were treated with 1 µl of 2.5 U/µl Benzonase (Sigma) for 10 mins, 30°C, shaking at 1000 rpm. Samples were then incubated with 5 µl (slurry) M2 anti-FLAG magnetic beads (Sigma) pre-washed in low-salt wash buffer (Table 2). Reactions were incubated with the anti-FLAG beads for 2 hours at 4°C, shaking at 1000 rpm. Supernatants were removed and kept (S: see Figure 5.2). Anti-FLAG beads and bound proteins were washed 2x in low salt wash (LSW) buffer (Table 2) and resuspended in 20 µl LSW buffer. FLAG peptide (LRI, peptide synthesis facility) was then added to a final concentration of 0.5 mg/ml and beads and bound proteins were incubated for 30 mins at 4°C with shaking at 1000 rpm. Eluate (IP: see Figure 5.2) was removed and kept. 2x SDS PAGE loading buffer was added to both IP and S samples to a final concentration of 1x. 50% of samples were loaded onto 3-8% TRIS-Acetate polyacrylamide gels. Electrophoresis was carried out at 150V for 1.5 hours. Gels were transferred to nitrocellulose membranes and immunoblotting performed as described in section 2.4.2.

2.12 Crosslinking Assays

To analyse protein-protein interactions during pre-RC formation, reactions were set up as for “Reconstitution of Mcm2-7 loading” reactions (section 2.9), using equimolar amounts of pairwise combinations of tagged proteins (refer to Tables 1 and 2). Reactions were incubated, washed, and DNA and bound proteins cleaved

from the magnetic beads as described in section 2.9. The only difference was that for photocleavage DNA-beads were suspended in 15 µl LSW buffer and not 20 µl. This did not affect the efficiency of photocleavage.

Reactions were then treated with 1 µl of 2.5 U/µl Benzonase (Sigma) for 10 mins, 30°C, shaking at 1000 rpm. The crosslinking reagent BS3 (Pierce) was added to final concentrations of 0, µM 25 µM and 50 µM. Reactions were then incubated at 24°C, 30 mins with shaking 1000 rpm. TRIS-HCl pH 7.5 was added to a final concentration of 50 mM to quench the crosslinking and reactions were incubated for 15 mins at 24°C with shaking at 1000 rpm. Samples were then denatured by incubating for 5 mins at 95°C in denaturing buffer (1% SDS, 0.05 M TRIS-HCl pH 8.0, 1 mM DTT). Reactions were then diluted 10x in RIPA buffer containing no SDS (300 mM NaCl, 1% NP-40, 0.5% deoxycholate, 50 mM TRIS-HCl pH 8.0, 1 mM DTT). Samples were then incubated with with 5 µl (slurry) M2 anti-FLAG magnetic beads (Sigma) pre-washed in RIPA buffer containing 0.1% SDS. Reactions were incubated with the anti-FLAG beads for 2 hours at 4°C, shaking at 1000 rpm. Supernatants were removed. Beads and bound proteins were washed twice in LSW buffer (Table 2) then and resuspended in 20 µl LSW buffer. FLAG peptide (LRI, peptide synthesis facility) was then added to a final concentration of 0.5 mg/ml and beads and bound proteins were incubated for 30 mins at 4°C with shaking at 1000 rpm. Eluate (IP: see Figure 5.2) was removed and kept. 2x SDS PAGE loading buffer was added to both IP and S samples to a final concentration of 1x. 50% of samples were loaded onto 3-8% TRIS-Acetate polyacrylamide gels. Electrophoresis was carried out at 150 V for 1.5 hours. Gels were transferred to nitrocellulose membranes and immunoblotting performed as described in section 2.4.2.

2.13 Primers

Table 3 Primers

Primer	Sequence	Target
AM1	CTGGGATCCATGTCAGCTATACCA	*CDC6*
AM2	CTGCTCGAGCTAGTGAAGGAAAGGTTTC	*CDC6*
AM51	TATAATTCTAGAATGGAAGGCTCAACGGGA	*MCM3*
AM52	TATAATGTCGACTGATCAGACTCTCCAAACTTTATCG	*MCM3*
AM53	TATAATGTCGACTGAGCTTGCTGGTTGTCTGAC	*MCM3*
AM54	TATAATTCTAGAATGAACTCTGGATCCCCAATC	*MCM3*
AM71	GTACTGAGATCTATGTCCGGTTCTGCTGCTAGTGG	*9X MYC*
AM72	GTACTGAGATCTGTTCAAGTCTTCTTCTG	*9X MYC*
AM75	CAGTACCACCGGTGCTTCACCTTGGAAGTACAAG	*CBP-TEV*
AM81	GATCCATGGACGATTATAAAGATGACGATGACAAGG ATTATAAAGATGACGATGACAAGGATTATAAAGATGA CGATGACAAGG	*3X FLAG*
AM86	GATCCCTTGTCATCGTCATCTTTATAATCCTTGTCAT CGTCATCTTTATAATCCTTGTCATCGTCATCTTTATAA TCGTCCATG	*3X FLAG*
AM88	GGGAAAGAGAAAAGAAAAAAATTGATCTATCGATTT CAATTCAATTCAAT ATCGATGAATTCGAGCTCG	*NA*
AM89	ACACTTACGCTGAATTGGAAAAGTTGTTGAAGACTG TTTTGAACACTTTG CGTACGCTGCAGGTCGAC	*NA*
AM117	GTACTGCACCGGTGATGTCCGGTTCTGCTGCTAGT GG	*9x MYC*
AM119	CAGTACCACCGGTGCGCTAGTGGA	*9x MYC*
AM120	GTACTGGGCGCGCCATGTCCGGTTCTGCTGCTAGT GG	*9x MYC*

AM122	CAGTACGGCGCGCCCGCTAGTGGA	*9x MYC*
AM140	CCGGTGATGGACGATTATAAAGATGACGATGACAAG GATTATAAAGATGACGATGACAAGGATTATAAAGATG ACGATGACAAG G CA	*3x FLAG*
AM141	CCGGTGCCTTGTCATCGTCATCTTTATAATCCTTGT CATCGTCATCTTTATAATCCTTGTCATCGTCATCTTTA TAATCGTCCATCA	*3x FLAG*
AM142	CGCGCCATGGACGATTATAAAGATGACGATGACAAG GATTATAAAGATGACGATGACAAGGATTATAAAGATG ACGATGACAAGGG	*3x FLAG*
AM143	CGCGCCCCTTGTCATCGTCATCTTTATAATCCTTGT CATCGTCATCTTTATAATCCTTGTCATCGTCATCTTTA TAATCGTCCATGG	*3x FLAG*
GC090	GTACTGCCCGGGATGAAGAGAAGATGGAAGAAG	*CBP-TEV*
ARS305-F-PC-bio-Eco	GGTGTATGCATGCTACTGTTTGAATTCCCATTATCGA AGGCAC	*ARS305*
ARS305-F-bio-Eco	GGTGTATGCATGCTACTGTTTGAATTCCCATTATCGA AGGCAC	*ARS305*
ARS305-F	CCATTATCGAAGGCAC	ARS305
ARS305-R	CTCTAGCAAAAAGTCTAC	*ARS305*
M13 F	GTAAAACGACGGCCAGT	*NA*
M13-F-bio	GTAAAACGACGGCCAGT	*NA*
M13 R	CAGGAAACAGCTATGAC	*NA*

2.14 Plasmids

Table 4 Plasmids

Plasmid	Cloning Vector	Insert	Reference
pAM3	pGEX-6p-1	*CDC6*	This study & Frigola et al., 2013
pAM4	pGEX-6p-1	*E224G CDC6*	This study
pAM5	pMal-C2P	*MCM3*	This study & Frigola et al., 2013
pAM6	pMal-C2P	*C-terminal MCM3*	This study & Frigola et al., 2013
pAM7	pMal-C2P	*N-terminal MCM3*	This study & Frigola et al., 2013
pAM8	pJF17	*9Myc (5′ ORC3)*	This study
pAM9	pJF17	*9Myc (5′ ORC4)*	This study
pAM10	pJF18	*9Myc (5′ ORC5)*	This study
pAM11	pJF18	*9Myc (5′ ORC6)*	This study
pAM14	pJF17	*3FLAG (5′ ORC3)*	This study
pAM15	pJF17	*3FLAG (5′ ORC4)*	This study
pAM16	pJF18	*3FLAG (5′ ORC5)*	This study
pAM17	pJF18	*3FLAG (5′ ORC6)*	This study
pAM18	pJF19	*3FLAG (5′ ORC1)*	This study
pAM21	pJF5	*CBP-TEV (5′ Mcm3)*	This study
pAM22	pJF2	*9Myc (5′ Cdt1)*	This study
pAM27	pAM21	*9Myc (5′ Mcm3)*	This study
pAM28	pJF2	*3FLAG (5′ Cdt1)*	This study
pAM36	pAM3	*9Myc (5′ Cdc6)*	This study

pAM37	pAM3	*3FLAG (5' Cdc6)*	This study & Frigola et al., 2013
pAM38	pJF5	*CBP-TEV- single SgrA1 site (5' Mcm3)*	This study
pJF17	pRS303	*ORC3-GAL1-10-ORC4*	Frigola et al., 2013
pJF18	pRS304	*ORC5-GAL1-10-ORC6*	Frigola et al., 2014
pJF19	pRS306	*CBP-TEV-ORC1-GAL1-10-ORC2*	Frigola et al., 2015
pET15b-*CDC6*	pET15b	*CDC6*	G. Perkins (unpublished)
pET15b-E224G-*CDC6*	pET15b	*CDC6*	G. Perkins (unpublished)
p305BP	pBR322	*ARS305*	Huang & Kowalski, 1996
pJF5	pRS306	*MCM2-GAL1-10-MCM3*	Frigola et al., 2013
pJF2	pRS303	*GAL4-GAL1-10-CDT1*	Frigola et al., 2013
pYM21	pYM6	*9x MYC*	Janke et al., 2004
pBP83	pYM21	*3x FLAG*	Boris Pfander and Frigola et al., 2013
pAM36	pAM3	*9x MYC*	This study
pAM37	pAM3	3x FLAG	This study

2.15 Yeast strains

Table 5 Yeast strains

Strain	*Genotype*	Reference
ySD-ORC	*W303-1a pep4::KanMx4 bar1:: Hph-NT1 his3-11::HIS3pJF17 trp1-1::TRP1pJF18 ura3-1::URA3pJF19*	Frigola et al., 2013
W3031a	*MATa ade2-1 ura3-1 his3-11 trp1-1 leu2-3 can1-100*	Rothstein, 1983
yJF38	*W303-1a pep4::KanMx4 bar1::Hph-NT1 his3-11::HIS3pJF2 trp1-1::TRP1pJF3 leu2-3::LEU2pJF4 ura3-1::URA3pJF6*	Frigola et al., 2013
yDR11	*YSC15 GAL1-10-ORC1::GAL1-10-ORC1-TAPTCP(URA3)*	Remus et al., 2009
yDR17	*W303-1a pep4::LEU2 bar1::TRP1 mcm4::MCM4-3xFLAG(kanMX)*	Remus et al., 2010
yJF1	*W303-1a pep4::KanMx4 bar1::Hph-NT1*	Jordi Frigola
yJF21	*W303-1a pep4::KanMx4 bar1::Hph-NT1 his3-11::HIS3pJF2 trp1-1::TRP1pJF3 leu2-3::LEU2pJF4*	Jordi Frigola
yAM1	*W303-1a bar1::Hyg pep4::KanMX ura::URApJF19*	This study
yAM2	*W303-1a bar1::Hyg pep4::KanMX trp1::TRP1pJF18*	This study
yAM3	*W303-1a bar1::Hph-NT1 pep4::KanMX4 his3::HIS3pJF17*	This study
yAM4	*W303-1a bar1::Hph-NT1 pep4::KanMX4 trp1::TRP1pJF18 his3::HIS3pJF17*	This study
yAM5	*W303-1a bar1::Hph-NT1 pep4::KanMX4 ura3::URA3pJF19 his3::HIS3pJF17*	This study
yAM6	*W303-1a bar1::Hph-NT1 pep4::KanMX4 ura3::URA3pJF19 trp1::TRP1pJF18*	This study
yAM8	*W303-1a bar1::Hph-NT1 pep4::KanMX4 trp1::TRP1pJF18 ura3::URA3pAM18 his3::HIS3pJF17*	This study
yAM11	*W303-1a bar1::Hph-NT1 pep4::KanMX4 trp1::TRP1pJF18 ura3::URA3pJF19 his3::HIS3pAM8*	This study
yAM12	*W303-1a bar1::Hph-NT1 pep4::KanMX4 trp1::TRP1pJF18 ura3::URA3pJF19 his3::HIS3pAM14*	This study
yAM13	*W303-1a bar1::Hph-NT1 pep4::KanMX4 trp1::TRP1pJF18 ura3::URA3pJF19 his3::HIS3pAM9*	This study

yAM14	*W303-1a bar1::Hph-NT1 pep4::KanMX4 trp1::TRP1pJF18 ura3::URA3pJF19 his3::HIS3pAM15*	This study
yAM15	*W303-1a bar1::Hph-NT1 pep4::KanMX4 trp1::TRP1pAM10 ura3::URA3pJF19 his3::HIS3pJF17*	This study
yAM16	*W303-1a bar1::Hph-NT1 pep4::KanMX4 trp1::TRP1pAM16 ura3::URA3pJF19 his3::HIS3pJF17*	This study
yAM17	*W303-1a bar1::Hph-NT1 pep4::KanMX4 trp1::TRP1pAM11 ura3::URA3pJF19 his3::HIS3pJF17*	This study
yAM18	*W303-1a bar1::Hph-NT1 pep4::KanMX4 trp1::TRP1pAM17 ura3::URA3pJF19 his3::HIS3pJF17*	This study
yAM22	*W303-1a pep4::KanMx4 bar1::Hph-NT1 trp1-1::TRP1pJF3 leu2-3::LEU2pJF4 ura3-1::URA3pAM21*	This study
yAM25	*W303-1a pep4::KanMx4 bar1::Hph-NT1 his3-11::HIS3pJF2 trp1-1::TRP1pJF3 leu2-3::LEU2pJF4 ura3-1::URA3pAM27*	This study
yAM33	*W303-1a pep4::KanMx4 bar1::Hph-NT1 his3-11::HIS3pJF2 trp1-1::TRP1pJF3 leu2-3::LEU2pJF4 ura3-1::URA3pAM21*	This study
yAM34	*W303-1a pep4::KanMx4 bar1::Hph-NT1 trp1-1::TRP1pJF3 leu2-3::LEU2pJF4 ura3-1::URA3pAM21 his3-11::HIS3pAM22*	This study
yAM35	*W303-1a pep4::KanMx4 bar1::Hph-NT1 trp1-1::TRP1pJF3 leu2-3::LEU2pJF4 ura3-1::URA3pAM21 his3-11::HIS3pAM28*	This study
yAM37	*W303-1alpha pep4::KanMx4 bar1::Hph-NT1 ura3-1::URA3pAM21*	This study
yAM43	*W303-1a pep4::KanMx4 bar1:: Hph-NT1 his3-11::HIS3pJF17 trp1-1::TRP1pJF18 ura3-1::URA3pJF19::ORC2-9xMYC*	This study
yAM44	*W303-1a pep4::KanMx4 bar1:: Hph-NT1 his3-11::HIS3pJF17 trp1-1::TRP1pJF18 ura3-1::URA3pJF19::ORC2-3xFLAG*	This study

2.16 Antibodies

Table 6 Antibodies

Primary Antibody	Dilution	Secondary antibody	Dilution
Anti-Mcm2 (Santa Cruz Biotechnology yN-19, sc-6680)	1:2000	Anti-goat-HRP (Stratech Scientific)	1:2000
Anti-Mcm5 (Santa Cruz Biotechnology yC-19, sc-6687)	1:2000	Anti-goat-HRP (Stratech Scientific)	1:2000
Anti-Mcm7 (Santa Cruz Biotechnology yN-19, sc-6688)	1:2000	Anti-goat-HRP (Stratech Scientific)	1:2000
Anti-Orc6 (CRUK, SB49)	1:2000	Anti-mouse-HRP (Dako)	1:5000
Anti-Cdc6 (CRUK, 98H/5)	1:2000	Anti-mouse-HRP (Dako)	1:5000
Anti-FLAG M2-HRP (Sigma)	1:20000	N/A	N/A
Anti-MBP (maltose binding protein)–HRP (NEB)	1:2000	N/A	N/A
Anti-Myc (CRUK, 9E10)	1:2000	Anti-mouse-HRP (Dako)	1:5000

Chapter 3. Using electrophoretic mobility shift assays to characterise intermediates in pre-RC formation

3.1 Introduction

The replicative helicase Mcm2-7 is loaded at origins into inactive pre-replicative complexes (pre-RCs) by the combined actions of three proteins: ORC, Cdc6 and Cdt1. *In vitro* reconstitution of pre-RC assembly has shown that Mcm2-7 is loaded as a symmetrical head-to-head double hexamer around double stranded DNA (Remus et al., 2009, Evrin et al., 2009).

ATP binding and hydrolysis are essential for pre-RC formation (see Chapter 1, section 1.2.2.3 for details). At least 12 of the 14 proteins that participate in pre-RC assembly are members of the AAA^+ (ATPases Associated with diverse cellular Activities) family of proteins (Iyer et al., 2004). Analysis of mutations in conserved ATP binding motifs of ORC, Cdc6 and Mcm2-7 has demonstrated that these elements are essential *in vivo* (Weinreich et al., 1999, Klemm and Bell, 2001, Schwacha and Bell, 2001, Perkins and Diffley, 1998). In budding yeast, ATP binding by ORC is essential for its binding to origin DNA (Bell and Stillman, 1992) and Mcm2-7 loading requires ATP hydrolysis by ORC and Cdc6 (Bowers et al., 2004, Klemm and Bell, 2001, Randell et al., 2006, Perkins and Diffley, 1998, Seki and Diffley, 2000).

ATP binding and hydrolysis thus play a major role in eukaryotic helicase (Mcm2-7) loading. Although there have been many advances in our knowledge of pre-RC formation, the specific functions of each of the pre-RC AAA^+ proteins in Mcm2-7 loading are still not very well understood. One question that arises from this is: what are the precise roles of ATP binding and hydrolysis in Mcm2-7 loading?

In a further layer of complexity, budding yeast ORC binds to a consensus site at origins of replication (ACS: see Chapter 1, section 1.2.1.1) and reconstitution studies indicate that ORC and Cdc6 load the Mcm2-7 double hexamer in a

concerted manner from two single Mcm2-7/Cdt1 heptamers (Evrin et al., 2009, Remus et al., 2009). This leads to several intriguing questions: is a symmetrical double hexamer of Mcm2-7 loaded by one ORC molecule located asymmetrically on one side of the origin? If so, how? How do ORC and Cdc6 catalyse this reaction? What role does ATP play in this process? To address these questions, we aimed to characterise possible intermediate stages in pre-RC formation, since this could provide a step-by-step view of Mcm2-7 loading.

Mcm2-7 loading, both *in vivo* and *in vitro,* has been defined as the generation of Mcm2-7 complexes that remain bound to DNA even after treatment with high salt (Donovan et al., 1997, Bowers et al., 2004, Remus et al., 2009, Evrin et al., 2009). *In vitro* reconstitution of Mcm2-7 loading using purified proteins and linear, origin-containing DNA coupled to paramagnetic beads (DNA-beads) has previously been described (Remus et al., 2009, Evrin et al., 2009). In the presence of ATP, ORC and Cdc6 load Mcm2-7/Cdt1 into a high-salt wash resistant double hexamer with concurrent release of Cdc6 and Cdt1 (Remus et al., 2009, Evrin et al., 2009). However, when ATP hydrolysis is prevented by incubation with ATPγS (a slowly hydrolysed ATP analogue), all the pre-RC components are recruited to DNA-beads after a low salt wash but are removed by high-salt extraction (Remus et al., 2009, Evrin et al., 2009). Thus, in the presence of ATPγS, ORC, Cdc6, Cdt1 and Mcm2-7 are all present on DNA-beads under low-salt wash conditions. Figure 3.1 summarizes the complexes that can be determined using this system.

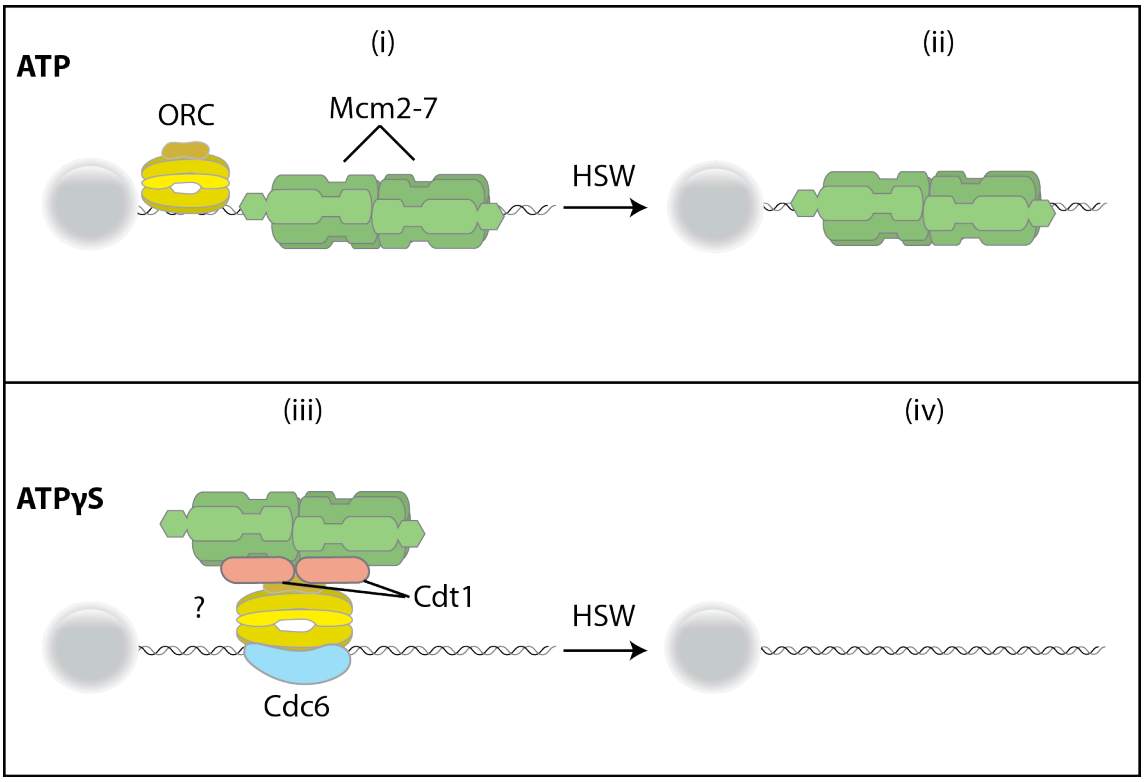

Figure 3.1 Pre-RC assembly and intermediates *in vitro*

(i) In the presence of ATP, ORC and Mcm2-7 are stably bound to DNA. (ii) A high salt wash (HSW) of DNA beads (grey ellipse) removes ORC, but the Mcm2-7 complex remains bound. (iii) In the presence of ATPγS, all pre-RC components are recruited to the DNA. A possible arrangement (?) of the proteins in shown. (iv) High salt extraction removes all proteins from the DNA-beads in ATPγS.

I hypothesised that characterising the "ATPγS complex" (Figure 3.1 (iii)) would provide insight into the role of ATP binding in the Mcm2-7 loading reaction. Such a complex may represent an intermediate stage, when ATP is bound but not yet hydrolysed. We reasoned that it would be informative to examine this ATPγS intermediate. Towards this aim, proteins of the pre-RC were purified for use in biochemical assays. Where possible proteins were expressed and purified from budding yeast cells arrested in G1 phase. During G1 phase, the levels of Cdk activity are low which is important as high Cdk levels prevent assembly of pre-RCs from S phase until the end of mitosis (Dahmann et al., 1995, Detweiler and Li, 1998, Piatti et al., 1996). G1 phase is therefore a period of competence for pre-RC formation and this has also been demonstrated *in vitro* (Seki and Diffley, 2000).

I employed these purified proteins in electrophoretic mobility shift assays (EMSAs) to examine pre-RC reactions assembled in ATP and in ATPγS. An electrophoretic mobility shift assay (EMSA) or band shift assay is a common *in vitro* electrophoresis technique used to examine protein-DNA interactions. This assay can determine whether a protein or mixture of proteins binds the nucleic acid sequence in question and can often reveal whether a single protein or complex is involved in the binding. The EMSA technique is based on the observation that protein:DNA complexes migrate slower than free linear DNA when subjected to native (non-denaturing) polyacrylamide or agarose gel electrophoresis (Garner and Revzin, 1981). The speed at which different molecules move through a porous gel matrix subjected to an electric field is determined by their size and charge. Binding of a protein to DNA creates a larger structure that is less mobile and therefore migrates more slowly compared to unbound DNA. For visualisation purposes, the DNA can be radiolabelled with P^{32} by 5' end labelling.

The gel matrix and low ionic strength of the electrophoresis running buffer help to stabilise interaction complexes and sometimes even labile complexes can be resolved (Fried and Crothers, 1981). This is important since intermediates formed during pre-RC assembly could be unstable. EMSA was previously used successfully to show that Cdc6 binds to ORC in an ATP dependent manner and alters the pattern of origin binding (Speck et al., 2005). However, a full pre-RC containing the Mcm2-7 complex had never been examined by EMSA. For these reasons I considered the EMSA to be an appropriate technique for examining pre-RC reactions and possible intermediates.

In this chapter I will describe how purified proteins for EMSA were prepared and tested and I will present results obtained from EMSA analysis of pre-RC reactions assembled in the presence of ATP and ATPγS.

3.2 Preparation of proteins and DNA for electrophoretic mobility shift assays

In order to analyse pre-RC formation by EMSA, the following steps were required:

1. Purification of pre-RC proteins
2. Preparation of radiolabelled target DNA
3. Assembly of proteins on target DNA in the presence of ATP or ATPγS
4. Electrophoresis of reactions on agarose or native polyacrylamide gels
5. Visualisation of band migration patterns by exposure to film or a phosphorimager screen.

Here I will describe how proteins and target DNA were prepared.

3.2.1 Protein purification for EMSA analysis

I purified proteins of the pre-RC for use in electrophoretic mobility shift assays (EMSAs). ORC and Mcm2-7/Cdt1 were purified from yeast cells arrested in G1 phase with the mating pheromone α-factor. Proteins were purified as described in Remus et al., 2009, with minor modifications in salt type and concentration. The purification is described below (also see Chapter 2).

ORC was purified from a yeast strain overexpressing all six subunits (Orc1-6) as additional copies from the inducible *GAL1-10* promoter. A tandem affinity purification (TAP) of ORC was carried out using a TAP-TCP tag fused to the C-terminus of Orc1 (see materials and methods). The TAP-TCP tag differs in its arrangement compared to a TAP tag (Puig et al., 2001). In the TAP-TCP tag a TEV protease site is located proximal to the protein followed sequentially by calmodulin binding peptide (CBP) and protein A (Remus et al., 2009). Using this tag, calmodulin affinity chromatography was carried out, followed by a TEV protease digest to remove the entire TAP-TCP tag and finally residual tagged protein was removed by passage over IgG sepharose. This was followed by Superdex 200 gel-filtration and MonoQ ion exchange chromatography to remove a complex containing a truncated version of Orc1. This resulted in a stoichiometric ORC complex of six subunits (Figure 3.2A).

Endogenous Mcm2-7/Cdt1, in which the C-terminus of the Mcm4 subunit was fused to a 3x FLAG epitope, was purified from G1 phase yeast extracts by anti-FLAG immunoaffinity chromatography followed by Superdex 200 gel-filtration chromatography (Figure 3.2B). This resulted in a stoichiometric complex of Mcm2-7 that co-purified with Cdt1 and eluted from the Superdex 200 column in the same fraction as thyroglobulin (670 kDa) (Figure 3.2A), consistent with the predicted molecular weight of Mcm2-7/Cdt1 (676 kDa).

Since Cdc6 is rapidly degraded during G1 phase in budding yeast (Drury et al., 2000), it was expressed in insect cells from a baculovirus vector. Cdc6, containing a 6x His tag at its N-terminus, was purified by Ni-NTA chromatography followed by Superdex 200 gel-filtration chromatography (Figure 3.2 C). Purified Cdc6 migrates in SDS PAGE as a doublet as it is phosphorylated in insect cells (Remus et al., 2009). Importantly, both phosphorylated Cdc6 and Cdc6 lacking all eight CDK phosphorylation sites (non phosphorylated in insect cells) function equally well in loading the Mcm2-7 complex *in vitro* (Remus et al., 2009).

Since these purified proteins were to be used to examine pre-RC formation by EMSA, it was important to ascertain that the proteins were functional. In order to test the activity of the purified proteins, I examined their ability to assemble pre-RCs *in vitro* (Figure 3.2D) as described in Remus et al., 2009, as a readout of functionality. Purified ORC, Cdc6 and Mcm2-7/Cdt1 were added to ARS305-containing DNA coupled to paramagnetic beads by a biotin-streptavidin linkage (DNA-beads). Proteins bound to the DNA-beads were detected by boiling the DNA-beads in SDS sample buffer followed by SDS PAGE and immunoblotting (Figure 3.2D; see Figure 1.5 for a schematic of *in vitro* pre-RC reconstitution). Antibodies against Orc6, Mcm2, Mcm5 and Mcm7 were used in this case and acted as readout for ORC and Mcm2-7 binding to DNA-beads. Mcm2 and Mcm5 are located on the opposite side of the MCM ring to Mcm7 (see Figure 1.3); this allowed us to monitor binding of both halves of Mcm2-7 to the DNA-beads.

In reactions containing ATP, DNA-beads bound Orc6, Mcm2, 7 and Mcm5 (Figure 3.2D, lane 1). A high salt wash (HSW; 0.5 M NaCl) of this reaction removed Orc6 but a substantial fraction of the MCM subunits remained bound (Figure 3.2D, lane

2). In the presence of ATPγS, the DNA-beads bound Orc6, Mcm2, 7 and Mcm5 after a low salt wash (Figure 3.2D, lane 3), however these proteins were removed by high salt extraction (Figure 3.2D, lane 4). Therefore, the Mcm2-7 complex was stably loaded in a high salt resistant manner in ATP and recruited in a salt labile manner in ATPγS. These data confirmed that the purified proteins were competent for pre-RC assembly *in vitro*.

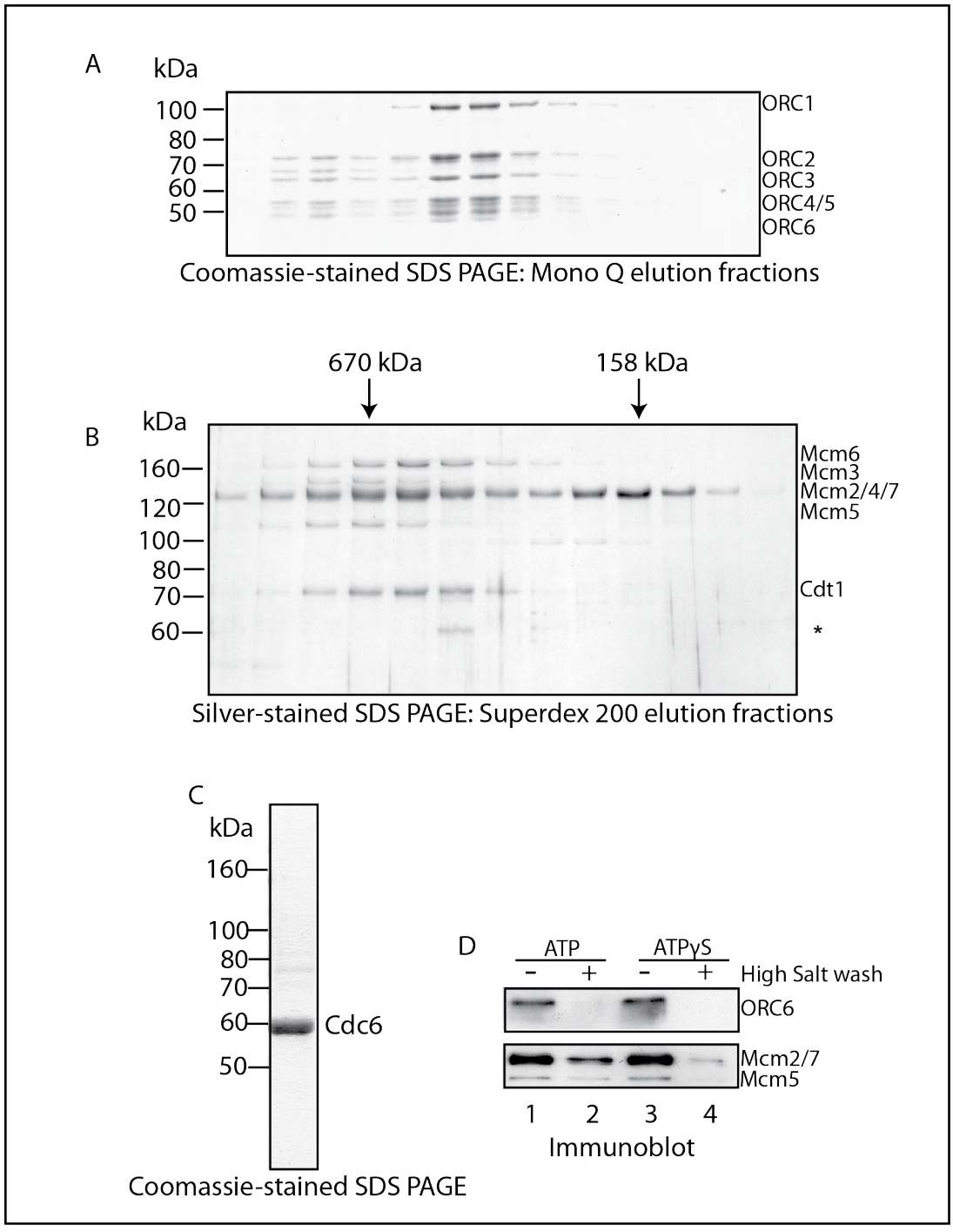

Figure 3.2 Preparation of proteins for EMSA analysis of pre-RC formation

(A) Purified ORC (MonoQ) analysed by SDS PAGE and Coomasie staining. ORC was purified G1 arrested yeast cells. Orc1 is TAP-tagged in this strain. * represents a contaminant. (B) Purified Mcm2-7/Cdt1 (gel filtration) analysed by SDS PAGE and silver staining. Mcm2-7/Cdt1 was purified from G1 arrested yeast cells where Mcm4 is FLAG-tagged at its C-terminus. (C) Purified His-Cdc6 from baculovirus in insect cells, analysed by SDS PAGE and Coomassie staining. (D) *In vitro* reconstitution of pre-RC assembly to test purified proteins; visualised by immunoblotting. Purified ORC and Cdc6 can load Mcm2-7 in a salt resistant manner in ATP only.

3.2.2 Preparation of DNA for EMSA analysis

To examine pre-RC formation by EMSA analysis, we required target DNA containing an origin of replication. In *S.cerevisiae,* origins of replication are known as ARSs (autonomously replicating sequences). The target DNA (probe) I generated consists of 247 bp of DNA derived from ARS305 and contains the A element (11 bp sequence known as the ACS) and B elements but not the surrounding sequences. The 247 bp probe was designed based on sequences that had been used successfully for EMSA and footprinting experiments with ORC and Cdc6 on origin DNA (Speck et al., 2005, Santocanale and Diffley, 1996).

In order to visualise DNA migration patterns following electrophoresis (step 5 above), I radiolabeled the 247 bp origin DNA probe at the 5' end using [γ-^{32}P]ATP and T4 polynucleotide kinase (see materials and methods).

3.3 EMSA analysis using ORC and Cdc6

To begin to characterise pre-RC assembly by EMSA, I examined the binding of ORC to DNA and the effect of Cdc6 on this binding. Purified ORC either with or without Cdc6 was incubated with the 247 bp probe in the presence of ATP. Reactions were performed with varying amounts of poly dI-dC (non-specific DNA). The addition of non-specific DNA acts as a competitor, reducing non-specific interactions between labelled probe and the proteins in question. Binding reactions containing end-labelled probe DNA were subjected to electrophoresis on a 3.5% native polyacrylamide gel. Following electrophoresis, the gel was dried, exposed to a Phosphorimager screen and scanned to document the results.

In Figure 3.3, lanes 1-8 show ORC binding to probe DNA, whilst lanes 9-16 show the effect of the addition of Cdc6 on this binding. Addition of ORC alone to the DNA probe, in the absence of competitor DNA, resulted in a slower migrating band compared to probe alone (Figure 3.3A, compare lanes 1 and 8). As competitor DNA was added, the ORC-DNA complex appeared to migrate faster through the gel (Figure 3.3A, lanes 2-7). Probably, ORC was titrated away from the origin DNA and bound unlabelled competitor DNA. The slower migrating DNA-ORC band

observed in the absence of competitor DNA, could represent multiple ORC molecules binding. Whilst, the faster migrating bands (lanes 2-7) could be fewer ORC molecules binding to the probe DNA.

Incubation of Cdc6 alone with probe DNA did not result in the formation of a novel band. However, a band was observed in the well indicating a probable aggregation of Cdc6 on the DNA (Figure 3.3A, lane 16). Addition of Cdc6 to the ORC-DNA complex induced formation of a slower migrating band, under conditions of low competitor DNA (Figure 3.3A, compare lanes 6 and 14, bands indicated by red stars). As the amount of competitor DNA was increased, this slower migrating band was no longer observed. Instead a faster migrating band at the level of ORC alone was detected (Figure 3.3A, lanes 9-12). Noticeably, these bands in lanes 9-12 were more intense than the bands observed in the presence of ORC alone (lanes 2-5). It appears that in these reactions, ORC binding to DNA was slightly stabilised and Cdc6 binding to ORC-DNA was inhibited.

I was unable to explain why the addition of Cdc6 to ORC-DNA did not give rise to a double band in all reactions as had been previously described in Speck et al., 2005. In addition, it was unclear why the addition of competitor DNA inhibited Cdc6 binding to ORC-DNA. Interestingly, a study in *Xenopus* egg extracts demonstrated that there is a minimum length of DNA required for Mcm2-7 binding (Edwards et al., 2002). Mcm2-7 binding was found to increase with the increase in DNA length whilst ORC binding was unaffected (Edwards et al., 2002). Cdc6 binding to different lengths of DNA was not, however examined by the authors (Edwards et al., 2002).

For these reasons, I asked whether 247 bp ARS 305 was capable of supporting Mcm2-7 loading *in vitro*. The reconstitution of Pre-RC assembly *in vitro* is usually performed using 1 kb origin-containing DNA.

To determine whether 247 bp DNA could support Mcm2-7 loading, I coupled this sequence to streptavidin-coated paramagnetic beads via a biotin linkage. Purified proteins were incubated with 247 bp DNA-beads or 1 kb DNA-beads in the presence of ATP or ATPγS. The DNA-beads were then subjected to washes (see

Figure 1.5) and binding of pre-RC proteins to the DNA-beads was assessed by immunoblotting. Figure 3.3B shows that, after incubation with purified proteins, in reactions containing ATP or ATPγS, both 1 kb and 247 bp DNA-beads bind Orc6 (Top panel; lanes 1, 3, 5 & 7). In this case, the detection of Orc6 acts as a surrogate for ORC binding and this result is consistent with data from Edwards et al., 2002 showing that ORC binding is unaffected by DNA length.

In the presence of ATP; Mcm2, Mcm5 and Mcm7 bound DNA beads containing 1 kb ARS305 but very little bound 247 bp ARS305 (Figure 3.3B, lanes 1 & 5). Any Mcm2, Mcm5 and Mcm7 that was bound to the 247 bp DNA-beads was removed by a high salt extraction whereas a substantial proportion remained bound to the 1 kb DNA-beads (compare lanes 2 & 6). Here, the detection of Mcm2, Mcm5 and Mcm7 was used as a surrogate for the Mcm2-7 complex.

In the presence of ATPγS; Mcm2, 5 and 7 all bound 1 kb DNA-beads and were removed by a high salt wash as expected (lanes 7 & 8). However, only Mcm2 and Mcm7 could be detected on 247 bp DNA-beads in in ATPγS, and this binding was less than that of 1 kb DNA-beads. Interestingly, Mcm2 and 7 appeared to bind 247 bp DNA better in ATPγS compared to ATP (Figure 3.3B bottom panel, compare lanes 1 & 3). This indicates that perhaps ATP hydrolysis somehow causes release of the MCM subunits from 247 bp DNA. In conclusion, 247 bp DNA-beads were not capable of supporting Mcm2-7 loading *in vitro*.

In light of this, I proceeded with EMSA analyses using a 1 kb probe.

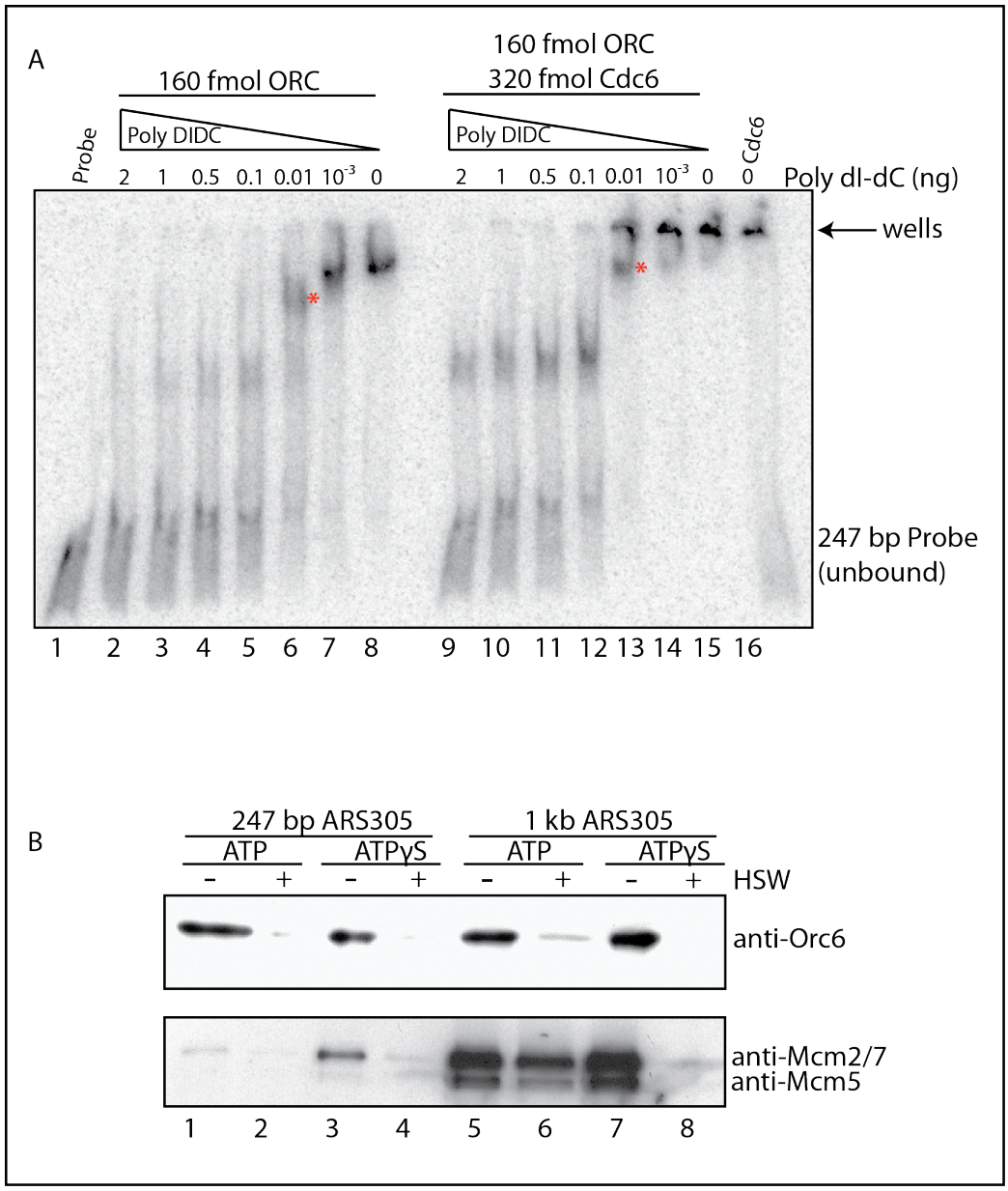

Figure 3.3 EMSA analysis of ORC and Cdc6 binding - 247 bp DNA does not support Mcm2-7 loading *in vitro*

(A) EMSA analysis of ORC and Cdc6 binding to 247 bp ARS 305. Radiolablled 247 bp ARS305 (P^{32} end labelled) was incubated with ORC, Cdc6 and titrations of polyDIDC at 30°C for 30 mins. The whole reaction was then loaded onto a 3.5% native polyacrylamide gel. 100 V for 3 hours. Red stars show the same reaction without (lane 6) or with (lane 13) the addition of Cdc6 for comparison.

(B**)** Reconstitution of Pre-RC assembly *in vitro* using 247 bp ARS305 vs 1 kb ARS305. ORC, Cdc6 and Mcm2-7 were incubated with either 247 bp or 1 kb ARS305 coupled to paramagnetic beads in the presence of ATP or ATPγS. The DNA-beads were then washed in low/high salt (HSW: high salt wash) and bound proteins analysed by SDS PAGE and immunoblotting against the proteins indicated.

3.4 EMSA analysis using 1 kb ARS305

Since the 247 bp ARS305 fragment did not support Mcm2-7 loading, EMSAs were subsequently performed using a 1 kb fragment of ARS305 (contains the A element, B elements and surrounding sequences) radiolabelled at its 5' end with P^{32}. To begin to characterise the pre-RC by EMSA on 1kb ARS305, I first examined binding of ORC to this 1 kb probe and the effect of Cdc6 on ORC-DNA complexes.

ORC either with or without different amounts of Cdc6 was incubated with the 1 kb ARS 305 probe in the presence of ATP. In these reactions I used a low amount of competitor DNA (0.01 ng poly dIdC) that was found to be permissible for ORC-Cdc6-DNA complex formation in Figure 3.3. A crosslinking reagent, glutaraldehyde was then added to a subset of reactions. Glutaraldehyde is a homobifunctional amine-reactive crosslinker, meaning that both of its ends react with primary amines. This forms a covalent bond between two proteins. Glutaraldehyde has previously been used successfully in EMSAs to study T-antigen binding to the SV40 origin of DNA replication (Dean et al., 1987). In our case, glutaraldehyde was used to stabilise nucleoprotein complexes in the reactions. Following crosslinking, reactions were subjected to electrophoresis on a 0.8% agarose gel (due to the larger size of the probe). Following electrophoresis, the gel was dried, exposed to a Phosphorimager screen and scanned to visualise the results.

Figure 3.4 shows the effect of addition of different amounts of Cdc6 to ORC-DNA complexes either in the absence or presence of glutaraldehyde crosslinking (lanes 2-6 and 9-13 respectively). Addition of ORC alone to the 1 kb origin DNA probe, resulted in a slower migrating band compared to the unbound linear DNA probe (Figure 3.4, lanes 7 & 14). In contrast, addition of Cdc6 alone to the DNA probe did not result in a novel band compared to unbound probe (Figure 3.4, lanes 8 & 15). Interestingly, addition of glutaraldehyde gave rise to a slower migrating band in ORC-DNA reactions (Figure 3.4, compare lanes 7 and 14). This indicates that in the absence of glutaraldehyde crosslinking, ORC was probably dissociating from the origin DNA during the gel electrophoresis.

As Cdc6 was added to ORC-DNA, a slower migrating smear was formed in lanes 2-7, indicating the formation of a ternary complex of ORC-Cdc6-DNA. However the smearing suggests that this complex was dissociating during electrophoresis. In reactions where glutaraldehyde crosslinking had been performed, the addition of Cdc6 resulted in bands in the wells of the gel (lanes 9-14). Possibly, crosslinking produced a structure that was large and did not enter the gel.

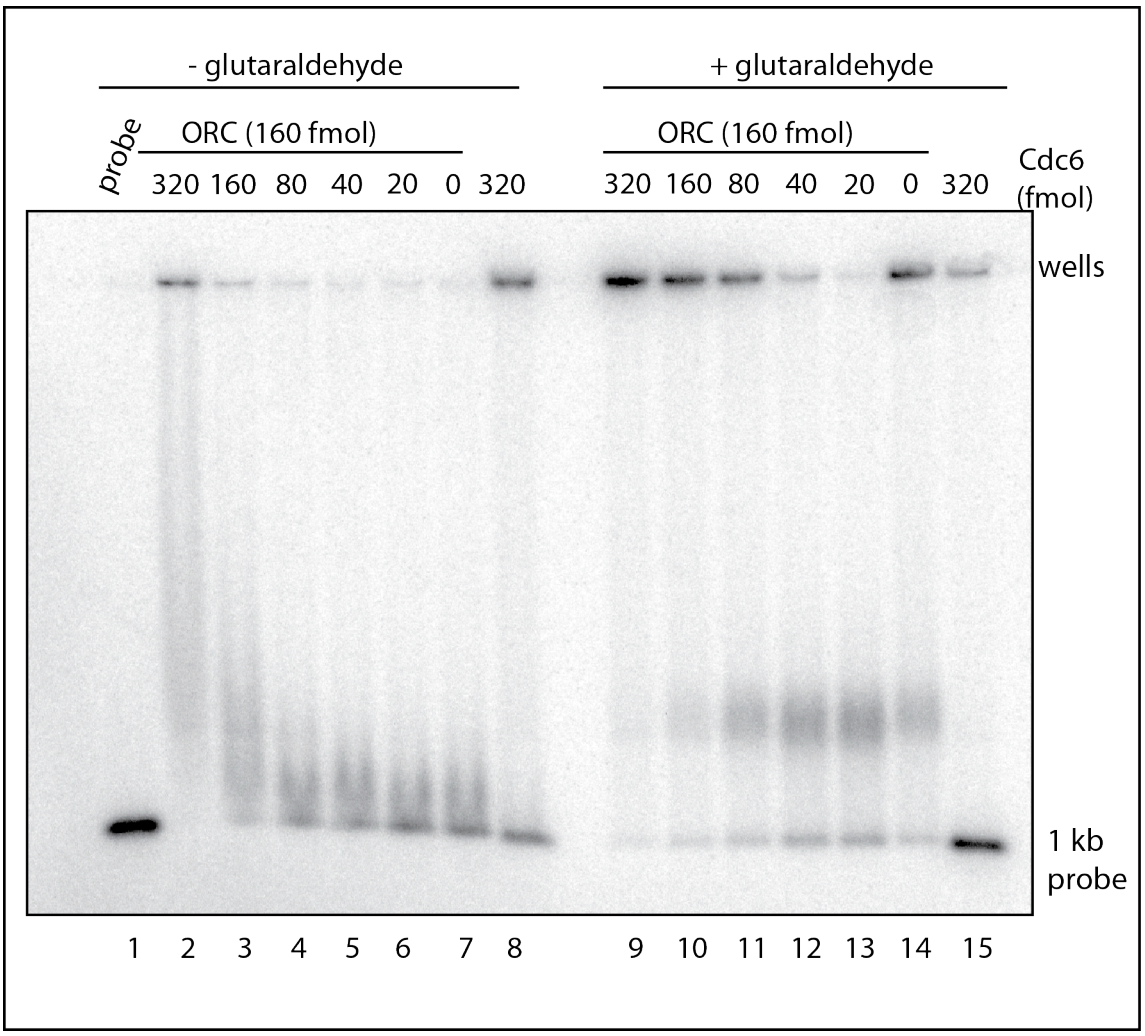

Figure 3.4 EMSA analysis of ORC and Cdc6 on 1 kb origin DNA

ORC and Cdc6 form complexes on origin DNA.
Purified ORC and Cdc6 were incubated with a 1 kb origin DNA probe in the presence of ATP for 30 mins at 30°C. Glutaraldehyde was then added to a final concentration of 0.1% for 5 mins. The reactions were quenched with TRIS-HCl pH 7.5 and loaded on a 0.8% agarose gel and run for 16 hours at 25 V.

In order to visualise stable nucleoprotein complexes, I optimised the electrophoretic conditions of the EMSAs to minimise crosslinked species in the wells. Electrophoresis times were reduced to minimise complex dissociation.

Upon establishing appropriate EMSA electrophoresis conditions, I proceeded to examine pre-RC formation in ATP and ATPγS. As discussed before, we reasoned that the "ATPγS reaction" could represent an intermediate in pre-RC formation where ATP is bound but not yet hydrolysed and could provide valuable information about Mcm2-7 loading. This EMSA was performed to visualise the DNA in ATPγS reactions and how its migration pattern was altered compared to reactions set up in ATP. In addition, a full pre-RC had never been examined in this manner.

Reactions containing ORC, Cdc6 and Mcm2-7/Cdt1 were assembled on the 1 kb origin probe in the presence of ATP or ATPγS. Glutaraldehyde was added to a subset of reactions to crosslink any intermediates formed and a low amount of competitor DNA (0.01 ng poly dIdC, as previously) was present in all samples. Following crosslinking, reactions were subjected to electrophoresis on a 0.8% agarose gel. The gel was then dried, exposed to a Phosphorimager screen and scanned to visualise the results.

Figure 3.5 shows the results of this EMSA analysis and is divided into four panels. The first two panels show results of reactions assembled in ATP in the absence or presence of glutaraldehyde crosslinking (lanes 2-8 and 9-15 respectively). The next two panels show results obtained from reactions assembled in ATPγS in the absence or presence of glutaraldehyde crosslinking (lanes 16-22 and 23-29 respectively). Lane 1 shows unbound 1kb origin DNA-probe.

ORC alone formed distinct complexes with 1 kb ARS 305, both in ATP and in ATPγS (Figure 3.5, lanes 2, 9, 16 & 23). Addition of glutaraldehyde to ORC-DNA produced a slower migrating smear in reactions containing ATP or ATPγS (lanes 9 & 23).

There were no detectable novel bands with Cdc6 and/or Mcm2-7/Cdt1 alone (Figure 3.5, lanes 3, 10, 17 & 24, and 4, 11, 18 & 25 respectively). This is consistent with studies showing that Cdc6 can only bind origins in the presence of ORC (Liang et al., 1995, Seki and Diffley, 2000) and that ORC and Cdc6 are required to load the Mcm2-7 complex onto chromatin (Donovan et al., 1997).

Complexes were observed when Cdc6 was added to ORC-DNA (Figure 3.5, lanes 5, 12, 19 & 26) that were distinct from ORC-DNA complexes. Again, the addition of glutaraldehyde to ORC-Cdc6 reactions, produced a slower migrating smear, indicating that crosslinking stabilised the ORC-Cdc6-DNA complex (compare lane 5 to 12 and lane 19 to 26).

Slower migrating complexes were observed in reactions containing ORC and Mcm2-7/Cdt1 (Figure 3.5, lanes 6, 13, 20 & 27) that were distinct from ORC-DNA and ORC-Cdc6-DNA complexes. When pre-RC assembly is reconstituted *in vitro*, we cannot detect Mcm2-7/Cdt1 binding to the origin in the absence of Cdc6. It is possible that the EMSA stabilises a weak interaction between ORC and Mcm2-7/Cdt1, and that is why a slower migrating product can be seen here. There were no novel bands or smears observed in reactions containing Cdc6 and Mcm2-7/Cdt1 (Figure 3.5, lanes 7, 14, 21 & 28) as Cdc6 requires ORC to bind DNA (Liang et al., 1995, Seki and Diffley, 2000).

There were some interesting differences between reactions in ATP and reactions in ATPγS. The full pre-RC reaction containing ORC, Cdc6 and Mcm2-7/Cdt1 produced a larger slower migrating smear in ATPγS containing reactions compared to ATP containing reactions (Figure 3.5, compare lanes 15 to 29). This indicates that in the presence of ATPγS, a larger or more complex structure is formed that migrates more slowly during electrophoresis. Indeed, in ATPγS, all loading components including Ccd6 and Cdt1 are bound at origins (Remus et al., 2009). This structure could thus be larger than the Mcm2-7 double hexamer formed in ATP.

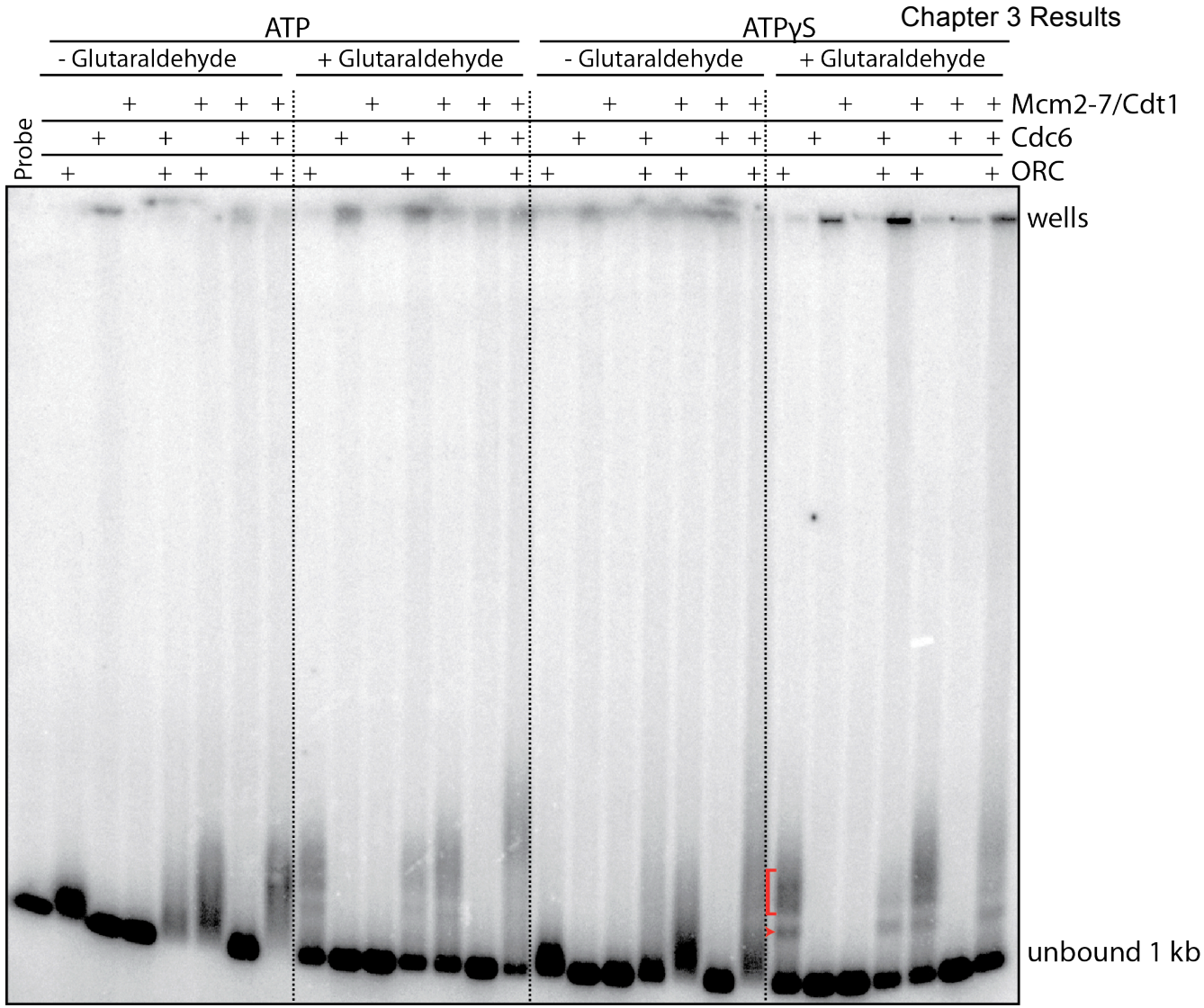

Figure 3.5 EMSA of the pre-RC on 1 kb origin DNA

Reactions were assembled using 160 fmol ORC, 160 fmol Cdc6 and 320 fmol Mcm2-7/Cdt1 in either ATP or ATPγS. Reactions were incubated for 30 mins at 30°C with 1 kb ARS305 probe DNA. Glutaraldehyde was then added to a final concentration of 0.1% for 5 mins in a subset of reactions. The reactions were quenched with TRIS-HCl pH 7.5 and whole reactions were loaded onto a 0.8% agarose gel (100 V, 5 hours). The gel was dried and exposed to a phosphorimager screen and scanned using a Typhoon scanner. The red triangle indicates a prominent band. The red bracket indicates a slower migrating smear.

We noticed a prominent band that formed in the presence of ORC in crosslinked reactions and most clearly in ATPγS crosslinked reactions (Figure 3.5, lane 23, red triangle). In addition, there was a slower migrating smear above this band (Figure 3.5, lane 23, red bracket). This smear appeared to alter in migration upon the addition of Cdc6 and/or Mcm2-7, whilst the band remained constant (compare Figure 3.5, lanes 23, 26, 27 and 29). It is possible that the band observed with ORC could be one ORC molecule binding specifically to the ARS consensus sequence whilst the slower migrating smear, that appears to be a precursor for the full reaction, could represent more than one ORC bound to DNA. It has been suggested that association of multiple ORC molecules with origin DNA is required for efficient Mcm2-7 loading in fission yeast (Takahashi et al., 2003). Another possibility is that the slower migrating smear could represent looping of the DNA, onto which the Mcm2-7 complex could be loaded.

In light of this, we next asked whether the band we observed in the ORC containing reactions represents ORC binding specifically to the ARS consensus sequence. To address this question, EMSAs were set up using either a WT ARS 305 probe or a mutant ARS305 probe. The mutant or A^- ARS305 probe contains an 8 bp XhoI linker in place of the wild-type sequence in the ARS consensus sequence (ACS) (Huang and Kowalski, 1996). This mutation inactivates function of the origin (Huang and Kowalski, 1996).

Reactions were assembled with either ORC or all pre-RC components (ORC, Cdc6 and Mcm2-7/Cdt1) on WT or A^- ARS305 in ATP or ATPγS. All samples were crosslinked with glutaraldehyde and reactions were subjected to electrophoresis on a 0.8% agarose gel. The gel was dried, exposed to a Phosphorimager screen and scanned.

Figure 3.6 shows the results of pre-RC reactions assembled in ATP (first panel) or ATPγS (second panel) on WT or A^- ARS305 DNA. Lanes 1 and 4 show the unbound linear WT ARS305 and A^- probes respectively. Addition of ORC to probe DNA resulted in slower migrating products (lanes 2, 5, 7 and 9). Consistent with previous results, a prominent band formed in the ATPγS reaction containing ORC

(Figure 3.6, lane 7). However, this band appeared to be absent from the A$^-$ ARS305 reaction (Figure 3.6, lane 9). This indicates that the ORC band is specific to WT ARS305 and represents ORC binding to the ACS. A slower migrating smear above the ORC band appeared in both WT and A$^-$ ARS305 reactions containing ORC alone, in ATP and in ATPγS (Figure 3.6, lanes 2, 5, 7 and 9). In addition, there seemed to be little or no difference between the full pre-RC reaction (ORC + Cdc6 + Mcm2-7/Cdt1) assembled on WT or A$^-$ ARS305 (Figure 3.6, compare lanes 3, 6, 8 and 10).

These data indicate that the 'specific ORC band' may not be required to form the pre-RC. This is consistent with data from Remus et al. 2009 showing that Mcm2-7 loading occurs on A$^-$ ARS1 just as efficiently as on WT ARS1 (ARS1 is another well characterised origin of DNA replication in budding yeast). The loading capacity of A$^-$ ARS1 is only reduced when competitor DNA is added (Remus et al., 2009). Interestingly, *S.cerevisiae* is the only known species to contain a sequence specific binding site for ORC.

Taken together these data suggest that ORC binds specifically at the ACS but this binding is not required for formation of the pre-RC. This specific band could represent one ORC molecule binding in a specific manner whereas the precursor for pre-RC formation could consist of multiple ORC molecules or DNA looping.

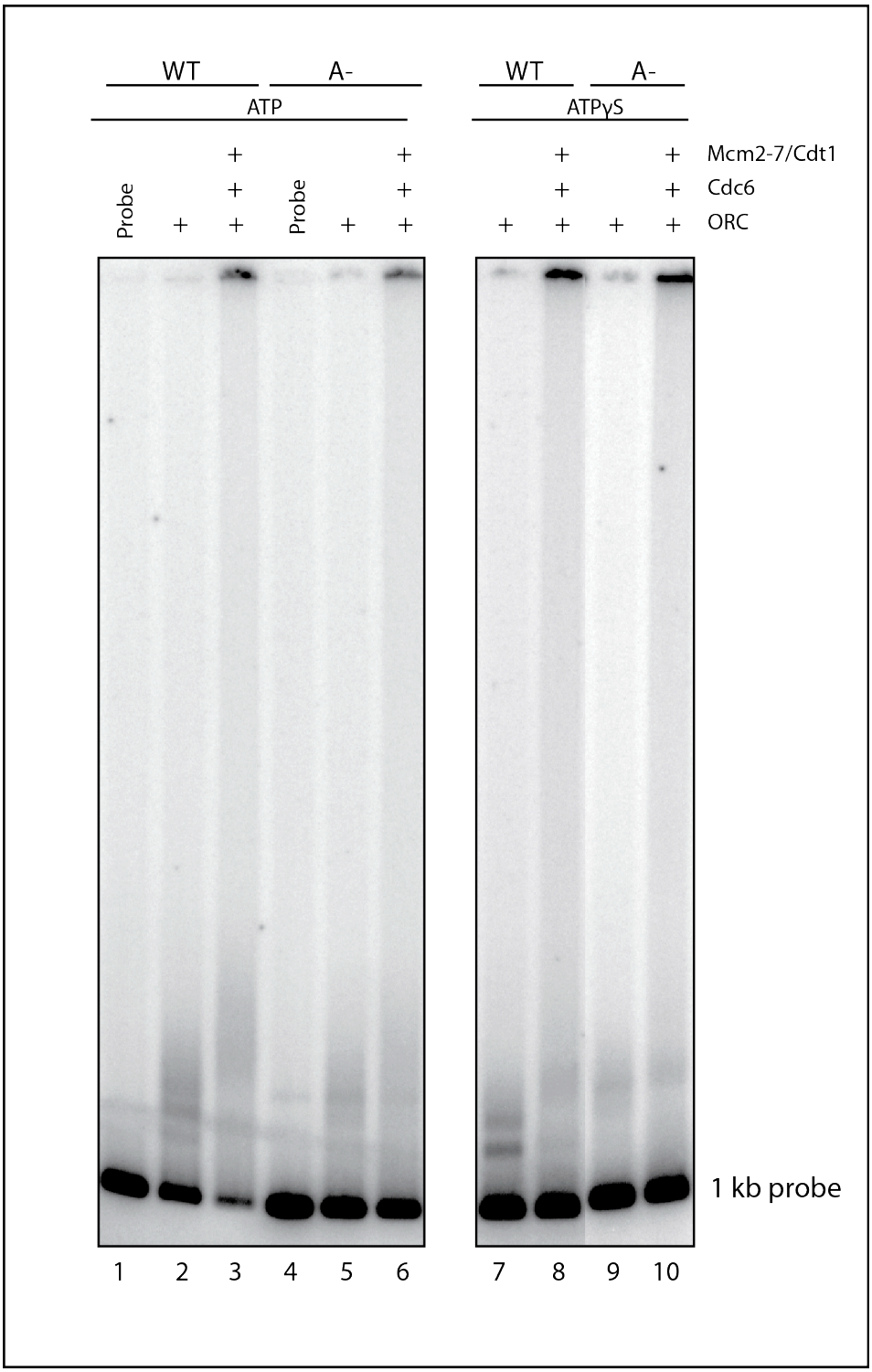

Figure 3.6 EMSA of the pre-RC on 1 kb WT ARS305 vs. 1 kb A$^-$ ARS305

Reactions were assembled as in Figure 3.4 on either 1 kb WT ARS305 or 1 kb A$^-$ ARS305. All reactions were crosslinked with glutaraldehyde and whole reactions were loaded on a 0.8% agarose gel (100 V, 5 hours).

3.5 Conclusions

To gain insight into the mechanism of Mcm2-7 loading, I set out to characterise intermediates in pre-RC formation. EMSA was used as a tool to characterise the "ATPγS complex", which may represent an intermediate stage in which ATP is bound by components of the pre-RC but not yet hydrolysed.

Proteins of the pre-RC were purified as described in Remus et al. 2009, and tested for their ability to load the Mcm2-7 complex *in vitro*. EMSA analysis of ORC and Cdc6 binding was carried out on 247 bp ARS305 DNA. Addition of Cdc6 to ORC-DNA did not give rise to a distinct novel band in all reactions. A study in *Xenopus* egg extracts showed that a minimum of 82 bp is required for weak Mcm2-7 binding and that this Mcm2-7 binding increases with DNA length, whereas ORC binding remains constant (Edwards et al., 2002). I therefore examined whether 247 bp of ARS305 was capable of Mcm2-7 loading *in vitro* when compared to 1 kb ARS305. I found that 247 bp could not support Mcm2-7 loading *in vitro* as Mcm2, 5 and 7 were only capable of binding DNA-beads in the presence of ATPγS and low salt.

These data are consistent with Edwards et al., 2002, and suggest that there is a threshold length required in order for proper Mcm2-7 loading to occur. If a pre-RC intermediate involved looping of the DNA then 247 bp could be too short, even if the A element and B elements were present. This may also explain why the EMSA with ORC and Cdc6 on 247 bp DNA did not give a clear result upon addition of Cdc6 to ORC-DNA (Figure 3.3A).

In addition, I observed some Mcm2-7 binding on 247 bp DNA in the absence of ATP hydrolysis (in ATPγS) that was then released upon ATP hydrolysis. A similar "ATP-dependent release" of Mcm2-7 has been observed in instances where reaction components are missing or when ORC has been inactivated by CDK phosphorylation (Frigola et al., 2013).

EMSAs were subsequently performed on 1 kb ARS305. Full pre-RC reactions (containing ORC, Cdc6 and Mcm2-7) assembled in ATPγS produced a larger,

slower migrating smear than those set up in ATP. This suggests that the ATPγS complex is a larger/more complex structure than the ATP complex where Cdc6 and Cdt1 are known to dissociate. We observed a prominent band that formed in the presence of ORC in ATPγS crosslinked reactions. By using mutant (A^-) ARS305, I established that this band represents ORC binding specifically to the ACS.

In addition to the specific ORC binding band, I detected a slower migrating smear in ORC containing reactions that appears to be the precursor for pre-RC formation. It is interesting to postulate that the specific band is one ORC molecule binding at the ACS, whilst the precursor smear could be multiple ORC molecules that act together to load the Mcm2-7 complex.

Whilst EMSA analysis provided some insight into intermediates in pre-RC formation (ATPγS complex), this information was limited and results were somewhat difficult to interpret. I therefore subsequently used different strategies to address whether multiple ORC molecules load the Mcm2-7 complex. I set out to examine the stoichiometry of loading factors during pre-RC formation using epitope tagged proteins. This will be discussed in the subsequent chapters.

Chapter 4. Fusion of the pre-RC proteins to 3x FLAG or 9x Myc peptide tags

4.1 Introduction

ORC, Cdc6 and Cdt1 act together to load a double hexamer of Mcm2-7 onto origin DNA (See Chapter 1, section 1.2.2.3) and the Mcm2-7 hexamers are thought to be loaded in a concerted manner (Remus et al., 2009). Budding yeast ORC binds at a specific site on DNA replication origins (ACS, see Chapter 1, section 1.2.2.3) and it is thought that one ORC molecule binds at this site. If this is true, how can one ORC molecule recruit and load two Mcm2-7 hexamers simultaneously? Would this require that different ORC subunits interact with each hexamer? On the other hand, it is possible that multiple ORCs and/or multiple Cdc6 molecules function in pre-RC formation. Perhaps two ORC-Cdc6 assemblies load one Mcm2-7/Cdt1 each, in opposite orientations. It is also possible that the Mcm2-7 hexamers are loaded sequentially by one ORC-Cdc6 complex. Several intriguing questions arise from this: what is the stoichiometry of loading factors during pre-RC formation? How many ORC, Cdc6 and Cdt1 molecules function in loading the Mcm2-7 complex? Are the Mcm2-7 hexamers indeed loaded in a concerted manner or sequentially? Information on protein stoichiometry would provide considerable insight into how Mcm2-7 can be loaded into a double hexamer.

In addition to deciphering protein stoichiometry during pre-RC formation, we need a better understanding of how licensing factors are positioned relative to each other to load the Mcm2-7 double hexamer. This leads to the question: which proteins interact during pre-RC assembly? Very little is known about protein-protein interactions in pre-RC formation. A study in 2007 suggested that Orc6 interacts with Cdt1 to recruit the Mcm2-7 complex (Chen et al., 2007), however there are likely to be other interactions involved in forming the double hexamer. An informative first step would be to examine protein-protein interactions in the context of the “ATPγS complex” (Figure 3.1 iii). This is because in the “ATPγS complex”, all the pre-RC components (ORC, Cdc6 and Mcm2-7/Cdt1) are stabilised at the origin in an ATP-bound state (Figure 3.1 iii). Examining any protein-protein interactions in

this complex would provide a clearer picture of how licensing factors are positioned during pre-RC formation.

To begin to construct a model of how a pre-RC is assembled, we sought to examine the stoichiometry and interactions of loading factors. To do this, we devised a peptide tagging strategy that would allow examination of both the stoichiometry and interactions of pre-RC proteins.

Peptide tagging, first described by Munro and Pelham in 1984 (Munro and Pelham, 1984), is a useful technique whereby a gene product is made immunoreactive to an already existing antibody. The process involves inserting a polynucleotide encoding a short continuous epitope into a gene of interest and then expressing the gene in an appropriate host. Peptide tagging enables simple detection of the protein product of the tagged gene.

I chose to fuse the 3x FLAG and 9x Myc peptide tags to each of the pre-RC polypeptides. There were several reasons for this. Firstly, specific antibodies against both of these peptide tags are readily available. Indeed, there are very few available antibodies against each of the 14 pre-RC polypeptides (6 ORC subunits, 6 Mcm2-7 subunits, Cdc6 and Cdt1). Secondly, the presence of tandem copies of the tags (3x FLAG and 9x Myc) significantly improves signal strength, which therefore makes detection of the protein fused to the peptide tag very sensitive. Finally, by using a single antibody against 3x FLAG or 9x Myc, I could quantitatively compare antibody signals across protein-tag fusions.

I examined protein stoichiometry and protein-protein interactions during pre-RC formation by combining 3x FLAG and 9x Myc-tagged licensing proteins and using immunoaffinity purification and crosslinking techniques coupled with antibody detection and quantification. These experiments and their results will be discussed in Chapters 5 and 6.

In this chapter I will present how proteins fused to 3x FLAG or 9x Myc peptide tags were generated for stoichiometry and interaction studies and how these proteins

were functionally assessed for their competency to load the Mcm2-7 complex *in vitro*.

4.2 Fusion of 3x FLAG or 9x Myc peptides to the N-terminus of Cdc6

To examine the stoichiometry and interactions of Cdc6 during pre-RC formation, I purified Cdc6 fused to a 3x FLAG or 9x Myc peptide tag. In this section, I will describe the approach taken to achieve this.

Previous work in the laboratory had established protocols for purification of Cdc6 from baculovirus expression in insect cells (Remus et al., 2009). Fusion of a peptide tag to a gene in baculovirus vectors involves several stages. Subsequent expression and purification of the tagged protein from insect cells is both laborious and time consuming. In contrast, the expression of proteins in *E.coli* is relatively easy and rapid. In addition, fusion of a peptide tag to a gene in this system is by simple cloning. For these reasons, I generated Cdc6 from an *E.coli* expression system to simplify peptide tagging and purification.

Briefly, I cloned *S.cerevisiae* Cdc6 in an expression plasmid where Cdc6 was fused to a GST (Glutathione S-transferase) tag at its N-terminus (see materials and methods, section 2.5.1). This GST-Cdc6 fusion contained a PreScission Protease recognition sequence at the 5' end of Cdc6 to facilitate removal of the GST tag during protein purification. The GST tag is composed of 220 amino acid residues and dimerises when purified. The removal of the GST tag is sometimes desirable to eliminate the possibility that it interferes with protein function.

This GST-Cdc6 expression plasmid was expressed in *E.coli* cells and Cdc6 was purified by glutathione chromatography and eluted with PreScission Protease (modified from Speck et al. 2005). The eluate was then subjected to hydroxyapatite chromatography using an elution gradient of salt (Figure 4.1B). The elution pattern from hydroxyapatite chromatography is shown in a Coomassie-stained polyacrylamide gel in Figure 4.1B. One advantage of this purification is that it is

less laborious than the baculovirus expression system. In addition, Cdc6 expressed from baculovirus in insect cells is phosphorylated (Figure 4.1A) (Remus et al., 2009). In *S.cerevisiae* phosphorylation of Cdc6 promotes its ubiquitin-mediated proteolysis (Drury et al., 1997, Sanchez et al., 1999). It is therefore the un-phosphorylated form of Cdc6 that is active in pre-RC formation. Cdc6 purified from *E.coli* is not phosphorylated (Figure 4.1B), making it ideal for further studies. Figure 4.1C shows the final purified preparations of Cdc6 from both baculovirus and *E.coli* expression systems.

It was important to establish that Cdc6 purified from this *E.coli* expression system was functional, as I intended to use the system for fusion of tags to Cdc6 and purification of tagged-Cdc6. These protein preparations were then to be used for stoichiometry and interaction studies. To ascertain that Cdc6 purified from *E.coli* was functional, I assessed its ability to load the Mcm2-7 complex *in vitro* (see Figure 1.5). This was compared to Cdc6 purified from baculovirus expression, which has previously been shown to be functional for pre-RC formation (Mcm2-7 loading) *in vitro* (Remus et al., 2009). Mcm2-7 loading, both *in vivo* and *in vitro,* has been defined as the generation of Mcm2-7 complexes that remain bound to DNA even after treatment with high salt (Donovan et al., 1997, Bowers et al., 2004, Remus et al., 2009, Evrin et al., 2009).

E.coli-purified or baculovirus-purified Cdc6 was incubated with purified ORC, Mcm2-7/Cdt1 (Figure 3.3) and origin DNA which was bound to magnetic beads by a biotin-streptavidin linkage (DNA-beads) (refer to Chapter 3, section 3.2.1). Mcm2-7 loading was assessed by immunoblotting. We used an antibody against Mcm2 as a surrogate for the Mcm2-7 complex, and an antibody against Orc6 as a surrogate for the ORC complex.

Figure 4.1D shows that Mcm2 bound to DNA-beads in ATP in a high salt wash resistant manner in reactions containing Cdc6 purified from *E.coli* and reactions containing Cdc6 purified from baculovirus expression (lanes 1, 2, 5 & 6). In ATPγS however, Mcm2 could only bind DNA-beads under low salt conditions and was removed upon high salt extraction (Figure 4.1D, lanes 3, 4, 7 & 8). Orc6 bound

DNA-beads only under low salt conditions in both ATP and ATPγS as expected (Figure 4.1D).

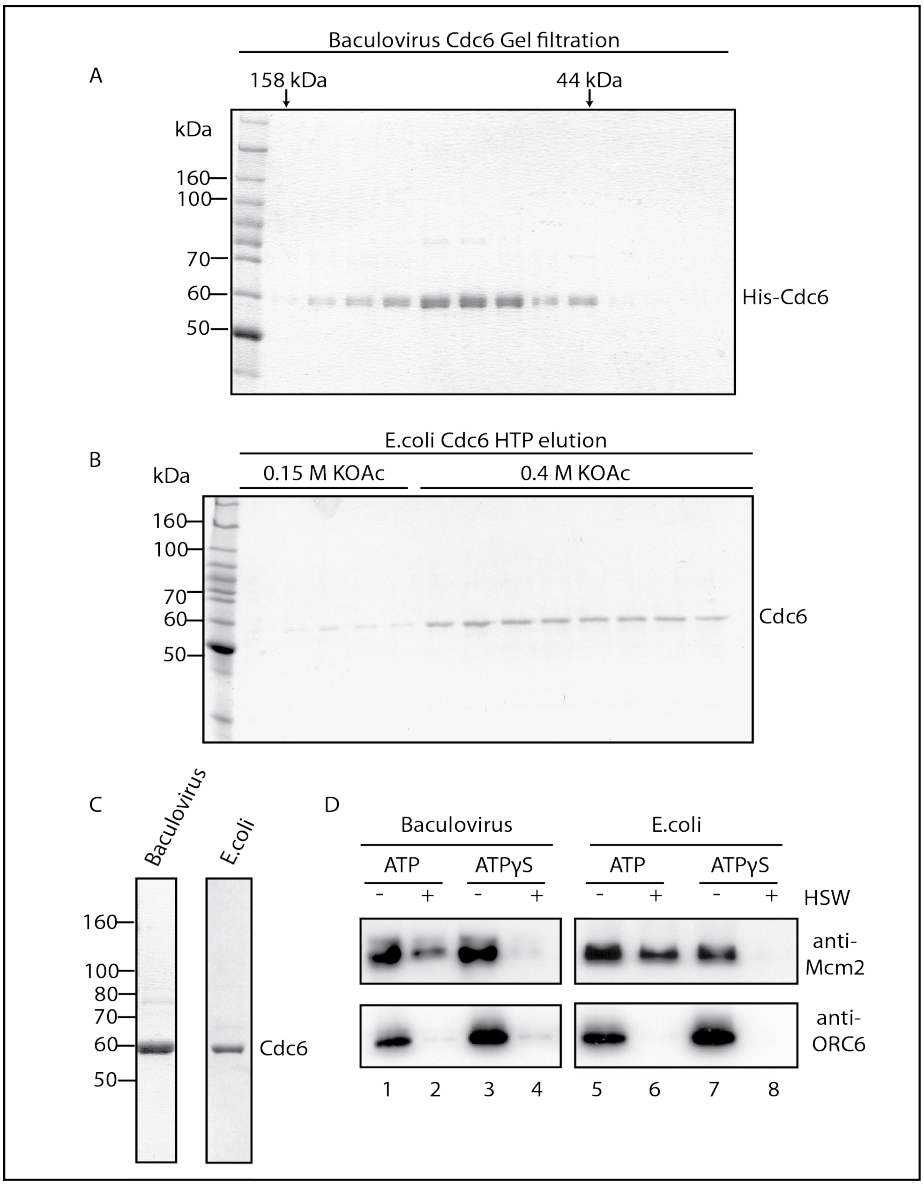

Figure 4.1 Purification of Cdc6 from *E.coli vs.* baculovirus expression in insect cells

(A) SDS PAGE followed by Coomassie staining of the gel filtration profile of 6x His-Cdc6 purified from baculovirus expressed in insect cells. (B) SDS PAGE followed by Coomassie staining of the hydroxyapatite (HTP) elution profile of Cdc6 purified from *E.coli.* (C) Final purifications of Cdc6. SDS PAGE, Coomassie stained. (D) *In vitro* Mcm2-7 loading, comparing MCM loading by *E.coli* Cdc6 vs. baculovirus Cdc6. Reactions were assembled in ATP or ATPγS on ARS305 DNA beads. HSW: high salt wash. Equimolar amounts of Cdc6 were used along with purified ORC and Mcm2-7/Cdt1 (purifications shown in Figure 3.3). Bound proteins were analysed by immunoblotting.

Therefore, Cdc6 purified from *E.coli* was able to load the Mcm2-7 complex onto origin DNA-beads in a salt resistant manner in ATP and there appeared to be no difference in MCM loading efficiency between Cdc6 from *E.coli* and Cdc6 from baculovirus expression. These data confirmed that Cdc6 expressed and purified from *E.coli* was competent for pre-RC assembly *in vitro*.

Upon establishing that Cdc6 purified from E.coli was functional for Mcm2-7 loading *in vitro*, I proceeded with fusion of 3x FLAG or 9x Myc to Cdc6 in the plasmid expressing GST-Cdc6. Briefly, polynucleotides encoding a 9x Myc or a 3x FLAG peptide were inserted at the 5' end of the Cdc6 gene. This gave rise to two constructs illustrated in Figure 4.2. This cloning strategy maintained the PreScission Protease cleavage site for removal of the GST tag following purification. It was important to remove this GST tag, since it dimerises and this property could affect the results of stoichiometry studies.

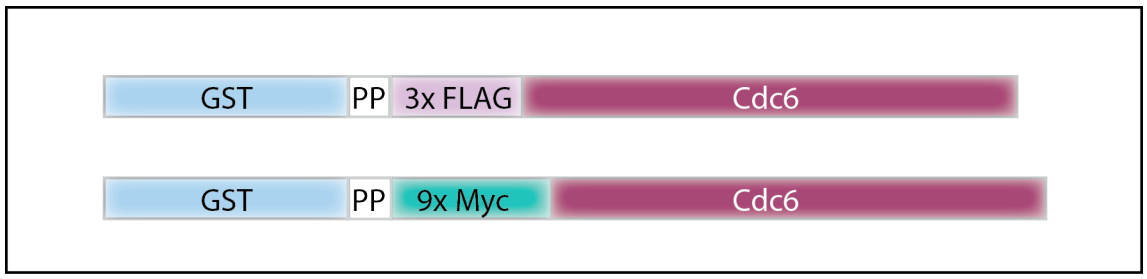

Figure 4.2 Schematic of *CDC6* fused to 3x FLAG or 9x Myc

3x FLAG or 9x Myc tag cloned into single restriction site 5' of Cdc6 in GST expression plasmid. Resulting constructs are illustrated. PP: PreScission protease cleavage site. Cleavage at the PP site with the protease cleaves off the GST tag, resulting in 3 x FLAG or 9x Myc tagged-Cdc6.

The plasmids containing 3x FLAG or 9x Myc-tagged Cdc6 were then expressed and purified from *E.coli* as described for untagged Cdc6. Cleavage with PreScission Protease removed the GST tag resulting in purified Cdc6, fused to either a 3x FLAG or 9x Myc peptide tag at its N-terminus. Purifications of 3x FLAG-Cdc6 and 9x Myc-Cdc6 are shown alongside untagged Cdc6 in a Coomassie stained polyacrylamide gel in Figure 4.3A (top panel). Immunoblots against FLAG

and Myc were performed and demonstrated that the peptide tags were fused to the purified Cdc6 proteins (Figure 4.3A, bottom panel).

I next examined the ability of the tagged versions of Cdc6 to load the Mcm2-7 complex *in vitro*. This was to ensure that the 9x Myc or 3x FLAG tags did not interfere with the function of Cdc6. To do this I employed *in vitro* reconstitution of Mcm2-7 loading, with minor adaptations described below (also see: Frigola et al., 2013).

Firstly, the ARS305 replication origin was amplified using an oligonucleotide primer containing a photocleavable biotin as described in (Tsakraklides and Bell, 2010). Photocleavable biotin (PC-biotin) is a non-nucleosidic moiety that is used here to incorporate a UV-cleavable biotin molecule onto the 5' end of ARS305. The biotin is separated from the 5'-end nucleotide base of ARS305 by a photo-cleavable group and a long chain alkyl spacer arm. The PCR product was then conjugated to streptavidin coated paramagnetic beads (DNA-beads). The photocleavable group can be selectively cleaved from the paramagnetic beads by illumination with UVA light. The photocleavage has been optimised to minimise DNA damage by irradiating for 10 min at 330 nm (Frigola et al., 2013). The reason photocleavable ARS305 DNA-beads were used in this case was to allow selective examination of DNA-bound proteins, as opposed to proteins that may be bound to magnetic beads. Previously, ARS305 DNA was coupled to paramagnetic beads via a biotin-streptavidin linkage that was not cleavable.

To assess the functionality of tagged-Cdc6: purified ORC, Cdc6 and Mcm2-7/Cdt1 (Figure 4.3B) were incubated with the photocleavable DNA-beads in the presence of ATP. Washes were performed to remove unbound proteins, as outlined in Figure 1.5. The DNA and bound proteins were released from the beads by UVA irradiation, as described above (also see Materials and Methods, section 2.9.2). Finally, proteins bound to the DNA were analysed by SDS PAGE followed by silver staining. Previously, DNA-bead-bound proteins were analysed by immunoblotting. An advantage of silver staining is that we can observe all bound proteins without the need for specific antibodies. However, it must be noted that not all proteins are

stained equally by silver staining. In addition, DNA-bound proteins can be compared and quantified.

Figure 4.3C shows that the Mcm2-7 complex was loaded in a high salt wash (HSW) resistant manner in reactions containing ORC, untagged Cdc6 and ATP (Figure 4.3C, lanes 1 & 2). ORC and Cdc6 were detected only under low salt conditions and were washed away with high salt (Figure 4.3C, lanes 1 & 2). The Mcm2-7 complex was also loaded in a high salt wash resistant manner in reactions containing ORC, ATP and 3x FLAG Cdc6 or 9 x Myc Cdc6 (Figure 4.3C, lanes 3, 4, 5 & 6). In these reactions ORC and 3 x FLAG Cdc6 bound only under low salt conditions and were washed away with high salt (Figure 4.3C, lanes 3, 4, 5 & 6). However, 9x Myc Cdc6 was not removed by high salt extraction (Figure 4.3C, lanes 6). This suggests that 9x Myc-Cdc6 might precipitate on the DNA, which will be discussed further in Chapter 5.

These results showed that Cdc6 fused to a 3x FLAG or 9x Myc at its N-terminus was functional for loading the Mcm2-7 complex onto origin DNA-beads *in vitro* in a high salt resistant manner, just as efficiently as untagged Cdc6.

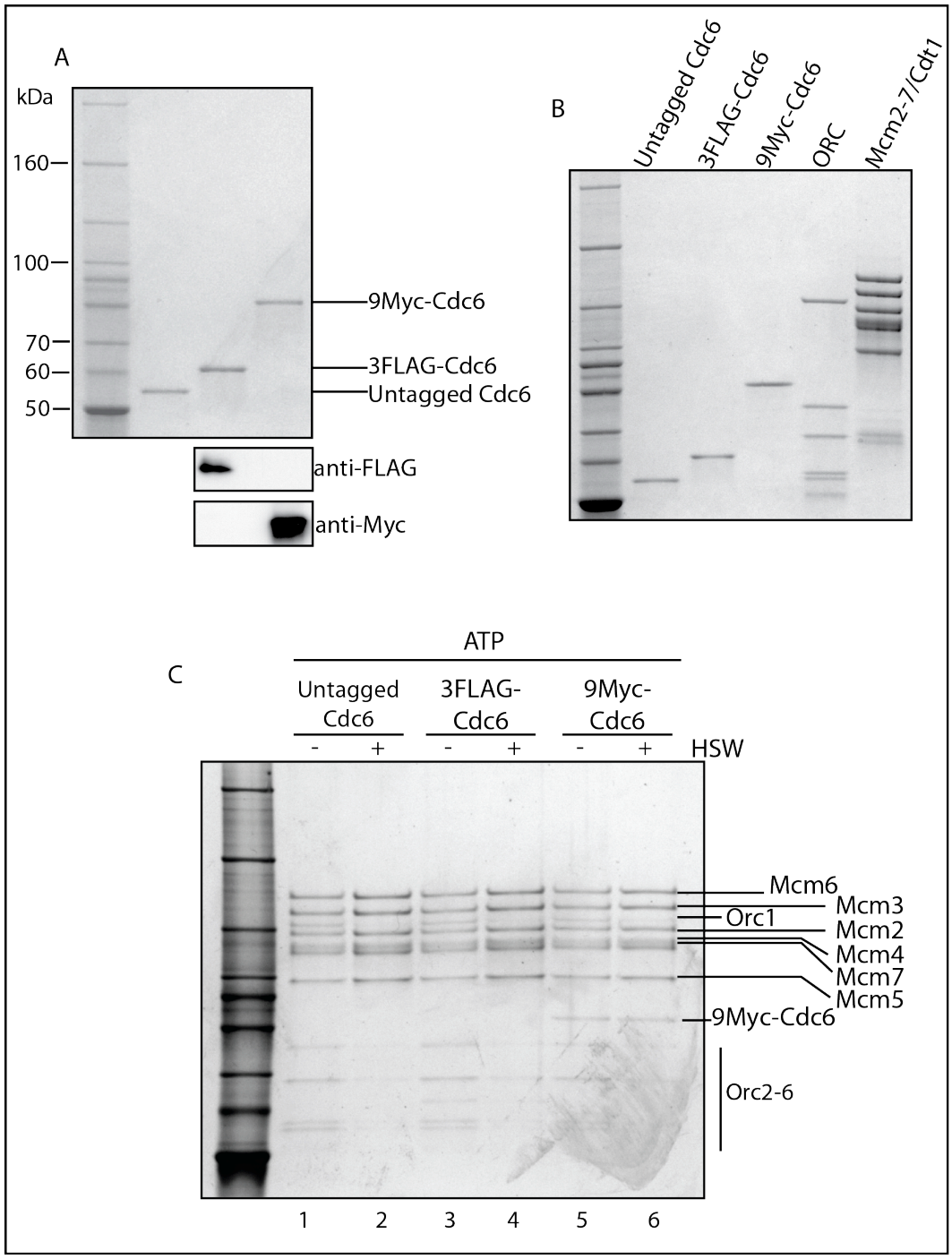

Figure 4.3 3x FLAG and 9x Myc-tagged Cdc6

(A) Coomassie stained SDS PAGE of purified untagged, 3x FLAG tagged and 9x Myc tagged Cdc6. (B) Coomassie stained SDS PAGE of 100% Inputs for *in vitro* loading assays. (C) *In vitro* loading assay. Proteins were incubated with origin DNA coupled to magnetic streptavidin beads via a photocleavable biotin linkage. Unbound proteins were washed away, HSW: high salt wash. DNA was cleaved from the beads and bound proteins were examined by SDS PAGE & silver staining.

4.3 Fusion of 3x FLAG or 9x Myc peptides to the ORC subunits

In order to examine the stoichiometry and interactions of ORC, I introduced 3x FLAG or 9x Myc peptide tags on each of the six ORC subunits. In this section I will describe the strategy I employed to achieve this.

At the start of my PhD, methods had been developed in the lab to express and purify ORC from a yeast strain overexpressing all six ORC subunits as additional copies from the inducible *GAL1-10* promoter (Remus et al., 2009). This required 50 L of cells per purification due to low protein expression, which was both laborious and time consuming.

In order to improve this process, each of the ORC genes was codon optimised to increase protein expression. The codon-optimised genes were synthesised (Geneart®) and cloned into bi-directional *GAL1-10* overexpression vectors and the plasmids were subsequently integrated at targeted sites in the yeast genome (Lucy Drury and Anne Early). This gave rise to a yeast strain, similar to that above, where all six codon optimised ORC genes are expressed as additional copies from the inducible *GAL1-10* promoter (see Frigola et al., 2013). In this strain Orc1 is fused to a Calmodulin Binding Peptide (CBP) tag at its 5' end. The CBP tag was chosen since purification of ORC using the CBP as part of the TAP-TCP tag (see Chapter 3, section 3.2.1) was previously shown to give rise to a functional, stoichiometric complex of ORC in a simple two-step purification process (see Figure 3.2).

Purification of codon optimised ORC was performed by calmodulin-affinity purification followed by gel filtration chromatography (described in Frigola et al., 2013). Codon optimisation of the ORC subunits greatly improved protein expression levels and purification yielded approximately 1 mg of protein from 2 L of cells as opposed to 50 L (purified codon optimised ORC is shown in Figure 4.3B).

Since the purification of codon optimised ORC was very efficient, I decided to utilise this system to tag each of the ORC subunits (Orc1-6) with a 3x FLAG or a 9x Myc tag and purify ORC complexes with a single tag.

4.3.1 Fusion of a 3x FLAG peptide to the N-termini of the ORC subunits

A polynucleotide encoding the 3x FLAG peptide tag was introduced at the 5' end of each of the codon optimised genes in the *Gal1-10* overexpression plasmids. The plasmids containing an ORC gene fused to the 3x FLAG DNA sequence were then separately integrated in a targeted manner into yeast background strains. This resulted in six yeast strains each overexpressing the codon-optimised ORC complex with a 3x FLAG tag fused to the N-terminus of one subunit.

The tagged complexes were then expressed and purified from G1 phase arrested yeast extracts via the CBP tag at the N-terminus of Orc1. These purifications were performed exactly as for untagged ORC. I purified all the tagged complexes in an identical manner for consistency. The resulting tagged complexes are shown in Figure 4.4A. I obtained five complexes each with a single 3x FLAG tag, plus an additional untagged complex.

Purification of ORCs containing 3xFLAG-Orc1, 3x FLAG-Orc3, 3xFLAG-Orc4, 3xFLAG-Orc5 or 3xFLAG-Orc6 yielded five stoichiometric complexes containing Orc1-6 with a single tagged subunit (Figure 4.4A). The tagged subunit in each case shifts up in SDS PAGE by an amount equivalent to the molecular weight of 3x FLAG (Figure 4.4A).

Purification of ORC containing 3x FLAG-Orc2 resulted in a sub-stoichiometric complex consisting mainly of Orc1. It has been shown that the N-terminal portion of Orc2 interacts with Orc6 in the ORC complex (Sun et al., 2012). Possibly the presence of a tag inhibited this interaction and caused the complex to disassemble. As an alternative, Orc2 was tagged with 3x FLAG at its C-terminus. This allowed formation of a stoichiometric ORC complex and shall be discussed later (section 4.3.3).

The next step was to test whether the tagged ORC complexes were capable of loading the Mcm2-7 complex onto DNA, in a manner similar to untagged ORC. This was to ensure that the 3x FLAG tags did not interfere with the function of ORC. To do this, I again examined Mcm2-7 loading *in vitro* as a read out of functionality.

Equimolar amounts of untagged or tagged ORC complexes (Figure 4.4A), Cdc6 and Mcm2-7/Cdt1 were incubated with origin DNA-beads in the presence of ATP or ATPγS. Unbound proteins were removed (see Figure 1.5) and the DNA was cleaved from the beads by UVA irradiation as described previously. DNA-bound proteins were analysed by SDS PAGE and silver staining. In reactions containing an ORC complex with a 3x FLAG tag at the N-terminus of Orc1: Mcm2-7 was loaded in ATP in a high salt wash (HSW) resistant manner (Figure 4.4B, lanes 3 & 4). This Mcm2-7 loading was undistinguishable from that in reactions containing untagged ORC (Figure 4.4B, compare lanes 2 & 4). In ATPγS, Mcm2-7 was detected in low salt only and was quantitatively removed by high salt extraction (Figure 4.4B, lanes 5, 6, 7 and 8). ORC bound DNA in ATP and ATPγS and was quantitatively removed by high salt (Figure 4.7B). An ORC complex containing 3x FLAG-Orc1 was therefore able to load the Mcm2-7 complex onto origin DNA *in vitro* in a manner similar to untagged ORC.

Similarly, the other tagged ORC complexes were capable of loading Mcm2-7 in a salt resistant manner in ATP (Figure 4.4C) and of recruiting the Mcm2-7 complex in ATPγS in a salt labile manner (Figure 4.4D). *In vitro* Mcm2-7 loading by ORC complexes containing 3x FLAG-Orc3 or 3x FLAG-Orc4 appeared undistinguishable from that by untagged ORC (Figure 4.4C). Salt-resistant Mcm2-7 loading in ATP by ORC complexes containing 3x FLAG-Orc5 or 3x FLAG-Orc6 appeared to be slightly reduced compared to that by untagged ORC (Figure 4.4C). Recruitment of the Mcm2-7 complex in ATPγS (after a low salt wash) was similar for both untagged and tagged ORCs (Figure 4.4D). These data provided information about the functionality of ORC complexes containing 3x FLAG peptide tags that will be important for stoichiometry and interactions studies (presented in Chapters 5 & 6).

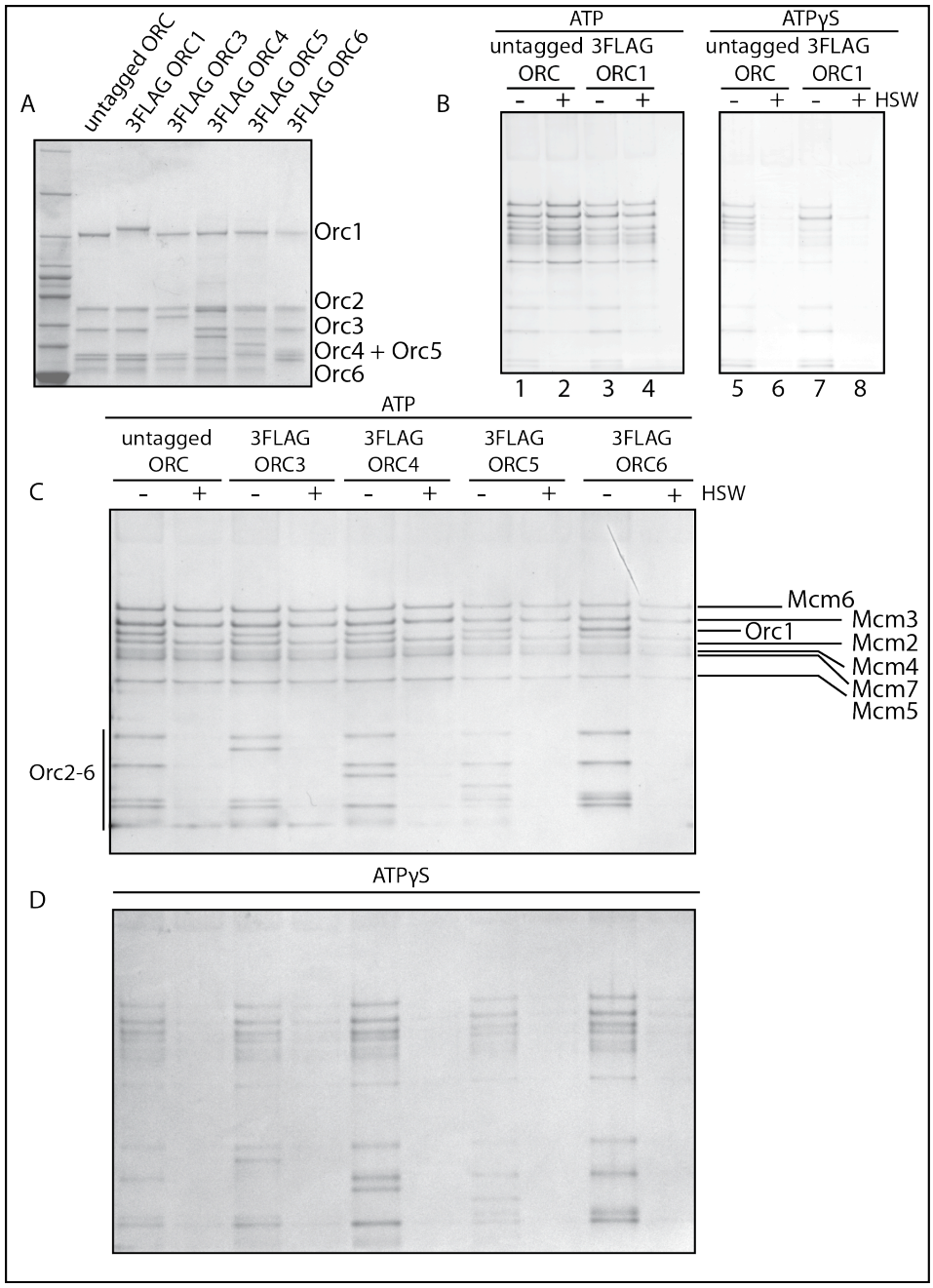

Figure 4.4 ORC complexes with single 3x FLAG tags can load the Mcm2-7 complex onto origin DNA

(A) Coomassie stained SDS PAGE of final purified ORC complexes with a 3x FLAG tag on each subunit. Tagged subunit is indicated above. (B) 3x FLAG Orc1 in an ORC complex can load the Mcm2-7 complex. Reconstitution of pre-RC assembly using untagged and 3x FLAG tagged Orc1. Assay performed in ATP or in ATPγS on photocleavable DNA-beads. HSW: high salt wash. DNA cleaved off beads by UVA irradiation. Proteins bound to DNA are detected by silver staining. (C) ORC complexes with single 3x FLAG tags on Orc3, 4, 5 & 6, can load the Mcm2-7 complex. *In vitro* loading assay in ATP as described for B. (D) ORC complexes with single 3x FLAG tags on Orc3, 4, 5 & 6, can recruit the Mcm2-7 complex. *In vitro* loading assay in ATPγS as described for B.

4.3.2 Fusion of a 9x Myc peptide to the N-termini of the ORC subunits

In order to fuse each of the ORC subunits to a 9x Myc peptide, a strategy similar to that outlined for the 3x FLAG peptide-fusions was employed. Polynucleotides encoding 9x Myc peptides were inserted at the 5' ends of each of the codon optimised ORC genes in the *Gal1-10* overexpression plasmids. I was unable to obtain clones for *9x MYC-ORC1*. I did, however, obtain constructs for the other *ORC* genes. As described previously, the plasmids containing *9x MYC-ORC* fusions were separately integrated into target sites in yeast background strains. This generated five yeast strains each overexpressing the ORC complex with a 9x Myc peptide tag fused to the N-terminus of one subunit.

The 9x Myc-tagged ORC complexes were expressed and purified as for the 3x FLAG tagged complexes. Figure 4.5 shows a Coomassie-stained polyacrylamide gel of the purified 9x Myc-tagged ORC complexes. As in the case of 3x FLAG-Orc2, upon purification, the ORC complex containing 9x Myc-Orc2 disassembled (data not shown). Purification of ORC complexes containing 9x Myc-Orc3, 9x Myc-Orc4 or 9x Myc-Orc5 resulted in three stoichiometric complexes (Figure 4.5). Purification of an ORC complex containing 9x Myc-Orc6 resulted in a stoichiometric complex of Orc1-5 that appeared to be lacking 9x Myc-tagged Orc6. Mass spectrometric analysis confirmed that the complex consisted of Orc1-5 with substoichiometric amounts of 9xMyc-Orc6 and several chaperones. Perhaps the 9x Myc tag disrupted Orc6 interaction with the other ORC subunits inducing its release from the complex. The presence of chaperones in the purified complex also indicates that the complex was perhaps not correctly folded. Further analysis by immunoblotting (Figure 4.5, bottom panel) showed that 9x Myc-Orc6 was present in substoichiometric amounts when compared to 9x Myc-tagged subunits from the other purified ORC complexes. Since I was unable to obtain 9x Myc-Orc1, 9x Myc-Orc2 and 9x Myc-Orc6, these subunits were fused to 9x Myc at their C-termini. Results of this tagging approach are discussed in section 4.3.3.

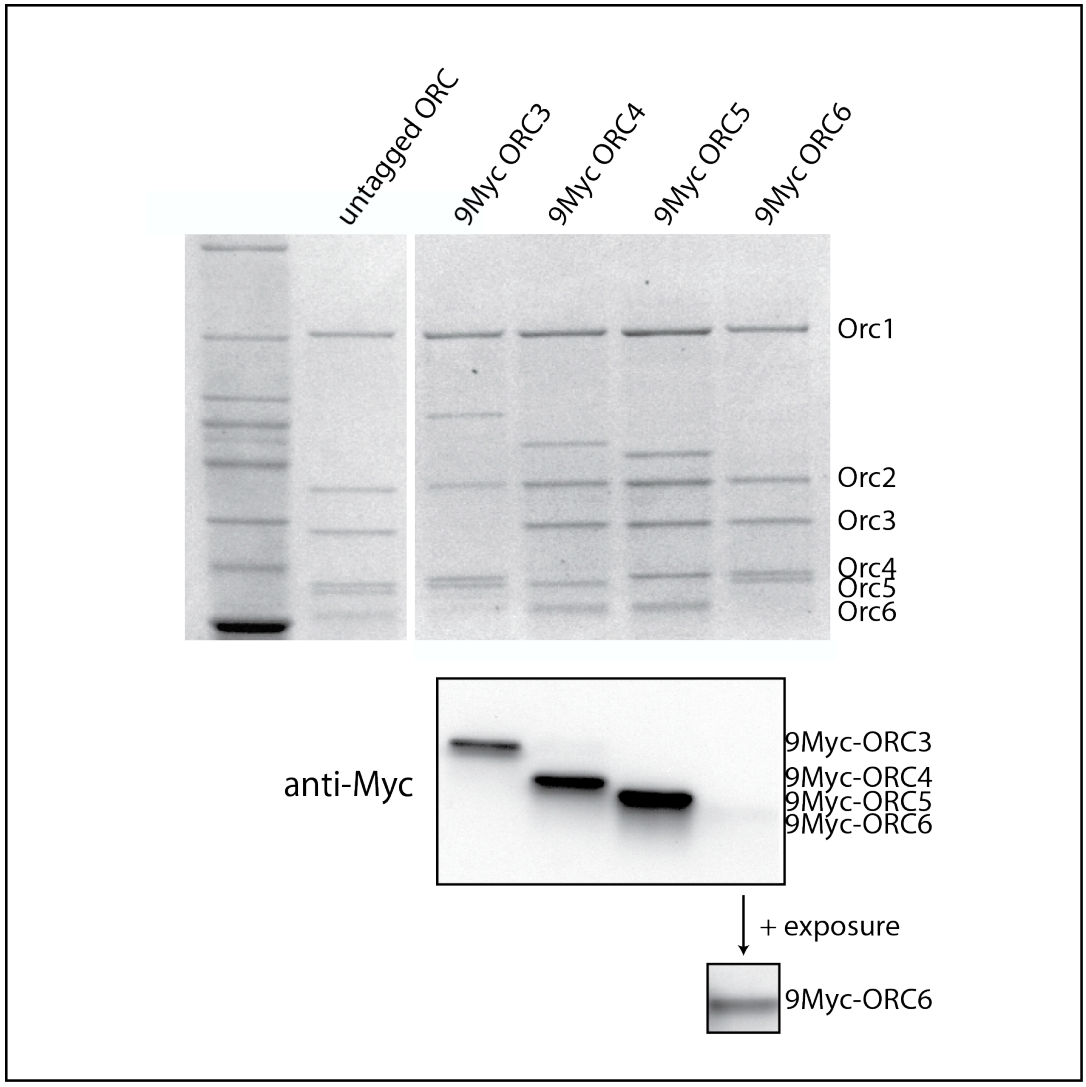

Figure 4.5 ORC complexes with single 9x Myc tags

Top panel, Coomassie stained polyacrylamide gel showing purified ORC complexes containing a 9x Myc tag on a single subunit. Tagged Orc3, Orc4, Orc5 and Orc6 are shown alongside untagged ORC. Bottom panel, immunoblot against Myc showing the presence of the 9x Myc tag on the indicated subunits. 9x Myc Orc6 is present in substoichiometric amounts and can only be visualised upon increased exposure of the immunoblot.

I next tested whether the 9x Myc-tagged complexes obtained were suitable for Mcm2-7 loading *in vitro*. ORC complexes containing 9x Myc-Orc3, 9x Myc-Orc4 or 9x Myc-Orc5 were tested alongside untagged ORC. The tagged proteins were incubated with purified Cdc6 and Mcm2-7/Cdt1 on photocleavable origin DNA-beads in the presence of ATP or ATPγS. Washes were performed as in Figure 1.5

to remove unbound proteins, DNA was cleaved off the paramagnetic beads (as previously), and DNA-bound proteins examined by SDS PAGE followed by silver staining. Figure 4.6A (lanes 1, 3, 5 & 7) shows that in the presence of ATP: ORC (tagged and untagged) and Mcm2-7 were detected. High salt extraction of DNA-beads quantitatively removed ORC but not Mcm2-7 (lanes 2, 4, 6 & 8). Figure 4.6B shows that in the presence of ATPγS: ORC, Cdc6 (band overlaps with Orc5) and Mcm2-7/Cdt1 could be detected by silver staining, only in low salt-washed reactions (lanes 1, 3, 5 & 7). High salt extraction quantitatively removed all proteins from the DNA-beads (lanes 2, 4, 6 & 8). From these results I concluded that ORC complexes containing 9x Myc-Orc3, 9x Myc-Orc4 or 9x Myc-Orc5 could load the Mcm2-7 complex *in vitro* and were therefore competent for use in assays examining stoichiometry and interactions.

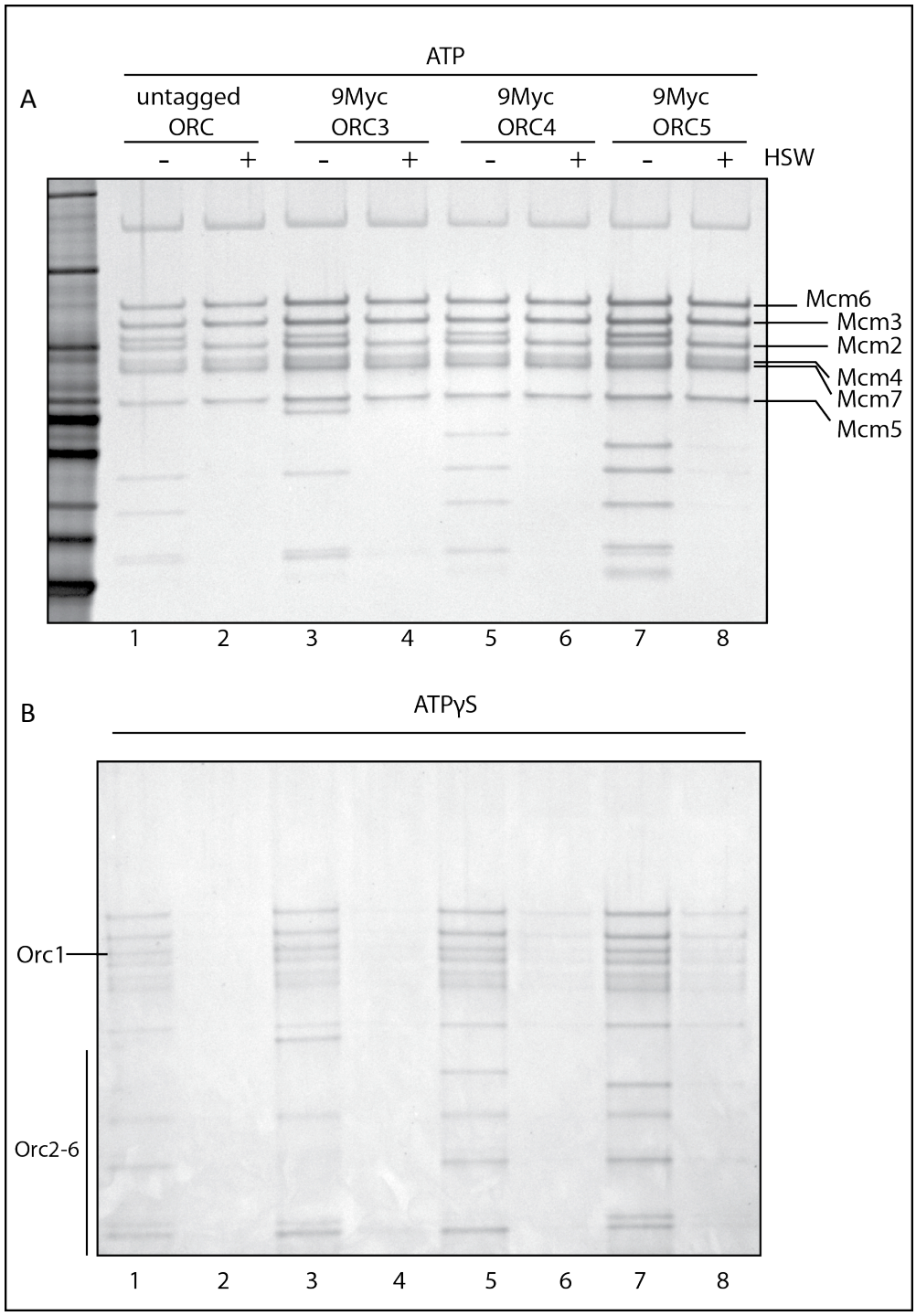

Figure 4.6 Testing 9x Myc-tagged Orc3, Orc4 and Orc5 for their ability to load Mcm2-7 *in vitro*.

9x Myc Orc3, Orc4 or Orc5 in an ORC complex can load the Mcm2-7 complex *in vitro*. Pre-RC assembly reconstitution performed in ATP (top panel) and in ATPγS (bottom panel) on photocleavable DNA-beads. HSW: high salt wash. DNA cleaved off beads by UVA irradiation. Proteins bound to DNA are detected by silver staining.

4.3.3 Fusion of 3x FLAG or 9x Myc peptides to the C-termini of the ORC subunits

Since I was unable to obtain ORC complexes containing 3x FLAG-Orc2, 9x Myc-Orc1, 9x Myc-Orc2 or 9x Myc-Orc6, I set out to generate C-terminally tagged versions of these subunits. To achieve this, I used a PCR-based strategy to introduce polynucleotide sequences encoding the peptide tags to the 3' ends of those codon optimised ORC genes in a yeast strain. Since the DNA sequence of codon optimised ORC genes differs from that of endogenous ORC genes, I was able to target PCR cassettes containing 3x FLAG or 9x Myc sequences to the 3' ends of codon optimised Orc1, Orc2 and Orc6. In this manner, I obtained yeast strains expressing codon optimised ORC with either *ORC2-3x FLAG* or *ORC2-9x MYC.* I was however unable to obtain yeast strains expressing *ORC1-9x MYC* nor *ORC6-9x MYC*.

ORC complexes containing Orc2-3x FLAG or Orc2-9x Myc were expressed and purified as described in 4.3.2. Figure 4.7A shows a Coomassie-stained polyacrylamide gel of the purified complexes. Both purifications resulted in stoichiometric complexes with a peptide tag fused to the C-terminus of Orc2 (indicated in Figure 4.7A). Both tagged ORC complexes were then tested for their ability to support Mcm2-7 loading *in vitro*. This was to verify that the peptide tags on Orc2 did not interfere with ORC function. Purified ORC (tagged or untagged), Cdc6 and Mcm2-7/Cdt1 were incubated with ARS305 DNA-beads in the presence of ATP or ATPγS. DNA-beads were washed as previously and DNA and bound proteins cleaved from the beads by UVA irradiation. Bound proteins were examined by SDS PAGE followed by silver staining.

Figure 4.7B shows that in the presence of ATP: Mcm2-7 and ORC bound DNA-beads, whether or not Orc2 was fused to a peptide tag (lanes 1, 3 & 5). Following high salt extraction, Mcm2-7 remained bound whilst ORC was quantitatively removed (lanes 2, 4 & 6). In the presence of ATPγS: ORC, Cdc6 (band overlaps with Orc5) and Mcm2-7/Cdt1 were detected after a low salt wash (Figure 4.7C, lanes 1, 3 & 5); however, these were all quantitatively removed by high salt extraction (Figure 4.7C, lanes 2, 4 & 6).

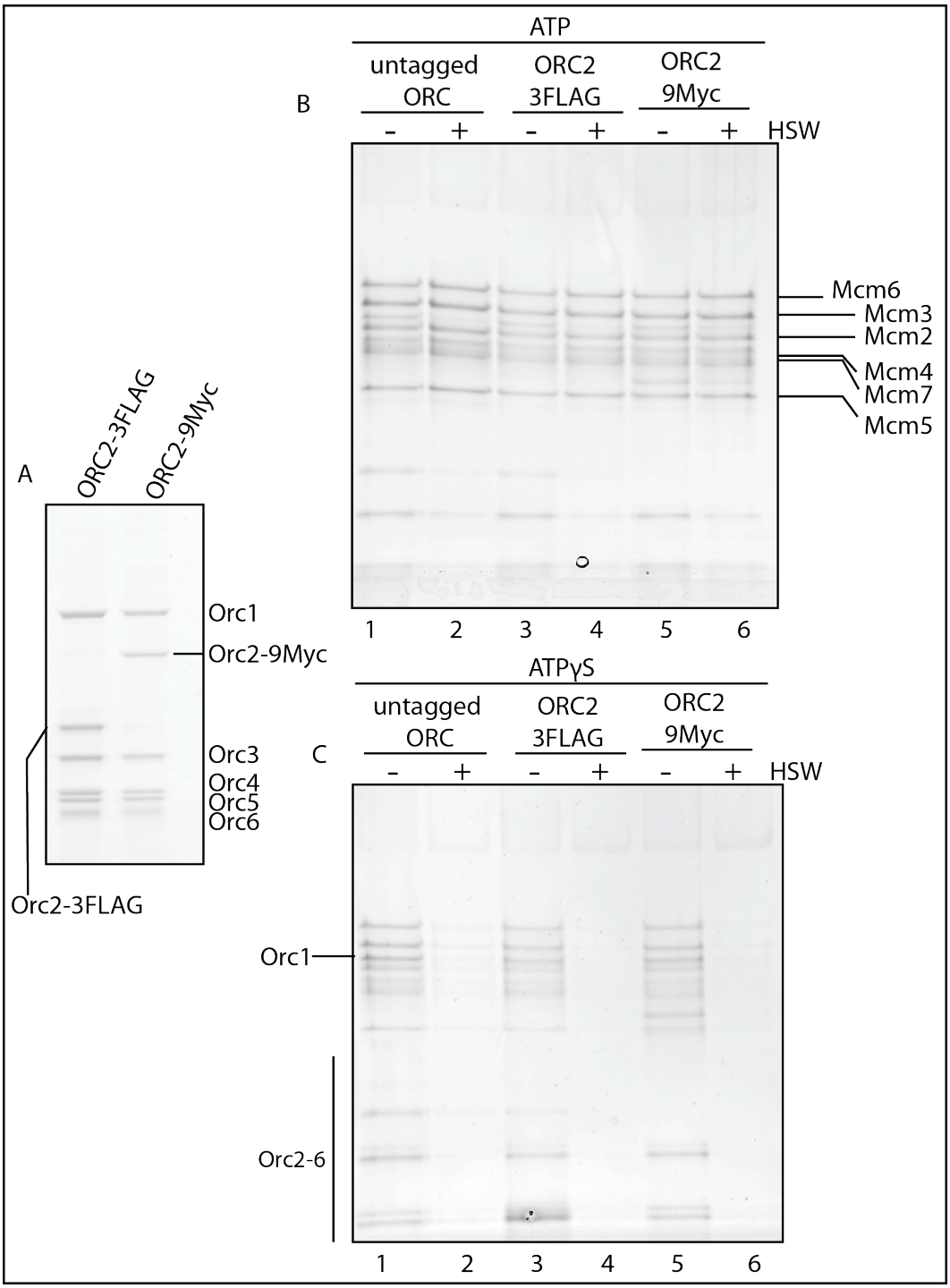

Figure 4.7 C-terminal fusions of 9x Myc or 3x FLAG to Orc2 in the ORC complex

(A) Coomassie stained SDS PAGE of purified ORC complexes containing either a 3x FLAG or a 9x Myc on the C-terminus of Orc2. (B) Pre-RC assembly reconstitution performed in ATP on photocleavable DNA-beads. HSW: high salt wash. DNA cleaved off beads by UVA irradiation. Proteins bound to DNA are detected by silver staining. Orc2-3x FLAG and Orc2-9x Myc are capable of loading the Mcm2-7 complex *in vitro*. (C) As in B, except reconstitution performed in the presence of ATPγS.

These data show that ORC complexes containing Orc2-3x FLAG or Orc2-9x Myc were capable of supporting Mcm2-7 loading *in vitro* and were therefore suitable for use in stoichiometry or interaction assays.

4.4 Fusion of 3x FLAG or 9x Myc peptides to the Mcm2-7/Cdt1 subunits

In the presence of ATP, a double hexamer of Mcm2-7 is loaded around double stranded DNA. Since single Mcm2-7/Cdt1 heptamers have not been visualised (by EM) on DNA (Remus et al., 2009), it is thought that the Mcm2-7 double hexamer is loaded in a concerted manner. In order to resolve whether the Mcm2-7 hexamers are loaded sequentially or in a concerted manner, I wanted to examine the stoichiometry of Mcm2-7 prior to ATP hydrolysis (ATPγS). I also wanted to characterise MCM interactions during pre-RC formation. For these reasons, I fused one of the Mcm2-7 subunits to a 3x FLAG or 9x Myc peptide.

In chapter 3, I described how endogenous Mcm2-7/Cdt1 was purified from G1 arrested yeast extracts. This purification required 100 L of cells due to low expression levels and was therefore time consuming and laborious. In order to improve this procedure, a yeast strain was generated where all of the Mcm2-7 subunits and Cdt1 are expressed from the inducible *GAL1-10* promoter (Jordi Frigola) (Frigola et al., 2013). This increased expression levels of Mcm2-7/Cdt1 whereby 1-1.5 mg of protein could be obtained from 2 L of cells. In this strain, Mcm3 is fused to a 3x FLAG peptide tag at its N-terminus. Purification was achieved by anti-FLAG immunoaffinity purification, followed by gel filtration chromatography. This results in a stoichiometric complex of Mcm2-7/Cdt1 that elutes from gel filtration in the same fraction as thyroglobulin (670 kDa). Figure 4.8A (lane 3) shows a Coomassie-stained polyacrylamide gel of this purified Mcm2-7/Cdt1 complex containing 3x FLAG-Mcm3.

Since one of the Mcm2-7 subunits was to be fused to a 9x Myc or a 3x FLAG peptide and not both, anti-FLAG immunoaffinity purification could not be used as a means of purifying the complex. To circumvent this problem, I fused Mcm3 to a

CBP tag at its N-terminus. I chose the CBP tag as it had been previously used to purify ORC with successful results. Fusion of Mcm3 to CBP was achieved by introducing a polynucleotide encoding the CBP at the 5' end of Mcm3 in a *GAL1-10* overexpression plasmid. This plasmid was then integrated into a targeted site in a yeast background strain. Mcm2-7/Cdt1 containing CBP-Mcm3 was purified by calmodulin affinity and gel filtration chromatographies. Figure 4.8A (lane 4) shows a Coomassie-stained Mcm2-7/Cdt1 complex containing Mcm3 fused to CBP at its N-terminus. The presence of the CBP tag on Mcm3 then allowed for fusion of the other MCM/Cdt1 subunits to 3x FLAG or 9x Myc peptides and purification of each Mcm2-7/Cdt1 complex in a consistent manner using the CBP tag.

Before proceeding with generating 3x FLAG or 9x Myc-tagged Mcm2-7/Cdt1 complexes, I asked whether Mcm2-7/Cdt1 with a CBP-Mcm3 could be loaded onto DNA-beads *in vitro* in a manner similar to Mcm2-7/Cdt1 containing 3x FLAG-Mcm3. Purified ORC, Cdc6, and the tagged versions of Mcm2-7/Cdt1 (Figure 4.8A) were incubated with origin DNA-beads in the presence of ATP. Washes were performed (Figure 1.5) and the DNA was cleaved from the beads by photocleavage as before. Bound proteins were analysed by SDS PAGE followed by silver staining. Figure 4.8B shows that ORC and Cdc6 can load Mcm2-7/Cdt1 with CBP-Mcm3 or 3x FLAG-Mcm3 in a salt resistant manner with concomitant release of Cdc6 and Cdt1. A high salt wash (HSW) removed ORC but not Mcm2-7. This shows that Mcm2-7/Cdt1 complexes with either a 3x FLAG-Mcm3 or a CBP-Mcm3 are functional for loading *in vitro*. In addition, the presence of a CBP tag on Mcm3 did not appear to alter the Mcm2-7 loading efficiency (Figure 4.8B, compare lanes 2 &4).

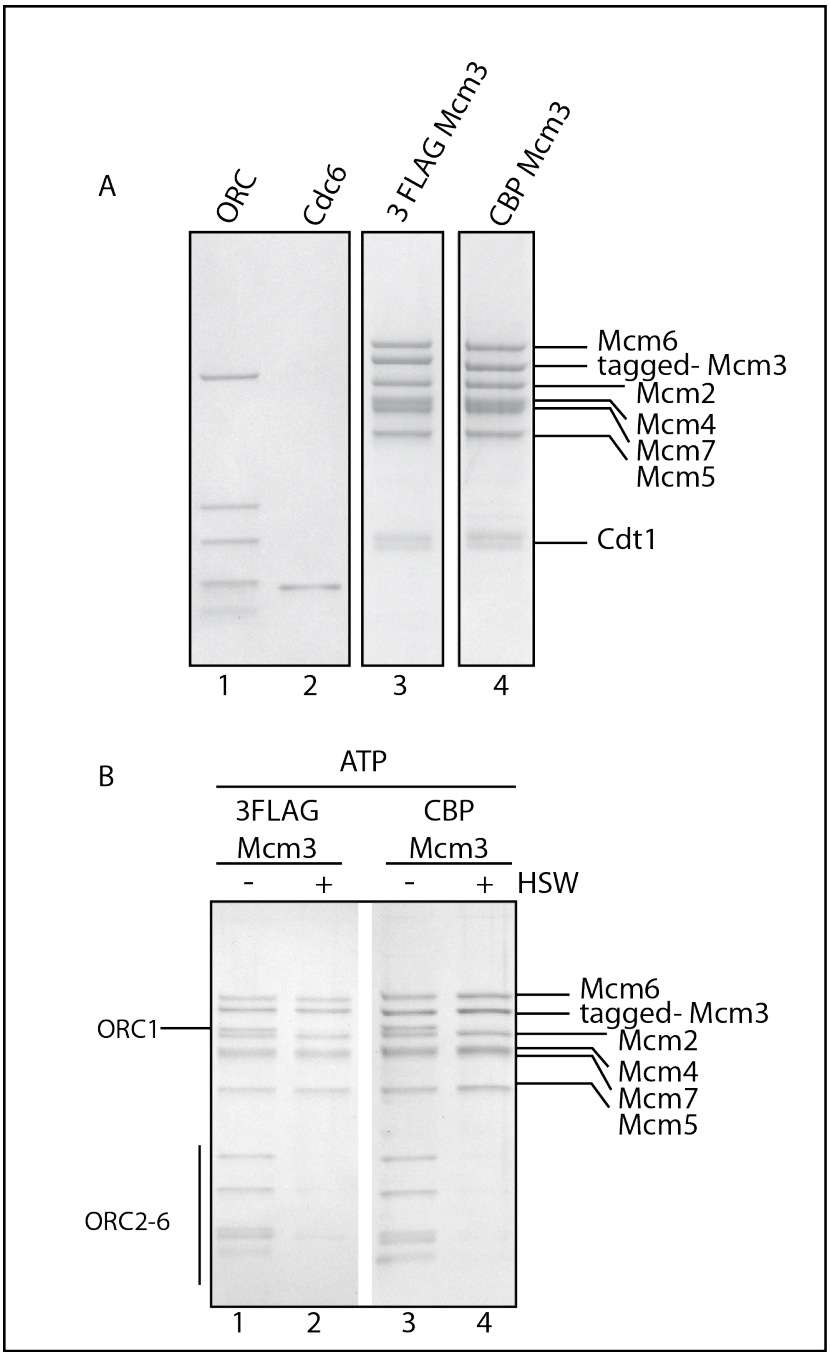

Figure 4.8 Comparison of Mcm2-7/Cdt1 containing 3x FLAG-Mcm3 or CBP-Mcm3

(A) Coomassie stained SDS PAGE of purified proteins (100% inputs for B). (B) Mcm2-7/Cdt1 with 3x FLAG-Mcm3 or CBP-Mcm3 is functional for loading *in vitro*. Purified proteins shown in A, were incubated with origin DNA-beads in the presence of ATP. Unbound proteins were washed away (see Figure 1.5), DNA was cleaved from the beads by UVA irradiation and bound proteins were examined by SDS PAGE followed by silver staining.

In order to examine Mcm2-7/Cdt1 stoichiometry and interactions, I focussed on generating Mcm2-7/Cdt12 complexes containing tagged-Mcm3. The reasons why Mcm3 was chosen will be discussed in Chapter 6. Since a Mcm2-7/Cdt1 complex containing 3x FLAG-Mcm3 was already available, I generated another MCM complex with 9x Myc-Mcm3

A polynucleotide sequence encoding the 9x Myc peptide was inserted at the 5' end of *MCM3* in the *GAL1-10* overexpression plasmid that expressed CBP-Mcm3. This gave rise to: *CBP-9x MYC-MCM3*, whereby I could still utilize the CBP tag for purification purposes. This plasmid was then integrated at a target site in a yeast strain. This generated a yeast strain overexpressing all Mcm2-7/Cdt1 subunits with a 9x Myc peptide tag fused to the N-terminus of Mcm3. I expressed and purified this Mcm2-7/Cdt1 complex by calmodulin affinity and gel filtration chromatographies. The final purified Mcm2-7/Cdt1 complex containing CBP-9myc-Mcm3 is shown in Figure 4.9A (lane 4).

I then assessed whether the Mcm2-7/Cdt1 complex with a 9x Myc tag on Mcm3 (9x Myc-CBP-Mcm3) was functional for loading by ORC and Cdc6 *in vitro*. The purified proteins (Figure 4.9A) were incubated with origin DNA-beads in the presence of ATP and washes were performed as previously (Figure 1.5). DNA was removed from the beads by photocleavage and SDS PAGE followed by silver staining assessed bound proteins. Figure 4.9B shows that ORC and Cdc6 loaded Mcm2-7 in a high-salt wash resistant manner. This was true whether Mcm2-7 contained 3x FLAG-Mcm3 or 9x Myc-Mcm3. ORC was removed by high salt extraction as expected (Figure 4.12B, lanes 2 & 4). These data show that ORC and Cdc6 could load Mcm2-7 complexes containing 3x FLAG-Mcm3 or 9x Myc-CBP-Mcm3 *in vitro* and these complexes were therefore suitable for use in stoichiometry or interaction studies.

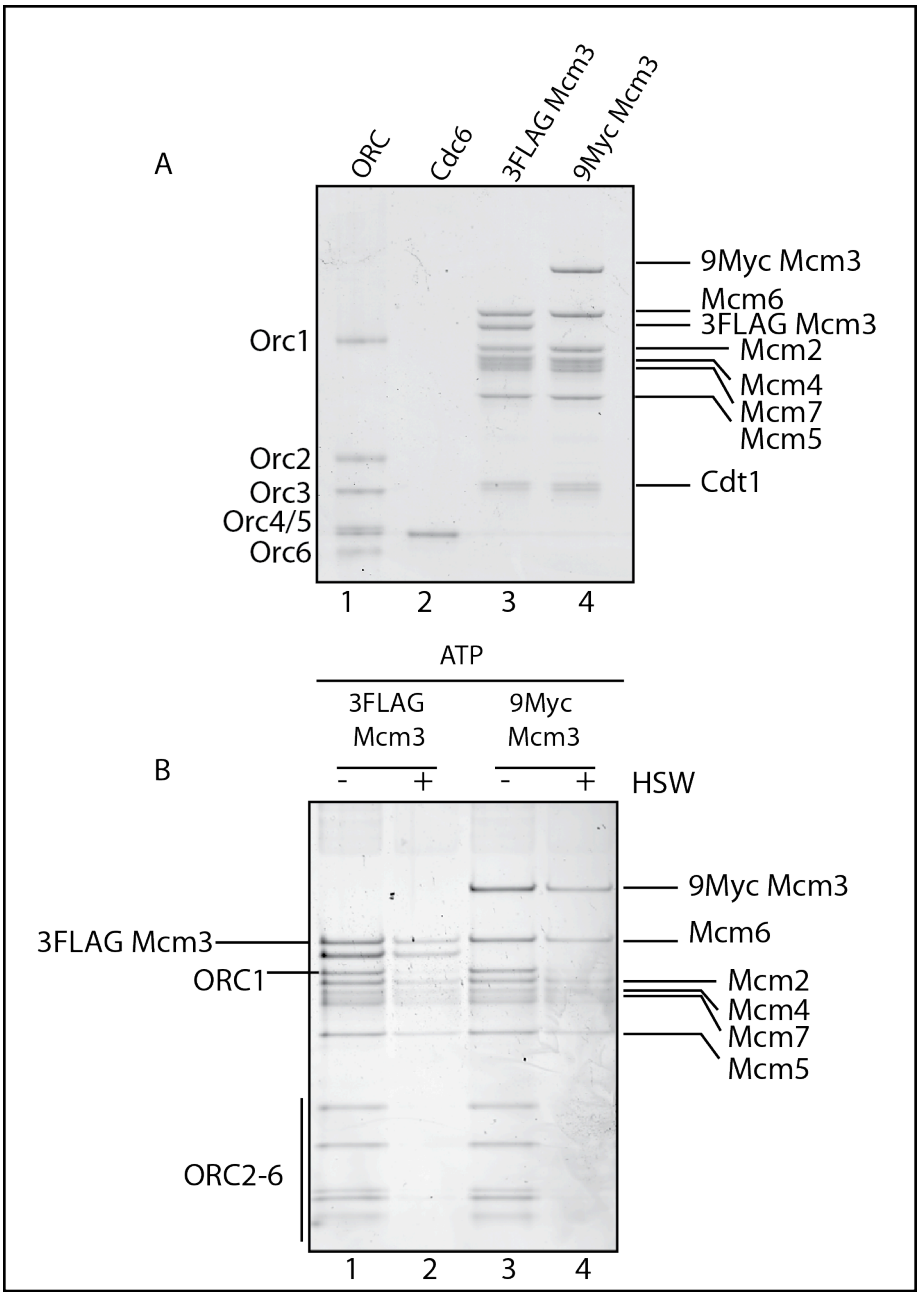

Figure 4.9 Purification and functional testing of 9x Myc-Mcm3 in the Mcm2-7/Cdt1 complex

(A) Coomassie stained SDS PAGE of purified proteins (100% inputs for B). Purified ORC, Cdc6, Mcm2-7/Cdt1 (3x FLAG-Mcm3) and Mcm2-7/Cdt1 (9x Myc-Mcm3) are shown. (B) Test of whether tagged complexes are functional for loading by ORC and Cdc6. Purified proteins shown in A were incubated with ARS305 DNA-Beads in the presence of ATP. Unbound proteins were washed away (see Figure 1.5), DNA was cleaved from the beads by UVA irradiation and bound proteins were examined by SDS PAGE followed by silver staining.

4.4.1 Fusion of 3x FLAG or 9x Myc peptides to the N-terminus of Cdt1 in the Mcm2-7/Cdt1 complex

Since a double hexamer of Mcm2-7 is loaded onto origin DNA upon ATP hydrolysis, and this loading is thought to occur in a concerted manner, it seems possible that multiple Cdt1 molecules act in the recruitment (prior to ATP hydrolysis; ATPγS) of Mcm2-7 to ORC-Cdc6.

In order to examine the stoichiometry of Cdt1 in the "ATPγS complex" I generated 3x FLAG-tagged and 9x Myc-tagged versions of this protein. Polynucleotides encoding a 9x Myc peptide or a 3x FLAG peptide were inserted at the 5' end of *CDT1* in a *GAL1-10* overexpression plasmid. This plasmid was integrated into a yeast background strain expressing CBP-Mcm3 in a targeted manner. I expressed and purified Mcm2-7/Tagged-Cdt1 by calmodulin affinity and gel filtration chromatographies. The final purified Mcm2-7/Cdt1 complexes containing 3x FLAG-Cdt1 or 9x Myc-Cdt1 are shown in Figure 4.10A. Since 9x Myc-Cdt1 could not be distinguished after SDS PAGE, as it overlaps with other bands, I performed an immunoblot against FLAG and Myc (Figure 4.10A, bottom panel). This confirmed the presence of the peptide tags on Cdt1.

I next assessed whether 3x FLAG or 9x Myc-tagged Cdt1 was functional for Mcm2-7 loading *in vitro*. ORC, Cdc6 and Mcm2-7/tagged-Cdt1 were incubated with origin DNA-beads in the presence of ATP. Washes were performed as described previously. DNA was isolated from the beads by photocleavage and bound proteins assessed by SDS PAGE and silver staining. Figure 4.10B shows that MCM complexes containing 3x FLAG-Cdt1 or 9x Myc-Cdt1 were recruited after a low salt wash and that a proportion of these complexes was resistant to high salt extraction (HSW). ORC bound under low salt conditions and was quantitatively removed by a high salt wash (Figure 4.10B). This showed that Cdt1 with a 3x FLAG or 9x Myc tag fused to its N-terminus is functional for Mcm2-7 loading *in vitro* and could therefore be used to examine Cdt1 stoichiometry during pre-RC formation.

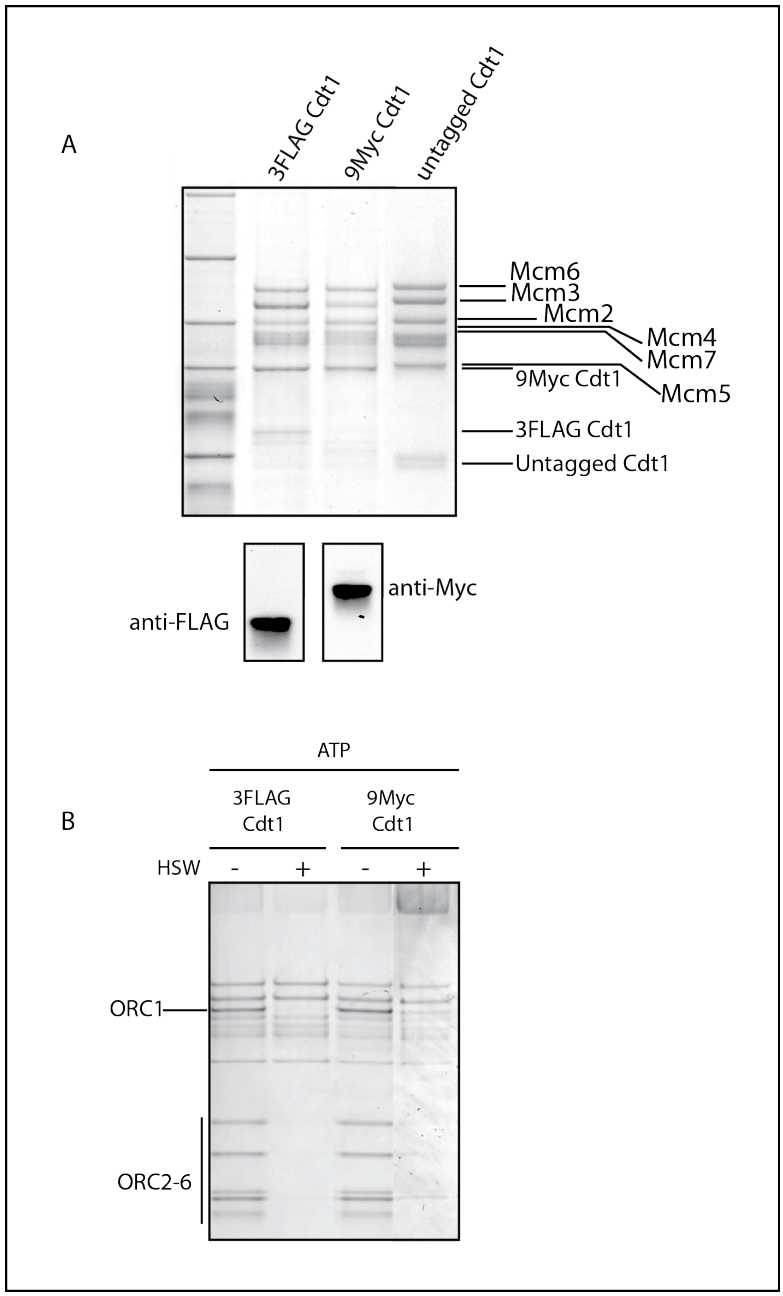

Figure 4.10 Cdt1 with a 3x FLAG or 9x Myc tag fused to its N-terminus is functional for Mcm2-7 loading

(A) Coomassie stained SDS PAGE of purified Mcm2-7/Cdt1 complexes containing 3x FLAG-Cdt1, 9x Myc-Cdt1 or untagged Cdt1. Bottom panel shows an immunoblot against the epitope tags (antibodies indicated). (B) Test of whether tagged complexes are functional for loading by ORC and Cdc6. Tagged complexes were incubated with ORC, Cdc6 and ARS305 DNA-Beads in the presence of ATP. Unbound proteins were washed away (see Figure 1.5), DNA was cleaved from the beads by UVA irradiation and bound proteins were examined by SDS PAGE followed by silver staining.

4.5 Conclusions

In order to examine protein stoichiometry and interactions during pre-RC formation, I set out to generate 3x FLAG or 9x Myc-tagged versions of each of the loading factors (ORC, Cdc6 and Mcm2-7/Cdt1).

I generated purified 9x Myc Cdc6 and 3x FLAG Cdc6 both of which were found to be functional since they were capable of supporting *in vitro* loading of the Mcm2-7 complex. I also generated purified ORC complexes containing 3x FLAG-Orc1, 3x FLAG-Orc3, 3x FLAG-Orc4, 3x FLAG-Orc5, 3x FLAG-Orc6, 9x Myc-Orc3, 9x Myc-Orc4 or 9x Myc-Orc5. Orc2 could not be fused to a peptide tag at its N-terminus, I therefore prepared ORC complexes containing Orc2 fused to a 3x FLAG or a 9x Myc at its C-terminus. I also found that Orc6 could not support a 9x Myc peptide tag. The tagged ORC complexes were found to be functional for Mcm2-7 loading *in vitro*.

To examine Mcm2-7 stoichiometry prior to double hexamer formation, I generated a Mcm2-7/Cdt1 complex containing 9x Myc-CBP-Mcm3. A complex containing 3x FLAG-Mcm3 was already available. I also generated complexes containing 9x Myc-Cdt1 or 3x FLAG-Cdt1 to assess the stoichiometry of Cdt1. These tagged complexes were tested for their ability to be loaded by ORC and Cdc6 *in vitro* and were found to be functional.

This peptide tagging approach created a basis with which I could address intriguing questions about protein stoichiometry and interactions during pre-RC formation. I hoped to use these tagged proteins in analyses to provide some clues into how the Mcm2-7/Cdt1 complex is loaded from a single hetero-heptamer into a double hexamer of Mcm2-7.

Chapter 5. Stoichiometry of pre-RC assembly factors.

5.1 Introduction

ORC and Cdc6 load Mcm2-7/Cdt1 from a single hetero-heptamer into a symmetrical head-to-head double hexamer of Mcm2-7. There are several possibilities of how Mcm2-7 double hexamer loading may occur. For example, one ORC-Cdc6 complex could load two Mcm2-7/Cdt1 hexamers sequentially through the action of ATP hydrolysis. Another possibility is that two ORC-Cdc6 assemblies load one Mcm2-7/Cdt1 each, in opposite orientations. There are several other possibilities that could include looping of the DNA and/or the involvement of multiple Cdc6 molecules.

To try and distinguish between these possibilities and gain insight into how a double hexamer of Mcm2-7 is loaded, we asked: what is the stoichiometry of pre-RC factors during Mcm2-7 loading?

Before Mcm2-7 double hexamer formation, ORC, Cdc6, Cdt1 and Mcm2-7 are "recruited" to origin DNA. This complex is short lived, but can be distinguished *in vitro* when ATP hydrolysis is inhibited by the use of ATPγS (Figure 3.1 iii). In this "ATPγS complex", all the pre-RC components (ORC, Cdc6, Mcm2-7 and Cdt1) are retained at the origin in an ATP-bound state (Figure 3.1 iii). In contrast, upon ATP hydrolysis, Cdc6 and Cdt1 are released (Figure 3.1 i). The "ATPγS complex" is therefore a useful intermediate to study the stoichiometry of each of the pre-RC factors.

In light of this, we asked: how many molecules of ORC, Cdc6, Cdt1 and Mcm2-7 are involved in the initial recruitment of Mcm2-7/Cdt1 to ORC-Cdc6. To address this question, I made use of the peptide tagged pre-RC proteins (Chapter 4) and studied their stoichiometry in the context of the ATPγS complex. I used an approach outlined in Figure 5.1. Briefly, I combined differently tagged proteins (for example 3x FLAG-Cdc6 and 9x Myc-Cdc6) in the presence of other pre-RC

proteins, ATPγS and origin DNA-beads (Figure 5.1, step 1). I then washed off unbound proteins (Figure 5.1, step 2) and performed an immunoaffinity purification using anti-FLAG magnetic beads (Figure 5.1, step 3). Bound proteins were then eluted with 3x FLAG peptide and I examined the eluate for the presence of both the 3x FLAG and the 9x Myc-tagged protein (Figure 5.1, step 4). In this manner I was able to gain insight into the stoichiometry of pre-RC factors during recruitment of Mcm2-7 to ORC-Cdc6.

In this chapter I will describe the results obtained from stoichiometry experiments using peptide tagged protein preparations (see Chapter 4 for details of peptide tagging with 3x FLAG and 9x Myc).

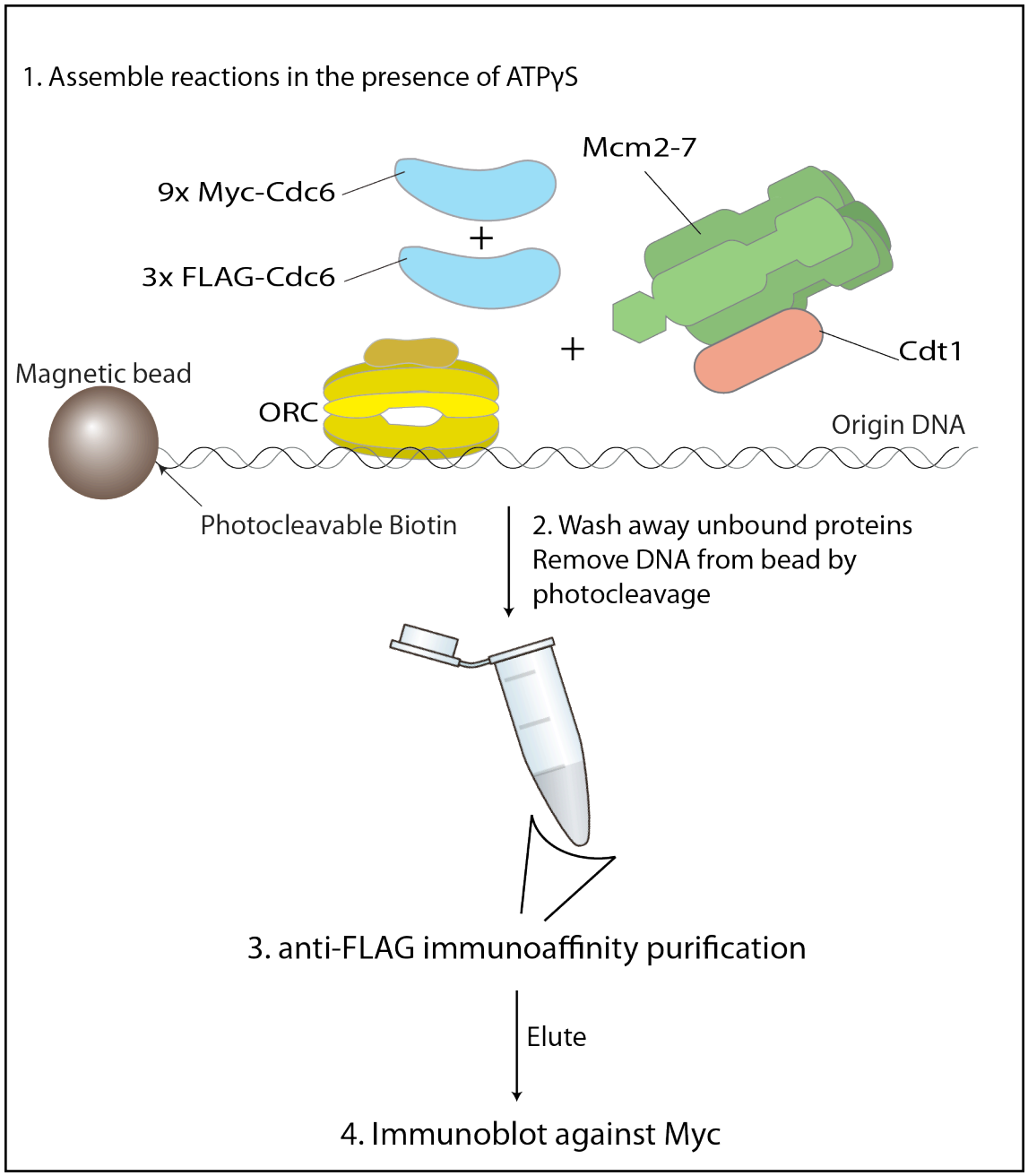

Figure 5.1 Strategy to examine protein stoichiometry during pre-RC assembly.

In this example, we are asking whether there are one or more Cdc6 molecules prior to ATP hydrolysis (ATPγS) by combining equimolar amounts of 9x myc-tagged Cdc6 and 3x FLAG-tagged Cdc6. Steps involved in this approach are numbered.

5.2 Stoichiometry of ORC

In Chapter 3, EMSA analysis revealed that a prominent band formed in the presence of ORC and DNA that represented ORC binding specifically to the ACS at the origin (Chapter 3, sections 3.3 & 3.4). In addition to this prominent band, we also observed a slower migrating smear that appeared to be a precursor for pre-RC formation. We hypothesised that the slower migrating smear could represent multiple ORC molecules binding the DNA in order to load the Mcm2-7 complex. In addition, we reasoned that it was probable that multiple ORC molecules were involved in pre-RC formation since the Mcm2-7 double hexamer was thought to be loaded in a concerted manner (Remus et al., 2009). To address this, I examined the stoichiometry of ORC during the initial recruitment of Mcm2-7/Cdt1 to origin DNA.

In order to examine the stoichiometry of ORC, I made use of the peptide tagged protein preparations from Chapter 4. The approach I took is outlined in Figure 5.1. I chose an ORC complex containing 3x FLAG-Orc3 and another ORC complex containing 9x Myc-Orc3. Both of these tagged complexes appeared to load the Mcm2-7 complex *in vitro* as efficiently as untagged ORC (See Figures 4.4 & 4.6), indicating that the tags did not adversely affect functionality of the ORC complexes. I combined equimolar amounts of 3x FLAG-Orc3 and 9x Myc-Orc3 (Figure 5.3A), Cdc6 and Mcm2-7/Cdt1 (Figure 5.3B) in the presence of ATPγS and origin DNA-beads. Unbound proteins were washed away using a low salt wash buffer (to preserve interactions) and the DNA with bound proteins was cleaved from the beads by UVA irradiation as previously (section 4.2). At this stage reactions were treated with an endonuclease, Benzonase®, to degrade the DNA. This was to eliminate the possibility that more than one pre-RC assembly reaction was taking place on the same piece of DNA, which would alter the results. Following this, an immunoaffinity purification using anti-FLAG M2 magnetic beads was performed. 3x FLAG-Orc2 and bound proteins were eluted by competitive elution with a 3x FLAG peptide. The eluate and unbound proteins were subjected to SDS PAGE and examined by immunoblotting. Figure 5.2 shows a flow chart of the steps involved in this experiment.

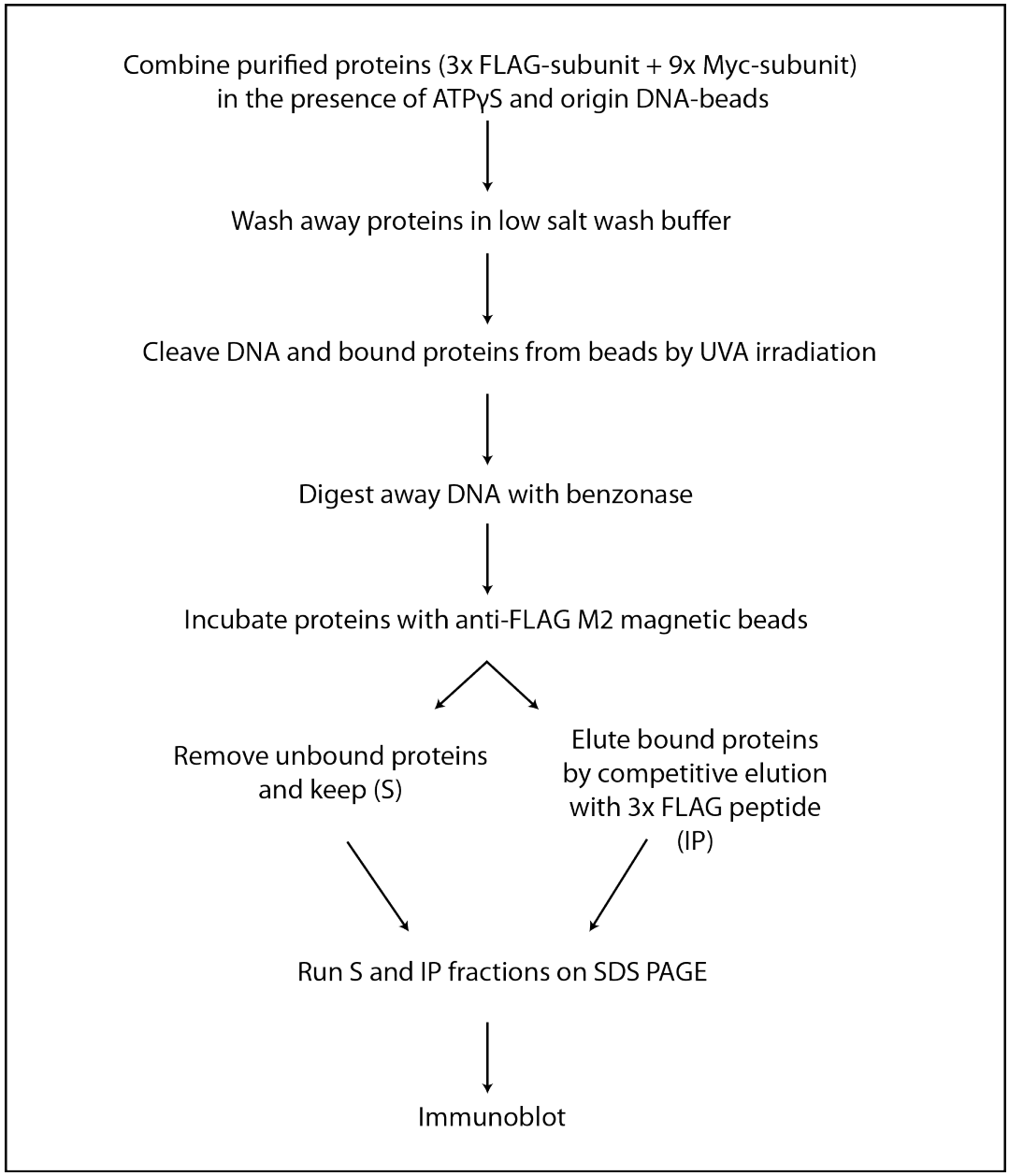

Figure 5.2 Strategy to examine stoichiometry of pre-RC factors

Figure 5.3C shows the results of this experiment. “IP” refers to the fraction eluted from anti-FLAG beads whilst “S” refers to the fraction that was bound to the DNA-beads but did not bind anti-FLAG beads (see Figure 5.2). Lanes 1 & 2 show that 3x FLAG-Orc3 was eluted from anti-FLAG beads (IP). This shows that 3x FLAG-Orc3 bound the origin DNA-beads and could be immunoaffinity purified and eluted. Lanes 3 & 4 show that no detectable 9x Myc-Orc3 was eluted from anti-FLAG

beads. Instead, 9x Myc-Orc3 was detected in the unbound fraction (lane 4, S). This shows that 9x Myc-Orc3 bound the origin DNA-beads but was not eluted from anti-FLAG magnetic beads. 9x Myc-Orc3 was therefore capable of binding DNA-beads but did not elute non-specifically following anti-FLAG immunoaffinity purification. The above was also true when 3x FLAG-Orc3 and 9x Myc-Orc3 were combined in the presence of DNA-beads. Both 3x FLAG-Orc3 and 9x Myc-Orc3 bound DNA-beads but only 3x FLAG-Orc3 was detected in the elution (IP) fraction (lanes 5 & 6).

Lanes 7 & 8 show that in reactions containing 3x FLAG-Orc3 and 9x Myc-Orc3 with Cdc6 and DNA-beads: both 3x FLAG-Orc3 and 9x Myc-Orc3 bound DNA-beads but only 3x FLAG-Orc3 was detected in the elution (IP) fraction. An immunoblot against Cdc6 shows that very little of this protein co-immunoprecipitated with 3x FLAG-Orc3. This was unexpected as Cdc6 forms a complex with ORC on DNA (Coleman et al., 1996, Santocanale and Diffley, 1996). Cdc6 was instead detected in the “S” fraction (lane 8), indicating that Cdc6 had bound the DNA-beads in the presence of ORC. Perhaps in this case, most of the Cdc6 in the reaction was in complex with 9x Myc-Orc3 and therefore did not co-purify with 3x FLAG-Orc3.

Lanes 9 & 10, show that in reactions containing 3x FLAG-Orc3, 9x Myc-Orc3, Mcm2-7/Cdt1 and DNA-beads: only 3x FLAG-Orc3 and not 9x Myc-Orc3 was detected in the elution fraction (IP) as above. Mcm2 was not detected either in the unbound (S) or the elution fractions (IP), this is because Mcm2-7 requires Cdc6 to associate with origins (Donovan et al., 1997).

Lanes 11 & 12 show that in reactions containing 3x FLAG-Orc3, 9x Myc-Orc3, Cdc6 and Mcm2-7/Cdt1 and DNA-beads: both 3x FLAG-Orc3 and 9x Myc-Orc3 bound DNA-beads but only 3x FLAG-Orc3 was detected in the elution (IP) fraction. This shows that 9x Myc-Orc3 could not be co-immunoprecipitated with 3x FLAG-Orc3, even when all pre-RC components were present. Lanes 11 & 12 also show that a proportion of Cdc6 and Mcm2 could be co-immunoprecipitated with 3x FLAG-Orc3. This indicates that an ATPγS complex was formed, but that this complex did not contain 3x FLAG-Orc3 and 9x Myc-Orc3 together.

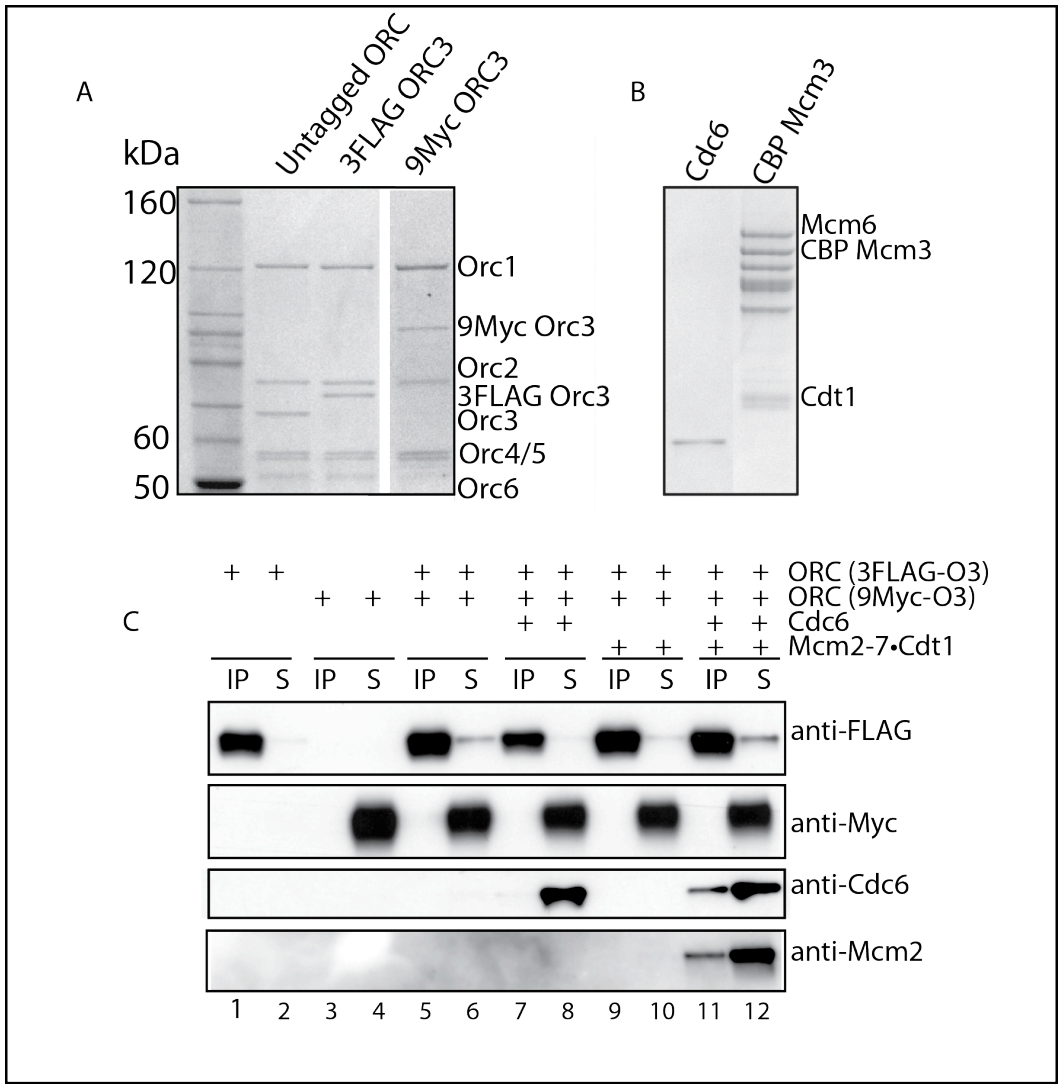

Figure 5.3 Stoichiometry of ORC

(A) Coomassie stained SDS PAGE of ORC complexes containing 3x FLAG-Orc3 or 9x Myc-Orc3 alongside untagged ORC. (B) Coomassie stained SDS PAGE of purified Cdc6 and Mcm2-7/Cdt1 used in the stoichiometry experiment. (C). Reactions were assembled in the presence of ATPγS and origin DNA-beads. Reactions were then treated as outlined in Figure 5.1. Both IP and S fractions were subjected to SDS PAGE followed by immunoblotting with the indicated antibodies. 50% of IP and 50% of S fractions was loaded per immunoblot well.

Taken together, these data suggest that contrary to our hypothesis, only one ORC molecule is involved in the initial recruitment of Mcm2-7/Cdt1 to ORC-Cdc6.

5.3 Stoichiometry of Cdc6

Although I only detected one ORC molecule during the recruitment of Mcm2-7/Cdt1 to ORC-Cdc6, it is still possible that multiple Cdc6 molecules function during this process. For example, a single ORC in combination with two Cdc6 molecules could recruit two Mcm2-7/Cdt1 complexes into a DNA loop. I therefore asked: what is the stoichiometry of Cdc6 during pre-RC formation?

To determine whether one or more Cdc6 molecules is involved in the initial recruitment of Mcm2-7/Cdt1, I used the peptide-tagged proteins 3x FLAG-Cdc6 and 9x Myc-Cdc6 (Chapter 4, section 4.2) and the strategy outlined in section 5.2 (also see Figures 5.1 & 5.2). Both 3x FLAG and 9x Myc-tagged Cdc6 were functional for Mcm2-7 loading *in vitro* (Figure 4.3), indicating that the tags did not interfere with the function of Cdc6.

To examine Cdc6 stoichiometry, 3x FLAG-Cdc6 and 9x Myc-Cdc6 were combined with ORC, Mcm2-7/Cdt1 (Figure 5.4A), DNA-beads and ATPγS. This experiment was carried out exactly as described for ORC in section 5.2.

Figure 5.4B (lanes 1 & 2) shows that 3x FLAG-Cdc6 was not present either in the elution fraction (IP) or the unbound fraction (S) in the absence of ORC. This is expected, as Cdc6 is not recruited to origins in the absence of ORC (Coleman et al., 1996, Santocanale and Diffley, 1996). Lane 3 shows that in reactions containing 9x Myc-Cdc6 and DNA, 9x Myc-Cdc6 was not immunoaffinity purified by anti-FLAG beads. However, lane 4 shows that 9x Myc-Cdc6 bound to the DNA-beads in the absence of ORC. This binding to the DNA likely represents 9x Myc-Cdc6 precipitating on the DNA, as Cdc6 requires ORC for binding. In addition, in reactions containing 9x Myc-Cdc6, 3x FLAG-Cdc6 and DNA: both 9x Myc-Cdc6 and 3x FLAG-Cdc6 were detected in eluates and unbound fractions (lanes 5 & 6). This indicates that 9x Myc-Cdc6 was causing precipitation of 3x FLAG-Cdc6 as well as itself precipitating on the DNA. In agreement with this, when 9x Myc-Cdc6 was tested for functionality in Mcm2-7/Cdt1 loading *in vitro*, 9x Myc-Cdc6 appeared to stick to the DNA-beads, even following a high salt wash (Figure 4.3C).

Due to this apparent precipitation or aggregation property of 9x Myc-Cdc6, I was unable to interpret the results of this experiment and we decided to try a different approach.

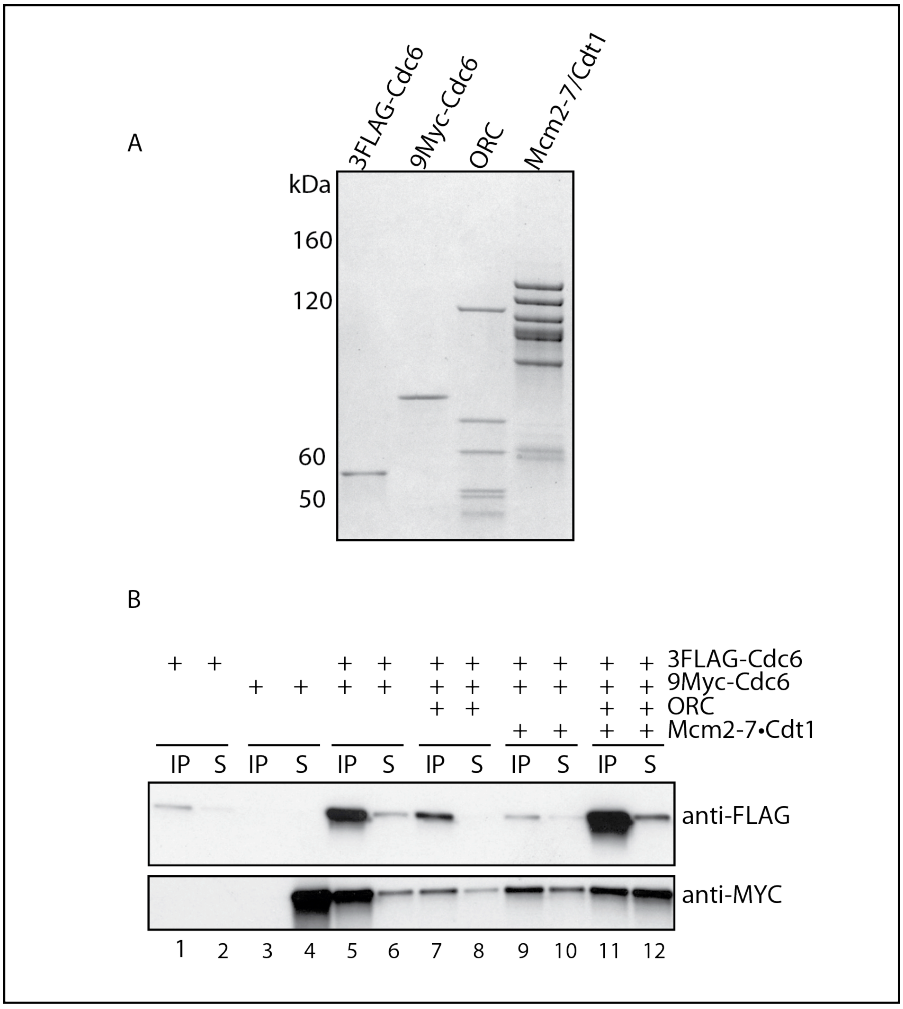

Figure 5.4 Stoichiometry of Cdc6 using 3x FLAG-Cdc6 and 9x Myc-Cdc6

(A) Coomassie stained SDS PAGE of inputs (100%). (B) Reactions were assembled in the presence of ATPγS and origin DNA-beads. Reactions were then treated as outlined in Figure 5.1. Both IP and S fractions were subjected to SDS PAGE followed by immunoblotting with the indicated antibodies. 50% of IP and 50% of S fractions was loaded per immunoblot well.

Since 9x Myc-Cdc6 appeared to precipitate on DNA and affect the results of experiments, I decided to use untagged Cdc6 as a substitute. A monoclonal antibody against Cdc6 was available, making the use of Cdc6 feasible and we also

knew that untagged Cdc6 was functional (Chapter 4, section 4.2). In addition, the 3x FLAG epitope tag, fused to the N-terminus of Cdc6, causes a change in molecular weight that allowed me to distinguish 3x FLAG-Cdc6 from untagged Cdc6 (Figure 5.5A).

I therefore proceeded to examine Cdc6 stoichiometry in the initial recruitment of Mcm2-7/Cdt1 to ORC-Cdc6 using 3x FLAG-Cdc6 and untagged Cdc6.
The exact same experiment as above was repeated with 3x FLAG-Cdc6 and untagged Cdc6. The steps involved are outlined in Figures 5.1 and 5.2.

Figure 5.5 shows that 3x FLAG Cdc6 could not be immunoaffinity purified in the absence of ORC (lane 1). 3x FLAG Cdc6 was also unable to bind DNA-beads in the absence of ORC (lane 2). This was also true of untagged Cdc6 (lanes 3 & 4) and when 3x FLAG-Cdc6 and untagged Cdc6 were combined in the absence of ORC (lanes 5 & 6). This showed that untagged Cdc6 did not aggregate and precipitate on the DNA, as had been the case for 9x Myc-Cdc6.

Both 3x FLAG-Cdc6 and untagged Cdc6 bound DNA-beads in the presence of ORC (Figure 5.5, lanes 7 & 8). However, only 3x FLAG could be immunoaffinity purified from this reaction (lane 7). This was also true when all pre-RC components were present (lanes 11 & 12). Untagged Cdc6 was only detected in the unbound (S) fraction, indicating that it bound DNA-beads but could not be co-purified with 3x FLAG-Cdc6. In this reaction, a fraction of Mcm2 co-purified with 3x FLAG-Cdc6 (lane 11), indicating that a complex was formed in ATPγS, but this complex only contained either 3x FLAG-Cdc6 or untagged Cdc6 and not both.

These results suggest that only one molecule of Cdc6 is involved in the recruitment of Mcm2-7/Cdt1 to ORC-Cdc6.

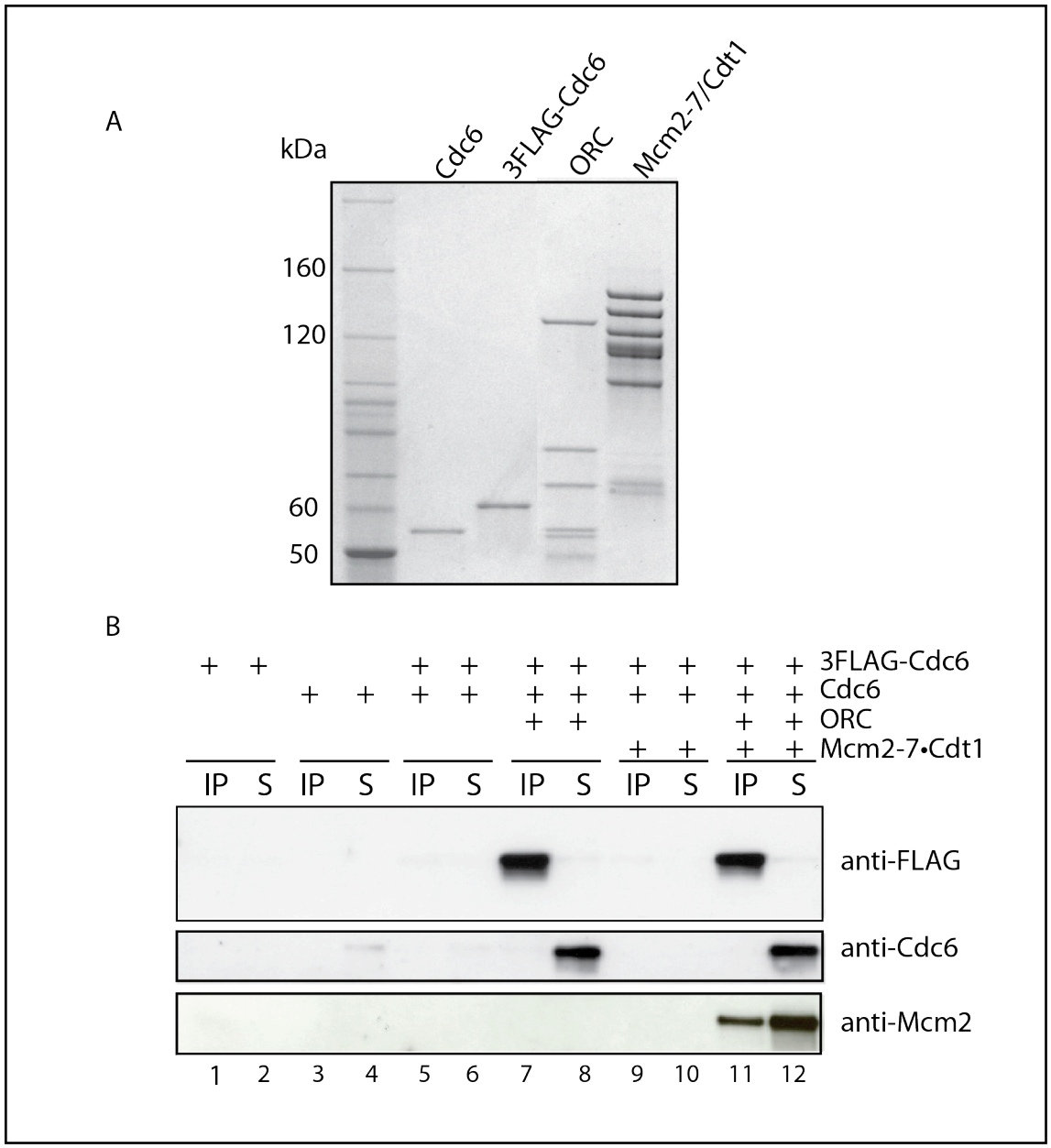

Figure 5.5 Stoichiometry of Cdc6, using 3x FLAG-Cdc6 and untagged Cdc6

(A) Coomassie stained SDS PAGE of inputs (100%). (B) Reactions were assembled in the presence of ATPγS and origin DNA-beads. Reactions were then treated as outlined in Figure 5.1. Both IP and S fractions were subjected to SDS PAGE followed by immunoblotting with the indicated antibodies. 50% of IP and 50% of S fractions was loaded per immunoblot well.

5.4 Stoichiometry of the Mcm2-7 Complex

Based on electron microscopy studies, the Mcm2-7 double hexamer appeared to be loaded onto DNA in a cooperative fashion, (Remus et al., 2009). Mcm2-7/Cdt1 double heptamers were never seen prior to loading and Mcm2-7 single hexamers were never observed on DNA after loading (Remus et al., 2009). This suggested that the Mcm2-7 hexamers are loaded in a concerted manner. However, our results indicated that one molecule of ORC and one molecule of Cdc6 act in the initial recruitment of Mcm2-7/Cdt1 to ORC-Cdc6. It was therefore perplexing how one ORC-Cdc6 complex could load two Mcm2-7 hexamers simultaneously. To address whether Mcm2-7 hexamers are loaded in a concerted or sequential manner, we asked: what is the stoichiometry of Mcm2-7? We know that upon ATP hydrolysis the Mcm2-7 complex is loaded as a double hexamer. But, how many Mcm2-7 molecules are present when ATP hydrolysis is blocked? Insight into the stoichiometry of Mcm2-7 prior to loading (before ATP hydrolysis), would give some insight into whether the Mcm2-7 hexamers are loaded sequentially or simultaneously.

To examine Mcm2-7 stoichiometry, I used Mcm2-7 complexes containing a 3x FLAG or a 9x Myc epitope tag at the N-terminus of Mcm3 (Chapter 4, section 4.4). Both of these complexes were found to be functional for pre-RC formation *in vitro*. These complexes were combined in equimolar amounts with ORC, Cdc6 (Figure 5.6A) and origin DNA-beads. The reactions were performed in the presence of ATP or ATPγS. Here I could take advantage of the fact that in the presence of ATP, the Mcm2-7 complex is loaded as a double hexamer, and I should therefore detect both 3x FLAG-tagged and 9x Myc-tagged Mcm3. This acted as a useful positive control. ATPγS was used to block ATP hydrolysis and examine the stoichiometry of Mcm2-7 prior to loading. The experiment was then carried out as described previously and in Figures 5.1 and 5.2.

Figure 5.6B shows immunoblots against the FLAG and Myc epitopes. The first panel (lanes 1-6) shows fractions eluted from anti-FLAG immunoaffinity purification (IP). The second panel (lanes 7-12) shows fractions that did not bind anti-FLAG beads, but were bound to DNA-beads (S). Lanes 1 & 4, show that 9x Myc-Mcm3

was not eluted from anti-FLAG immunoaffinity purification in the absence of 3x FLAG-Mcm3. This shows that there was no background binding of the 9x Myc tag to the anti-FLAG beads. 9x Myc-Mcm3 was still, however, able to bind DNA-beads in the presence of ORC and Cdc6 (lanes 7 & 10). Lane 2 shows that 9x Myc-Mcm3 was co-immunoprecipitated with 3x FLAG-Mcm3 in the presence of ATP. This indicates that a double hexamer of Mcm2-7 was formed in the presence of ATP. Lane 3 shows that this co-immunoprecipitation was dependent on ORC. Lane 9 shows that ORC was required for binding of both 3x FLAG and 9x Myc-tagged Mcm3 to DNA-beads.

In contrast, lane 5 (Figure 5.6) shows that when ATP hydrolysis was blocked by incubation with ATPγS, only 3x FLAG Mcm3 could be immunoaffinity purified and 9x Myc Mcm3 was only detected in the unbound fraction (lane 11). This was dependent on the presence of ORC (lanes 6 & 12).

These results indicate that prior to ATP hydrolysis, one copy of Mcm2-7 is recruited to ORC-Cdc6. ATP hydrolysis then somehow causes double hexamer assembly. This suggests that the Mcm2-7 hexamers are loaded one at a time through the action of ATP hydrolysis. Indeed, a recent study by Evrin et al. showed that in the absence of ATPase activity, Mcm2-7 association with origin DNA is restricted to a single hexamer (Evrin et al., 2013).

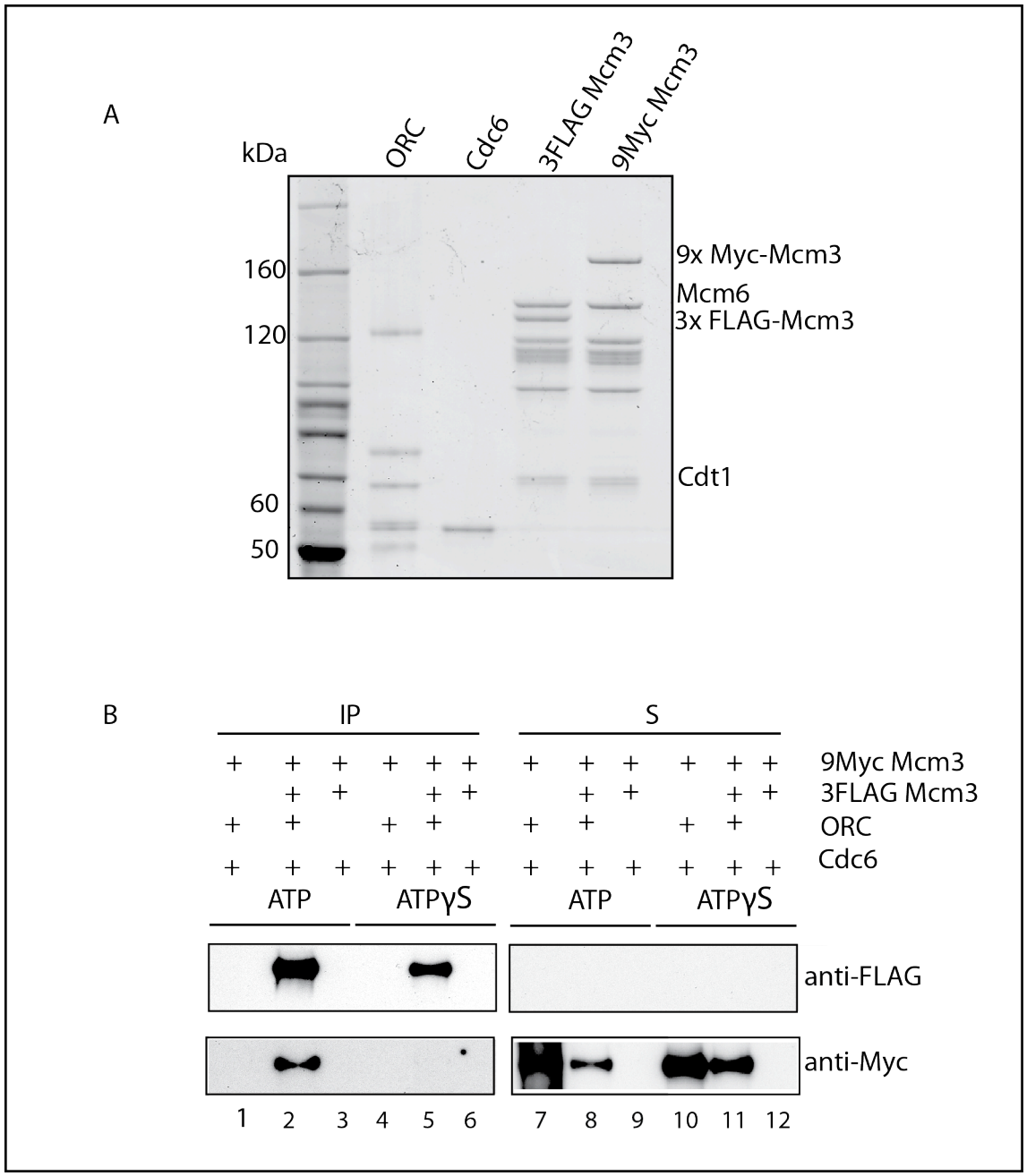

Figure 5.6 Stoichiometry of Mcm2-7

A single copy of Mcm3 is detected in the absence of ATP hydrolysis.
(A) Coomassie stained SDS PAGE of inputs (100%). (B) Reactions were assembled in the presence of ATP or ATPγS and origin DNA-beads. Reactions were then treated as outlined in Figure 5.1. Both IP and S fractions were subjected to SDS PAGE followed by immunoblotting with the indicated antibodies. 50% of IP and 50% of S fractions was loaded per immunoblot well.

5.4.1 Stoichiometry of the Mcm2-7 complex in the absence of Cdc6 ATPase activity

Whilst examining the stoichiometry of Mcm2-7, we found that prior to ATP hydrolysis, the Mcm2-7 complex is most likely recruited to ORC-Cdc6 as a single hexamer. Following ATP hydrolysis, Mcm2-7 is a double hexamer that encircles double stranded DNA (Remus et al., 2009, Evrin et al., 2009). This indicates that ATP hydrolysis induces double hexamer formation.

Orc1-Orc5 and Cdc6 are members of the AAA+ family of proteins (Iyer et al., 2004) however, only Orc1 and Cdc6 have been shown to hydrolyse ATP (Randell et al., 2006, Bowers et al., 2004, Klemm et al., 1997). The AAA+ proteins have several conserved elements that are important for ATP binding and hydrolysis, including the Walker A and Walker B domains (see Chapter 1, section 1.2.2.1). The Walker A motif of *S.cerevisiae* Cdc6 is thought to be important for ATP binding. A mutation in a conserved lysine of the Walker A motif of Cdc6 is lethal *in vivo*, inhibits Cdc6 interaction with ORC and prevents Mcm2-7 loading onto chromatin (Perkins and Diffley, 1998, Weinreich et al., 1999). In contrast, the Walker B motif of Cdc6 is required for ATP hydrolysis (Randell et al., 2006). Mutation of a conserved glutamic acid to a glycine residue (E224G) in the Walker B motif of Cdc6 causes dominant lethality *in vivo* (Perkins and Diffley, 1998) and a block in Mcm2-7 loading *in vitro* (Randell et al., 2006). In light of this, we asked whether the ATPase activity of Cdc6 regulates Mcm2-7 double hexamer formation.

To address this question, I cloned Cdc6 harbouring a mutation in the Walker B motif (E224G) into a GST expression plasmid. E224G-Cdc6 was expressed and purified from *E.coli* as for Cdc6 (purification by Jordi Frigola; see Chapter 4, section 4.2). I next tested whether Cdc6 harbouring a mutation in its Walker B motif (E224G) was defective in Mcm2-7 loading *in vitro* in our system. ORC, Cdc6 and Mcm2-7 were incubated with origin DNA-beads in the presence of ATP. Washes were performed as described previously (Figure 1.5). DNA was isolated from the beads by photocleavage and bound proteins assessed by SDS PAGE and silver staining.

Figure 5.7 shows the results of this experiment. Lanes 1-6 show Mcm2-7 loading in the presence of increasing amounts of Cdc6. Lanes 7-12 show Mcm2-7 loading in the presence of increasing amounts of E224G-Cdc6. Lanes 1 & 2 (Figure 5.6) show that Mcm2-7 was loaded onto DNA-beads in a high salt resistant manner, in the presence of Cdc6. This salt resistant loading of Mcm2-7 was not greatly affected by increasing amounts of Cdc6 (lanes 3-6). Lanes 7 & 8 show that Mcm2-7 was also loaded onto DNA-beads in a high salt resistant manner, in the presence of E224G- Cdc6. As the amount of E224G Cdc6 was increased, the amount of salt resistant loaded Mcm2-7 decreased.

This was somewhat surprising, as the E224G-Cdc6 mutant has previously been shown to be defective in Mcm2-7 loading (Randell et al., 2006). However, we did observe a decrease in Mcm2-7 loading as more E224G-Cdc6 was added to the reactions. These results imply that the E224G-Cdc6 protein may be unstable or may perhaps aggregate when high amounts are used, thus impairing its function in Mcm2-7 loading. This may help to explain the discrepancy between our result and that of others. These data also imply that the ATP hydrolysis of Cdc6 is not required for Mcm2-7 loading, or that it is not the only ATPase activity required.

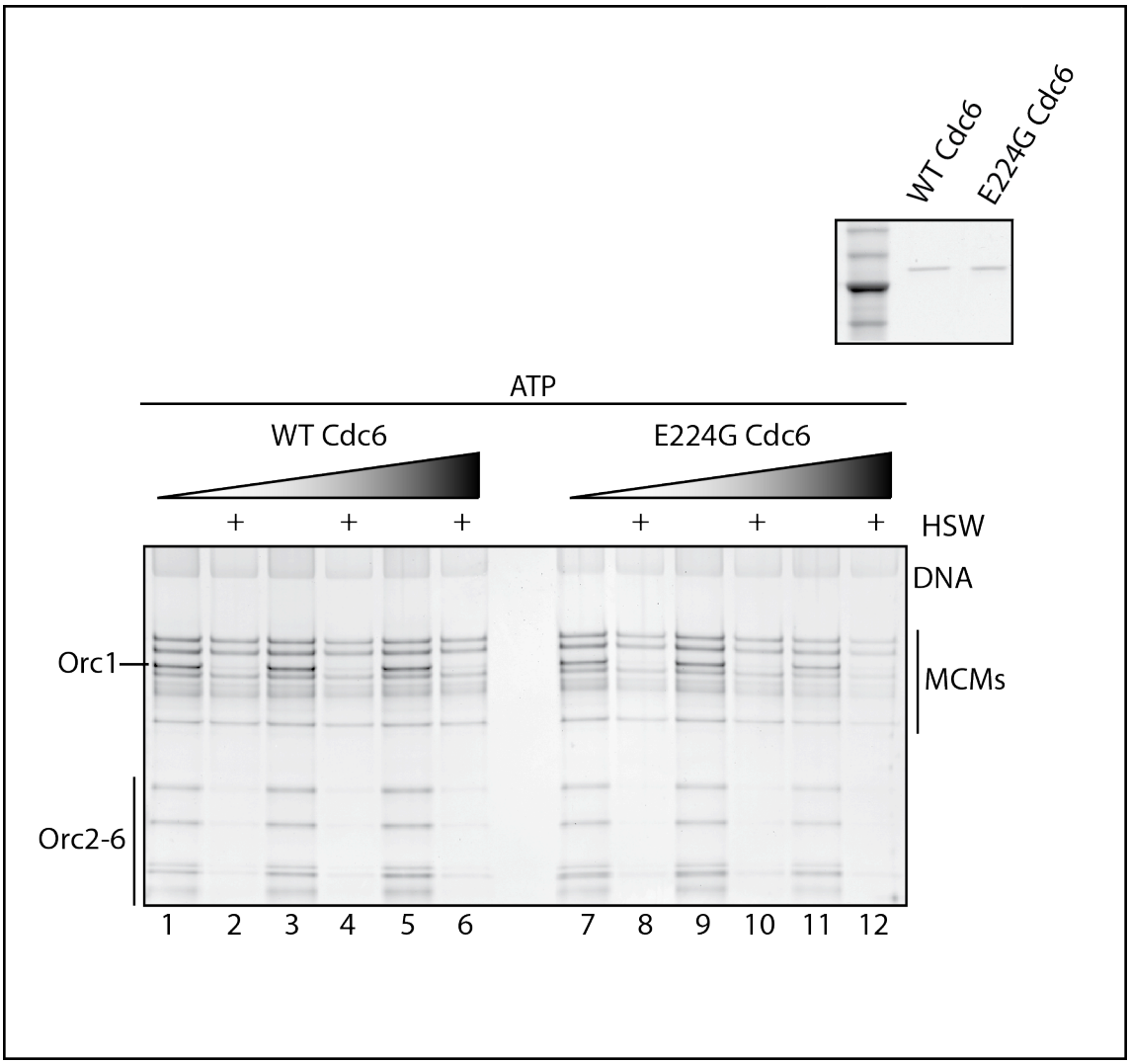

Figure 5.7 Cdc6 ATP hydrolysis is not required for Mcm2-7 loading *in vitro*

Top panel shows purified Cdc6 (WT Cdc6) and Walker B mutant Cdc6 (E224G Cdc6). Those are the inputs (100%) used for lanes 1, 2, 7 and 8. Bottom panel shows *in vitro* reconstitution of pre-RC formation in the presence of increasing amounts of Cdc6 (WT Cdc6) or Walker B mutant Cdc6 (E224G Cdc6). Purified ORC, Cdc6, or E224G-Cdc6, and Mcm2-7/Cdt1 were incubated with origin DNA-beads in the presence of ATP. DNA-beads were washed as outlined in Figure 1.5. 50% of the reactions were then subjected to SDS PAGE and silver staining. HSW: High salt wash.

Once I established that Cdc6 harbouring a mutation in the Walker B motif was in fact functional for Mcm2-7 loading, we proceeded to ask whether the ATPase activity of Cdc6 regulates Mcm2-7 double hexamer formation. To address this question, I again utilised Mcm2-7/Cdt1 complexes containing 3x FLAG-Mcm3 or 9x

Myc-Mcm3. These complexes were combined with ORC and Cdc6 or E224G Cdc6 in the presence of ATP or ATPγS and DNA-beads. Here I used low amounts of both Cdc6 and E224G Cdc6 that showed approximately equal loading of Mcm2-7 in Figure 5.7 (lanes 2 & 8). The reactions were treated as previously (see Figures 5.1 & 5.2) and the results were analysed by SDS PAGE followed by immunoblotting.

Figure 5.8 shows the result of this experiment. In the top half of this figure (separated by a black line), the IP fractions are shown. These are the fractions that were eluted following anti-FLAG immunoaffinity purification. The bottom half of the figure shows the fractions that did not bind the anti-FLAG resin, but that did bind DNA-beads. The figure is further separated into reactions performed in the presence of ATP or ATPγS.

Lanes 1 & 2 show that 9x Myc-Mcm3 did not elute from anti-FLAG immunoaffinity purification in the absence of 3x FLAG-Mcm3. 9x Myc did, however, bind the DNA-beads (bottom panel, lanes 1 & 2). Lane 3 shows that 3x FLAG-Mcm3 and 9x Myc-Mcm3 co-purified in the presence of ATP, ORC and Cdc6. A proportion of the "double Mcm3" complex was resistant to a high salt wash (lane 4). Lane 5 shows that 3x FLAG-Mcm3 and 9x Myc-Mcm3 also co-purified in the presence of ATP, ORC and E224G Cdc6. A proportion of this binding was also resistant to high salt extraction (lane 6). However, the binding of both 3x FLAG and 9x Myc-tagged Mcm3 in the presence of E224G Cdc6 appeared to be less than that of Cdc6 (compare lanes 3 & 5).

Lanes 7-10 (Figure 5.7) show that 3x FLAG-Mcm3, but not 9x Myc-Mcm3 was immunoaffinity purified in the presence of ATPγS in a salt labile manner. This is consistent with the results presented in section 5.4, indicating that one Mcm2-7 hexamer is recruited prior to ATP hydrolysis. This recruitment of a single hexamer appears to occur whether Cdc6 or E224G-Cdc6 is present in the reaction. However, the recruitment of 3x FLAG-Mcm3 by E224G-Cdc6, appeared to be less than that recruited by Cdc6 (compare lanes 7 & 9). In the ATPγS reactions, I detected Cdc6 but not E224G Cdc6 in the immunoaffinity purified fractions (lanes 7 & 9). Instead

E224G was detected in the unbound fraction. This indicates that whilst E224G was able to recruit Mcm2-7/Cdt1, it did not form a stable “ATPγS complex”.

These data suggest that Cdc6 harbouring an E to G mutation in the Walker B motif is still capable of loading a double hexamer of Mcm2-7 onto DNA. This loading, however, appears to be less efficient than Mcm2-7 loading by Cdc6. This indicates that ATP hydrolysis by Cdc6 plays some role in Mcm2-7 loading, but that ATP hydrolysis by other reaction components is likely to contribute to double hexamer formation.

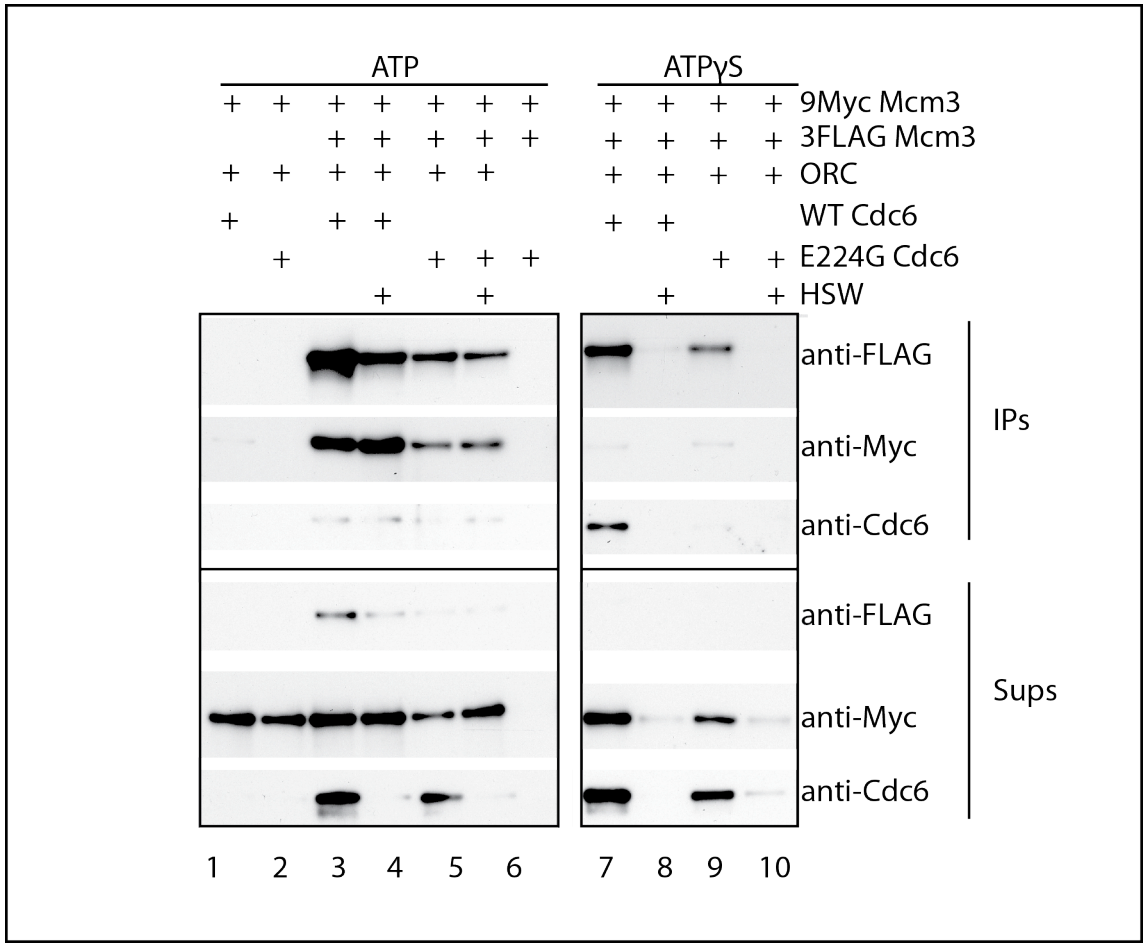

Figure 5.8 of Cdc6 Mcm2-7 stoichiometry in the absence of the ATPase activity of Cdc6

Reactions were assembled in the presence of ATP or ATPγS and origin DNA-beads. Reactions were then treated as outlined in Figure 5.1. Both IP and S fractions were subjected to SDS PAGE followed by immunoblotting with the indicated antibodies. 50% of IP and 50% of S fractions was loaded per immunoblot well.

5.5 Stoichiometry of Cdt1

A study in 2011 suggested that multiple Cdt1 molecules are involved in Mcm2-7 loading onto origin DNA (Takara and Bell, 2011). Data from Takara et al. (2011) indicated that in the absence of ATP hydrolysis, at least two Cdt1 molecules are recruited to the origin.

Since I detected that one Mcm2-7 complex is present at the recruitment stage (prior to ATP hydrolysis) and Cdt1 in *S.cerevisiae* is associated with Mcm2-7, it was difficult to reconcile how multiple Cdt1 molecules and a single Mcm2-7 hexamer could be involved at the recruitment stage. I therefore decided to examine the stoichiometry of Cdt1 in the absence of ATP hydrolysis.

To examine Cdt1 stoichiometry, I used Mcm2-7/Cdt1 complexes containing a 3x FLAG or a 9x Myc epitope tag at the N-terminus of Cdt1 (Chapter 4, section 4.4.1). Both of these complexes were found to be functional for pre-RC formation *in vitro*. These complexes were combined in equimolar amounts with ORC, Cdc6 (Figure 5.8A) and origin DNA-beads. ATPγS was used to block ATP hydrolysis to facilitate study of the stoichiometry of Cdt1 during the recruitment stage of Mcm2-7. The experiment was then carried out as described previously (see Figures 5.1 & 5.2).

Figure 5.9 (bottom panel) shows immunoblots against 3x FLAG-Cdt1 and 9x Myc-Cdt1. Lanes 1-3 show fractions eluted from anti-FLAG immunoaffinity purification. Lanes 4-6 show fractions that did not bind the anti-FLAG beads, but that were bound to DNA-beads prior to purification. Lane 1 shows that 9x Myc-Cdt1 did not elute from anti-FLAG immunoaffinity purification in the absence of 3x FLAG-Cdt1, and therefore did not bind non-specifically to the anti-FLAG beads. 9x Myc-Cdt1 was detected in the unbound (S) fraction, indicating that Mcm2-7/9x-Myc-Cdt1 was recruited to DNA-beads (lane 4). Lane 2 shows that 3x FLAG-Cdt1 was immunoaffinity purified by anti-FLAG beads. However, 9x Myc-Cdt1 did not co-purify with 3x FLAG-Cdt1. Instead 9x Myc-Cdt1 was detected in the unbound fraction (lane 5), indicating that Mcm2-7/9x Myc-Cdt1 was capable of binding DNA-beads, but did not form a complex with 3x FLAG-Cdt1. Even upon increased exposure of the immunoblot (bottom panel), no 9x Myc-Cdt1 was detected in lane 2.

Lanes 3 and 6 show that the recruitment of both 3x FLAG-Cdt1 and 9x Myc-Cdt1 to DNA-beads was ORC-dependent.

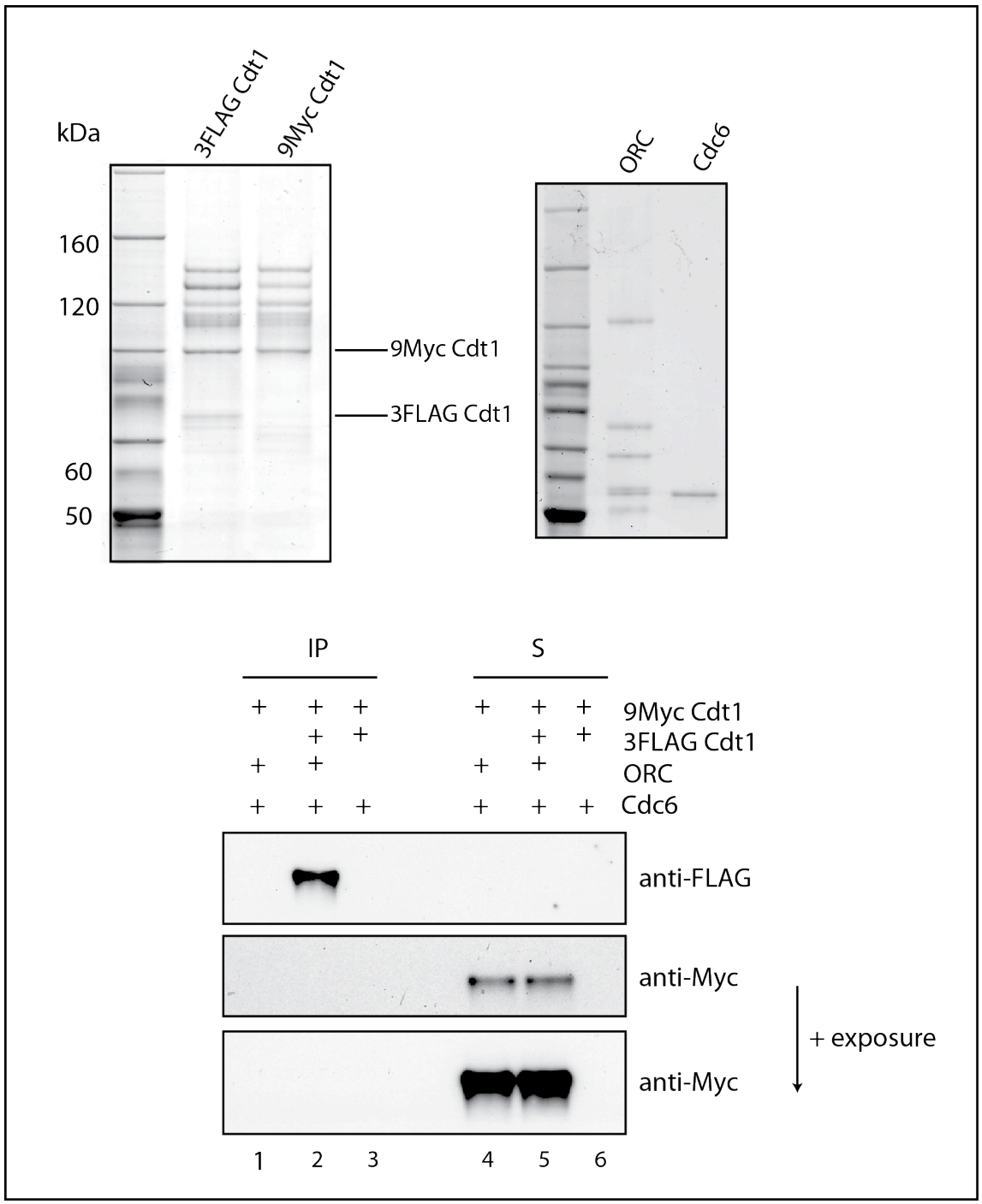

Figure 5.9 Stoichiometry of Cdt1 in the absence of ATP hydrolysis

One molecule of Cdt1 appears to be present prior to ATP hydrolysis. (A) Coomassie stained SDS PAGE of inputs (100%). (B) Reactions were assembled in the presence of ATPγS and origin DNA-beads. Reactions were then treated as outlined in Figure 5.1. Both IP and S fractions were subjected to SDS PAGE followed by immunoblotting with the indicated antibodies. 50% of IP and 50% of S fractions was loaded per immunoblot well.

These data suggest that contrary to a previous study, only one molecule of Cdt1 is involved in the initial recruitment of Mcm2-7 to ORC-Cdc6.

The above experiment was performed in the presence of the endonuclease, Benzonase® to digest the DNA (see Figure 5.2). This was to eliminate the possibility that more than one pre-RC assembly reaction occurred on a single piece of DNA. However, it is possible that the DNA helps to stabilise a Mcm2-7 helicase loading intermediate. Indeed, Takara et al. (2011) examined the stoichiometry of Cdt1 in the absence of any deoxyribonuclease (DNase) treatment. It is possible that a loosely associated second copy of Cdt1 could have been lost owing to Benzonase® treatment, I therefore decided to re-examine the stoichiometry of Cdt1 in the absence of endonuclease treatment.

To analyse Cdt1 stoichiometry in the absence of DNA digestion, the same experiment as above was carried out either in the presence or absence of Benzonase®. Figure 5.10 shows immunoblots against 3x FLAG-cdt1 and 9x Myc-Cdt1. Lanes 1-6 show fractions eluted from anti-FLAG immunoaffinity purification in the presence or absence of Benzonase® treatment. Lanes 7-12 show fractions that did not bind the anti-FLAG beads in the presence or absence of Benzonase® treatment, but that were bound to DNA-beads prior to purification.

Figure 5.10 shows that 9x Myc-Cdt1 did not elute non-specifically following anti-FLAG immunoaffinity purification in the absence of 3x FLAG-Cdt1, and this was unaffected by the absence of Benzonase® treatment (lanes 1 & 4). 9x Myc-Cdt1 was, however, able to bind DNA-beads, both in the presence and absence of Benzonase® treatment (lanes 7 & 10). 3x FLAG-Cdt1 was eluted following anti-FLAG immunoaffinity purification, whether or not benzonase treatment was performed (lane 2 & 5). 9x Myc-Cdt1 did not co-purify with 3x FLAG-Cdt1 when these two complexes were combined in the presence of ORC and Cdc6 (lanes 2 & 5). This was regardless of the absence of benzonase treatment. Indeed, 9x Myc was detected in the “S” fraction, indicating that it was bound to DNA-beads but did not co-purify with 3x FLAG-Cdt1. Both the elution of 3x FLAG-Cdt1 and the binding of 9x Myc-Cdt1 to DNA-beads were dependent on the presence of ORC (lanes 3, 6, 9 & 12).

Taken together these data suggest that there is only one copy of Cdt1 involved in the initial recruitment of Mcm2-7 to ORC-Cdc6. This appears to be true regardless of the presence of DNA during the immunoaffinity purification step.

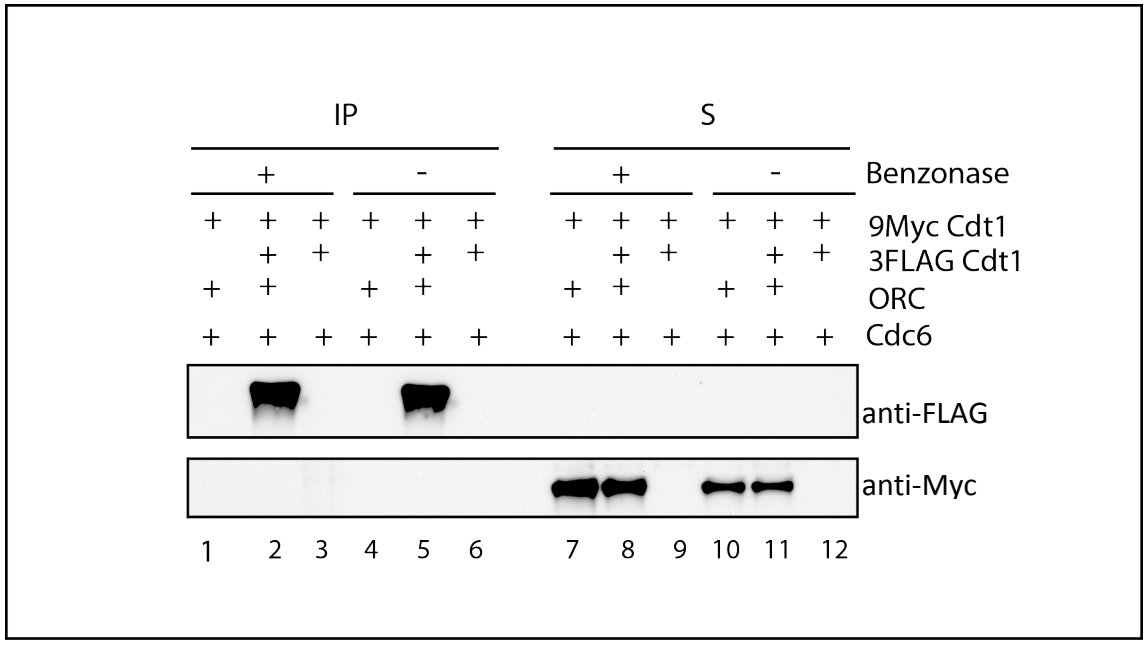

Figure 5.10 Stoichiometry of Cdt1 in the presence or absence of Benzonase® endonuclease

Reactions were assembled in the presence of ATPγS and origin DNA-beads. Reactions were then treated as outlined in Figure 5.1, except water instead of benzonase was added to a subset of reactions. Both IP and S fractions were subjected to SDS PAGE followed by immunoblotting with the indicated antibodies. 50% of IP and 50% of S fractions was loaded per immunoblot well.

5.6 Conclusions

Although it is clear that ORC, Cdc6 and Cdt1 function together to load a double hexamer of Mcm2-7 onto origin DNA, little is known about the stoichiometry of loading factors prior to double hexamer formation. Or at which stage the double hexamer is formed. In this chapter, I examined the stoichiometry of pre-RC assembly factors. Using peptide-tagged proteins from Chapter 4, I determined the stoichiometry of ORC, Cdc6, Mcm2-7 and Cdt1 during pre-RC formation.

By using ORC complexes containing a 3x FLAG tag or a 9x Myc tag, I identified that a single copy of ORC is present at the origin prior to ATP hydrolysis. I then used 3x FLAG-Cdc6 and untagged Cdc6 and revealed that there is also likely to be only one molecule of Cdc6 present prior to ATP hydrolysis.

I subsequently examined the stoichiometry of Mcm2-7 and found that one copy of Mcm3 is present before ATP hydrolysis, whilst two copies are present after ATP hydrolysis. This suggests that a single Mcm2-7 hexamer is recruited to ORC-Cdc6 prior to ATP hydrolysis and that the Mcm2-7 hexamers are loaded in a sequential manner through the action of ATP hydrolysis.

Since the presence of two Mcm2-7 hexamers was found to require ATP hydrolysis, I examined double hexamer formation in the absence of ATPase activity by Cdc6. Using a mutant version of Cdc6 that is defective in ATP hydrolysis (E224G-Cdc6), I revealed that in fact Mcm2-7 loading *in vitro* can still occur, but that this loading decreases as the amount of E224G-Cdc6 used is increased. This may be due to aggregation properties of this mutant, and perhaps the presence of higher amounts of the protein exacerbate precipitation or aggregation, making E224G-Cdc6 less available for Mcm2-7 loading. This may help to explain why my results differ from those published by Randell et al. (2006) and Evrin et al. (2013), who found that E224G-Cdc6 was defective in Mcm2-7 loading *in vitro*.

I then went on to examine the stoichiometry of Mcm2-7 in the presence of E224G Cdc6. I found that two copies of Mcm3 could be detected in the presence of ATP, and these two copies were resistant to a high salt extraction. However, the amount

of Mcm3 that was bound appeared to be slightly less than that loaded by Cdc6 (non-mutated).

These data indicate that ATP hydrolysis by Cdc6 plays a role in double hexamer formation, however, it is not the defining factor. ATP hydrolysis by other pre-RC factors must therefore contribute to Mcm2-7 double hexamer formation. Orc1 of the ORC complex has been shown to hydrolyse ATP, and is thought to play a role in reiterative Mcm2-7 loading (Bowers et al., 2004). However, a recent study by Evrin et al. (2013) showed that Orc1 ATPase is not required for pre-RC formation *in vitro*. New data from our laboratory show that ATP hydrolysis by the MCM subunits play a role in pre-RC formation (Gideon Coster, unpublished data). It will be interesting to uncover the roles of individual ATPases and their contribution to Mcm2-7 double hexamer formation.

I also examined the stoichiometry of Cdt1 prior to ATP hydrolysis. A study had previously indicated that multiple copies of Cdt1 were involved in recruiting Mcm2-7 to ORC-Cdc6 (Takara and Bell, 2011). It was difficult to reconcile how multiple Cdt1 molecules could be present at the recruitment stage (when ATP hydrolysis is blocked), when I only detected one Mcm2-7 complex. Particularly since in *S.cerevisiae* Cdt1 is associated with Mcm2-7. To examine the stoichiometry of Cdt1 I used Mcm2-7/Cdt1 complexes containing a 3x FLAG tag or a 9x Myc tag fused to the N-terminus of Cdt1. I was only able to detect one copy of Cdt1 when ATP hydrolysis was blocked and this was not due to loss of a second copy by DNase treatment.

The above stoichiometry data have been confirmed by recent studies that show that in the presence of ATPγS an OCCM (ORC, Cdc6, Cdt1, Mcm2-7) complex is formed that contains a single copy of each of the licensing factors (Evrin et al., 2013, Sun et al., 2013).

Chapter 6. Mcm3 is required for Mcm2-7/Cdt1 recruitment to DNA-bound ORC-Cdc6

6.1 Introduction

Mcm2-7/Cdt1 is loaded onto origin DNA from a single heteroheptamer into a double hexamer of Mcm2-7 wrapped around double stranded DNA. Reconstitution of this reaction *in vitro* has previously been described (Refer to Chapter 1, section 1.2.2.3). In the presence of ATP: ORC and Cdc6 load Mcm2-7/Cdt1 onto origin DNA coupled to magnetic beads (DNA-beads) in a salt resistant manner, with concomitant release of Cdc6 and Cdt1. When ATP hydrolysis is blocked by incubation with a slowly hydrolysed analogue, ATPγS: ORC, Cdc6, Cdt1 and Mcm2-7 are all recruited to the DNA-beads but are removed by a high salt wash.

To investigate the individual roles of Cdt1 and the Mcm2-7 subunits, each of these proteins was purified separately (Jordi Frigola) (Frigola et al., 2013). The individual subunits were tested for recruitment to origin DNA-beads by ORC and Cdc6 (ATPγS, low salt wash). Only Mcm3 (without the other Mcm2-7/Cdt1 subunits) was recruited in a Cdc6-dependent manner (Jordi Frigola) (Frigola et al., 2013). Furthermore, a Mcm2-7 complex lacking Mcm3 could not be recruited to ORC-Cdc6 whereas a Mcm2-7 complex lacking Mcm4 could still be recruited (Frigola et al., 2013). These results indicated that Mcm3 plays a crucial rule in Mcm2-7 recruitment to ORC-Cdc6.

In this chapter I will describe how we further investigated the role of Mcm3 in the recruitment of Mcm2-7 to ORC-Cdc6 (in collaboration with Jordi Frigola).

6.2 The C-terminus of Mcm3 is crucial for recruitment of Mcm2-7 to ORC-Cdc6

Mcm3 comprises an amino-terminal (N-terminal) domain, a AAA+ domain and an extended C-terminal tail (Figure 6.1A, also see Figure 1.3). The N-terminal and AAA+ domains of Mcm3 are common amongst all the Mcm2-7 subunits, however,

the C-terminal extension is of unknown function. A Mcm2-7 complex containing a 3x FLAG epitope at the C-terminus of Mcm3 (Mcm3-3x FLAG) was found to be non functional in pre-RC formation *in vitro* (Frigola et al., 2013). Mcm3-3xFLAG was defective both in Mcm2-7 recruitment to ORC-Cdc6 in the presence of ATPγS and in Mcm2-7 loading in ATP. In light of this, we hypothesised that the C-terminus of Mcm3 plays a role in pre-RC assembly.

To further examine the C-terminus of Mcm3, we performed a multiple alignment of Mcm3 from a variety of eukaryotic species (Figure 6.1B). We identified a conserved domain at the extreme C-terminus of Mcm3 that is not found in the other Mcm2-7 subunits (Figure 6.1B).

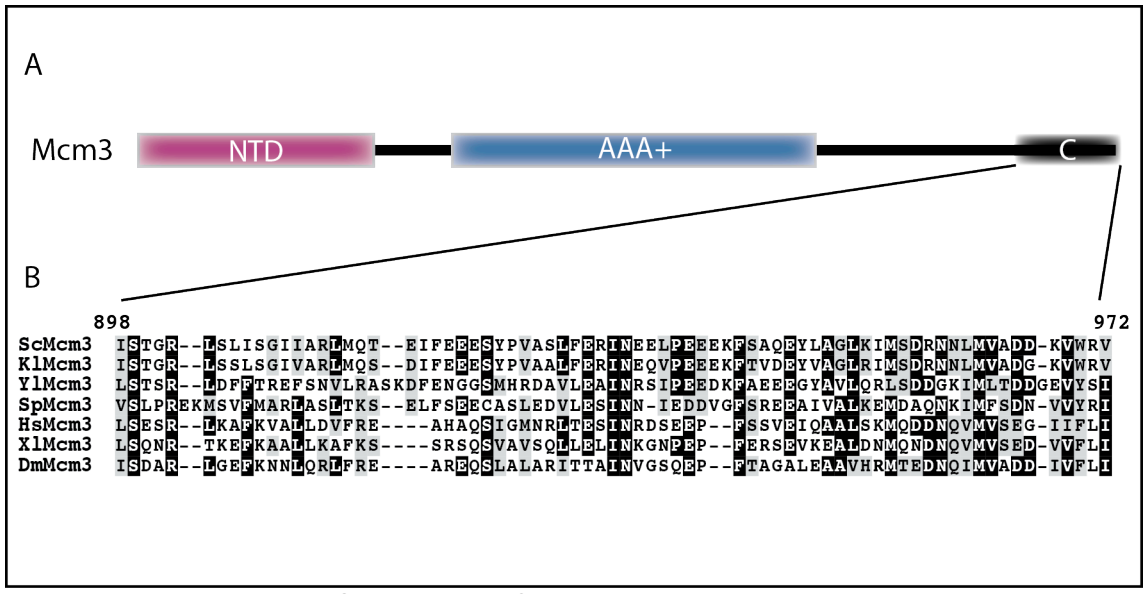

Figure 6.1 The extreme C-terminus of Mcm3 is highly conserved

(A) Domain architecture of Mcm3. NTD: Amino-terminal domain. (B) Alignment of Mcm3 from a variety of eukaryotic species. Residue numbers above correspond to *S.cerevisiae* Mcm3. Sc: *Saccharomyces cerevisiae*, Kl: *Kluyveromyces lactis*, Yl: *Yarrowia lipolytica*, Sp: *Schizosaccharomyces pombe*, Hs: *Homo sapiens*, Xl: *Xenopus laevis*, Dm: *Drosophila melanogaster*

To investigate the role of the *S.cerevisiae* C-terminal tail of Mcm3, I constructed N- and C-terminal deletions of Mcm3. The deletion constructs were based on secondary structure predictions (Phyre) and conservation. I generated three versions of Mcm3: full length (FL) Mcm3, N-terminal (N-term) Mcm3 lacking the C-terminal 194 amino acid residues and C-terminal (C-term) Mcm3 composed of the conserved C-terminal 194 amino acid residues (Figure 6.2A).

The full length and truncated versions of Mcm3 (Figure 6.2A) containing N-terminal fusions to maltose binding protein (MBP) were expressed and purified from *E.coli* (See Materials and Methods, sections 2.5.8 and 2.7.8). The proteins were purified by amylose affinity chromatography. Figure 6.2B shows a Coomassie-stained polyacrylamide gel of the purified Mcm3 preparations.

I then asked whether the Mcm3 deletions had an effect on recruitment of Mcm3 to ORC-Cdc6. To address this, full length MBP-Mcm3, or MBP-tagged deletions were incubated with ORC, Cdc6 and origin DNA-beads in the presence of ATPγS. Unbound proteins were removed by a low salt wash and DNA with bound proteins was cleaved from the beads by UVA irradiation (see Chapter 4, section 4.2). Proteins recruited to the DNA were examined by SDS PAGE and immunoblotting. Here I took advantage of the MBP peptide tag and immunoblots were performed using an anti-MBP monoclonal antibody. Figure 6.2C shows the results of this experiment. Consistent with previous results, full length Mcm3 (FL Mcm3) was recruited to the origin DNA in an ORC- and Cdc6-dependent manner (Figure 6.2A, top panel). An N-terminal fragment of Mcm3 lacking the C-terminal 194 amino acids could not be detected, even when both ORC and Cdc6 were present (Figure 6.2C, middle panel). This indicates that the extreme C-terminus of Mcm3 is necessary for Mcm3 recruitment to ORC-Cdc6. Finally, the small fragment (C-term Mcm3) containing the C-terminal 194 amino acids of Mcm3 could be recruited in an ORC and Cdc6-dependent manner. This indicates that the C-terminus of Mcm3 is both necessary and sufficient for Mcm3 recruitment to ORC-Cdc6.

The N-terminal fragment of Mcm3 was assembled into a Mcm2-7/Cdt1 complex and its ability to recruit and load Mcm2-7 was tested (Jordi Frigola). This version of

Mcm3, lacking its C-terminal domain, was completely defective in recruiting Mcm2-7 to ORC-Cdc6 (Frigola et al., 2013).

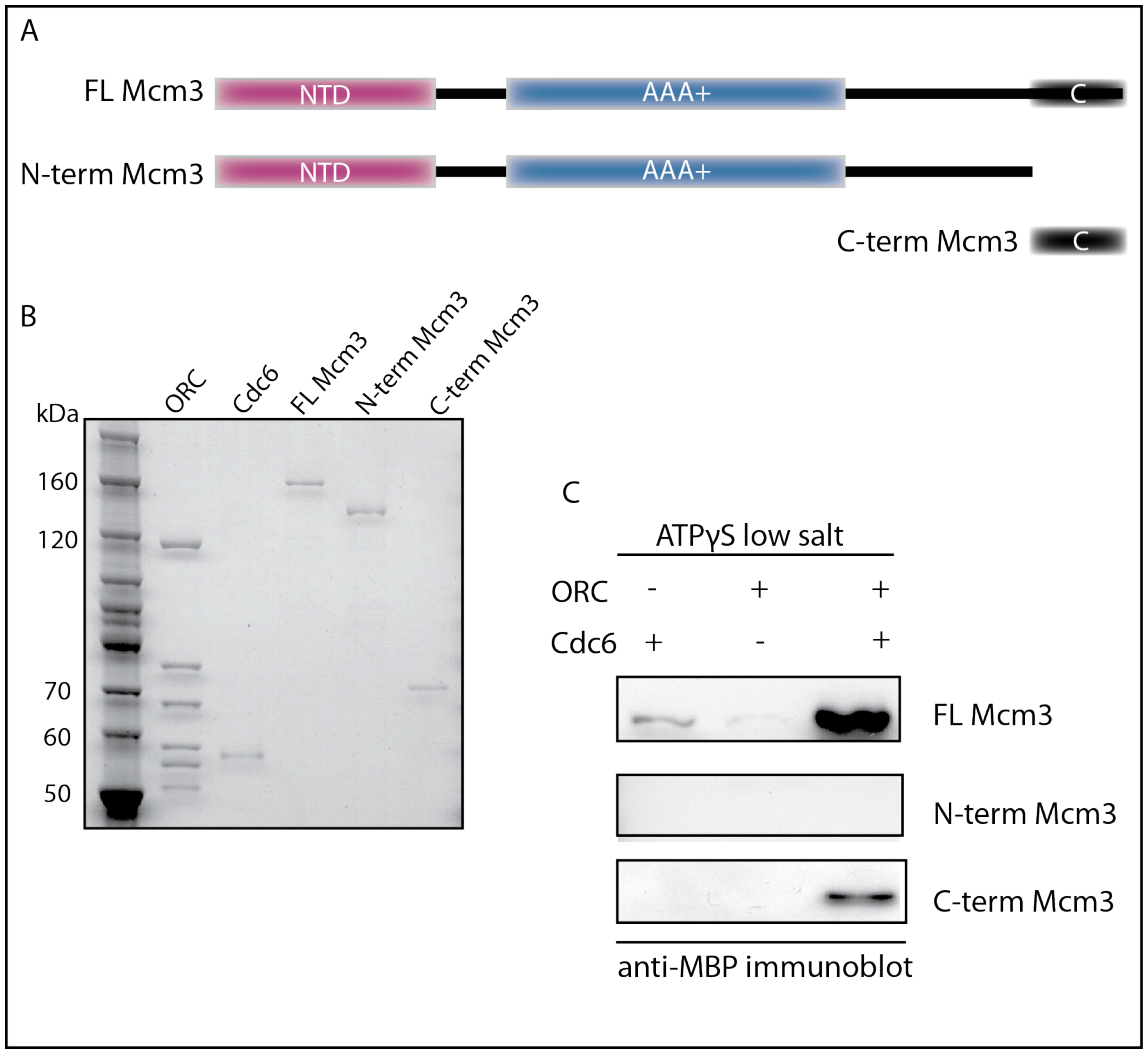

Figure 6.2 The C-terminus of Mcm3 is required for Mcm2-7 recruitment

(A) Schematic of full length Mcm3 and truncations. The N-terminal portion of Mcm3 (N-term Mcm3) lacks the C-terminal 194 amino acid residues. The C-terminal portion of Mcm3 (C-term Mcm3) consists of only the C-terminal conserved 194 residues. (B) Coomassie-stained SDS PAGE of inputs to test Mcm3 recruitment to ORC-Cdc6. All Mcm3 purifications are fused to a MBP tag at their N-termini. (C) Immunoblot to assess Mcm3 recruitment to ORC-Cdc6. ORC, Cdc6 and Mcm3 or Mcm3 truncations, were incubated with origin DNA-beads in the presence of ATPγS. Unbound proteins were removed by a low salt wash and DNA with bound proteins was cleaved from the beads by UVA irradiation. Proteins were assessed by SDS PAGE followed by immunoblotting with a monoclonal antibody against MBP.

Together these data pointed towards a role for the C-terminus of Mcm3 in Mcm2-7 recruitment to DNA-bound ORC-Cdc6.

To further examine the role of the C-terminus of Mcm3 in Mcm2-7/Cdt1 recruitment, a series of C-terminal amino acid substitution mutants were generated in full length untagged Mcm3 (Jordi Frigola, Figure 6.3A) based on the conservation of the C-terminus of Mcm3. These mutant proteins were assembled into full Mcm2-7/Cdt1 complexes and assessed for their ability to recruit and load Mcm2-7/Cdt1 onto origin DNA-beads. The Mcm3-11 and Mcm3-12 single mutants, as well as the Mcm3-13 double mutant (Figure 6.3A) were completely defective in recruiting Mcm2-7/Cdt1 to ORC-Cdc6 (Frigola et al., 2013). This showed that the C-terminus of Mcm3 is crucial for recruitment of all Mcm2-7 subunits to ORC-Cdc6.

To determine the importance of the C-terminus of Mcm3 *in vivo*, I studied Mcm3 complementation in a *S.cerevisiae* diploid background. The *S.cerevisiae* diploid strain, W303, was transformed with PCR cassettes containing a *URA3* marker and either *MCM3 wt*, *mcm3-11*, *mcm3-12*, or *mcm3-13* (Figure 6.3A). Heterozygotes were selected and subjected to sporulation and tetrad dissection.

Figure 6.3B shows the growth of spores on rich media. Transformation of *MCM3 wt* in the diploid background gave rise to four spores that grew equally well (Figure 6.3B, first panel). Transformation of *mcm3-11* in the diploid background gave rise to four spores, of which two exhibited growth defects (Figure 6.3B, second panel & C). The spores exhibiting the growth defect expressed the *URA3* marker indicating that *mcm3-11* was present as a single copy. This shows that *MCM3* with a single amino acid substitution in the very last amino acid could only support very slow growth when compared to *MCM3 wt* (Figure 6.3C). Panels 3 & 4 show that only two spores were viable when the diploid yeast strain was transformed with either *mcm3-12* or *mcm3-13.* The viable spores tested negative for the presence of the *URA3* marker. This shows that both *mcm3-12* and *mcm3-13* were unable to support growth when present as single copies.

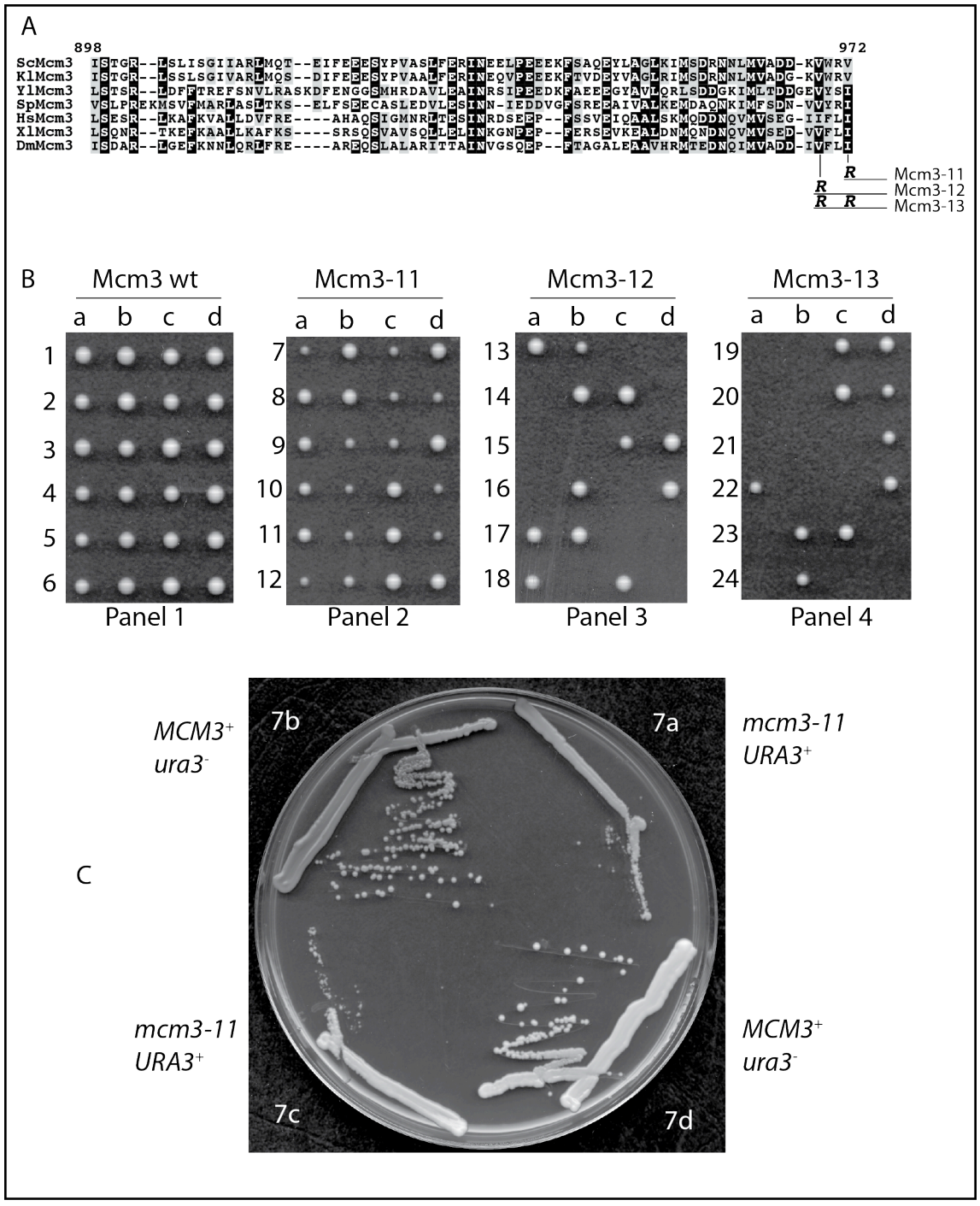

Figure 6.3 Mutations in the C-terminus of Mcm3 affect viability

(A) Aligment of the C-terminus of Mcm3, as in Figure 6.1B. The position of various mutants is shown by vertical lines, and the mutant amino acid residue is shown at the bottom of the line. Allele names are on the right (*mcm3-11*, *mcm3-12*, and *mcm3-13*). (B) The diploid strain W303 was transformed with PCR cassettes containing the *URA3* marker and *MCM3 wt*, *3-11*, *3-12* or *3-13* mutants. Heterozygotes were selected and subjected to sporulation and tetrad dissection. The numbers indicate different tetrads analysed, while the four spores of each tetrad are labeled from a to d. (C) Each spore from tetrad number 7 (*mcm3-11*) was streaked out on a YPD plate to examine growth.

Taken together these data indicate that a domain at the C-terminus of Mcm3 is required for recruiting Mcm2-7/Cdt1 to ORC-Cdc6 and that this function is necessary for viability.

6.3 Interactions of Mcm3 with ORC-Cdc6

The described data indicate that after ATP-dependent binding by ORC and Cdc6, Mcm2-7/Cdt1 is recruited by interaction between the extreme C-terminus of Mcm3 and DNA-bound ORC-Cdc6. In light of this, we next asked: which subunits of ORC-Cdc6 does Mcm3 interact with? Insight into Mcm3 interactions would provide a better understanding of how licensing factors are positioned relative to each other during recruitment of Mcm2-7/Cdt1 to ORC-Cdc6. Particularly since we know the subunit organisation of Mcm2-7 and ORC.

In order to examine the interactions of Mcm3 with ORC-Cdc6, I utilised the tagged protein preparations generated in Chapter 4. I used a cross-linking strategy combined with the peptide-tagged proteins to characterise the interactions of Mcm3 (outlined in Figure 6.4).

I used the crosslinker BS3 that contains an amine-reactive *N*-hydroxysulfosuccinimide (NHS) ester at each end of an 8-carbon spacer arm. The NHS esters react with primary amines (-NH_2) to form stable amide bonds. Primary amines exist at the N-terminus of each polypeptide chain and in the side chain of lysine (K) residues. In this approach I introduced the BS3 crosslinker in limiting, sub-saturating amounts to generate pairs of covalently crosslinked proteins. The BS3 cross-linker has a short 11.4 Å spacer arm, meaning that I could cross-link proteins that were in close proximity to one another, and therefore were likely to interact. For all of these reasons, I chose BS3 as a suitable crosslinking reagent to characterize Mcm3 interactions.

Pairwise combinations of tagged proteins (3x FLAG and 9x Myc-tagged) were combined in the presence of ATPγS and origin DNA-beads (Figure 6.4, step 1). I then introduced the BS3 crosslinker under limiting conditions to generate pairs of covalently crosslinked proteins (Figure 6.4, step 2). The mixture was denatured in

1% SDS and subjected to immunoaffinity purification with anti-FLAG beads (Figure 6.4, steps 3 & 4). Bound proteins were eluted by competitive elution with a 3x FLAG peptide and the eluate was examined by immunoblotting to identify interactions (Figure 6.4, step 6). A flow chart of the steps involved in this experiment is shown in Figure 6.5.

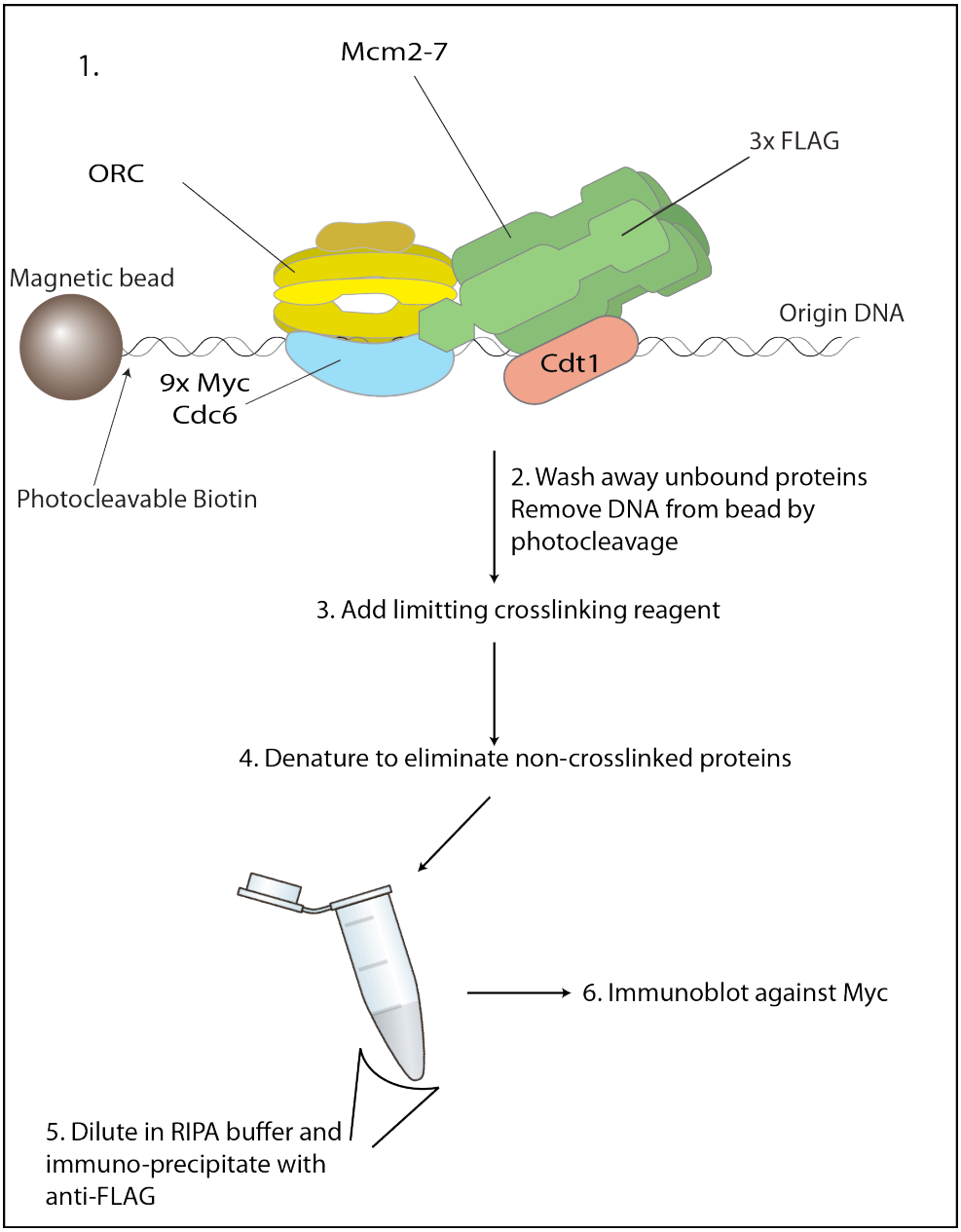

Figure 6.4 Strategy to examine pairwise interactions during pre-RC assembly

In this example, we are asking whether there is an interaction between Cdc6 (9x myc-tagged) and Mcm3 (3x FLAG-tagged). The steps involved are numbered in the figure.

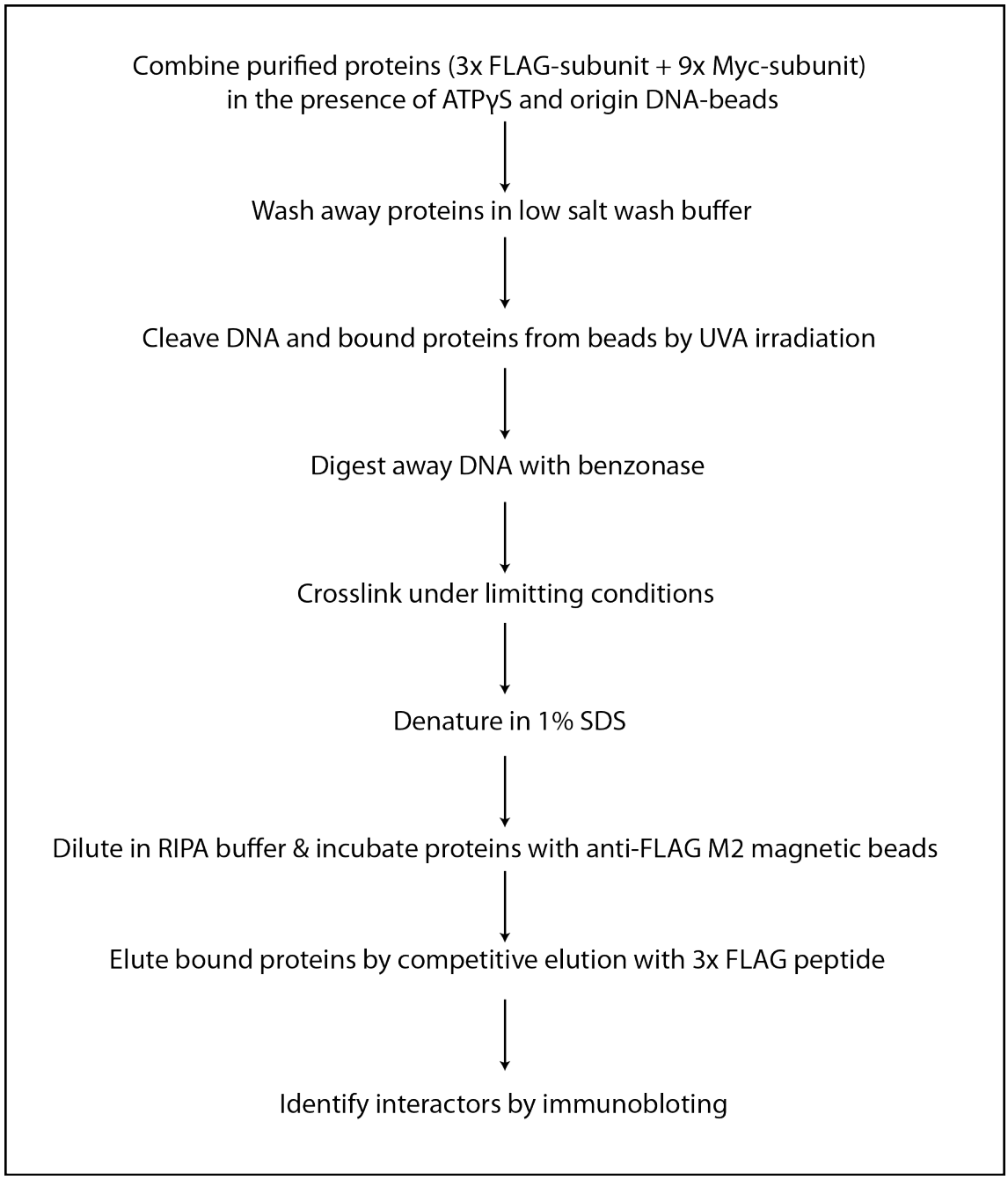

Figure 6.5 Flowchart of strategy to examine interactions of Mcm3

Using the described approach, I first asked whether Mcm3 interacts with Cdc6. For this, I used Mcm3 N-terminally fused to a 9x Myc peptide in the Mcm2-7/Cdt1 complex (9x Myc-Mcm3) and Cdc6 fused to a 3x FLAG tag at its N-terminus (3x FLAG-Cdc6) (See Chapter 4). These tagged proteins were combined with ORC and DNA-beads in the presence of ATPγS and subjected to crosslinking as above. I then performed an immunoaffinity purification (IP) of 3x FLAG-Mcm3 under denaturing conditions and tested the IP for the presence of Myc and FLAG-tagged proteins.

Figure 6.6A shows a Coomassie-stained polyacrylamide gel of the purified proteins used in this experiment. Figure 6.6B shows immunoblots against the FLAG and Myc peptide tags. Lanes 1, 2 and 4 (Figure 6.6B) show that 3x FLAG-Cdc6 was immunoaffinity purified in an ORC-dependent manner. Addition of the BS3 cross-linker induced the formation of higher order cross-links (lanes 3 & 5). In this case, the anti-FLAG antibody gave rise to background bands that were Cdc6-dependent and BS3-independent (indicated in Figure 6.6B). These were background bands produced by interaction of the anti-FLAG antibody with FLAG-tagged protein preparations.

Lanes 7-12 show that some un-crosslinked 9x Myc-Mcm3 bound non-specifically to anti-FLAG beads. However, upon the addition of BS3, crosslinked bands were observed that were dependent on the immunoaffinity purification of 3x FLAG-Cdc6 (lanes 9 & 11). The crosslinked bands were not observed in the absence of BS3 (lane 7), ORC (lanes 8 & 10) nor 3x FLAG-Cdc6 (lane 12).

These data show that 9x Myc-Mcm3 specifically cross-linked to 3x FLAG-Cdc6. This indicates that Mcm3 interacts with Cdc6 during Mcm2-7/Cdt1 recruitment to DNA-bound ORC-Cdc6.

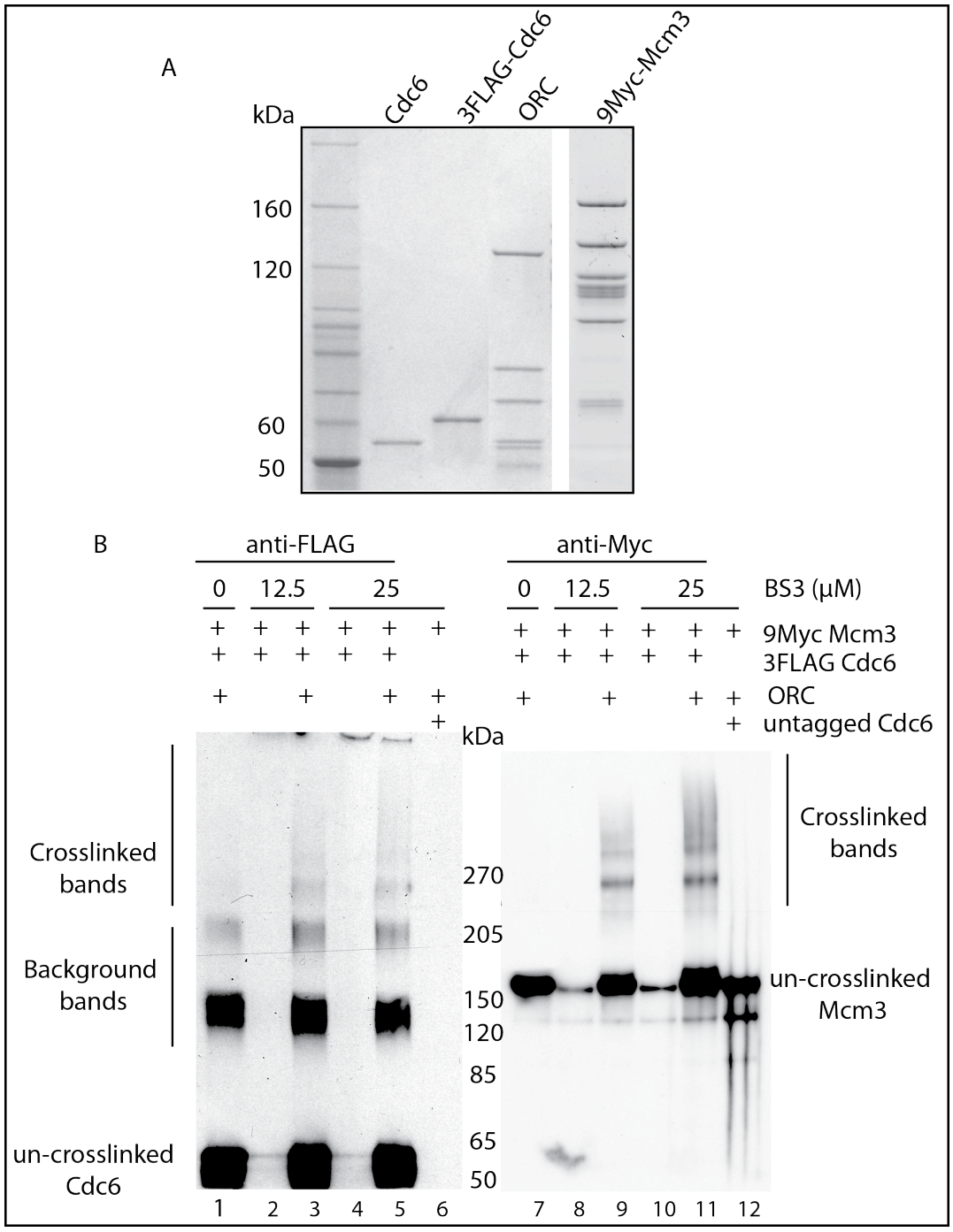

Figure 6.6 Mcm3 interacts with Cdc6 during Mcm2-7/Cdt1 recruitment to ORC-Cdc6-DNA

(A) Coomassie-stained SDS PAGE of 100% input proteins. (B) SDS PAGE and immunoblotting against FLAG and Myc after denaturing IP. Tagged proteins were incubated with ORC and origin DNA-beads in the presence of ATPγS and subjected to cross-linking with the indicated amounts of BS3 (described in Figure 6.5). Cross-linking was quenched with TRIS-HCl pH 7.5. The mixture was denatured in 1% SDS and the 3x FLAG-tagged Cdc6 was immunoprecipitated. Proteins covalently bound to Cdc6 were identified by SDS PAGE followed by immunoblotting

Upon identifying that Mcm3 most likely interacts with Cdc6, I went on to ask whether Mcm3 interacts with any of the ORC subunits, and if so which subunits. To address this question, I again used peptide-tagged protein preparations (described in Chapter 4). Since I obtained more 3x FLAG-tagged ORC subunits than 9x Myc-tagged subunits, I decided to utilise 3x FLAG-tagged ORC complexes and 9x Myc-tagged Mcm3. The only exception was the use of 9x Myc-Orc2 with 3x FLAG-Mcm3. This was because upon examination of 3x FLAG-Orc2, I was unable to detect the FLAG tag by immunoblotting. This could be due to an error during the PCR-based tagging approach. The tagged and untagged protein preparations used to examine Mcm3 interactions with ORC are shown in Figure 6.7.

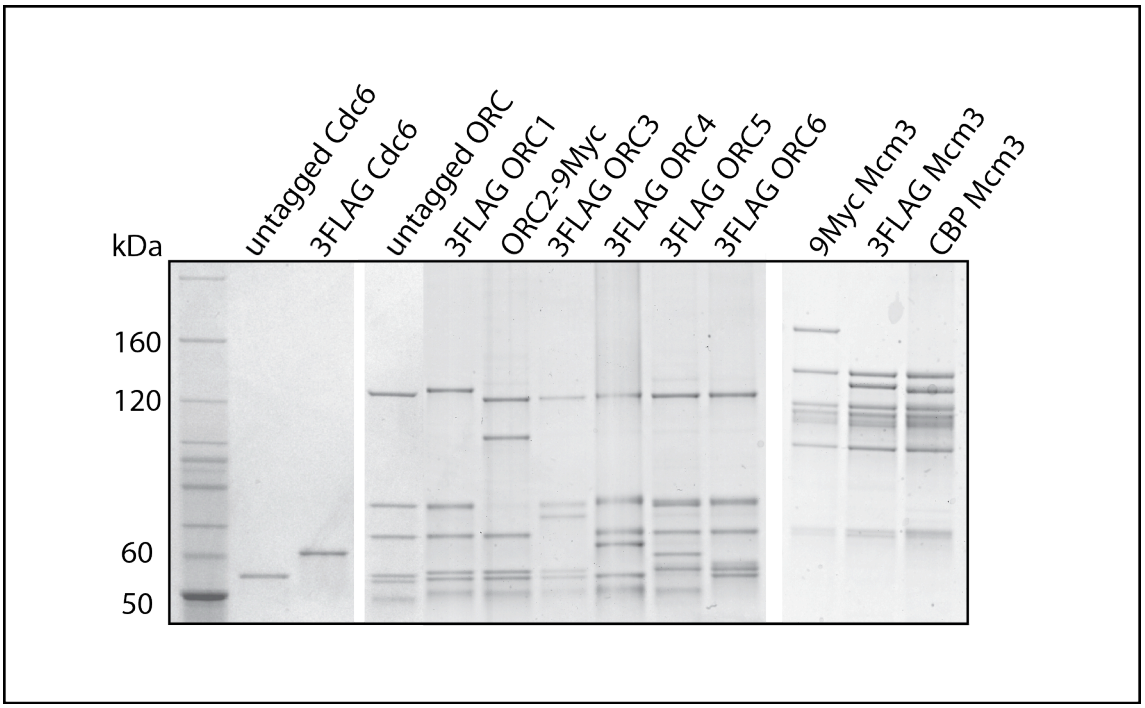

Figure 6.7 Coomassie stained SDS PAGE of protein preparations for Mcm3 interaction studies

100% of inputs for Figure 6.8 are shown.

Pairwise combinations of the tagged proteins were combined with origin DNA-beads in ATPγS and cross-linked as described above. 3x FLAG-tagged proteins were then immunoaffinity purified (IP) under denaturing conditions and the IP was tested for the presence of the 9x Myc-tagged proteins by immunoblotting.

Figure 6.8 shows immunoblots against the FLAG and Myc epitope tags. Lane 1 & 16 show that in the absence of a 3x FLAG-tagged protein, no bands were observed in the anti-FLAG blot. Under these conditions, un-crosslinked 9x Myc-Mcm3 and un-crosslinked 9x Myc-Orc2 (indicated by a red star) appeared to bind non-specifically to anti-FLAG beads (lanes 1-16). Lanes 2-15 show that 3x FLAG-tagged proteins were immunoaffinity purified by the anti-FLAG beads. Addition of BS3 resulted in the formation of crosslinked bands in the anti-FLAG immunoblot (lanes 3, 5, 7, 9, 11, 13 & 15). This indicates that higher order crosslinks were formed between immunoaffinity purified 3x FLAG-tagged proteins and binding partners. Again background bands were observed in the anti-FLAG immunoblot, but addition of the BS3 crosslinker gave rise to novel bands, compared to background (Figure 6.8, top panel)

The IP was tested for the presence of 9x Myc-tagged proteins. The anti-Myc immunoblot shows that higher order cross-links were only formed when 9x Myc-Orc2 and 3x FLAG-Mcm3 were combined (lane 5) or when 9x Myc-Mcm3 was combined with 3x FLAG-Cdc6 (lane 15). This indicates that Mcm3 specifically cross-linked to Orc2 and Cdc6.

Together these data suggest that Mcm3 interacts with Orc2 and Cdc6 during Mcm2-7/Cdt1 recruitment to ORC-Cdc6.

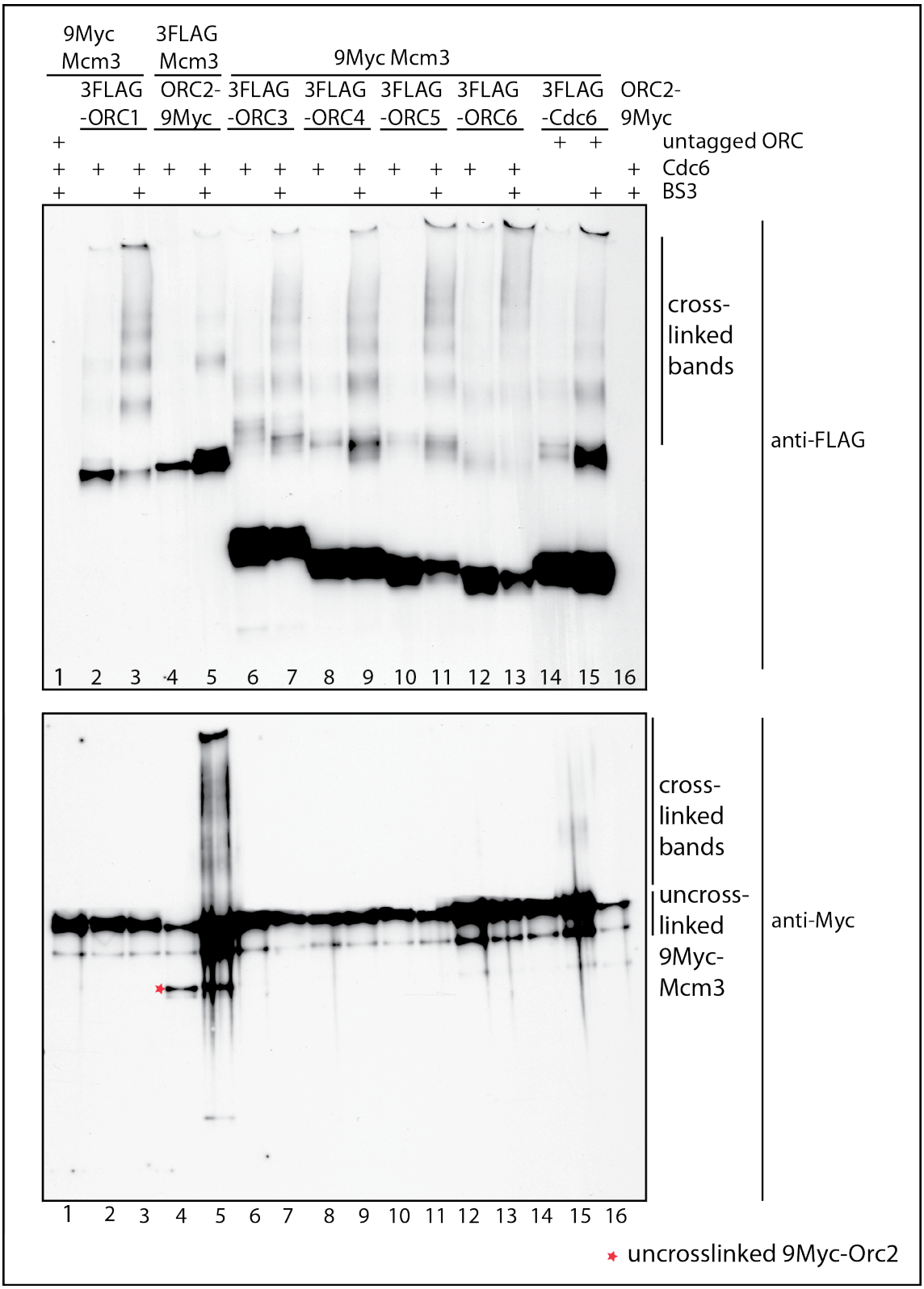

Figure 6.8 Mcm3 cross-links to Orc2 and Cdc6

SDS PAGE and immunoblotting against FLAG and Myc after denaturing IP. Tagged and untagged proteins (as shown) were incubated with origin DNA-beads in the presence of ATPγS and subjected to cross-linking with 25μM of BS3 (described in Figure 6.5). Cross-linking was quenched with TRIS-HCl pH 7.5. The mixture was denatured in 1% SDS and the 3x FLAG-tagged proteins were immunoprecipitated. Proteins covalently bound to 3x FLAG-tagged proteins were identified by SDS PAGE followed by immunoblotting with indicated antibodies.

6.4 Conclusions

In this Chapter I showed that Mcm3, in the absence of the other Mcm2-7/Cdt1 subunits, can be recruited (ATPγS, low salt wash) in an ORC- and Cdc6-dependent manner (in collaboration with Jordi Frigola). I also showed that a conserved C-terminal domain of Mcm3 (194 amino acid residues) is required for Mcm3 recruitment to ORC-Cdc6. Mutations in this conserved C-terminal tail resulted in growth defects *in vivo* and were defective for Mcm2-7 recruitment and loading *in vitro* (Jordi Frigola). I characterised the interaction partners of Mcm3 during Mcm2-7/Cdt1 recruitment to ORC-Cdc6 and found that Mcm3 formed cross-links with Cdc6 and Orc2.

Taken together, these data suggest that during pre-RC formation, Mcm2-7/Cdt1 is recruited to origins via an interaction between the C-terminus of Mcm3 and ORC-Cdc6. This interaction appears to be mediated by Orc2 and Cdc6. Indeed in a recent paper, the authors detected an interaction between Mcm3 and Cdc6 during Mcm2-7/Cdt1 recruitment (Sun et al., 2013).

Mcm2-7 is loaded onto DNA as a head-to-head double hexamer. Formation of the Mcm2-7 double hexamer is dependent on ATP hydrolysis. Further analysis has shown that both Mcm2-7 hexamers require the C-terminus of Mcm3 (Frigola et al., 2013). In addition, Mcm3 binding was found to trigger ATP hydrolysis by ORC and Cdc6 which correlates with release of recruited Mcm2-7 (Frigola et al., 2013). This indicates that the initial recruitment of Mcm2-7 to ORC-Cdc6 is an ATP-independent process that occurs by Mcm3 interaction with ORC-Cdc6 and that ATP hydrolysis breaks this contact.

Based on data presented in Chapter 5, and published data (Fernandez-Cid et al., 2013), it appears that the recruitment and loading of the Mcm2-7 hexamers occurs sequentially. This sequential recruitment and loading of Mcm2-7 is probably mediated by the C-terminal interaction of Mcm3 with ORC-Cdc6. Formation of the Mcm2-7 double hexamer also requires Cdt1 (Fernandez-Cid et al., 2013). It is still unclear how these mechanisms function together to load two Mcm2-7 hexamers

that lie head-to-head on one side of ORC-Cdc6. It will be interesting to further dissect these mechanisms.

Chapter 7. Discussion

ORC, Cdc6 and Cdt1 function together to load a double hexamer of Mcm2-7 around double stranded DNA in an ATP dependent manner (Evrin et al., 2009, Remus et al., 2009). How exactly do ORC, Cdc6 and Cdt1 coordinate loading of a double hexamer of Mcm2-7? Is one ORC molecule required for this loading? Or is Mcm2-7 loading achieved by binding of two ORC molecules on either side of the origin? A similar question may be asked of Cdc6. How are the ATPase activities of the loading proteins coordinated for double hexamer formation? Which proteins are required to interact during helicase loading?

This thesis aimed to address some of these questions by characterising the biochemical architecture of pre-RC formation using the yeast *S.cerevisiae* as a model system. In particular, I focused on identifying the stoichiometry of loading factors and some of their interactions. The experiments discussed in previous chapters have produced the following conclusions:

- 247 bp of DNA containing the ACS and B elements of ARS305 could not support Mcm2-7 loading *in vitro* when compared to 1 kb of DNA containing the ACS, B elements and surrounding sequences of ARS305. This suggests that there is a threshold length required for pre-RC formation, as previously demonstrated in *Xenopus* egg extracts (Edwards et al., 2002).

- One molecule of ORC and one molecule of Cdc6 recruit Mcm2-7/Cdt1 prior to ATP hydrolysis.

- One molecule of Mcm2-7 is recruited to ORC-Cdc6 when ATP hydrolysis is blocked. In the presence of ATP, two molecules of Mcm2-7 were detected. This suggests that the Mcm2-7 hexamers are loaded in a step-wise, sequential manner.

- One molecule of Cdt1 appears to be involved in the recruitment of Mcm2-7 to DNA-bound ORC-Cdc6.

- ATP hydrolysis by Cdc6 appears to be dispensable for Mcm2-7 loading/double hexamer formation. Blocking Cdc6 ATPase activity caused only a minor reduction in Mcm2-7 loading.

- Mcm3 is required for Mcm2-7/Cdt1 recruitment to ORC-Cdc6 (Jordi Frigola) and a conserved C-terminal domain of Mcm3 is necessary for this recruitment.

- Mcm3 interacts with Orc2 and Cdc6 during Mcm2-7/Cdt1 recruitment to DNA-bound ORC-Cdc6.

These data support a model for origin licensing whereby one molecule of ORC and Cdc6 recruit a Mcm2-7/Cdt1 heteroheptamer via interaction between Mcm3 and Orc2/Cdc6. The C-terminus of Mcm3 appears to be required for this recruitment. However, it is still unclear how a single heteroheptamer of Mcm2-7/Cdt1 transitions into a double hexamer of Mcm2-7. In this chapter I suggest a model for Mcm2-7 recruitment and double hexamer formation based on results from this thesis and published data.

7.1 Recruitment of Mcm2-7/Cdt1 to ORC-Cdc6 prior to ATP hydrolysis

Before helicase loading, ORC, Cdc6, Cdt1 and Mcm2-7 are recruited to origin DNA. This is a short-lived complex that can only be detected *in vitro* when ATP hydrolysis is blocked, for example by the use of the slowly hydrolysable analogue, ATPγS. Since single hexamers of Mcm2-7 were never observed on DNA by EM (Remus et al., 2009) and multiple Cdt1 molecules were detected in ATPγS (Takara and Bell, 2011), it was thought that both Mcm2-7 hexamers are loaded in a concerted manner to form the Mcm2-7 double hexamer. In addition, Cdt1 was found to interact with Orc6 and this ORC subunit appeared to have two Cdt1 interaction sites (Takara and Bell, 2011, Chen et al., 2007). In yeast, Cdt1 is associated with

the Mcm2-7 complex. This therefore provided a possible mechanism for loading of two Mcm2-7 hexamers at the same time via Cdt1 interaction with Orc6.

7.1.1 A one-to-one stoichiometry during recruitment of Mcm2-7/Cdt1 to DNA-bound ORC-Cdc6

There are several possibilities for how Mcm2-7 double hexamer loading may occur. For example, one ORC-Cdc6 complex could load two Mcm2-7/Cdt1 hexamers sequentially through the action of ATP hydrolysis. Another possibility is that two ORC-Cdc6 assemblies load one Mcm2-7/Cdt1 each, in opposite orientations. To further dissect how a double hexamer of Mcm2-7 is formed, I studied the stoichiometry of licensing factors during the recruitment stage of origin licensing. Using peptide-tagged proteins (Chapter 4), I found that one molecule of each of the licensing factors (ORC, Cdc6, Mcm2-7 and Cdt1) is involved in the recruitment of Mcm2-7/Cdt1 to DNA-bound ORC-Cdc6 (Chapter 5). Other studies have recently validated these results. Evrin et al. showed that in the absence of ATP hydrolysis, one hexamer of Mcm2-7 is recruited to the origin (Evrin et al., 2013).

Furthermore, Sun et al. performed cryo-EM on the recruitment stage (ATPγS intermediate) and observed a one-to-one stoichiometry of each of the licensing factors in a complex they termed the OCCM (ORC, Cdc6, Cdt1, Mcm2-7) (Sun et al., 2013). The cryo-EM study of the OCCM revealed that the C-terminal AAA^+ motor domains of the Mcm2-7 hexamer are extensively engaged with the ORC-Cdc6 N-terminal AAA^+ domains. Interestingly, the authors also observed that ORC-Cdc6 in the OCCM undergoes a structural rearrangement into a right-handed spiral encircling the dsDNA (Sun et al., 2013). This is reminiscent of the replication factor C clamp loader (Sun et al., 2013, Kelch et al., 2011) and suggests a conserved mechanism of action. It is still unclear whether DNA passes through the OCCM structure, although a linear continuous density was observed passing from outside ORC-Cdc6 into the Mcm2-7 central channel (Sun et al., 2013). It is possible that the Mcm2-7 complex already encircles the DNA in this OCCM ATPγS intermediate, but the hexamer is probably partially loaded since the OCCM is removed from DNA by high salt extraction.

Taken together, these data suggest that the Mcm2-7 hexamers are loaded sequentially and not simultaneously to form the loaded Mcm2-7 double hexamer.

7.1.2 The role of Mcm3 in the recruitment of Mcm2-7/Cdt1 to ORC-Cdc6-DNA

Mcm3 was found to be required for the initial recruitment of Mcm2-7/Cdt1 to ORC-Cdc6-DNA (Frigola et al., 2013). In Chapter 6 I showed that a 194-residue C-terminal conserved region of Mcm3 was necessary and sufficient for this recruitment. This is in agreement with the cryo-EM structure of the OCCM, which suggests that the C-termini of the Mcm2-7 subunits interact with ORC-Cdc6 (Sun et al., 2013). In addition, the recruitment of both Mcm2-7 hexamers requires the C-terminal domain of Mcm3 (Frigola et al., 2013). Using peptide-tagged proteins (Chapter 4) and crosslinking under limiting conditions, I found that Mcm3 interacts with Orc2 and Cdc6 during Mcm2-7 recruitment to ORC-Cdc6-DNA (Chapter 6). Sun et al. also observed an interaction between Mcm3 and Cdc6 (Sun et al., 2013), but did not examine interactions between Mcm3 and the ORC complex (Sun et al., 2013). In the cryo-EM structure of the OCCM complex, Mcm3 appears to be distal to both Cdc6 and Orc2. It is possible that this structure is trapped at a later stage where the Mcm2-7 complex has undergone conformational changes. Indeed, the authors confirmed the interaction between Mcm3 and Cdc6 by co-immunoaffinity purification and not from the cryo-EM structure. Since the C-terminus of Mcm3 is required for Mcm2-7/Cdt1 recruitment to ORC-Cdc6, it is likely that this C-terminal domain interacts with Orc2 and Cdc6. This remains to be tested.

These data suggest that Mcm2-7/Cdt1 is recruited to DNA-bound ORC Cdc6 via the C-terminus of Mcm3, which likely interacts with Orc2 and Cdc6.

7.1.3 The role of Cdt1 in recruitment of Mcm2-7 to DNA-bound ORC-Cdc6

Recent data has shown that in contrast to previous reports in crude extracts, Cdt1 is not required for the initial recruitment of Mcm3, 5 and 7 to origins but does play some role in recruiting Mcm2, 4 and 6 (Frigola et al., 2013). It is likely that Cdt1 plays a role in stabilising the Mcm2-7 ring during its initial recruitment to ORC-Cdc6.

Cdt1 interacts with the C-terminal tail of Mcm6 (Yanagi et al., 2002). The C-terminus of Mcm6 was recently found to inhibit Mcm2-7 binding to ORC-Cdc6 in the absence of Cdt1 (Fernandez-Cid et al., 2013). Interaction between Cdt1 and Mcm6 appears to alleviate this autoinhibitory property, allowing the MCM complex to interact with ORC-Cdc6 (Fernandez-Cid et al., 2013). It is likely that binding of Cdt1 to Mcm6 facilitates recruitment of Mcm2, 4 and 6 to ORC-Cdc6-DNA. Previous reports had suggested that an interaction between Cdt1 and Orc6 was necessary for Mcm2-7 recruitment and loading (Chen and Bell, 2011, Chen et al., 2007), however other data has subsequently shown that ORC lacking the Orc6 subunit is still able to recruit the Mcm2-7/Cdt1 complex as efficiently as the full ORC complex (Frigola et al., 2013). In agreement with this, Fernandez-Cid et al. showed that Orc1-5 could recruit Cdc6 and Mcm2-7/Cdt1 to DNA in the presence of ATPγS (Fernandez-Cid et al., 2013). These results suggest that an interaction between Cdt1 and Orc6 is not required for recruitment of Mcm2-7 to ORC-Cdc6-DNA.

7.1.4 A model for recruitment of Mcm2-7/Cdt1 to DNA-bound ORC-Cdc6

Taken together, these data support a new model for the initial recruitment of Mcm2-7/Cdt1 to ORC-Cdc6-DNA. I thus propose the following model (Figure 7.1). ORC binds ATP and is recruited to origin DNA by a combination of DNA sequence and chromatin structure (See Chapter 1, section 1.2.1.1). Upon entry into G1 phase, ORC recruits one molecule of Cdc6, which is also ATP-bound. Together, DNA-bound ORC and Cdc6 recruit a single heteroheptamer of Mcm2-7/Cdt1 via Mcm3 interaction with Orc2 and Cdc6. It seems probable that the Mcm2-7 hexamers do not require the interaction of multiple Cdt1 molecules with Orc6. Instead, it is likely that the role of Cdt1 is to stabilise the Mcm2-7 hexamer during its recruitment to ORC-Cdc6-DNA and to relieve an autoinhibitory property of the C-terminus of Mcm6. Figure 7.1 shows a schematic of this new model for Mcm2-7/Cdt1 recruitment to ORC-Cdc6.

In order to fully understand pre-RC assembly, the initial recruitment of Mcm2-7/Cdt1 to ORC-Cdc6-DNA will need to be further characterised. For example,

interactions between Cdc6 and the ORC subunits have yet to be examined. The 3x FLAG and 9x Myc-tagged protein preparations (Chapter 4) will likely be of use in investigating these interactions. In addition, although we now know that Mcm3 interacts with Orc2 and Cdc6, there are likely to be other interactions between the MCM subunits and ORC-Cdc6. Insight into protein-protein interactions would provide a better understanding of how the individual licensing factors are positioned relative to each other during recruitment of Mcm2-7/Cdt1 to ORC-Cdc6-DNA. It is also unclear when the Mcm2-7 ring opens to encircle DNA. It is possible that the Mcm2-7 complex already encircles DNA in the OCCM complex, however, this will need to be further examined.

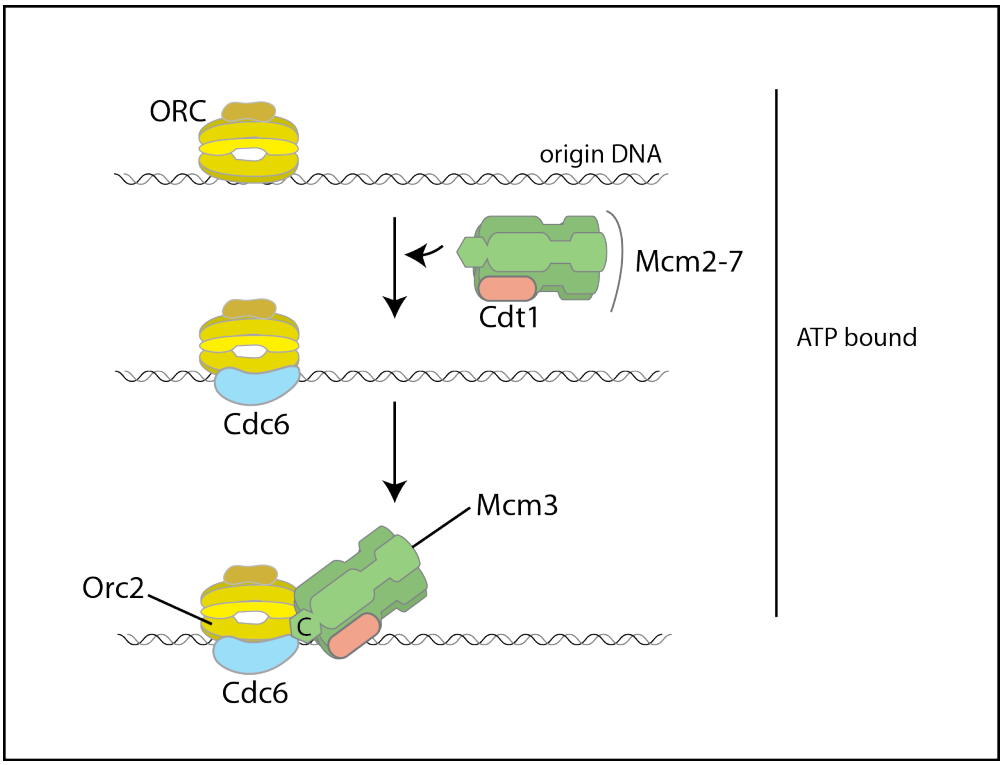

Figure 7.1 A model for Mcm2-7/Cdt1 recruitment to ORC-Cdc6-DNA

Model for recruitment of Mcm2-7/Cdt1 to ORC-Cdc6 prior to ATP hydrolysis. ORC binds to origins of DNA replication in an ATP dependent manner. In yeast, ORC binds origins throughout the cell cycle. Cdc6, bound to ATP, then binds ORC in late M/G1 phase of the cell cycle. Mcm2-7/Cdt1 is recruited to ORC-Cdc6-DNA via interaction of Mcm3 with Orc2 and Cdc6. The C-terminus of Mcm3 is required for the recruitment of Mcm2-7/Cdt1 to ORC-Cdc6-DNA. In this complex, there is a single copy of each of the licensing factors, indicating that the Mcm2-7 hexamers are loaded sequentially.

7.2 Loading the recruited Mcm2-7 hexamer into a double hexamer around double stranded DNA

Upon ATP hydrolysis, Mcm2-7 hexamers are loaded around double-stranded DNA as head-to-head double hexamers with their N-termini pointing towards each other (Evrin et al., 2009, Gambus et al., 2011, Remus et al., 2009). The loading of the Mcm2-7 double hexamer also involves concomitant release of Cdc6 and Cdt1. There is therefore a complex transition between the OCCM prior to ATP hydrolysis and the Mcm2-7 double hexamer following ATP hydrolysis. The results of this thesis and recent studies have revealed that there is a single copy of each of the licensing factors prior to ATP hydrolysis. In addition, it appears that both Mcm2-7 hexamers that form the loaded double hexamer require an interaction between the C-terminal tail of Mcm3 and ORC-Cdc6 as well as Cdt1 interaction with Mcm6 (Fernandez-Cid et al., 2013, Frigola et al., 2013). How do two hexamers of Mcm2-7 use the same interaction interfaces during loading and yet end up in opposite orientations on one side of the ORC complex (Figure 7.2)?

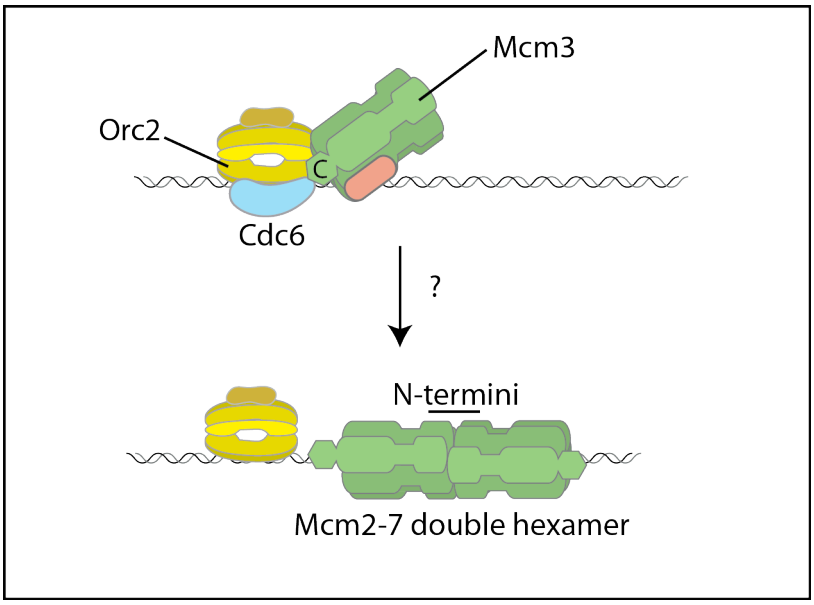

Figure 7.2 How is a double hexamer of Mcm2-7 loaded around double stranded DNA?

The OCCM is shown on top with an interaction between the C-terminus of Mcm3 and ORC-Cdc6. This OCCM transitions to a Mcm2-7 double hexamer bound around double-stranded DNA upon ATP hydrolysis. This also involves release of Cdc6 and Cdt1.

7.2.1 An intermediate in Mcm2-7 double hexamer formation – the OCM complex

Although we know that ATP hydrolysis is required for assembly of the Mcm2-7 double hexamer, it is unclear what stage of assembly requires this ATP hydrolysis. A recent study examined time-resolved Mcm2-7 loading *in vitro* in ATP and found that Mcm2-7 double hexamer formation is a slow process (Fernandez-Cid et al., 2013). The authors observed ATP hydrolysis-dependent release of Cdt1 prior to Cdc6 release. This resulted in a salt-sensitive intermediate complex consisting of ORC, Cdc6 and Mcm2-7 (OCM) (Fernandez-Cid et al., 2013). The OCM complex was found to consist of one copy each of ORC, Cdc6 and Mcm2-7. In this study the OCM formed in seconds, whilst formation of a salt-stable double hexamer of Mcm2-7 took several minutes. In addition, the OCM appears to be a salt-sensitive complex (Fernandez-Cid et al., 2013), indicating that this intermediate contains a partially loaded Mcm2-7 complex. This leads to the question: at what stage is the Mcm2-7 complex properly loaded? The mechanism for transition from an OCM to a Mcm2-7 double hexamer is still unknown.

Interaction of the C-terminus of Mcm3 with DNA-bound ORC-Cdc6 was found to stimulate the ATPase activity of ORC-Cdc6 (Frigola et al., 2013). This ATP hydrolysis was shown to promote the release of Mcm2-7 from ORC-Cdc6-DNA in the absence of Cdt1 (Frigola et al., 2013). Indeed, Cdt1 appears to block ATP hydrolysis by ORC-Cdc6 (Fernandez-Cid et al., 2013). It is possible that stimulation of ORC-Cdc6 ATPase activity by Mcm3 occurs after OCM formation (i.e. Cdt1 release) and acts to break the contact between Mcm2-7 and DNA-bound ORC-Cdc6 This would release ORC-Cdc6 to recruit and load the next Mcm2-7/Cdt1 heteroheptamer through another round of ATP hydrolysis. How the next Mcm2-7 hexamer would be loaded in an opposite orientation to the first hexamer is still unclear. Would this require formation of a second OCM? Samson et al. recently suggested a model for pre-RC formation (Samson and Bell, 2013). The authors suggest that the release of Cdt1 destabilises the Mcm2-7 complex and induces rearrangement of the hexamer into an “open book conformation” consisting of two halves. They further speculate that recruitment of the second hexamer via Mcm3

and Cdt1 would bind to the two halves of the open book generating a double hexamer or “closed book”.

In order to decipher how the Mcm2-7 double hexamer is loaded, further analysis is required. It will be interesting to examine the OCM complex further, for example by characterising protein-protein interactions and whether these differ compared to interactions in the OCCM. Another interesting aspect would be to map the inter-Mcm2-7 interactions in the loaded double hexamer. This would give insight into how the two hexamers are oriented with respect to each other in the double hexamer and perhaps tell us something about how the double hexamer is formed. It would also be informative to examine the OCM complex by cryo-EM and compare it to the OCCM ATPγS complex.

7.2.2 The role of ATP hydrolysis by ORC and Cdc6 in Mcm2-7 loading

ATP hydrolysis is required for Mcm2-7 double hexamer formation. At least 12 of the 14 proteins that participate in pre-RC assembly are members of the AAA^+ family of proteins (Iyer et al., 2004). Orc1, Cdc6 and Mcm2-7 are all capable of hydrolysing ATP. This raises the question: what is the role of the individual ATPase activities during pre-RC formation?

Studies in yeast extracts dissected distinct functions for the ATPase activities of ORC and Cdc6 in pre-RC formation (Bowers et al., 2004, Randell et al., 2006). A point mutation in the Walker B motif of Cdc6 (E224G-Cdc6), that inhibits ATP hydrolysis but not ATP binding, appeared to block Mcm2-7 loading (Randell et al., 2006). In addition, blocking ATP hydrolysis by ORC, by mutating a catalytically essential arginine finger in Orc4, reduced the number of Mcm2-7 complexes bound at origins (multiple Mcm2-7 complexes are normally loaded at origins). This suggested an absence of reiterative Mcm2-7 loading (Bowers et al., 2004). Importantly, mutations that eliminate ORC ATP hydrolysis in *S.cerevisiae* do not support viability (Bowers et al., 2004). This led to a model that sequential ATP hydrolysis by Cdc6 then ORC is required for proper Mcm2-7 loading at origins. A study by Ying and Gautier found that *Xenopus* Mcm2-7 ATPase mutants were

competent for Mcm2-7 loading (Ying and Gautier, 2005). The role of Mcm2-7 ATPase activity in pre-RC formation in yeast was therefore not tested.
In Chapter 5 I showed that E224G-Cdc6, harbouring a point mutation in its Walker B domain that blocks ATP hydrolysis, was competent for Mcm2-7 loading *in vitro*. This is in contrast to previous data from Randell et al. (2006). I only observed a reduction in Mcm2-7 loading when the amount of mutant Cdc6 used was increased. This suggests that the E224G-Cdc6 protein preparation is unstable which may explain why others were unable to detect Mcm2-7 loading. Indeed Evrin et al. found that this Walker B mutant led to some Mcm2-7 loading (Evrin et al., 2013).

In vivo, the E224G-Cdc6 mutant was found to be dominant negative when overexpressed from the *GAL* promoter (Perkins and Diffley, 1998). However, another study found that Cdc6 containing a double alanine mutation in the Walker B motif was functional *in vivo* and exhibited a normal S-phase (Weinreich et al., 1999). In this study, the Cdc6 Walker B mutant was expressed at endogenous levels and WT Cdc6 was expressed from a *MET3* promoter and repressed with methionine. An explanation for these data could be that mutations in the Walker B motif of Cdc6 somehow inhibit the release of Cdc6 from DNA after Mcm2-7 loading. Overexpression of such a mutant, as in the Perkins and Diffley study (1998) would cause replication origins in the cell to be occupied by Cdc6 that could not be released for Mcm2-7 loading in the next cell cycle, thus leading to a loss of viability.

These data indicate that the role of the Walker B motif of Cdc6 in pre-RC formation is still unclear. Analysis of a sensor-1 mutant of Cdc6 that is defective in ATP hydrolysis showed that ATP hydrolysis by Cdc6 is important for Cdt1 release and OCM formation (Fernandez-Cid et al., 2013). There is therefore likely to be a role for ATP hydrolysis by Cdc6 in pre-RC formation, but this role remains to be fully characterised and understood.

As mentioned previously, ATP hydrolysis by Orc1 is dependent on an arginine finger in Orc4. Blocking ATP hydrolysis by mutating this arginine finger (ORC4R) leads to a single round of Mcm2-7 loading *in vitro* and reiterative MCM loading is inhibited (Bowers et al., 2004). This mutation of ORC is also lethal *in vivo* (Bowers et al., 2004). However, Evrin et al. recently showed that the ORC4R mutant was

capable of producing a double hexamer of Mcm2-7 that was salt-resistant (Evrin et al., 2013). The authors concluded that Orc1 ATPase is not required for pre-RC assembly. Having said that, a Walker B mutant of Orc1, defective in ATP hydrolysis, was found to block Cdt1 release, thus preventing OCM formation (Fernandez-Cid et al., 2013).

There are therefore conflicting data surrounding the roles of ATP hydrolysis by ORC and Cdc6. There appear to be different phenotypes for different ATPase mutants. This could perhaps be due to effects on ATP binding rather than ATP hydrolysis. It is also likely that several of these mutations affect protein stability or proper folding, thus making results difficult to interpret. It is clear that ATP hydrolysis is required for Mcm2-7 double hexamer formation, but the distinct roles of ORC and Cdc6 ATPases will need to be further analysed and clarified. Unpublished data (Gideon Coster) indicate that the Mcm2-7 ATPases also play a role in pre-RC formation. It will be interesting to dissect the individual roles of the ATPases in Mcm2-7 double hexamer formation.

7.3 A model for Mcm2-7 double hexamer assembly

Taking all these data together, I propose the following model for Mcm2-7 double hexamer assembly (Figure 7.3). In the OCCM complex, it is probable that the Mcm2-7 ring encircles DNA (Figure 7.3, step 1). Following OCCM formation, ATP hydrolysis promotes release of Cdt1 forming the OCM complex (Figure 7.3, step 2). This ATP hydrolysis is likely to be mediated by ORC and Cdc6. The ATPases of Mcm2-7 could also be involved in this step. I propose that release of Cdt1 triggers another round of ATP hydrolysis, which is possibly mediated by Mcm3 activating the ATPase activities of ORC-Cdc6. This ATP hydrolysis could induce release of the Mcm2-7 complex from ORC-Cdc6 (step 3). This would free up DNA-bound ORC-Cdc6 to recruit another Mcm2-7/Cdt1 heteroheptamer via interaction of Mcm3 with Orc2 and Cdc6 (step 4). It is possible that the recruitment of each Mcm2-7 hexamer occurs on a DNA loop. In Chapter 3, I showed that 247 bp of ARS305 DNA could not support Mcm2-7 loading. It is likely that 247 bp of DNA is too short to form a DNA loop. If this is true, it may explain why Mcm2-7 loading could not

occur, but ORC binding was unaffected. Another study has also shown that there is a DNA length requirement for MCM loading in *Xenopus*. It is therefore a possibility that looping of the DNA is required for Mcm2-7 loading. In addition, a DNA loop would allow two hexamers loaded sequentially to interact at the same interfaces with ORC-Cdc6 (Figure 7.3). Following recruitment of the second Mcm2-7/Cdt1 heteroheptamer, I suggest that a further two rounds of ATP hydrolysis occur. The first inducing release of Cdt1, forming another OCM complex (step 5) and the second triggering release of Mcm2-7 from ORC-Cdc6 (step 6).

Finally, I propose that ATP hydrolysis by Cdc6 itself would induce its release and a Mcm2-7 double hexamer would form by sliding of the hexamers on the duplex DNA towards each other. Sliding of Mcm2-7 double hexamers on double stranded DNA has been previously observed (Evrin et al., 2013, Remus et al., 2009).

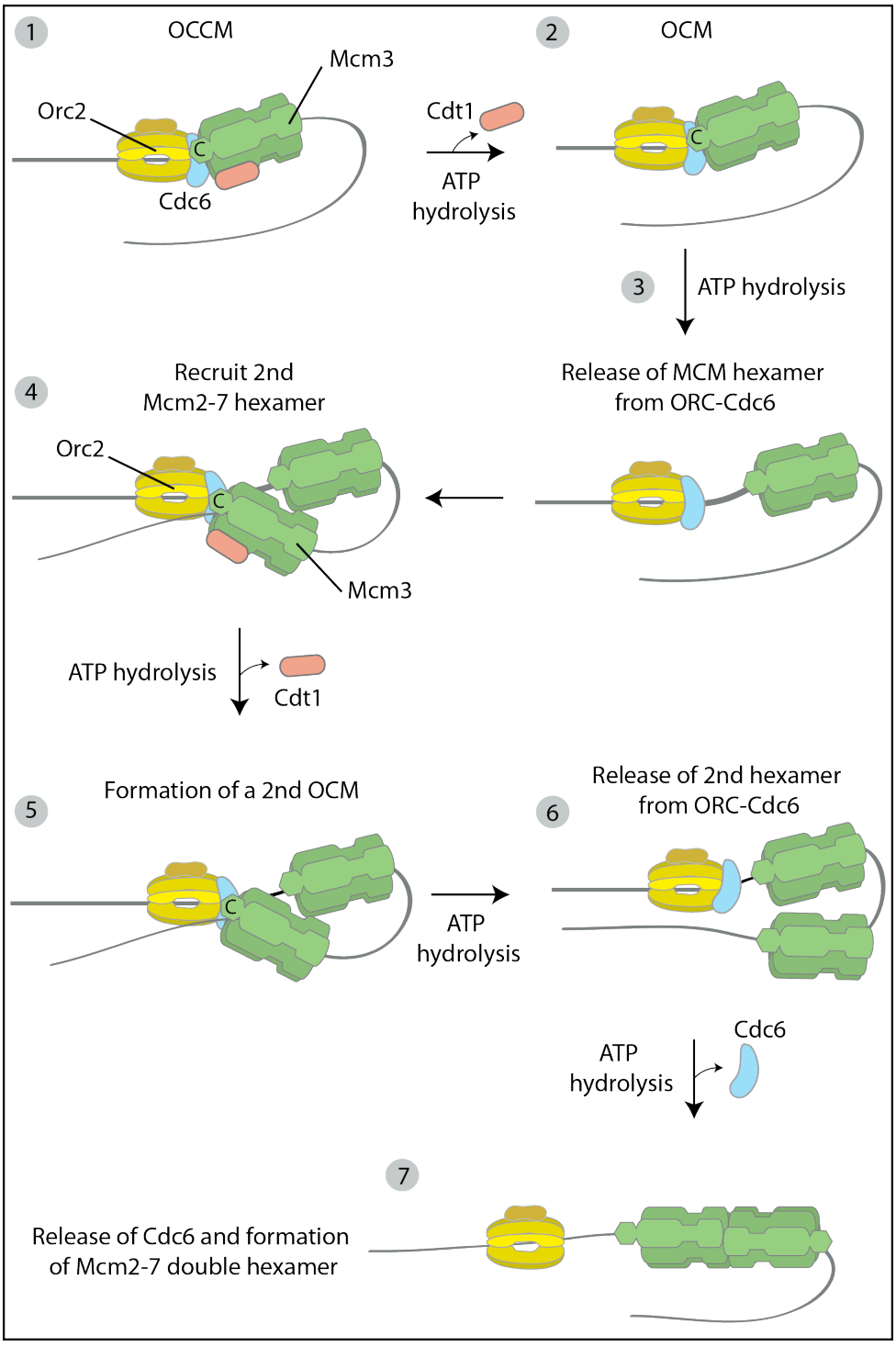

Figure 7.3 A model for Mcm2-7 double hexamer formation.

1) Formation of the OCCM (refer to Figure 7.1). 2) ATP hydrolysis induces Cdt1 release and formation of the OCM. 3) Another round of ATP hydrolysis releases Mcm2-7 from ORC-Cdc6. 4) A second Mcm2-7 hexamer is recruited to ORC-Cdc6-DNA via Mcm3 interaction with Orc2 and Cdc6. 5) & 6) Two rounds of ATP hydrolysis induce formation of a second OCM and then release of Mcm2-7 from ORC-Cdc6. 7) Cdc6 is released, and the Mcm2-7 double hexamer is formed by sliding of the hexamers towards each other.

This model is highly speculative at this stage. In order to increase our understanding of pre-RC formation, it will be crucial to further analyse intermediates in Mcm2-7 double hexamer formation. For example, EM with rotary shadowing would provide insight into the structure of the DNA during Mcm2-7 loading and whether the DNA does indeed form a loop. This could be performed on the OCM complex or indeed the OCCM complex.

The distinct roles of the ATPases should also be addressed and clarified. It is still not clear what the individual roles of ATP hydrolysis by ORC and Cdc6 are. In addition, it appears that the ATPases of Mcm2-7 also play a role in pre-RC formation. Characterising these roles by analysis of ATPase site mutants will be invaluable in the study of licensing.

Several of the Mcm2-7 subunits have N and C-terminal tails (Figure 1.3) that are unique to that particular subunit but conserved amongst species. It is possible that as for the C-terminal tail of Mcm3, these other tails play roles in pre-RC formation. It would therefore be interesting to examine the roles of the Mcm2-7 subunit tails.

Finally, further characterisation of protein-protein interactions during Mcm2-7 double hexamer formation would allow us to begin to construct a model for how the individual proteins are spatially oriented during pre-RC formation.

Addressing these points would provide insight into how the Mcm2-7 complex transitions from a heteroheptamer of Mcm2-7/Cdt1 to a double hexamer of Mcm2-7 loaded around double-stranded DNA.

Reference List

APARICIO, O. M., WEINSTEIN, D. M. & BELL, S. P. 1997. Components and dynamics of DNA replication complexes in S. cerevisiae: redistribution of MCM proteins and Cdc45p during S phase. *Cell,* 91**,** 59-69.

ARAI, K., YASUDA, S. & KORNBERG, A. 1981. Mechanism of dnaB protein action. I. Crystallization and properties of dnaB protein, an essential replication protein in Escherichia coli. *J Biol Chem,* 256**,** 5247-52.

ARIAS, E. E. & WALTER, J. C. 2007. Strength in numbers: preventing rereplication via multiple mechanisms in eukaryotic cells. *Genes Dev,* 21**,** 497-518.

ARIAS-PALOMO, E., O'SHEA, V. L., HOOD, I. V. & BERGER, J. M. 2013. The bacterial DnaC helicase loader is a DnaB ring breaker. *Cell,* 153**,** 438-48.

BAILEY, S., ELIASON, W. K. & STEITZ, T. A. 2007a. The crystal structure of the Thermus aquaticus DnaB helicase monomer. *Nucleic Acids Res,* 35**,** 4728-36.

BAILEY, S., ELIASON, W. K. & STEITZ, T. A. 2007b. Structure of hexameric DnaB helicase and its complex with a domain of DnaG primase. *Science,* 318**,** 459-63.

BARCENA, M., RUIZ, T., DONATE, L. E., BROWN, S. E., DIXON, N. E., RADERMACHER, M. & CARAZO, J. M. 2001. The DnaB.DnaC complex: a structure based on dimers assembled around an occluded channel. *EMBO J,* 20**,** 1462-8.

BELL, S. P. & DUTTA, A. 2002. DNA replication in eukaryotic cells. *Annu Rev Biochem,* 71**,** 333-74.

BELL, S. P. & KAGUNI, J. M. 2013. Helicase loading at chromosomal origins of replication. *Cold Spring Harb Perspect Biol,* 5.

BELL, S. P., KOBAYASHI, R. & STILLMAN, B. 1993. Yeast origin recognition complex functions in transcription silencing and DNA replication. *Science,* 262**,** 1844-1849.

BELL, S. P. & STILLMAN, B. 1992. ATP-dependent recognition of eukaryotic origins of DNA replication by a multiprotein complex. *Nature,* 357**,** 128-134.

BLOW, J. J. & GE, X. Q. 2009. A model for DNA replication showing how dormant origins safeguard against replication fork failure. *EMBO Rep,* 10**,** 406-12.

BLOW, J. J., GILLESPIE, P. J., FRANCIS, D. & JACKSON, D. A. 2001. Replication origins in Xenopus egg extract Are 5-15 kilobases apart and are activated in clusters that fire at different times. *J Cell Biol,* 152**,** 15-25.

BLOW, J. J. & LASKEY, R. A. 1988. A role for the nuclear envelope in controlling DNA replication within the cell cycle. *Nature,* 332**,** 546-8.

BOCHMAN, M. L., BELL, S. P. & SCHWACHA, A. 2008. Subunit organization of Mcm2-7 and the unequal role of active sites in ATP hydrolysis and viability. *Mol Cell Biol,* 28**,** 5865-73.

BOCHMAN, M. L. & SCHWACHA, A. 2009. The Mcm complex: unwinding the mechanism of a replicative helicase. *Microbiol Mol Biol Rev,* 73**,** 652-83.

BOGAN, J. A. & HELMSTETTER, C. E. 1997. DNA sequestration and transcription in the oriC region of Escherichia coli. *Mol Microbiol,* 26**,** 889-96.

BOOS, D., FRIGOLA, J. & DIFFLEY, J. F. X. 2012. Activation of the replicative DNA helicase: breaking up is hard to do. *Curr Opin Cell Biol*.

BOOS, D., SANCHEZ-PULIDO, L., RAPPAS, M., PEARL, L. H., OLIVER, A. W., PONTING, C. P. & DIFFLEY, J. F. X. 2011. Regulation of DNA Replication through Sld3-Dpb11 Interaction Is Conserved from Yeast to Humans. *Curr Biol,* 21**,** 1152-7.

BOOS, D., YEKEZARE, M. & DIFFLEY, J. F. 2013. Identification of a heteromeric complex that promotes DNA replication origin firing in human cells. *Science,* 340**,** 981-4.

BOWERS, J. L., RANDELL, J. C., CHEN, S. & BELL, S. P. 2004. ATP hydrolysis by ORC catalyzes reiterative Mcm2-7 assembly at a defined origin of replication. *Mol Cell,* 16**,** 967-78.

BOWMAN, G. D., O'DONNELL, M. & KURIYAN, J. 2004. Structural analysis of a eukaryotic sliding DNA clamp-clamp loader complex. *Nature,* 429**,** 724-30.

BRAMHILL, D. & KORNBERG, A. 1988. Duplex opening by DnaA protein at novel sequences in initiation of replication at the origin of the *E.coli* chromosome. *Cell,* 52**,** 743-755.

BROACH, J. R., LI, Y. Y., FELDMAN, J., JAYARAM, M., ABRAHAM, J., NASMYTH, K. A. & HICKS, J. B. 1983. Localization and sequence analysis of yeast origins of DNA replication. *Cold Spring Harb Symp Quant Biol,* 47 Pt 2**,** 1165-73.

BUJALOWSKI, W., KLONOWSKA, M. M. & JEZEWSKA, M. J. 1994. Oligomeric structure of Escherichia coli primary replicative helicase DnaB protein. *J Biol Chem,* 269**,** 31350-8.

CAMPBELL, J. L. & KLECKNER, N. 1990. *E. coli oriC* and the *dnaA* Gene Promoter are Sequestered from *dam* Methyltransferase Following the Passage of the Chromosomal Replication Fork. *Cell,* 62**,** 967-979.

CARPENTER, P. B., MUELLER, P. R. & DUNPHY, W. G. 1996. Role for a Xenopus Orc2-related protein in controlling DNA replication. *Nature,* 379**,** 357-360.

CARR, K. M. & KAGUNI, J. M. 2001. Stoichiometry of DnaA and DnaB protein in initiation at the Escherichia coli chromosomal origin. *J Biol Chem,* 276**,** 44919-25.

CAYROU, C., COULOMBE, P., PUY, A., RIALLE, S., KAPLAN, N., SEGAL, E. & MECHALI, M. 2012. New insights into replication origin characteristics in metazoans. *Cell Cycle,* 11**,** 658-67.

CAYROU, C., COULOMBE, P., VIGNERON, A., STANOJCIC, S., GANIER, O., PEIFFER, I., RIVALS, E., PUY, A., LAURENT-CHABALIER, S., DESPRAT, R. & MECHALI, M. 2011. Genome-scale analysis of metazoan replication origins reveals their organization in specific but flexible sites defined by conserved features. *Genome Res,* 21**,** 1438-49.

CHAKRABORTY, A., SHEN, Z. & PRASANTH, S. G. 2011. "ORCanization" on heterochromatin: linking DNA replication initiation to chromatin organization. *Epigenetics,* 6**,** 665-70.

CHEN, S. & BELL, S. P. 2011. CDK prevents Mcm2-7 helicase loading by inhibiting Cdt1 interaction with Orc6. *Genes Dev,* 25**,** 363-72.

CHEN, S., DE VRIES, M. A. & BELL, S. P. 2007. Orc6 is required for dynamic recruitment of Cdt1 during repeated Mcm2-7 loading. *Genes Dev,* 21**,** 2897-907.

CHEN, Z., SPECK, C., WENDEL, P., TANG, C., STILLMAN, B. & LI, H. 2008. The architecture of the DNA replication origin recognition complex in Saccharomyces cerevisiae. *Proc Natl Acad Sci U S A,* 105**,** 10326-31.

CHONG, J. P., HAYASHI, M. K., SIMON, M. N., XU, R. M. & STILLMAN, B. 2000. A double-hexamer archaeal minichromosome maintenance protein is an ATP-dependent DNA helicase. *Proc Natl Acad Sci U S A,* 97**,** 1530-1535.

COCKER, J. H., PIATTI, S., SANTOCANALE, C., NASMYTH, K. & DIFFLEY, J. F. X. 1996. An essential role for the Cdc6 protein in forming the pre-replicative complexes of budding yeast. *Nature,* 379**,** 180-2.

COLEMAN, T. R., CARPENTER, P. B. & DUNPHY, W. G. 1996. The *Xenopus* Cdc6 protein is essential for the initiation of a single round of DNA replication in cell-free extracts. *Cell,* 87**,** 53-63.

COSTA, A., ILVES, I., TAMBERG, N., PETOJEVIC, T., NOGALES, E., BOTCHAN, M. R. & BERGER, J. M. 2011. The structural basis for MCM2-7 helicase activation by GINS and Cdc45. *Nat Struct Mol Biol,* 18**,** 471-7.

DAHMANN, C., DIFFLEY, J. F. X. & NASMYTH, K. A. 1995. S-phase-promoting cyclin-dependent kinases prevent re-replication by inhibiting the transition of replication origins to a pre-replicative state. *Curr Biol,* 5**,** 1257-69.

DAVEY, M. J., FANG, L., MCINERNEY, P., GEORGESCU, R. E. & O'DONNELL, M. 2002. The DnaC helicase loader is a dual ATP/ADP switch protein. *Embo J,* 21**,** 3148-59.

DAVEY, M. J., INDIANI, C. & O'DONNELL, M. 2003. Reconstitution of the Mcm2-7p heterohexamer, subunit arrangement, and ATP site architecture. *J Biol Chem,* 278**,** 4491-9.

DEAN, F. B., DODSON, M., ECHOLS, H. & HURWITZ, J. 1987. ATP-dependent formation of a specialized nucleoprotein structure by simian virus 40 (SV40) large tumor antigen at the SV40 replication origin. *Proc Natl Acad Sci U S A,* 84**,** 8981-5.

DETWEILER, C. S. & LI, J. J. 1998. Ectopic induction of Clb2 in early G1 phase is sufficient to block prereplicative complex formation in *Saccharomyces cerevisiae*. *Proc. Natl. Acad. Sci. USA,* 95**,** 2384-2389.

DEVAULT, A., VALLEN, E. A., YUAN, T., GREEN, S., BENSIMON, A. & SCHWOB, E. 2002. Identification of Tah11/Sid2 as the ortholog of the replication licensing factor Cdt1 in Saccharomyces cerevisiae. *Curr Biol,* 12**,** 689-94.

DIFFLEY, J. F. X. 1996. Once and only once upon a time: Specifying and regulating origins of DNA replication in eukaryotic cells. *Genes Dev.,* 10**,** 2819-2830.

DIFFLEY, J. F. X. & COCKER, J. H. 1992. Protein-DNA interactions at a yeast replication origin. *Nature,* 357**,** 169-172.

DIFFLEY, J. F. X., COCKER, J. H., DOWELL, S. J., HARWOOD, J. & ROWLEY, A. 1995. Stepwise assembly of initiation complexes at budding yeast replication origins during the cell cycle. *J Cell Sci Suppl,* 19**,** 67-72.

DIFFLEY, J. F. X., COCKER, J. H., DOWELL, S. J. & ROWLEY, A. 1994. Two steps in the assembly of complexes at yeast replication origins in vivo. *Cell,* 78**,** 303-16.

DONOVAN, S., HARWOOD, J., DRURY, L. S. & DIFFLEY, J. F. X. 1997. Cdc6p-dependent loading of Mcm proteins onto pre-replicative chromatin in budding yeast. *Proc Natl Acad Sci U S A,* 94**,** 5611-6.

DRURY, L. S., PERKINS, G. & DIFFLEY, J. F. X. 1997. The Cdc4/34/53 pathway targets Cdc6p for proteolysis in budding yeast. *Embo J,* 16**,** 5966-76.

DRURY, L. S., PERKINS, G. & DIFFLEY, J. F. X. 2000. The cyclin-dependent kinase Cdc28p regulates distinct modes of Cdc6p proteolysis during the budding yeast cell cycle. *Curr Biol,* 10**,** 231-40.

EATON, M. L., GALANI, K., KANG, S., BELL, S. P. & MACALPINE, D. M. 2010. Conserved nucleosome positioning defines replication origins. *Genes Dev,* 24**,** 748-53.

EDWARDS, M. C., TUTTER, A. V., CVETIC, C., GILBERT, C. H., PROKHOROVA, T. A. & WALTER, J. C. 2002. MCM2-7 complexes bind chromatin in a distributed pattern surrounding the origin recognition complex in Xenopus egg extracts. *J Biol Chem,* 277**,** 33049-57.

ENEMARK, E. J. & JOSHUA-TOR, L. 2008. On helicases and other motor proteins. *Curr Opin Struct Biol,* 18**,** 243-57.

EVRIN, C., CLARKE, P., ZECH, J., LURZ, R., SUN, J., UHLE, S., LI, H., STILLMAN, B. & SPECK, C. 2009. A double-hexameric MCM2-7 complex is loaded onto origin DNA during licensing of eukaryotic DNA replication. *Proc Natl Acad Sci U S A,* 106**,** 20240-5.

EVRIN, C., FERNANDEZ-CID, A., ZECH, J., HERRERA, M. C., RIERA, A., CLARKE, P., BRILL, S., LURZ, R. & SPECK, C. 2013. In the absence of ATPase activity, pre-RC formation is blocked prior to MCM2-7 hexamer dimerization. *Nucleic Acids Res,* 41**,** 3162-72.

FANG, L., DAVEY, M. J. & O'DONNELL, M. 1999. Replisome assembly at oriC, the replication origin of E. coli, reveals an explanation for initiation sites outside an origin. *Mol Cell,* 4**,** 541-53.

FERENBACH, A., LI, A., BRITO-MARTINS, M. & BLOW, J. J. 2005. Functional domains of the Xenopus replication licensing factor Cdt1. *Nucleic Acids Res,* 33**,** 316-24.

FERNANDEZ-CID, A., RIERA, A., TOGNETTI, S., HERRERA, M. C., SAMEL, S., EVRIN, C., WINKLER, C., GARDENAL, E., UHLE, S. & SPECK, C. 2013. An ORC/Cdc6/MCM2-7 Complex Is Formed in a Multistep Reaction to Serve as a Platform for MCM Double-Hexamer Assembly. *Mol Cell,* 50**,** 577-88.

FLETCHER, R. J., BISHOP, B. E., LEON, R. P., SCLAFANI, R. A., OGATA, C. M. & CHEN, X. S. 2003. The structure and function of MCM from archaeal M. Thermoautotrophicum. *Nat Struct Biol,* 10**,** 160-7.

FOSS, M., MCNALLY, F. J., LAURENSON, P. & RINE, J. 1993. Origin recognition complex (ORC) in transcriptional silencing and DNA replication in *S. cerevisiae*. *Science,* 262**,** 1838-1844.

FRANCIS, L. I., RANDELL, J. C., TAKARA, T. J., UCHIMA, L. & BELL, S. P. 2009. Incorporation into the prereplicative complex activates the Mcm2-7 helicase for Cdc7-Dbf4 phosphorylation. *Genes Dev,* 23**,** 643-54.

FRICK, D. N. & RICHARDSON, C. C. 2001. DNA primases. *Annu Rev Biochem,* 70**,** 39-80.

FRIED, M. & CROTHERS, D. M. 1981. Equilibria and kinetics of lac repressor-operator interactions by polyacrylamide gel electrophoresis. *Nucleic Acids Res,* 9**,** 6505-25.

FRIEDMAN, K. L., BREWER, B. J. & FANGMAN, W. L. 1997. Replication profile of *Saccharomyces cerevisiae* chromosome VI. *Genes Cells,* 2**,** 667-678.

FRIGOLA, J., REMUS, D., MEHANNA, A. & DIFFLEY, J. F. 2013. ATPase-dependent quality control of DNA replication origin licensing. *Nature,* 495**,** 339-43.

FU, Y. V., YARDIMCI, H., LONG, D. T., GUAINAZZI, A., BERMUDEZ, V. P., HURWITZ, J., VAN OIJEN, A., SCHARER, O. D. & WALTER, J. C. 2011. Selective Bypass of a Lagging Strand Roadblock by the Eukaryotic Replicative DNA Helicase. *Cell,* 146**,** 931-941.

FUJITA, M. 2006. Cdt1 revisited: complex and tight regulation during the cell cycle and consequences of deregulation in mammalian cells. *Cell Div,* 1**,** 22.

FULLER, R. S., FUNNELL, B. E. & KORNBERG, A. 1984. The DnaA protein complex with the *E. coli* chromosomal replication origin (*oriC*) and other DNA sites. *Cell,* 38**,** 889-900.

GAMBUS, A., JONES, R. C., SANCHEZ-DIAZ, A., KANEMAKI, M., VAN DEURSEN, F., EDMONDSON, R. D. & LABIB, K. 2006. GINS maintains association of Cdc45 with MCM in replisome progression complexes at eukaryotic DNA replication forks. *Nat Cell Biol,* 8**,** 358-66.

GAMBUS, A., KHOUDOLI, G. A., JONES, R. C. & BLOW, J. J. 2011. MCM2-7 form double hexamers at licensed origins in Xenopus egg extract. *J Biol Chem,* 286**,** 11855-64.

GARG, P., STITH, C. M., SABOURI, N., JOHANSSON, E. & BURGERS, P. M. 2004. Idling by DNA polymerase delta maintains a ligatable nick during lagging-strand DNA replication. *Genes Dev,* 18**,** 2764-73.

GARNER, M. M. & REVZIN, A. 1981. A gel electrophoresis method for quantifying the binding of proteins to specific DNA regions: application to components of the

Escherichia coli lactose operon regulatory system. *Nucleic Acids Res,* 9**,** 3047-60.

GAVIN, K. A., HIDAKA, M. & STILLMAN, B. 1995. Conserved initiator proteins in eukaryotes [see comments]. *Science,* 270**,** 1667-71.

GE, X. Q., JACKSON, D. A. & BLOW, J. J. 2007. Dormant origins licensed by excess Mcm2-7 are required for human cells to survive replicative stress. *Genes Dev,* 21**,** 3331-41.

GERAGHTY, D. S., DING, M., HEINTZ, N. H. & PEDERSON, D. S. 2000. Premature structural changes at replication origins in a yeast minichromosome maintenance (MCM) mutant. *J Biol Chem,* 275**,** 18011-21.

GIETZ, D., ST. JEAN, A., WOODS, R. A. & SCHIESTL, R. H. 1992. Improved method for high efficiency transformation of intact yeast cells. *Nucleic Acids Res.,* 20**,** 1425.

GILLESPIE, P. J., LI, A. & BLOW, J. J. 2001. Reconstitution of licensed replication origins on *Xenopus* sperm nuclei using purified proteins. *BMC Biochem,* 2**,** 15.

GOSSEN, M., PAK, D. T., HANSEN, S. K., ACHARYA, J. K. & BOTCHAN, M. R. 1995. A Drosophila homolog of the yeast origin recognition complex [see comments]. *Science,* 270**,** 1674-7.

GREEN, B. M., FINN, K. J. & LI, J. J. 2010. Loss of DNA replication control is a potent inducer of gene amplification. *Science,* 329**,** 943-6.

GUARNE, A., ZHAO, Q., GHIRLANDO, R. & YANG, W. 2002. Insights into negative modulation of E. coli replication initiation from the structure of SeqA-hemimethylated DNA complex. *Nat Struct Biol,* 9**,** 839-43.

HARTWELL, L. H., MORTIMER, R. K., CULOTTI, J. & CULOTTI, M. 1973. Genetic control of the cell division cycle in yeast : V. Genetic analysis of *cdc* mutants. *Genetics,* 74**,** 267-286.

HELLER, R. C., KANG, S., LAM, W. M., CHEN, S., CHAN, C. S. & BELL, S. P. 2011. Eukaryotic Origin-Dependent DNA Replication In Vitro Reveals Sequential Action of DDK and S-CDK Kinases. *Cell,* 146**,** 80-91.

HENNESSY, K. M., CLARK, C. D. & BOTSTEIN, D. 1990. Subcellular localization of yeast CDC46 varies with the cell cycle. *Genes Dev.,* 4**,** 2252-2263.

HOFMANN, J. F. & BEACH, D. 1994. cdt1 is an essential target of the Cdc10/Sct1 transcription factor: requirement for DNA replication and inhibition of mitosis. *EMBO J,* 13**,** 425-34.

HOGAN, E. & KOSHLAND, D. 1992. Addition of extra origins of replication to a minichromosome suppresses its mitotic loss in *cdc6* and *cdc14* mutants of *Saccharomyces cerevisiae*. *Proc. Natl. Acad. Sci. USA,* 89**,** 3098-3102.

HSIAO, C. L. & CARBON, J. 1979. High-frequency transformation of yeast by plasmids containing the cloned yeast ARG4 gene. *Proc Natl Acad Sci U S A,* 76**,** 3829-33.

HUANG, R. Y. & KOWALSKI, D. 1996. Multiple DNA elements in ARS305 determine replication origin activity in a yeast chromosome. *Nucleic Acids Res,* 24**,** 816-23.

ILVES, I., PETOJEVIC, T., PESAVENTO, J. J. & BOTCHAN, M. R. 2010. Activation of the MCM2-7 helicase by association with Cdc45 and GINS proteins. *Mol Cell,* 37**,** 247-58.

ISHIMI, Y. 1997. A DNA helicase activity is associated with an MCM4, -6, and -7 protein complex. *J. Biol. Chem.,* 272**,** 24508-24513.

ITSATHITPHAISARN, O., WING, R. A., ELIASON, W. K., WANG, J. & STEITZ, T. A. 2012. The hexameric helicase DnaB adopts a nonplanar conformation during translocation. *Cell,* 151**,** 267-77.

IYER, L. M., LEIPE, D. D., KOONIN, E. V. & ARAVIND, L. 2004. Evolutionary history and higher order classification of AAA+ ATPases. *J Struct Biol,* 146**,** 11-31.

JACOB, F., BRENNER, S. & CUZIN, F. 1963. On the regulation of DNA replication in bacteria. *Cold Spring Harbor Symp. Quant. Biol.,* 28**,** 329-348.
JOHANSSON, E. & DIXON, N. 2013. Replicative DNA polymerases. *Cold Spring Harb Perspect Biol,* 5.
JOHANSSON, E., GARG, P. & BURGERS, P. M. 2004. The Pol32 subunit of DNA polymerase delta contains separable domains for processive replication and proliferating cell nuclear antigen (PCNA) binding. *J Biol Chem,* 279**,** 1907-15.
JOHNSON, A. & O'DONNELL, M. 2005. Cellular DNA replicases: components and dynamics at the replication fork. *Annu Rev Biochem,* 74**,** 283-315.
KAGUNI, J. M. 2006. DnaA: controlling the initiation of bacterial DNA replication and more. *Annu Rev Microbiol,* 60**,** 351-75.
KAMIMURA, Y., TAK, Y. S., SUGINO, A. & ARAKI, H. 2001. Sld3, which interacts with Cdc45 (Sld4), functions for chromosomal DNA replication in Saccharomyces cerevisiae. *Embo J,* 20**,** 2097-107.
KATAYAMA, T. 2008. Roles for the AAA+ motifs of DnaA in the initiation of DNA replication. *Biochem Soc Trans,* 36**,** 78-82.
KAWASAKI, Y., KIM, H. D., KOJIMA, A., SEKI, T. & SUGINO, A. 2006. Reconstitution of Saccharomyces cerevisiae prereplicative complex assembly in vitro. *Genes Cells,* 11**,** 745-56.
KELCH, B. A., MAKINO, D. L., O'DONNELL, M. & KURIYAN, J. 2011. How a DNA polymerase clamp loader opens a sliding clamp. *Science,* 334**,** 1675-80.
KIM, S., DALLMANN, H. G., MCHENRY, C. S. & MARIANS, K. J. 1996. tau couples the leading- and lagging-strand polymerases at the Escherichia coli DNA replication fork. *J Biol Chem,* 271**,** 21406-12.
KIMURA, H., NOZAKI, N. & SUGIMOTO, K. 1994. DNA polymerase alpha associated protein P1, a murine homolog of yeast MCM3, changes its intranuclear distribution during the DNA synthetic period. *Embo J,* 13**,** 4311-20.
KLEMM, R. D., AUSTIN, R. J. & BELL, S. P. 1997. Coordinate Binding of ATP and Origin DNA Regulates the ATPase Activity of the Origin Recognition Complex. *Cell,* 88**,** 493-502.
KLEMM, R. D. & BELL, S. P. 2001. ATP bound to the origin recognition complex is important for preRC formation. *Proc Natl Acad Sci U S A,* 98**,** 8361-7.
KOONIN, E. V. 1993. A common set of conserved motifs in a vast variety of putative nucleic acid-dependent ATPases including MCM proteins involved in the initiation of eukaryotic DNA replication. *Nucleic Acids Res.,* 21**,** 2541-2547.
KORNBERG, A. & BAKER, T. A. 1992. *DNA Replication,* United States of America, W. H. Freeman and Company.
KORNBERG, T. & GEFTER, M. L. 1972. Deoxyribonucleic acid synthesis in cell-free extracts. IV. Purification and catalytic properties of deoxyribonucleic acid polymerase III. *J Biol Chem,* 247**,** 5369-75.
KOWALSKI, D. & EDDY, M. J. 1989. The DNA unwinding element: A novel *cis*-acting component that facilitates opening of the *Escherichia coli* replication origin. *EMBO J.,* 8.
KUBOTA, Y., MIMURA, S., NISHIMOTO, S.-I., TAKISAWA, H. & NOJIMA, H. 1995. Identification of the yeast MCM3-related protein as a component of *Xenopus* DNA replication licensing factor. *Cell,* 81**,** 601-609.
KUSHNIROV, V. V. 2000. Rapid and reliable protein extraction from yeast. *Yeast,* 16**,** 857-60.
LABIB, K., DIFFLEY, J. F. X. & KEARSEY, S. E. 1999. G1-phase and B-type cyclins exclude the DNA-replication factor Mcm4 from the nucleus. *Nat Cell Biol,* 1**,** 415-22.
LABIB, K., KEARSEY, S. E. & DIFFLEY, J. F. X. 2001. MCM2-7 proteins are essential components of prereplicative complexes that accumulate cooperatively in the

nucleus during G1-phase and are required to establish, but not maintain, the S-phase checkpoint. *Mol Biol Cell,* 12**,** 3658-67.
LABIB, K., TERCERO, J. A. & DIFFLEY, J. F. X. 2000. Uninterrupted MCM2-7 function required for DNA replication fork progression. *Science,* 288**,** 1643-7.
LEBOWITZ, J. H. & MCMACKEN, R. 1986. The Escherichia coli dnaB replication protein is a DNA helicase. *J Biol Chem,* 261**,** 4738-48.
LEE, J. K. & HURWITZ, J. 2000. Isolation and characterization of various complexes of the minichromosome maintenance proteins of Schizosaccharomyces pombe. *J Biol Chem,* 275**,** 18871-8.
LEONARD, A. C. & GRIMWADE, J. E. 2010. Regulating DnaA complex assembly: it is time to fill the gaps. *Curr Opin Microbiol,* 13**,** 766-72.
LEONARD, A. C. & MECHALI, M. 2013. DNA Replication Origins. *Cold Spring Harb Perspect Biol*.
LIANG, C., WEINREICH, M. & STILLMAN, B. 1995. ORC and Cdc6p interact and determine the frequency of initiation of DNA replication in the genome. *Cell,* 81**,** 667-676.
LIKU, M. E., NGUYEN, V. Q., ROSALES, A. W., IRIE, K. & LI, J. J. 2005. CDK phosphorylation of a novel NLS-NES module distributed between two subunits of the Mcm2-7 complex prevents chromosomal rereplication. *Mol Biol Cell,* 16**,** 5026-39.
LOHMAN, T. M. & BJORNSON, K. P. 1996. Mechanisms of helicase-catalyzed DNA unwinding. *Annu Rev Biochem,* 65**,** 169-214.
LU, M., CAMPBELL, J. L., BOYE, E. & KLECKNER, N. 1994. SeqA: a negative modulator of replication initiation in E. coli. *Cell,* 77**,** 413-26.
LUTZMANN, M., GREY, C., TRAVER, S., GANIER, O., MAYA-MENDOZA, A., RANISAVLJEVIC, N., BERNEX, F., NISHIYAMA, A., MONTEL, N., GAVOIS, E., FORICHON, L., DE MASSY, B. & MECHALI, M. 2012. MCM8- and MCM9-deficient mice reveal gametogenesis defects and genome instability due to impaired homologous recombination. *Mol Cell,* 47**,** 523-34.
LUTZMANN, M. & MECHALI, M. 2008. MCM9 binds Cdt1 and is required for the assembly of prereplication complexes. *Mol Cell,* 31**,** 190-200.
MAINE, G. T., SINHA, P. & TYE, B. K. 1984. Mutants of *Saccharomyces cerevisiae* defective in the maintenance of minichromosomes. *Genetics,* 106**,** 365-85.
MAIORANO, D., CUVIER, O., DANIS, E. & MECHALI, M. 2005. MCM8 is an MCM2-7-related protein that functions as a DNA helicase during replication elongation and not initiation. *Cell,* 120**,** 315-28.
MAIORANO, D., MOREAU, J. & MECHALI, M. 2000. XCDT1 is required for the assembly of pre-replicative complexes in *Xenopus laevis*. *Nature,* 404**,** 622-5.
MAKI, H., MAKI, S. & KORNBERG, A. 1988. DNA Polymerase III holoenzyme of Escherichia coli. IV. The holoenzyme is an asymmetric dimer with twin active sites. *J Biol Chem,* 263**,** 6570-8.
MAKOWSKA-GRZYSKA, M. & KAGUNI, J. M. 2010. Primase directs the release of DnaC from DnaB. *Mol Cell,* 37**,** 90-101.
MARAHRENS, Y. & STILLMAN, B. 1992. A yeast chromosomal origin of DNA replication defined by multiple functional elements. *Science,* 255**,** 817-823.
MATSUI, M., OKA, A., TAKANAMI, M., YASUDA, S. & HIROTA, Y. 1985. Sites of DnaA protein binding in the replication origin of the *Escherichia coli* K-12 chromosome. *J. Mol. Biol.,* 184**,** 529-533.
MCGARRY, K. C., RYAN, V. T., GRIMWADE, J. E. & LEONARD, A. C. 2004. Two discriminatory binding sites in the Escherichia coli replication origin are required for DNA strand opening by initiator DnaA-ATP. *Proc Natl Acad Sci U S A,* 101**,** 2811-6.

MICKLEM, G., ROWLEY, A., HARWOOD, J., NASMYTH, K. & DIFFLEY, J. F. X. 1993. Yeast origin recognition complex is involved in DNA replication and transcriptional silencing. *Nature,* 366**,** 87-89.

MILLER, D. T., GRIMWADE, J. E., BETTERIDGE, T., ROZGAJA, T., TORGUE, J. J. & LEONARD, A. C. 2009. Bacterial origin recognition complexes direct assembly of higher-order DnaA oligomeric structures. *Proc Natl Acad Sci U S A,* 106**,** 18479-84.

MOTT, M. L., ERZBERGER, J. P., COONS, M. M. & BERGER, J. M. 2008. Structural synergy and molecular crosstalk between bacterial helicase loaders and replication initiators. *Cell,* 135**,** 623-34.

MOYER, S. E., LEWIS, P. W. & BOTCHAN, M. R. 2006. Isolation of the Cdc45/Mcm2-7/GINS (CMG) complex, a candidate for the eukaryotic DNA replication fork helicase. *Proc Natl Acad Sci U S A,* 103**,** 10236-41.

MUNRO, S. & PELHAM, H. R. 1984. Use of peptide tagging to detect proteins expressed from cloned genes: deletion mapping functional domains of Drosophila hsp 70. *EMBO J,* 3**,** 3087-93.

MURAMATSU, S., HIRAI, K., TAK, Y. S., KAMIMURA, Y. & ARAKI, H. 2010. CDK-dependent complex formation between replication proteins Dpb11, Sld2, Pol (epsilon}, and GINS in budding yeast. *Genes Dev,* 24**,** 602-12.

MUZI-FALCONI, M. & KELLY, T. J. 1995. Orp1, a member of the Cdc18/Cdc6 family of S-phase regulators, is homologous to a component of the origin recognition complex. *Proc Natl Acad Sci U S A,* 92**,** 12475-9.

NASMYTH, K. & NURSE, P. 1981. Cell division cycle mutants altered in DNA replication and mitosis in the fission yeast Schizosaccharomyces pombe. *Mol Gen Genet,* 182**,** 119-24.

NGUYEN, V. Q., CO, C. & LI, J. J. 2001. Cyclin-dependent kinases prevent DNA re-replication through multiple mechanisms. *Nature,* 411**,** 1068-73.

NICK MCELHINNY, S. A., GORDENIN, D. A., STITH, C. M., BURGERS, P. M. & KUNKEL, T. A. 2008. Division of labor at the eukaryotic replication fork. *Mol Cell,* 30**,** 137-44.

NIEVERA, C., TORGUE, J. J., GRIMWADE, J. E. & LEONARD, A. C. 2006. SeqA blocking of DnaA-oriC interactions ensures staged assembly of the E. coli pre-RC. *Mol Cell,* 24**,** 581-92.

NISHITANI, H., LYGEROU, Z., NISHIMOTO, T. & NURSE, P. 2000. The Cdt1 protein is required to license DNA for replication in fission yeast. *Nature,* 404**,** 625-8.

NISHITANI, H., TARAVIRAS, S., LYGEROU, Z. & NISHIMOTO, T. 2001. The human licensing factor for DNA replication Cdt1 accumulates in G1 and is destabilized after initiation of S-phase. *J Biol Chem,* 276**,** 44905-11.

OKA, A., SUGIMOTO, K., TAKANAMI, M. & HIROTA, Y. 1980. Replication Origin of the *Escherichia coli* K-12 Chromosome : The Size and Structure of the Minimum DNA Segment Carrying the Information for Autonomous Replication. *Mol. Gen. Genet.,* 178**,** 9-20.

PARK, J., LONG, D. T., LEE, K. Y., ABBAS, T., SHIBATA, E., NEGISHI, M., LUO, Y., SCHIMENTI, J. C., GAMBUS, A., WALTER, J. C. & DUTTA, A. 2013. The MCM8-MCM9 complex promotes RAD51 recruitment at DNA damage sites to facilitate homologous recombination. *Mol Cell Biol,* 33**,** 1632-44.

PERKINS, G. & DIFFLEY, J. F. X. 1998. Nucleotide-dependent prereplicative complex assembly by Cdc6p, a homolog of eukaryotic and prokaryotic clamp-loaders. *Mol Cell,* 2**,** 23-32.

PETERSEN, B. O., LUKAS, J., SORENSEN, C. S., BARTEK, J. & HELIN, K. 1999. Phosphorylation of mammalian CDC6 by Cyclin A/CDK2 regulates its subcellular localization. *EMBO J.,* 18**,** 396-410.

PIATTI, S., BOHM, T., COCKER, J. H., DIFFLEY, J. F. X. & NASMYTH, K. 1996. Activation of S-phase-promoting CDKs in late G1 defines a "point of no return" after which Cdc6 synthesis cannot promote DNA replication in yeast. *Genes Dev,* 10**,** 1516-31.

POMERANTZ, R. T. & O'DONNELL, M. 2007. Replisome mechanics: insights into a twin DNA polymerase machine. *Trends Microbiol,* 15**,** 156-64.

PUIG, O., CASPARY, F., RIGAUT, G., RUTZ, B., BOUVERET, E., BRAGADO-NILSSON, E., WILM, M. & SERAPHIN, B. 2001. The tandem affinity purification (TAP) method: a general procedure of protein complex purification. *Methods,* 24**,** 218-29.

PURSELL, Z. F., ISOZ, I., LUNDSTROM, E. B., JOHANSSON, E. & KUNKEL, T. A. 2007. Yeast DNA polymerase epsilon participates in leading-strand DNA replication. *Science,* 317**,** 127-30.

RANDELL, J. C., BOWERS, J. L., RODRIGUEZ, H. K. & BELL, S. P. 2006. Sequential ATP hydrolysis by Cdc6 and ORC directs loading of the Mcm2-7 helicase. *Mol Cell,* 21**,** 29-39.

RANDELL, J. C., FAN, A., CHAN, C., FRANCIS, L. I., HELLER, R. C., GALANI, K. & BELL, S. P. 2010. Mec1 Is One of Multiple Kinases that Prime the Mcm2-7 Helicase for Phosphorylation by Cdc7. *Mol Cell,* 40**,** 353-63.

RAO, P. N. & JOHNSON, R. T. 1970. Mammalian cell fusion: studies on the regulation of DNA synthesis and mitosis. *Nature,* 225**,** 159-64.

REHA-KRANTZ, L. J. & HURWITZ, J. 1978a. The dnaB gene product of Escherichia coli. I. Purification, homogeneity, and physical properties. *J Biol Chem,* 253**,** 4043-50.

REHA-KRANTZ, L. J. & HURWITZ, J. 1978b. The dnaB gene product of Escherichia coli. II. Single stranded DNA-dependent ribonucleoside triphosphatase activity. *J Biol Chem,* 253**,** 4051-7.

REMUS, D., BEALL, E. L. & BOTCHAN, M. R. 2004. DNA topology, not DNA sequence, is a critical determinant for Drosophila ORC-DNA binding. *Embo J,* 23**,** 897-907.

REMUS, D., BEURON, F., TOLUN, G., GRIFFITH, J. D., MORRIS, E. P. & DIFFLEY, J. F. X. 2009. Concerted loading of Mcm2-7 double hexamers around DNA during DNA replication origin licensing. *Cell,* 139**,** 719-30.

REMUS, D. & DIFFLEY, J. F. X. 2009. Eukaryotic DNA replication control: lock and load, then fire. *Curr Opin Cell Biol,* 21**,** 771-7.

ROMANOWSKI, P., MADINE, M. A., ROWLES, A., BLOW, J. J. & LASKEY, R. A. 1996. The Xenopus origin recognition complex is essential for DNA replication and MCM binding to chromatin. *Curr Biol,* 6**,** 1416-25.

ROWLES, A., TADA, S. & BLOW, J. J. 1999. Changes in association of the Xenopus origin recognition complex with chromatin on licensing of replication origins. *J. Cell Sci.,* 112**,** 2011-2018.

ROWLEY, A., COCKER, J. H., HARWOOD, J. & DIFFLEY, J. F. X. 1995. Initiation complex assembly at budding yeast replication origins begins with the recognition of a bipartite sequence by limiting amounts of the initiator, ORC. *Embo J,* 14**,** 2631-41.

SAMBROOK, J. & RUSSELL, D. W. 2001. *Molecular cloning : a laboratory manual,* Cold Spring Harbor, N.Y., Cold Spring Harbor Laboratory Press.

SAMSON, R. Y. & BELL, S. D. 2013. MCM loading--an open-and-shut case? *Mol Cell,* 50**,** 457-8.

SANCHEZ, M., CALZADA, A. & BUENO, A. 1999. The Cdc6 protein is ubiquitinated in vivo for proteolysis in Saccharomyces cerevisiae. *J Biol Chem,* 274**,** 9092-7.

SANCHEZ-PULIDO, L., DIFFLEY, J. F. X. & PONTING, C. P. 2010. Homology explains the functional similarities of Treslin/Ticrr and Sld3. *Curr Biol,* 20**,** R509-10.

SANTOCANALE, C. & DIFFLEY, J. F. X. 1996. ORC- and Cdc6-dependent complexes at active and inactive chromosomal replication origins in Saccharomyces cerevisiae. *Embo J,* 15**,** 6671-9.

SCHAPER, S. & MESSER, W. 1995. Interaction of the initiator protein DnaA of Escherichia coli with its DNA target. *J Biol Chem,* 270**,** 17622-6.

SCHWACHA, A. & BELL, S. P. 2001. Interactions between two catalytically distinct MCM subgroups are essential for coordinated ATP hydrolysis and DNA replication. *Mol Cell,* 8**,** 1093-104.

SEKI, T. & DIFFLEY, J. F. X. 2000. Stepwise assembly of initiation proteins at budding yeast replication origins in vitro. *Proc Natl Acad Sci U S A,* 97**,** 14115-20.

SHECHTER, D. F., YING, C. Y. & GAUTIER, J. 2000. The intrinsic DNA helicase activity of Methanobacterium thermoautotrophicum delta H minichromosome maintenance protein. *J Biol Chem,* 275**,** 15049-59.

SHEN, Z., SATHYAN, K. M., GENG, Y., ZHENG, R., CHAKRABORTY, A., FREEMAN, B., WANG, F., PRASANTH, K. V. & PRASANTH, S. G. 2010. A WD-repeat protein stabilizes ORC binding to chromatin. *Mol Cell,* 40**,** 99-111.

SHEU, Y. J. & STILLMAN, B. 2006. Cdc7-Dbf4 phosphorylates MCM proteins via a docking site-mediated mechanism to promote S phase progression. *Mol Cell,* 24**,** 101-13.

SHEU, Y. J. & STILLMAN, B. 2010. The Dbf4-Cdc7 kinase promotes S phase by alleviating an inhibitory activity in Mcm4. *Nature,* 463**,** 113-7.

SIDDIQUI, K., ON, K. F. & DIFFLEY, J. F. 2013. Regulating DNA Replication in Eukarya. *Cold Spring Harb Perspect Biol*.

SIDDIQUI, K. & STILLMAN, B. 2007. ATP-dependent assembly of the human origin recognition complex. *J Biol Chem,* 282**,** 32370-83.

SKARSTAD, K. & KATAYAMA, T. 2013. Regulating DNA replication in bacteria. *Cold Spring Harb Perspect Biol,* 5**,** a012922.

SLATER, S., WOLD, S., LU, M., BOYE, E., SKARSTAD, K. & KLECKNER, N. 1995. E. coli SeqA protein binds oriC in two different methyl-modulated reactions appropriate to its roles in DNA replication initiation and origin sequestration. *Cell,* 82**,** 927-36.

SPECK, C., CHEN, Z., LI, H. & STILLMAN, B. 2005. ATPase-dependent cooperative binding of ORC and Cdc6 to origin DNA. *Nat Struct Mol Biol,* 12**,** 965-71.

STINCHCOMB, D. T., STRUHL, K. & DAVIS, R. W. 1979. Isolation and characterisation of a yeast chromosomal replicator. *Nature,* 282**,** 39-43.

STRUHL, K., STINCHCOMB, D. T., SCHERER, S. & DAVIS, R. W. 1979. High-frequency transformation of yeast: Autonomous replication of hybrid DNA molecules. *Proc. Natl. Acad. Sci. USA,* 76**,** 1035-1039.

SUN, J., EVRIN, C., SAMEL, S. A., FERNANDEZ-CID, A., RIERA, A., KAWAKAMI, H., STILLMAN, B., SPECK, C. & LI, H. 2013. Cryo-EM structure of a helicase loading intermediate containing ORC-Cdc6-Cdt1-MCM2-7 bound to DNA. *Nat Struct Mol Biol,* 20**,** 944-51.

SUN, J., KAWAKAMI, H., ZECH, J., SPECK, C., STILLMAN, B. & LI, H. 2012. Cdc6-induced conformational changes in ORC bound to origin DNA revealed by cryo-electron microscopy. *Structure,* 20**,** 534-44.

SYMEONIDOU, I. E., TARAVIRAS, S. & LYGEROU, Z. 2012. Control over DNA replication in time and space. *FEBS Lett,* 586**,** 2803-12.

TAKAHASHI, T., OHARA, E., NISHITANI, H. & MASUKATA, H. 2003. Multiple ORC-binding sites are required for efficient MCM loading and origin firing in fission yeast. *EMBO J,* 22**,** 964-74.

TAKARA, T. J. & BELL, S. P. 2011. Multiple Cdt1 molecules act at each origin to load replication-competent Mcm2-7 helicases. *EMBO J,* 30**,** 4885-96.
TANAKA, S. & DIFFLEY, J. F. X. 2002. Interdependent nuclear accumulation of budding yeast Cdt1 and Mcm2-7 during G1 phase. *Nat Cell Biol,* 4**,** 198-207.
TANAKA, S., UMEMORI, T., HIRAI, K., MURAMATSU, S., KAMIMURA, Y. & ARAKI, H. 2007. CDK-dependent phosphorylation of Sld2 and Sld3 initiates DNA replication in budding yeast. *Nature,* 445**,** 328-32.
TANAKA, T., KNAPP, D. & NASMYTH, K. 1997. Loading of an Mcm protein onto DNA-replication origins is regulated by Cdc6p and CDKs. *Cell,* 90**,** 649-660.
TANAKA, T., UMEMORI, T., ENDO, S., MURAMATSU, S., KANEMAKI, M., KAMIMURA, Y., OBUSE, C. & ARAKI, H. 2011. Sld7, an Sld3-associated protein required for efficient chromosomal DNA replication in budding yeast. *EMBO J*.
THOMMES, P., KUBOTA, Y., TAKISAWA, H. & BLOW, J. J. 1997. The RLF-M component of the replication licensing system forms complexes containing all six MCM/P1 polypeptides. *EMBO J.,* 16**,** 3312-3319.
TORHEIM, N. K. & SKARSTAD, K. 1999. Escherichia coli SeqA protein affects DNA topology and inhibits open complex formation at oriC. *EMBO J,* 18**,** 4882-8.
TSAKRAKLIDES, V. & BELL, S. P. 2010. Dynamics of pre-replicative complex assembly. *J Biol Chem,* 285**,** 9437-43.
VAN HOUTEN, J. V. & NEWLON, C. S. 1990. Mutational analysis of the consensus sequence of a replication origin from yeast chromosome III. *Mol Cell Biol,* 10**,** 3917-25.
VOLKENING, M. & HOFFMANN, I. 2005. Involvement of human MCM8 in prereplication complex assembly by recruiting hcdc6 to chromatin. *Mol Cell Biol,* 25**,** 1560-8.
VON FREIESLEBEN, U., RASMUSSEN, K. V. & SCHAECHTER, M. 1994. SeqA limits DnaA activity in replication from oriC in Escherichia coli. *Mol Microbiol,* 14**,** 763-72.
WALTER, J. & NEWPORT, J. 2000. Initiation of eukaryotic DNA replication: origin unwinding and sequential chromatin association of Cdc45, RPA, and DNA polymerase alpha. *Mol Cell,* 5**,** 617-27.
WATSON, J. D. & CRICK, F. H. 1953. Molecular structure of nucleic acids; a structure for deoxyribose nucleic acid. *Nature,* 171**,** 737-8.
WEINREICH, M., LIANG, C. & STILLMAN, B. 1999. The Cdc6p nucleotide-binding motif is required for loading Mcm proteins onto chromatin. *Proc. Natl. Acad. Sci. USA,* 96**,** 441-446.
WHITTAKER, A. J., ROYZMAN, I. & ORR-WEAVER, T. L. 2000. Drosophila double parked: a conserved, essential replication protein that colocalizes with the origin recognition complex and links DNA replication with mitosis and the down-regulation of S phase transcripts. *Genes Dev,* 14**,** 1765-76.
WICKNER, S. & HURWITZ, J. 1975. Interaction of Escherichia coli dnaB and dnaC(D) gene products in vitro. *Proc Natl Acad Sci U S A,* 72**,** 921-5.
WILLIAMS, R. S., SHOHET, R. V. & STILLMAN, B. 1997. A human protein related to yeast Cdc6p. *Proc. Natl. Acad. Sci. USA,* 94**,** 142-7.
WILMES, G. M. & BELL, S. P. 2002. The B2 element of the Saccharomyces cerevisiae ARS1 origin of replication requires specific sequences to facilitate pre-RC formation. *Proc Natl Acad Sci U S A,* 99**,** 101-6.
WOHLSCHLEGEL, J. A., DWYER, B. T., DHAR, S. K., CVETIC, C., WALTER, J. C. & DUTTA, A. 2000. Inhibition of eukaryotic DNA replication by geminin binding to Cdt1. *Science,* 290**,** 2309-12.
YAN, H., MERCHANT, A. M. & TYE, B.-K. 1993. Cell cycle-regulated nuclear localisation of MCM2 and MCM3, which are required for the initiation of DNA

synthesis at chromosomal replication origins in yeast. *Genes Dev.,* 7**,** 2149-2160.

YANAGI, K., MIZUNO, T., YOU, Z. & HANAOKA, F. 2002. Mouse geminin inhibits not only Cdt1-MCM6 interactions but also a novel intrinsic Cdt1 DNA binding activity. *J Biol Chem,* 277**,** 40871-80.

YANG, S., YU, X., VANLOOCK, M. S., JEZEWSKA, M. J., BUJALOWSKI, W. & EGELMAN, E. H. 2002. Flexibility of the rings: structural asymmetry in the DnaB hexameric helicase. *J Mol Biol,* 321**,** 839-49.

YEKEZARE, M., GOMEZ-GONZALEZ, B. & DIFFLEY, J. F. 2013. Controlling DNA replication origins in response to DNA damage - inhibit globally, activate locally. *J Cell Sci,* 126**,** 1297-306.

YING, C. Y. & GAUTIER, J. 2005. The ATPase activity of MCM2-7 is dispensable for pre-RC assembly but is required for DNA unwinding. *EMBO J,* 24**,** 4334-44.

ZEGERMAN, P. & DIFFLEY, J. F. X. 2007. Phosphorylation of Sld2 and Sld3 by cyclin-dependent kinases promotes DNA replication in budding yeast. *Nature,* 445**,** 281-5.

ZHANG, J., YU, L., WU, X., ZOU, L., SOU, K. K., WEI, Z., CHENG, X., ZHU, G. & LIANG, C. 2010. The interacting domains of hCdt1 and hMcm6 involved in the chromatin loading of the MCM complex in human cells. *Cell Cycle,* 9**,** 4848-57.

ZHENG, L. & SHEN, B. 2011. Okazaki fragment maturation: nucleases take centre stage. *J Mol Cell Biol,* 3**,** 23-30.